

*Synthesis, structures and characterization of  
coordination compounds with the transition metals,  
Ni(II), Cu(II), Mn(II), Cr(III), Fe(III), using ligands based on  
iminodiacetic acid and N-heterocycles.*

Zur Erlangung des akademischen Grades eines

DOKTOR DER NATURWISSENSCHAFTEN

Von der Fakultät Chemie und Biowissenschaften der Universität Karlsruhe (TH)

**Dissertation**

von

**Dipl.-Chem. Maria Paula Juanico**

**aus Buenos Aires**

**Dekan : Prof. M. Kappes**

**1. Gutachter : Prof. A. K. Powell**

**2. Gutachter : Prof. W. Freyland**

**Tag der mündlichen Prüfung: 19.12.2003**



This thesis was completed in the period from January 2001 until December 2003 in the Institut für Anorganische Chemie der Universität Karlsruhe (TH) under the supervision of Prof. A. K. Powell.



## **Dedication:**

I would like to dedicate this thesis to my godfather Oscar Pedro Rovella, who died during my doctoral work on the Day of the Innocents in Uruguay. He was an economist, a government minister for family matters and a diplomat. He had both Jewish and Muslim friends, who all had respect for him. He knew both Sukarno and [“Che Guevara”], and was always able to keep calm in difficult situations. He inspires me not to lose courage to reach my goals.

Also I would like to dedicate this thesis at my uncle Carlitos Luis Oehninger, because I also admire him very much, and because he is a wonderful medic and was very fond of my father.

## **Dedicatoria:**

Deseo dedicar este doctorado a mi difunto padrino Oscar Pedro Rovella que falleció durante mi doctorado el día de los inocentes en Uruguay. El fue economista, director de asignaciones familiares y diplomático. Tuvo amigos tanto judíos como musulmanes, que lo respetaron mucho, conoció a Sukarno y a [“Che Guevara”] y siempre supo mantener la calma en situaciones difíciles. En él se inspira mi valentía para conseguir mis logros.

También deseo dedicar este doctorado a otra persona que admiro mucho, mi tío Carlitos Luis Oehninger, que es un gran médico y quería mucho a mi padre.



# Table of Contents

1	Chapter One: Introduction .....	1
2	Chapter Two: Research Objectives .....	3
3	Chapter Three: Molecule Based Magnets.....	4
3.1	Concepts in supramolecular chemistry .....	4
3.2	Magnetic properties of matter .....	7
3.2.1	Fundamental knowledge of magnetism .....	7
3.2.2	Types of magnetic properties .....	9
4	Chapter Four: Synthons .....	16
4.1	Organic Synthons .....	16
4.1.1	N-heterocycles based ligands .....	17
4.1.2	Ligands based on iminodiacetic acid .....	18
4.1.3	Carboxylate bridging modes .....	19
4.2	The metal ion synthons .....	20
4.3	The solvent synthon.....	20
4.4	The base as synthon.....	21
4.5	Synthetic strategies.....	21
4.6	Previous work on the ligands used.....	22
5	Chapter Five: Results and Discussion .....	26
5.1	Structure of $[\text{CuBr}_2(\text{C}_{14}\text{H}_{16}\text{N}_4)]$ , 1. ....	27
5.2	Structure of $[\text{CuCl}_2(\text{C}_{14}\text{H}_{16}\text{N}_4)] \cdot \text{H}_2\text{O}$ , 2. ....	29
5.3	Structure of $[\text{Cu}(\text{C}_{14}\text{H}_{16}\text{N}_4)_2]\text{Br}_2 \cdot 2\text{MeOH}$ , 3. ....	33
5.4	Structure of $[\text{CuCl}_2(\text{C}_{12}\text{H}_{12}\text{N}_2\text{O}_2)]$ , 4 .....	35
5.5	Structure of $[\text{Cu}_2\text{Cl}_4(1,3\text{-dipyridylpropane})_2] \cdot \text{H}_2\text{O}$ , 5.....	37
5.6	Structure of $[\text{Cu}_2(\text{OAc})_4(\text{C}_4\text{H}_4\text{N}_3\text{Br})]_\infty$ , 6. ....	39
5.6.1	Magnetic properties of 6 .....	41
5.7	Structure of $[\text{Cu}_2(\text{OAc})_4(\text{C}_4\text{H}_4\text{N}_3\text{Br})_2]$ , 7.....	43
5.8	Structure of $\text{K}_4[\text{Cu}(\text{OAc})_6(\text{HOAc})_4]$ , 8. ....	46
5.9	Structure of $[\text{Cu}_2(\text{OAc})_4\text{MnCl}_2(\text{H}_2\text{O})_4]_\infty$ , 9. ....	49
5.9.1	Magnetic properties of the compound 9.....	52
5.10	Structure of $\text{K}[\text{Cu}(\text{ida})\text{Cl}(\text{H}_2\text{O})_2]$ , 10.....	54
5.11	Structure of $\text{K}[\text{Cr}(\text{Hedta})\text{Cl}] \cdot \text{H}_2\text{O}$ , 11.....	57
5.12	Structure of $[\text{CuCl}(\text{H}_3\text{edta})] \cdot 2\text{H}_2\text{O}$ , 12. ....	60

5.13	Structure of [Cu(Hada) <sub>2</sub> ], 13.....	62
5.14	Structure of (pyrH).[Cr(ada) <sub>2</sub> ].3H <sub>2</sub> O 14 .....	64
5.15	Structure of {(pyrH)[Cu(heidi)(pyr)]Cl.2H <sub>2</sub> O} <sub>∞</sub> , 15. ....	66
5.16	Structure of [Cu(naphtyl-OH-ida).(H <sub>2</sub> O)], 16. ....	69
5.17	Structure of [Ni(Hhda-OH)(H <sub>2</sub> O) <sub>2</sub> ].H <sub>2</sub> O, 17.....	71
5.18	Structure of [Cr(hda-OH)(H <sub>2</sub> O)].2H <sub>2</sub> O, 18. ....	73
5.19	Structure of [Fe(hda-OH)(H <sub>2</sub> O) <sub>2</sub> ].2H <sub>2</sub> O, 19. ....	75
5.20	Structure of K <sub>5</sub> [Fe <sub>2</sub> (μ-O)(μ-NO <sub>3</sub> )(SO <sub>3</sub> -hda-OH) <sub>2</sub> ] .15H <sub>2</sub> O, 20.....	76
5.20.1	Magnetic properties of the compound 20.....	80
6	Chapter Six: Synthetic Methods. ....	83
6.1	Organic synthesis.....	83
6.1.1	Synthesis of the ligand L1. ....	83
6.1.2	Synthesis of the ligand L2. ....	83
6.1.3	Synthesis of the ligand L3. ....	83
6.1.4	Synthesis of the ligand L13. [109] .....	84
6.2	Inorganic synthesis.....	84
6.2.1	[CuBr <sub>2</sub> (C <sub>14</sub> H <sub>16</sub> N <sub>4</sub> )] 1 .....	84
6.2.2	[CuCl <sub>2</sub> (C <sub>14</sub> H <sub>16</sub> N <sub>4</sub> )].H <sub>2</sub> O 2 .....	84
6.2.3	[Cu(C <sub>14</sub> H <sub>16</sub> N <sub>4</sub> ) <sub>2</sub> ]Br <sub>2</sub> .2MeOH 3 .....	84
6.2.4	[CuCl <sub>2</sub> (C <sub>12</sub> H <sub>12</sub> N <sub>2</sub> O <sub>2</sub> )] 4 .....	85
6.2.5	[Cu <sub>2</sub> Cl <sub>4</sub> (1,3-dpp) <sub>2</sub> ].H <sub>2</sub> O 5 .....	85
6.2.6	[Cu <sub>2</sub> (OAc) <sub>4</sub> (C <sub>4</sub> H <sub>4</sub> N <sub>3</sub> Br)] <sub>∞</sub> 6.....	85
6.2.7	[Cu <sub>2</sub> (OAc) <sub>4</sub> (C <sub>4</sub> H <sub>4</sub> N <sub>3</sub> Br) <sub>2</sub> ] 7.....	85
6.2.8	K <sub>4</sub> [Cu(OAc) <sub>6</sub> (HOAc) <sub>4</sub> ] 8 .....	86
6.2.9	[Cu <sub>2</sub> (OAc) <sub>4</sub> MnCl <sub>2</sub> (H <sub>2</sub> O) <sub>4</sub> ] <sub>∞</sub> 9 .....	86
6.2.10	K[Cu(ida)Cl(H <sub>2</sub> O) <sub>2</sub> ] 10.....	86
6.2.11	K[Cr(Hedta)Cl].H <sub>2</sub> O 11 .....	86
6.2.12	[CuCl(H <sub>3</sub> edta)].2H <sub>2</sub> O 12 .....	87
6.2.13	[Cu(Hada) <sub>2</sub> ] 13 .....	87
6.2.14	[Cr(ada) <sub>2</sub> ](pyrH).3H <sub>2</sub> O 14 .....	87
6.2.15	{(pyrH)[Cu(heidi)(pyr)]Cl.2H <sub>2</sub> O} <sub>∞</sub> 15 .....	87
6.2.16	[Cu(naphthyl-OH-ida)(H <sub>2</sub> O)] 16.....	88
6.2.17	[Ni(hda-OH)(H <sub>2</sub> O) <sub>2</sub> ].H <sub>2</sub> O 17.....	88
6.2.18	[Cr(hda-OH)(H <sub>2</sub> O)].2H <sub>2</sub> O 18 .....	88



6.2.19	[Fe(hda-OH)(H <sub>2</sub> O) <sub>2</sub> ].2H <sub>2</sub> O 19	88
6.2.20	K <sub>5</sub> [Fe <sub>2</sub> (μ-O)(μ-NO <sub>3</sub> )(SO <sub>3</sub> -hda-OH) <sub>2</sub> ].15H <sub>2</sub> O 20	89
7	Chapter Seven: Experimental methods.....	90
7.1	X-ray-diffraction on single crystals. ....	90
7.2	FT-IR Spectroscopy .....	90
7.3	FT-NMR spectroscopy .....	90
7.4	Elemental Analysis .....	91
7.5	Magnetic Measurements.....	91
8	Chapter Eight: Crystallographic data.....	92
8.1	[CuCl <sub>2</sub> (C <sub>14</sub> H <sub>16</sub> N <sub>4</sub> )].H <sub>2</sub> O 2 : Bond lengths [Å] and angles [°]. ....	97
8.2	[Cu(C <sub>14</sub> H <sub>16</sub> N <sub>4</sub> ) <sub>2</sub> ]Br <sub>2</sub> .2MeOH 3 : Bond lengths [Å] and angles [°]. ....	97
8.3	[CuBr <sub>2</sub> (C <sub>14</sub> H <sub>16</sub> N <sub>4</sub> )] 1 : Bond lengths [Å] and angles [°].....	98
8.4	[Cu <sub>2</sub> Cl <sub>4</sub> (1,3-dpp) <sub>2</sub> ].H <sub>2</sub> O 5 : Bond lengths [Å] and angles [°]. ....	98
8.5	[Cu <sub>2</sub> (OAc) <sub>4</sub> (C <sub>4</sub> H <sub>4</sub> N <sub>3</sub> Br)] <sub>∞</sub> 6 : Bond lengths [Å] and angles [°].....	99
8.6	[Cu <sub>2</sub> (OAc) <sub>4</sub> (C <sub>4</sub> H <sub>4</sub> N <sub>3</sub> Br) <sub>2</sub> ] 7 : Bond lengths [Å] and angles [°]. ....	100
8.7	K <sub>4</sub> [Cu(OAc) <sub>6</sub> (HOAc) <sub>4</sub> ] 8 : Bond lengths [Å] and angles [°]. ....	101
8.8	[Cu <sub>2</sub> (OAc) <sub>4</sub> MnCl <sub>2</sub> (H <sub>2</sub> O) <sub>4</sub> ] <sub>∞</sub> 9 : Bond lengths [Å] and angles [°].....	103
8.9	K[Cu(ida)Cl(H <sub>2</sub> O) <sub>2</sub> ] 10 : Bond lengths [Å] and angles [°]. ....	103
8.10	K[Cr(Hedta)Cl].H <sub>2</sub> O 11 : Bond lengths [Å] and angles [°]. ....	105
8.11	[CuCl(H <sub>3</sub> edta)].2H <sub>2</sub> O 12 : Bond lengths [Å] and angles [°].....	106
8.12	[Cu(Hada) <sub>2</sub> ] 13 : Bond lengths [Å] and angles [°]. ....	108
8.13	[Cr(ada) <sub>2</sub> ](pyrH).3H <sub>2</sub> O 14 : Bond lengths [Å] and angles [°]. ....	109
8.14	{(pyrH).[Cu(heidi)(pyr)]Cl.2H <sub>2</sub> O} <sub>∞</sub> 15: Bond lengths [Å] and angles [°]. ....	110
8.15	[Cu(naphtyl-OH-ida)(H <sub>2</sub> O)] 16: Bond lengths [Å] and angles [°]. ....	111
8.16	[Ni(hda-OH)(H <sub>2</sub> O) <sub>2</sub> ].H <sub>2</sub> O 17: Bond lengths [Å] and angles [°].....	112
8.17	[Cr(hda-OH)(H <sub>2</sub> O)].2H <sub>2</sub> O 18: Bond lengths [Å] and angles [°].....	113
8.18	[Fe(hda-OH)(H <sub>2</sub> O) <sub>2</sub> ].2H <sub>2</sub> O 19: Bond lengths [Å] and angles [°].....	114
8.19	K <sub>5</sub> [Fe <sub>2</sub> (μ-O)(μ-NO <sub>3</sub> )(SO <sub>3</sub> -hda-OH) <sub>2</sub> ].15H <sub>2</sub> O 20 : Bond lengths [Å] and angles [°].	115
9	Chapter Nine : Conclusions.....	119
10	Chapter Ten: Bibliography .....	122
	Appendices A – C .....	129



## Chapter One: Introduction

In the last 12 years the development of molecular magnets has attracted increasing interest. Molecular based magnets have the advantage of possessing a defined structure, allowing for correlations between structure and magnetic properties. The past 5 years have also witnessed a rapid growth in supramolecular chemistry. Workers in the area of molecular magnetism are increasingly turning their attention to ways of inducing magnetic couplings and the secondary properties of molecular-based magnets, such as solubility, color and crystal packing as well as conductivity and photo induced effects. The goal of this work was the synthesis of compounds using synthons that are derivatives of iminodiacetic acid and N-heterocycles in combination with paramagnetic transition metal ions in order to achieve cooperative magnetic effects to form so-called molecular based magnets.

The purpose of the work presented here was to explore ways in which such approach could be applied to the field of molecular based magnetism. In this case, as well as the more familiar synthons at the disposal of the chemist the chosen transition metal ion also takes on a defining role. For example, Cr(III) with its  $d^3$  configuration results in kinetically inert octahedral complexes. Similarly, the  $d^9$  configuration of Cu(II) introduces rather flexible coordination geometries especially with the Jahn-Teller effect. Ni(II) with a  $d^8$  configuration can easily adopt 4, 5 and 6 coordination geometries. Combination of these transition metal ions in homometallic aggregates can produce cooperatives magnetic effects. They can also be combined in mixed-metal systems to give ferro- or ferrimagnetic couplings (Olivier Kahn et al.) [1]. The transition metal ions selected for the work presented here, Cu(II), Ni(II), Cr(III) and Fe(III), have the potential to form different compounds. The secondary functionalities, such as hydrophobic, hydrophilic, aliphatic or aromatic side groups of the ligand coordinating to metal-compound can be varied. This affects the structures and properties of the resulting compounds. The formation of these coordination compounds and their ordering in the crystal lattice is determined by the nature of the transition metal, the ligand, and the reaction conditions.

The synthetic procedure can also have an effect on the resulting material, for example the choice of concentration and ratios of the metal salt, ligand and base. New ligands, which can form radicals, were used and some mononuclear compounds were obtained. Synthetic strategies were used with a variety of ligands containing an iminodiacetic acid group with the

aim of producing molecular based magnets. Two molecular based magnets were synthesized,  $K_5[Fe_2(\mu-O)(\mu-NO_3)(SO_3-hda)_2].15H_2O$  and  $[Cu_2(OAc)_4MnCl_2(H_2O)_4]_\infty$  and magnetic measurements were obtained. Mononuclear complexes and polymers were produced in the synthesis of new compounds. Solvothermal reactions with mononuclear complexes and different metal salts were attempted to synthesize metal clusters, however these experiments were unsuccessful. Inert gas techniques with argon-atmosphere were used in order to stabilize metal complexes containing a quinone radical ligand. A colorless solution yielding red crystals was obtained from this ligand, however these were not single crystals, and were not suitable for an x-ray single crystal measurement. Only one metal-compound using this ligand has been reported in the literature to date [2].

Molecule-based magnets are an emerging class of magnetic materials that expand the materials properties typically associated with magnets to include low density, transparency, electrical insulation, and low temperature fabrication, as well as combine magnetic ordering with other properties such as photoresponsiveness. Essentially all of the common magnetic phenomena like ferro-, ferri-, and antiferromagnetism, associated with transition-metal based magnets can be found in molecule-based magnets. Molecule based magnets are molecular solids, which are composed of molecules that lack strong covalent bonding between them, maintain aspects of the parent molecular framework, and frequently are soluble. The representative attributes of molecule-based magnets are low density, mechanical flexibility, low-temperature processability, high strength, tuning of properties by means of organic chemistry, solubility, low environmental contamination, compatibility with polymers for composites, high magnetic susceptibilities, high magnetizations, high remanent magnetizations, low magnetic anisotropy, transparency and semiconducting and/or insulating dc electrical conductivity.

Although discovered less than two decades ago, magnets with ordering temperatures exceeding room temperature and with very high (27 kOe) and very low coercivities, and substantial eminent and saturation magnetizations are known [3].

## Chapter Two: Research Objectives

The purpose of the research presented in this thesis was to synthesize ligands based on iminodiacetic acid and on N-heterocycles, which can react with transition metals building interesting architectures and also molecule based magnets. The intention of these experiments was to construct and understand several different metal-ligand systems and to optimize the ambient conditions such as base, ligand concentration and solvent to encourage the self-assembly of supramolecular arrays influenced in two different particular ways by the ligand and type of metal ion. Furthermore, the incorporation of  $\pi$ -systems into ligating agents used allows both the manifestation of hydrophobic effects (such as  $\pi$ - $\pi$  interactions) and hydrophilic/chelating effects to be expressed in the organisation of the structures formed.

Also experiments using ligands with various side arms were side performed with different synthetic routes with the goal of forming compounds, which cyclise in a monomer or produce a dimer forming an oxo-bridge. A lot of monomers can be seen in this work, which are interesting in terms of the synthetic pathways, various characteristics and in the context of previous work. Also a reaction in argon-atmosphere was done using a ligand, which might give a radical. This gave a colourless solution with red crystals, which unfortunately were not suitable single crystals for x-ray-diffraction.

Some magnetic measurements were done at the University of Florence to evaluate the potential of some of the compounds formed. The approach of this work deals with the aspects of molecular organization, host-guest interactions, molecular communication, translocation and “transport”, replication and structural assembly.

A secondary aim of this work was to contribute to the ever expanding field of supramolecular chemistry. Every synthon is a parameter of the system and the possible variations of this parameters is large with the probability of achieving the right synthetic conditions very small. So to understand the role of the synthons in the synthetic process is time consuming.

Also the possibility of isolating mixed metal compounds where the different metal ions give rise to new and interesting magnetic qualities was explored. The work presented here led to the preparation and characterization of 20 compounds illustrating these approaches.

## Chapter Three: Molecule Based Magnets

There are two broad categories of magnets: (1) permanent magnets, which produce an external magnetic field that in turn produces a force on other magnets or on an electric current; and (2) nonpermanent magnets, which guide or deflect magnetic fields and have large magnetic moments in response to small electric currents.

Many molecule-based magnets contain metal ions; however, the organic moieties present in these molecules are key to their magnetic behavior. In some cases, the spin is on the organic fragment, i.e. it is a radical, which actively contributes to both the strength of the magnet and the spin coupling.

Molecule based magnets exhibit a wide variety of bonding and structural motifs. These include isolated molecules (zero-dimensional) and those with extended bonding within chains (1D), within layers (2D) and within (3D) network structures.

Some examples of molecule based magnets are: [Mn(III)OEP][C<sub>4</sub>(CN)<sub>6</sub>] (antiferromagnetic), Mn(II)/Cu(II)chains (ferrimagnetic), Mn(II) nitronyl nitroxide chains (ferrimagnetic), [Mn(III)(porphyrin)][TCNE] chains (ferrimagnetic), Mn[N(CN)<sub>2</sub>]<sub>2</sub> (weak ferromagnetic), V[TCNE]<sub>x</sub> (spin glass), Mn<sub>12</sub>-cluster (single molecule magnet) [3].

### 3.1 Concepts in supramolecular chemistry

The ultimate aim of supramolecular chemistry is to become the science of informed matter, i.e. it seeks to create functioning, organized small devices, which will be able to process information, by analogy with the marvelous examples, present in nature. The emergence of “chemistry between the molecules”, however, has done much to initiate a paradigm shift over the last 5 years, where concepts like molecular investigation and self assembly are transferred from biological processes to chemical nanosystems. What supramolecular chemistry has done for synthetic chemists is to alert them to the fact that chemical synthesis does not begin and end with the making and breaking of covalent bonds.

Supramolecular chemistry is often described as a rational and compressible science where the building blocks are assembled by design. It is often argued that published supramolecular structures were produced by an informed preconception, bond angles and spacer length.

While the raw materials of supramolecular chemistry would often not be regarded as challenging targets by chemists, the ways in which these materials behave upon mixing continues to earn respect for supramolecular chemists and provide supramolecular chemistry of some potentially useful molecular structures.

A widely used strategy for the assembly of supramolecular structures is the use of transition-metal centers like Fe(III) and their coordination chemistry. Metal centers, through their directional bonding, provide highly predictable corners or side units, which result in geometric shapes and polyhedra such as triangles [4], squares [5, 6], rectangles [7] and cubes [8]. There is a wide number of complexes available through metal-ion-directed self-assembly. Many coordination environments that metal centers can adopt are the fundamental building block for the formation of the vast range of geometries available with interesting ligands. The strategies used to form such assemblies have been the subject of extensive reviews [9, 10]. The concept of self-assembly has been extended to include the formation of helices [11] and other more complex three-dimensional structures [12 - 15].

In an example of supramolecular assembly leading to the formation of a molecular receptor, Hupp and coworkers have reported the synthesis of rhenium-based molecular squares capable of recognizing volatile organic compounds [16]. 4, 4'-Bipyridine and pyrazine self-assembled with rhenium to form neutral molecular squares with large internal cavities of 5 - 9 nm diameter. In addition, they displayed large zeolite-like channels in the crystalline solid state, which allowed guest transport by simple unidirectional diffusion. When tested for their selectivity properties, these materials show a distinction between small aromatic compounds and aliphatic molecules of almost identical size and volatility. They were also able to distinguish between benzene derivatives with either electron donating or electron withdrawing groups.

The ability to engage in reversible hydrogen-bond formation is a critical feature in the assembly of some of the most remarkable supramolecular architectures known. Systems that employ hydrogen bonding for the assembly of novel structural elements, such as proteins or carbohydrates continue to provide inspiration for the design of new supramolecular architectures. In general terms, hydrogen-bonded supramolecular assemblies, like metal-based systems, can be considered in terms of their dimensionality through different types of oxygen-bridges. Much work is being performed to better understand the factors governing the

formation of one-, two- and three- dimensional assemblies [17]. For example, one- and two-dimensional systems (including self-assembling macromolecular sheets, rosettes and ribbons) employ heterocyclic hydrogen-bond donors and acceptors. In these systems, the outcome of supramolecular assembly relies upon the geometry and donor number of components, and this area has recently been reviewed [18].

Hydrogen bonding has also been used extensively in the formation of the three-dimensional systems. A particularly interesting recent report in this area involves formation of an optically pure helicate by simple mixing of (1R,2R)-trans-1,2-diaminocyclohexane and (1R,2R)-trans-cyclohexane-1,2-dicarboxylic acid in water [19]. Formation of this assembly was shown to rely upon the matching of the chiralities of the acidic and basic components: when (1S,2S)-trans-1,2,-diaminocyclohexane is mixed with (1R,2R)-trans-cyclohexane-1,2-dicarboxylic acid, the diastereomeric salt fails to crystallize. Many other molecules have been assembled and it would be reasonable to suggest that these systems have been designed to assemble into preconceived architectures, although, even here, the assembly has been shown to be solvent dependent in some cases [20].

Examples of such structures are calixarene dimers which may be formed by way of hydrogen-bonding intermediaries such as 4,4'-bipyridine [21] or 2-aminopyrimidine [22]. Alternatively, calixarene "urea derivatives" can be prepared and used for formation of dimers [23 - 26].

It has also been demonstrated that when two calixarene units are covalently attached to a spacer in such a way that their urea units are oriented in opposite directions, association of the calixarene units leads to reversible formation of linear polymers described as "polycaps" [27].

In recent years Decurtins and coworkers have investigated the versatility and usefulness of two types of molecular building blocks, namely, tris-oxalato transition metal [28], and octacyanometalate complexes [29], for applications in the field of molecule-based magnets. Anionic, tris-chelated oxalato building blocks are able to build up two-dimensional honeycomb-layered structural motifs as well as three-dimensional decagon frameworks.

As a result, many coordination chemists since 1998 have come to the realization that it may be easier and more productive to develop legitimate routes to microscopic supramolecular structures by capitalizing on the large number of established high-yielding reactions in



coordination chemistry. Supramolecular chemistry deals with the association of several chemical bonds, in an organized way and according to well-defined concepts. Based on a molecular engineering approach, supramolecular structures can be designed from pre-formed building blocks, providing a promising route from chemistry to molecular nanotechnology. The supramolecular approach deals with the relevant aspects of molecular organization, host-guest interactions, molecular communication, translocation and “transport”, replication and structural assembly. Nanosized and molecular materials can exhibit a wide diversity of electronic and chemical properties, e.g., piezoelectricity, conductivity, ferroelectricity, ferromagnetism, second and third order light polarizabilities, molecular recognition, photophysical, photochemical, catalytic and electrocatalytic activity. They can be employed in an unlimited number of electronic devices and technological applications. Organized structures and self-assembly also cover a world-wide area, as exemplified by molecular films, membranes and liposome's, including polymeric supramolecular systems and supramolecular arrays, ladders and grids based on metal-complexes. The experimental design employed resembles a self-assembly approach directed by the metal-ligand affinities.

### 3.2 Magnetic properties of matter

The magnetic behaviour of para- and diamagnetic materials is characterized by magnetic susceptibility. The magnetic properties of a material are a direct image of its electronic ground state and can be used to elucidate questions of chemical structure [29, 30], the valence state of the atoms for example in mixed valence compounds [31] as well as the interpretation of phase transitions in solids [32].

#### 3.2.1 Fundamental knowledge of magnetism

If a sample is exposed to an outer magnetic field of the strength  $H$ , the magnetic induction  $B$  results in the sample from  $H$  and a contribution  $4\pi I$ , that comes from the sample itself:

$$B = H + 4\pi I \quad (1)$$

$I$  is the magnetization. For the relationship  $B/H$  (magnetic Permeability) the following is valid:

$$B/H = 1 + 4\pi(I/H) = 1 + 4\pi\chi \quad (2)$$

$\chi$  represents the volume magnetic susceptibility ( $\chi = \chi_v$ ). It is normal to give the magnetic susceptibility of a material with respect to its molecular weight. The so-called molar susceptibility  $\chi_{\text{mol}}$  is then defined through the equation:

$$\chi_{\text{mol}} = (\chi_M)/\rho \quad (3)$$

M is the molecular weight and  $\rho$  the density of the relevant compound. The classic methods for measuring magnetic properties have been developed by: Gouy, [33], Quinke [34, 35] and Faraday-Curie [14-17]; with these, the force with which a sample is attracted or repelled from a magnet field is measured. There are also the induction methods after Boersma [36] and Foner [37, 38] for investigating magnetic behaviour.

There are three principal origins for the magnetic moment of a free atom, the spins of the electrons, their orbital angular momentum about the nucleus and the change in the orbital moment induced by an applied magnetic field. The latter gives rise to a diamagnetic contribution, whereas the first two effects generate paramagnetic contributions.

$$\chi = M/H \text{ (CGS)} \quad \text{or} \quad \chi = \mu_0 M/H \text{ (SI)} \quad (4)$$

where M is the molar magnetic moment and H is the macroscopic magnetic field intensity and B in Tesla and H in  $\text{Am}^{-1}$ . The molecular susceptibility is often also referred to as  $\chi_M$  and the magnetic moment per gram is sometimes written as  $\sigma$ .

In general  $\chi$  is the algebraic sum of two contributions associated with different phenomena:

$$\chi = \chi^D + \chi^P \quad (5)$$

where  $\chi^D$  represents the diamagnetic susceptibility and  $\chi^P$  is the paramagnetic susceptibility. The former is negative and the latter is positive. When  $\chi^D$  dominates, the sample is said to be diamagnetic; it is repelled by the magnetic field. When  $\chi^P$  is the leading contribution, the sample is said to be paramagnetic; it is attracted by the magnetic field.

### 3.2.2 Types of magnetic properties

The magnetic properties of matter can be described in terms of temperature dependence of the magnetic susceptibility and divided into the following categories.

#### **Diamagnetism:**

Diamagnetism is a property of matter and is due to the interaction of the magnetic field with the motion of the electrons in their orbitals.  $\chi$  is independent of the magnetic field strength.  $\chi$  is negative. Diamagnetism occurs in all materials with electron pairs. Also ring currents are generated by induction when switching on the magnet field. The direction of the induced magnet field is countered according to Lenz's law. All materials have a diamagnetic component. In general, for paramagnetic compounds of low molecular weight, the additive method of Pascal's constants may be sufficient to estimate the diamagnetic contribution. In such cases, this contribution is small, estimated at  $5 \times 10^{-4}$  emu.mol<sup>-1</sup>.

#### **Paramagnetism:**

Any atom, ion or molecule that has one or more unpaired electrons is paramagnetic and will be attracted into a magnetic field.

$\chi$  is temperature dependent. The permanent magnetic moments of unpaired electrons are organized in the magnetic field so that their direction is aligned with the direction of the field. This yields an additional magnetic induction parallel to the applied magnetic field, therefore the value for  $\chi$  is positive,  $\chi > 0$ . The temperature dependence of the magnetic susceptibility is described by the Curie-law as:

$$\chi = C / T \quad (6)$$

where C is the Curie constant and T is the temperature. Below an ordering temperature  $T_C$  or  $T_N$  the interaction between the magnetic moments can lead to a spontaneous alignment of all moments respectively either parallel to each other, ferromagnetism, or antiparallel, antiferromagnetic or ferrimagnetism.

### Curie paramagnetism

For most paramagnetic substances with isolated magnetic moments, the magnetic susceptibility varies inversely with temperatures. This will be exemplified for  $s=1/2$  using an isolated spin.

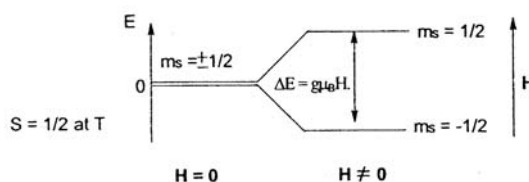


Fig.1 Energy diagram of an  $S=1/2$  spin in an external magnetic field along the z-axis [39].

For one mole spin =  $1/2$  particles in zero field the two levels  $m_s = \pm 1/2$  are degenerate. When a field  $H$  is applied along the positive z-axis the two levels split as illustrated in figure 1. The energy level of each is  $m_s g \mu_B H$ , which becomes  $-g \mu_B H/2$  for the lower level and  $+g \mu_B H/2$  for the upper level. The difference in energy between the two levels is therefore  $\Delta E = g \mu_B H$ , which for  $g = 2$  correspond to about  $1 \text{ cm}^{-1}$  at 10000 G.

The latter is the susceptibility expected in the case of an isolated spin follows the Curie-law. When the paramagnetic atoms or ions interact the Curie law is no longer valid and the magnetic exchange between spin carriers has to be calculated in a different way.

### Curie Weiss paramagnetism

When there are magnetic interactions between the spin carriers the Hamiltonian can be written as :

$$H = g\mu_B \vec{H} \cdot \vec{S} - 2J \sum_{ij} \vec{S}_i \cdot \vec{S}_j \quad (7)$$

Therefore using field approach, applicable to moderate magnetic fields, a new susceptibility can be written as:

$$M = C \frac{H}{T - \theta} \quad \text{with} \quad C = \frac{Ng^2 \mu_B^2}{4k_B} \quad \theta = \frac{zJ}{2k_B} \quad (8)$$

where  $\theta$  is the Weiss constant [39].

## Ferromagnetism

In a ferromagnetic system,  $\chi$  is temperature and field strength dependent. The permanent magnetic moments are paramagnetic above a certain temperature of  $T_c$  and below  $T_c$  ferromagnetic. The susceptibility follows the Curie Weiss law in the high temperature approximation with positive  $\theta$ :

$$\chi = C / (T - \theta) \quad \theta = \text{Weiss Temperature} \quad (9)$$

Classic examples for ferromagnetic materials are iron, cobalt, nickel and some alloys, that all are ferromagnetic at room temperature. Within the ferromagnetic substance, the interaction causes an alignment of the moments between the spins, i.e. it generates the spontaneous magnetization. With  $T = 0$  K, all moments are organized, with increasing temperature, more moments are increasingly in stimulated conditions and no longer orient parallel to  $M$ , with  $T > T_c$ , the directional distribution is on average anisotropic and the material behaves as a paramagnet. By cooling down the sample in the paramagnetic phase to a temperature  $T < T_c$ , spontaneous magnetization results. Weiss domains form following a temperature distribution. The magnetization direction is different from domain to domain, but even in a very weak field the domains align.

A steep increase of the magnetization curve is found near  $H = 0$  with a hysteresis loop and a spontaneous magnetization being observed. This spontaneous magnetization has applications in technology for example transformers.

The saturation magnetisation of a ferromagnet should correspond to the full alignment of all magnetic moments. Figure 2 shows the magnetic behaviour of an ideal ferromagnet. The exchange integral,  $J$  ( $\text{cm}^{-1}$ ), used to define the degree of coupling at any temperature when positive implies ferromagnetic coupling [39].

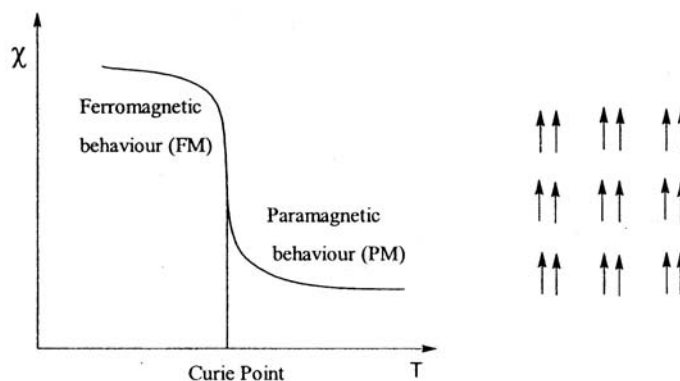


Fig. 2 Magnetic characteristics of an ideal ferromagnet. Left: temperature dependence of the magnetisation. Right: spontaneous alignment of the moments within a domain [39].

### Antiferromagnetism

In an anti-ferromagnetic system  $\chi$  is temperature and field strength dependent. The permanent magnetic moments are organized anti-parallel below the Néel-Temperature,  $T_N$ . Examples for antiferromagnetic materials are MnO and MnF<sub>2</sub>. Above  $T_N$  the susceptibility obeys a Curie-Weiss law with negative  $\theta$  and shows paramagnetic behaviour

$$\chi = C / (T - \theta) \quad (10)$$

where  $\theta$  is the Weiss-Temperature. Below  $T_N$  the value for  $\chi$  decreases with falling temperature.

Antiferromagnetism, like ferromagnetism, is also a consequence of cooperative interactions leading to long-range order. In antiferromagnetism magnetic interactions tend to align the moments antiparallel to each other resulting in no spontaneous magnetisation. Above a critical temperature, usually called the Néel temperature,  $T_N$ , thermal agitation destroys magnetic ordering and the material becomes a paramagnet that follows the Curie-Weiss law [39].

Figure 3 shows the magnetic behaviour of an ideal antiferromagnet. The negative  $J$  value implies antiferromagnetic coupling.

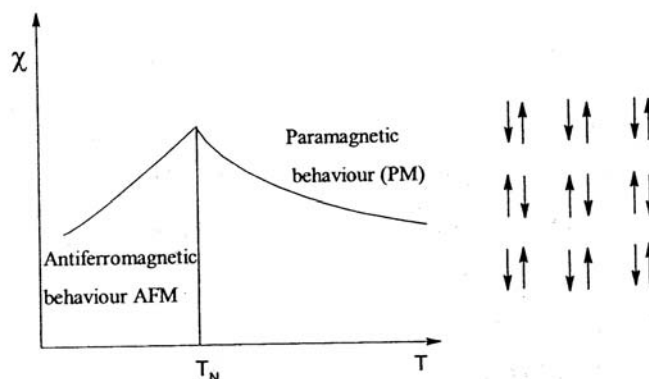


Fig. 3 Magnetic characteristics of an ideal antiferromagnet. Left: temperature dependence of the magnetisation. Right: spontaneous alignment of the moments within a domain [39].

### Ferrimagnetism

For a ferrimagnetic system  $\chi$  is temperature and field strength dependent. The permanent magnetic moments are directed in opposite pairs with spins of different magnitude. A spontaneous magnetization results. Examples for ferrimagnetic materials are: Ferrites,  $\text{MO.Fe}_2\text{O}_3$ ,  $M = \text{Fe}^{2+}$ ,  $\text{Ni}^{2+}$  etc., Lanthanide-Garnets,  $\text{Ln}_3\text{M}_5\text{O}_{12}$  with  $M = \text{Fe}^{3+}$ ,  $\text{Al}^{3+}$ ,  $\text{Ga}^{3+}$  etc.) and Lanthanide-Perovskites,  $\text{LnMO}_3$ ,  $M^{3+}$  metal cation. The strong temperature and field strength dependence is similar to that of the ferromagnetism.

The macroscopic behaviour of ferrimagnets resembles both that of ferromagnets in that these materials exhibit spontaneous magnetisation and that of antiferromagnets in that the magnetic interactions tend to align the magnetic moments antiparallel to each other. However, ferrimagnets differ from ferro- and antiferromagnets as they involve two or more magnetic species possessing different magnitudes of magnetic moment. The species can be different elements or a combination of an ion and a free radical or they can be just two different valence states of the same ion. Above  $T_c$ , a ferrimagnet becomes a paramagnet, which obeys the Curie-Weiss law. Figure 4 shows the magnetic behaviour of an ideal ferrimagnet. In the simplest case of a ferrimagnet with two sub-lattices whose respective magnetic moments,  $M_A$  and  $M_B$  are aligned antiparallel to each other, spontaneous magnetisation is the consequence of a lack of cancellation of sub-lattice magnetisation. Thus depending on the form and the

magnitude of the respective sub-lattice magnetisation  $M_A(T)$  and  $M_B(T)$ , the spontaneous magnetisation can vary widely in a ferrimagnet [39].

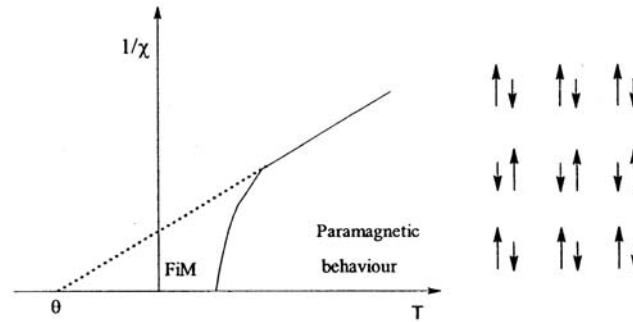


Fig. 4 Magnetic characteristics of an ideal ferrimagnet. Left: temperature dependence of the reciprocal susceptibility. Right: spontaneous alignment of the moments within a domain [39].

### Van Vleck Formula

The molar paramagnetic susceptibility characterizes the way in which an applied magnetic field  $H$  interacts with the angular momenta associated with the thermally populated states of a molecule. In classical mechanics, when a sample is perturbed by an external magnetic field, its magnetization is related to its energy variation through

$$M = - \partial E / \partial H \quad (11)$$

The macroscopic molar magnetization  $M$  is the obtained by summing the microscopic magnetizations  $\mu_n = - \partial E_n / \partial H$  weighted according to the Boltzmann distribution law, which leads to

$$M = N \sum_n (\partial E_n / \partial H) \exp(-E_n/kT) / \sum_n \exp(-E_n/kT) \quad (12)$$

except that this equation is often difficult to apply. Indeed it requires knowledge on the  $E_n = f(H)$  variations for all thermally populated states to calculate the  $(\partial E_n / \partial H)$  derivatives.



In 1932 Van Vleck proposed a simplification based on a few approximations. The first of them is that it is legitimate to expand the energies  $E_n$  according to the increasing powers of  $H$ . The second approximation is that  $H/kT$  is small with respect to unity. In other words, it is assumed that  $H$  is not too large and  $T$  not too small. The exponential in (12) may then be written as

$$\exp(-E_n/kT) = \exp(-E_n^{(0)}/kT) \exp(-E_n^{(1)}/kT) \quad (13)$$

and finally the susceptibility can be written:

$$\chi = N \sum_n (E_n^{(1)*} E_n^{(1)} / kT - E_n^{(2)}) \exp(-E_n^{(0)}/kT) / [\sum_n \exp(-E_n^{(0)}/kT)] \quad (14)$$

This equation (14) is the Van Vleck Formula. To apply this formula we only need the energy values.

If the only thermally populated state of a molecule is a spin singlet without first-order angular momentum, then the paramagnetic susceptibility is intuitively expected to be zero, and the measured susceptibility will be negative. The diamagnetic ground state may couple with excited states through the Zeeman perturbation provided that the energy gaps are not too large.  $\chi$  is then positive since all denominators are negative and temperature independent. This contribution is also called temperature-independent paramagnetism.

## Chapter Four: Synthons

### 4.1 Organic Synthons

The organic ligands used for complexation reactions in this research are given in figure 5. A list of ligand identifiers is given in table 1.

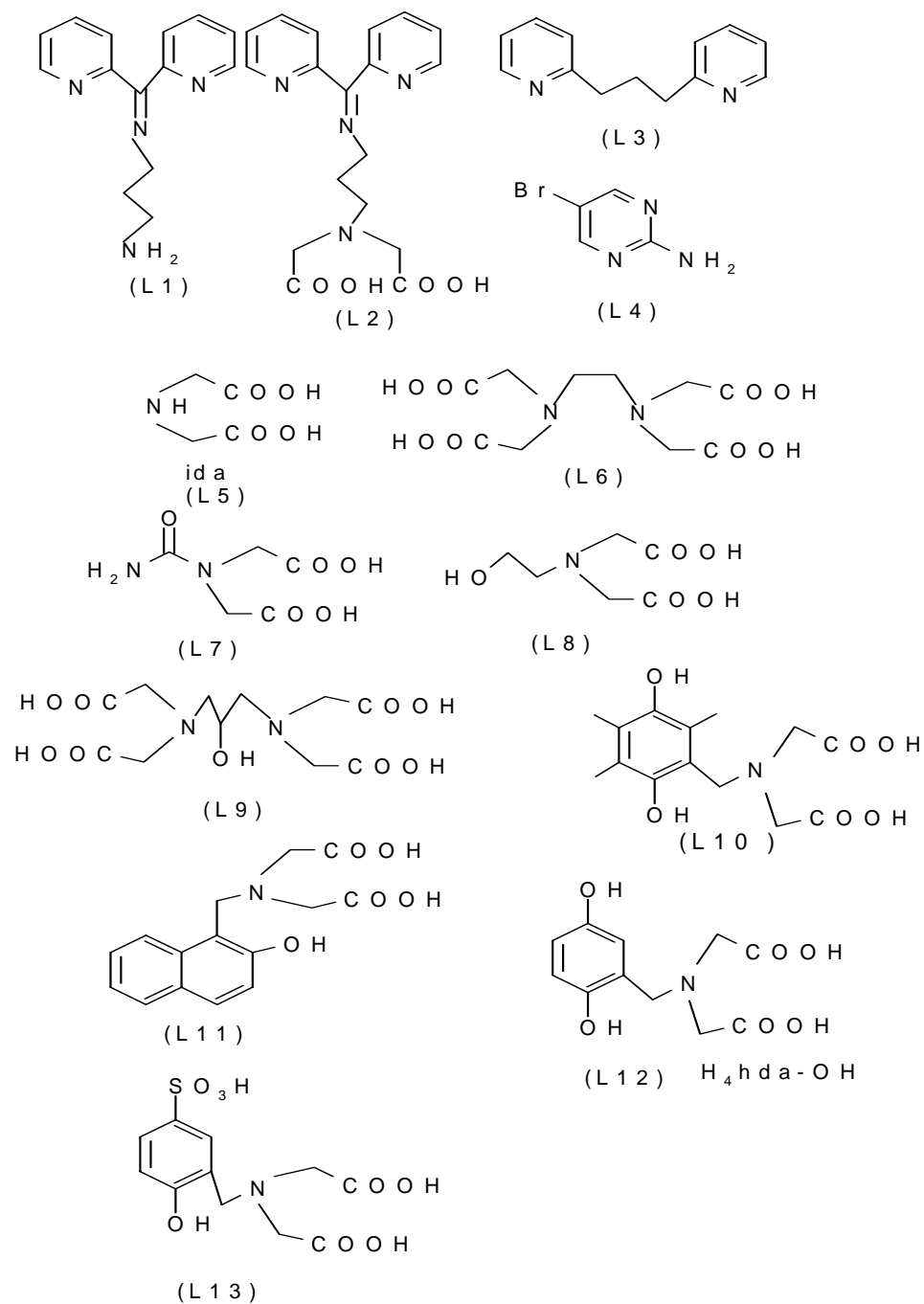


Fig. 5 Ligands used in this research and their identifiers.

- L1** N-[(1E)-Dipyridin-2-ylmethylene]propane-1,3-diamine  
**L2** [(Carboxymethyl)(3- {[ (1E)-dipyridin-2-ylmethylene]amino}propyl)amino]acetic acid  
**L3** 2-(3-Pyridin-2ylpropyl)pyridine  
**L4** 5-Bromo-2-pyrimidine-amine  
**L5** Iminodiacetic acid  
**L6** Ethyldiamine-N,N,N,N-tetraacetic acid  
**L7** [(Aminocarbonyl)(carboxymethyl) methylamino]acetic acid  
**L8** N-(2-Hydroxyethyl)iminodiacetic acid  
**L9** 1, 3-Diimino 2 hydroxy propane N, N N', N', tetraacetic acid  
**L10** [(Carboxymethyl)(2,5-dihydroxy-3,4,6-trimethylphenyl)methylamino]acetic acid  
**L11** [(Carboxymethyl)(2 hydroxy-1 naphthyl)methylamino]acetic acid  
**L12** [(Carboxymethyl)(2,5-dihydroxyphenyl)methylamino]acetic acid  
**L13** [(Carboxymethyl)(2-hydroxy-5-sulfophenyl)methylamino]acetic acid

Table 1 A list of organic ligands and their identifiers.

In each case the introduction of various groups can be included or changed to produce preferences for different supramolecular effects such as H-bonding,  $\pi$ - $\pi$  stacking, hydrophilic and hydrophobic regions and coordination bonds.

#### 4.1.1 N-heterocycles based ligands

Ligands containing pyridyl groups have been used extensively in coordination supramolecular chemistry and can be found in cyclic structures, grids and squares where strategically placed pyridyl coordination sites direct the crystal packing [40] or else simply provide  $\pi$ - $\pi$  stacking which can serve to arrange transition metal centers in chains [41]. These donor agents are particularly relevant to the efforts of molecular based magneto-chemists since they are relatively soft and so ideal partners for metals such Cu(II) ; but also induce a relatively large ligand field splitting and can give rise to spin-crossover compounds with iron, i.e. compounds where the metal ion centres can exist in the low or high spin form according to thermal, light or pressure induced crossovers [42].

The possibility to modulate a physical property following a predetermined strategy is of central importance for the development of molecular science. In this sense the lessons we learn from the synthesis of small molecules are important for the future rational design of

interacting molecular systems having desirable properties. Molecules that are characterized by high-spin electronic ground states are being actively investigated as possible building blocks for molecular magnets since they are good candidates for obtaining magnetic solids [43 - 47]. Some of the ligands used in this work are di-pyridylketone derivatives, (L1) and (L2).

It is well established that aldehydes and aliphatic ketones readily undergo addition to primary amines to produce Schiff bases, as shown in figure 6.

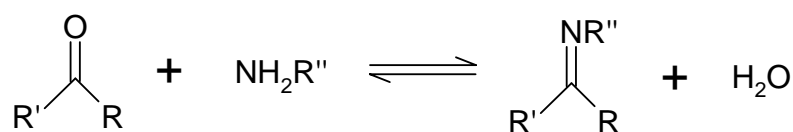


Fig. 6 The reversible reaction of an aldehyde or ketone with a primary amine results in the formation of a Schiff base.

However, when R and R' are aromatic groups, as in di-2-pyridylketone, the reactions require much more vigorous conditions. To shift the equilibrium to the product side, higher temperature, increased reaction time, and the use of a catalyst are generally required. Also, removal of water during the reaction greatly enhances product formation. To produce the desired Schiff base, it was found necessary to use a catalyst (BF<sub>3</sub>.etherate) and a Dean-Stark apparatus to remove water as it formed during the reaction. Compounds with long diamine chains did not react with dipyridylketone (dpk). These products are air sensitive and react with oxygen [48]. In the case of **L2**, the ligand hydrolyze easily as exemplified by the Cu(II)-dpk-compound described in chapter 5.

#### 4.1.2 Ligands based on iminodiacetic acid

Previous work in our group has shown the versatility of the iminodiacetic acid moiety for producing structures with 0, 1, 2 and 3 dimensional arrangements [52, 53]. Iminodiacetic acid ligands were used in order to crystallize metal-aggregates. The ligands can bind through their different donor groups to different metals. In its simplest form as the parent acid, H<sub>2</sub>ida, the ligand provides a tridentate NO<sub>2</sub> donor set as seen in simple monomers such as K[Fe(ida)<sub>2</sub>].3H<sub>2</sub>O [53]. In this case the ligand nearly always coordinates facially. If only one ligand is coordinated per metal ion center then there is the possibility to form hydroxo- or oxo-bridges to other metal centers in all three spatial directions as is seen in the Fe<sub>6</sub>

aggregates  $M_4[Fe_6O_2(OH)_6(ida)_6].nH_2O$  with ( $M = Na, K$ ) [53]. This represents the situation where solvent derived species provide the bridges between metal centers. Another possibility is bridging via the carboxylate groups and this has been observed for Cu(II) compounds [39].

Ligands derived from iminodiacetic acid adopt the general formula  $RN(CH_2COOH)_2$  and there are various possibilities to change the coordinating group R giving a tripodal ligand. The R groups which were explored in this work are shown in figure 7.

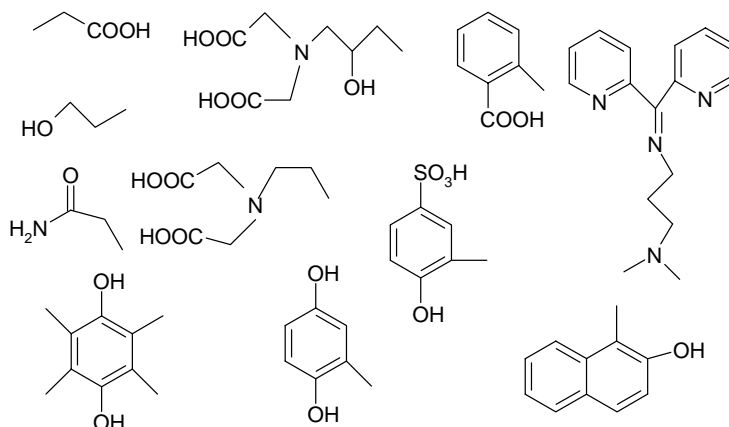


Fig.7 The R groups in  $RN(CH_2COOH)_2$ .

At this point it is worth detailing the possible carboxylate bridging modes and also the signs and magnitudes of their magnetic coupling.

#### 4.1.3 Carboxylate bridging modes

Carboxylates can coordinate and bridge in a variety of ways as shown in figures 8 and 9. These bridging modes can be used to modulate the overall magnetic behaviour of compounds linking metal centres into extended systems [39].

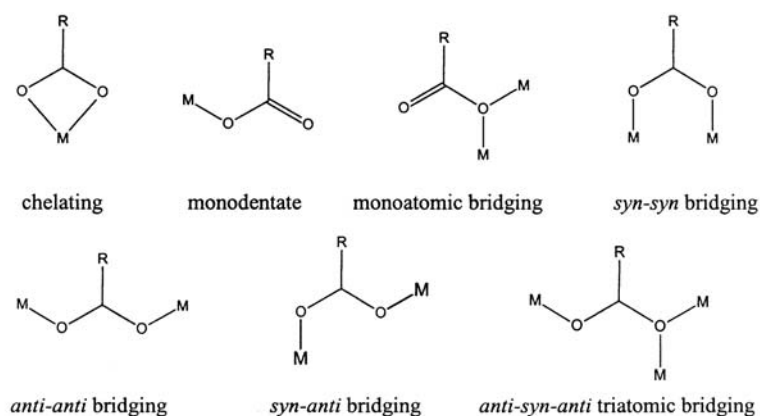


Fig. 8 Examples of monodentate and bidentate carboxylate coordination.

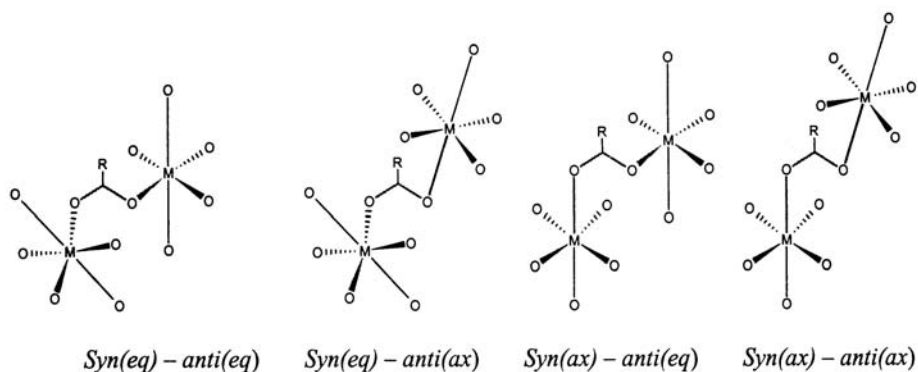


Fig. 9 Examples of bidentate carboxylate bridging modes.

## 4.2 The metal ion synthons

The choice of metal ion can direct the resulting structure through the ligand field effects; through the “softness” or “hardness” of given metal ions in a given oxidation state and spin configuration; and through its ability to undergo solvolysis reactions which is related to its Lewis acidity. The metal ions used in this work were Fe(III), Cu(II), Cr(III), Mn(II) and Ni(II). Also mixtures of two of these metal ions were tried in order to form mixed metal structures. Different synthetic strategies were tried out to achieve this. First both metals were mixed in a solution and to this solution the ligand solution with the base was added, and secondly the ligand solution with the base was added to the metal ion solution and after filtering was added to the solution of another metal ion. Also a Mn-monomer was used as a starting material. Attempts to produce mixed-metal systems using hydrothermal conditions also failed to yield any single crystals.

## 4.3 The solvent synthon

When a protic solvent is chosen then a metal ion can act to deprotonate it and this leads to bridging moieties between metal centres that are solvent rather than ligand derived. This is seen most often for Fe(III) high spin ions in aqueous media and recently, rather surprisingly given the softer nature of the ion, for Cu(II) in alcoholic media [39]. This might be a result of the fact that Cu(II) is a relatively good Lewis acid compared with most other M(II) ions, but it is still an intriguing point.

Protic solvents can also take part in H-bonding networks, which is another important supramolecular interaction, and in this way the change from H<sub>2</sub>O to MeOH can lead to a correspondingly dramatic change in crystal packing. Interesting clusters such as Cu<sub>12</sub> were synthesized in methanol [50] and in some cases the size of the cluster can be changed simply by dissolving one cluster in a different solvent as seen for the transformation of Mn<sub>12</sub> to Mn<sub>21</sub> in THF [51].

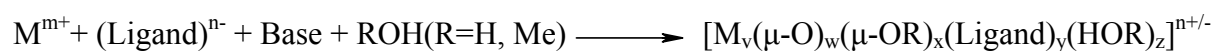
#### 4.4 The base as synthon

The purpose of the base is primarily to assist with deprotonation of the ligand or coordinated solvent molecules. However, this leads to the formation of a positively charged species either alkali metal cations or the protonated base and in cases where anionic coordination compounds are produced these can act as counterions. In this way the base can have different roles to play. Firstly, the strength of the base has been shown to have effects on degree of solvolysis with harder bases tending to lead directly to extended hydroxide and oxyhydroxide whereas softer bases allow for the trapping of fragments of extended solids as seen, for example, in the Fe<sub>17</sub> and Fe<sub>19</sub> species formed with H<sub>3</sub>heidi (an iminodiacetic acid derivative) [52]. Secondly, if the positively charged species forms part of the crystal structure then it can have structure-directing capabilities through H-bonding,  $\pi$ - $\pi$  stacking or coordination bonding effects exemplified for the based-derived counterions [NH<sub>4</sub>]<sup>+</sup>, [Hpyr]<sup>+</sup> and Na<sup>+</sup>. An example of NH<sub>4</sub><sup>+</sup> is given by the tetramer NH<sub>4</sub>[Fe<sub>4</sub>O(OH)(hpdta)<sub>2</sub>(H<sub>2</sub>O)<sub>4</sub>].12.5H<sub>2</sub>O synthesized in our group by Schmitt [51]. Also different Cu<sub>12</sub>-cluster systems were made in our group by Murugesu and King in their doctorate studies [39] with various alkali cations, which link the Cu<sub>12</sub>-structure via oxygen bridged alkali metal ion units. The size of the alkali-metal-cation seems to be important for organizing these clusters into supramolecular arrays [49].

#### 4.5 Synthetic strategies

As stated before, the aim of this work was to use selected organic synthons in combination with transition metal ion synthons and to investigate the resulting supramolecular structures. Reactions were also performed in protic solvents to allow for the possibility of oxide and hydroxide or alkoxide bridges forming [50, 51, 54].

Thus as an overall strategy and allowing for the possibility of including oxygen-containing ligands from the solvent we can write:



Although this strategy has been shown to be effective for yielding zero-dimensional metal aggregates as well as extended solids [50, 56] in the experiments performed in this work all the crystalline materials which were isolated turned out to be either monomers or else extended structures displaying a variety of packing effects. In this case we can regard the species  $[M_v(\text{O})_w(\text{OR})_x(\text{L})_y(\text{HOR})_z]^{n+/-}$  as the product formula for a monomer with  $v = 1$  or else as the repeating unit for an extended structure. Obviously all of the coordination compounds have non-zero values for  $v$  and  $y$ . The other species can have zero-values for  $w$ ,  $x$  and  $z$  and also  $n$ . The formulation does not include the supramolecular synthons of the counterions or solvent molecules, which may be present, but these are discussed at the relevant points in the next chapter, which describes the structures of the coordination compounds formed.

#### 4.6 Previous work on the ligands used

Derivatives of the ligand **L1** were synthesized and characterized, four new Schiff bases derived from 2,2'-dipyridyl ketene and some diamines were prepared and identified by NMR, IR; mass spectroscopy and elemental analysis. The electronic spectra in EtOH and  $\text{C}_6\text{H}_{12}$  were measured and interpreted. The metal complexes of these Schiff bases with divalent Cu, Co, Ni, Cd and trivalent Fe were studied by UV- visible spectrophotometry in neutral EtOH solutions. One of these Schiff bases, 2,2'-dipyridyl ketenylidene-N-1,3-diamine-2-propanol, is specific for Cu(II). The types of metal complexes, their stabilities and determination of micro quantities are discussed [57].

The stability of the complexes with **L1** with different metals such as Co(II), Ni(II), Cu(II), Zn(II), Cd(II), Ag(I) and Hg(II) were determined and also the effect of varying the alkane chain between the pyridyl groups. The most stable complexes are made with Hg and the stability decreases for 5-membered ring to 7-membered ring very drastically. [57]

The ligand **L3** is also a possible candidate for inducing spin-cross-over with iron [59]. Similar ligands to **L3** like 2,2'-bipyridine (bipy) were used [60]. The anomalous magnetic properties of the compound  $[\text{Fe}(\text{bipy})_2(\text{NCS})_2]$  were observed by Baker and Bobonich in the 1960s [61]. This compound undergoes a sharp spin transition at  $T_c \approx 213 \text{ K}$ , which can easily be monitored by thermal variation of the product  $\chi^*T$  where  $\chi$  is the molar magnetic



susceptibility and  $T$  is the temperature. The complete cooling and heating cycle does not indicate the occurrence of thermal hysteresis. A dimer with the ligand **L3** and  $\text{Ag}^+$  was synthesized [61]. The Ag-Ag distance within a cyclic unit is 7.455Å. Janiak postulated a stacking geometry [62].

Henderson has used the ligand iminodiacetic acid (ida) **L5** in his PhD [63]. He postulated how to control the product formation in the Fe/ida system. With a pH of 3-5 and a metal: ligand ratio of 1:1 the Fe-monomer  $[\text{Fe}(\text{ida})_2]^{2-}$  forms, while with a pH of 4-9 and the same mol ratio an hexamer  $[\text{Fe}_6(\mu_3\text{-O})_2(\mu_2\text{-OH})_6(\text{ida})_6]^{4-}$  results. In this work a Cu-ida-monomer has been isolated forming at pH 7 with 0.69 mmol Cu-salt and 0.69 mmol of **L5** in 20 ml solvent has been isolated. Also using a cosolvent can help to get crystals [54a].

Another Cu-monomer,  $[\text{Cu}(\text{ida})]\cdot 2\text{H}_2\text{O}$ , was synthesized by Podder [64]. The Cu ion is coordinated in a distorted octahedron and the approximate square plane around Cu formed by the imino N atom, the O atom of the water, the carboxyl O atom and another carboxyl O atom of the neighboring molecule forming a chain. The packing of this monomer consists in endless parallel chains along the **a**-axis. A Ni-ida **L5** monomer was also synthesized [65]. A Cu-ida **L5** monomer was also synthesized [66] where the Cu is coordinated in a distorted octahedron and the monomers forms in the packing parallel chains.

Iminodiacetic acid constitutes the functional group of an important and useful resin, commercially known as Chelex 100, where iminodiacetic acid is introduced into a matrix of a styrene divinyl benzene polymer. This resin shows unusually high preference for Cu and other heavy metals and thus makes this resin uniquely suitable for detection, estimation and removal of trace metals from biological fluids and enzyme systems ( Siegel & Degens, 1960). Moreover ligand exchange chromatography on Cu-loaded Chelex 100 (Goldstein, 1967) has been found to be an extremely useful technique for the rapid separation of nucleic acid compounds. A Cu-monomer with ethylenediamine-N,N,N'-triacetic-N'-3-propionic acid ( $\text{H}_4\text{ed3ap}$ ) was synthesized [67]. This ligand is similar to  $\text{H}_4\text{edta}$  **L6**. The  $[\text{Cu}(\text{ed3ap})]^{2-}$  and  $[\text{Mg}(\text{H}_2\text{O})]^{2+}$  octahedra form discrete units. The presence of 32 water molecules and the same number of carboxylate oxygens in the unit cell makes the system of hydrogen bonds very complicated.

With H<sub>4</sub>edta several monomers with Cr(III), Fe(III) and Ga(III) were synthesized [68]. Fe(III) is coordinated as a hexadentate and Cr(III) as a pentadentate with H<sub>4</sub>edta. A mixed-metal compound was also made with the ligand H<sub>4</sub>edta [69]. Also a V(III)-monomer was synthesized with H<sub>4</sub>edta [70], where the ligand coordinates to the vanadium (III) center in the quinquedentate fashion and depending on the nature of the coexisting anion, yields a “heptacoordinate or hexacoordinate” vanadium(III) complex [71]. This ligand interacts also as a bridging ligand. Many transition-metal ions take a coordination number of 6 when complexed with edta<sup>4-</sup>; such hexadentate structures with Cu(II) [72] and Cr(III) [73] are well known. Also a pentadentate complex of [Cu(H<sub>2</sub>edta)(H<sub>2</sub>O)] has been well established [74]. A review about the different coordination possibilities of H<sub>4</sub>edta with several transition metals was reported in 1977 by R. H. Nutall and D. M. Stalker [75]. Henderson has used also H<sub>3</sub>ada, and with this ligand he obtained Fe and Cr monomers. Also Coronado has written a review about the magnetic properties of H<sub>4</sub>edta complexes [77]. In this paper it was shown, that the bimetallic compounds of the H<sub>4</sub>edta family provides a set of magnetic systems for the investigation of low dimensional ferrimagnetism. Obviously, the low strength of antiferromagnetic interactions determined by the type of carboxylate bridges together with the good isolation of chains, these compounds only order at low temperatures.

Schmitt has synthesized tetramers with H<sub>3</sub>heidi and the magnetic properties were examined. It has typical ferrimagnetic behavior, where the interacting antiferromagnetic moments do not compensate. The field dependence of the magnetization was measured up to 6.5 T at two temperatures, 2.90 and 5.35 K. The curves reveal a rapid increase at low field, with a continuous decrease of the slope on increasing the field, typical of a system characterized by a ground state with  $S > 0$ . At the highest H/T value the magnetization is ca. 8.8  $\mu_B$ . Also Fe<sub>17</sub> and Fe<sub>19</sub>-clusters were synthesized with H<sub>4</sub>heidi [52]. A detailed investigation of their magnetic properties using ac and dc susceptibility measurements and EPR and Mössbauer spectroscopy reveals that at least one of the clusters the ground state spin cannot be smaller than  $S = 33/2$ . Some complexes with Co(II), Ni(II) and Cu(II) and the ligand **L11** were synthesized in 1971 [76]. These substances have a blue fluorescence in aqueous solution under UV light at pH 4-14, which increases in intensity with increasing pH and is maximal at pH 8. In daylight the reagent do not lose the intensity of this fluorescence for hours. Some 27 common metal cations were tested for their effect on fluorescence. Cu<sup>2+</sup>, Ni<sup>2+</sup>, and Fe<sup>3+</sup> quench the fluorescence almost completely, while Bi<sup>2+</sup>, Hg<sup>2+</sup> and Mn<sup>2+</sup> do so only partially. Thus the degree of inhibition may be used as a measure of stability of the metal complexes

formed by the ligand and sharp titration endpoints were found in many instances. Attempts were made in this work using ethylenediamine as base as Schmitt did in his PhD-work 2002 in our group. Using the ligands **L11**, **L12**, **L13** and ethylenediamine, attempts were made to build Fe<sub>8</sub>-clusters following the synthetic conditions [50]. However this resulted in the formation of microcrystalline solids. The target Fe-clusters have the basic core [Fe<sub>8</sub>(O)<sub>4</sub>(OH)<sub>4</sub>(XY-hda)(en)<sub>4</sub>]. The iron centers are arranged as a sort of tetragonally compressed cube with each outer face in the figure consisting of four iron centers, three linked through a μ<sub>3</sub>-oxo with fourth center linked by a bridging hydroxide to one of these three centers. In addition, one of the carboxylate groups of the ligand bridges across the base of the face.

The ligand **L12** is commercially available. This ligand showed poor antitumor activity against leukemia P388 [78]. Some complexes of chromium were made with this ligand and the luminescence of them was observed in 1976 [79]. Also voltametric studies were made. Complexes with Co(II), Ni(II), Zn(II) and Mn(II) were synthesized in 1970 [80].

The ligand **L13** is a new ligand although similar molecules have been reported. The reagent 3-bis (carboxymethyl)aminomethyl-2-hydroxy-5-sulfobenzoic acid, the same ligand but with two iminodiacetic groups, was synthesized via the corresponding chloromethyl derivatives, in which Cl was replaced by the amine group in iminodiacetic acid. It is able to form a betaine structure with a proton attached to N and the dissociated sulfo-group. The stability constants of monoprotic and aprotic 1:1 complexes are: Mg(II), 8.2; Cu(II), 10.6, 15.8; Co(II), 7.8, 13.4; Ni(II), 8.3, 14.0; and Fe(III), 19.5, respectively. Co(II), Cu(II), Fe(III), and Al(III) hydroxides were prepared in the presence of a similar ligand to **L13** at pH 11.5, 11.5, 11.0, and 6-7, respectively.

Derivatives of **L13** were synthesized [81] and chelates compounds were formed with most metal ions, including a hexadentate complex with Fe(III). With ligand **L13** an interesting supramolecular structure incorporating Fe(III)dimers is observed.

Ligands **L4-L9** were commercially available and were purchased from Aldrich and Sigma or Lancaster and used as received. Ligands **L10-L13** were synthesized by Dr. J.P. Hill and Dr. W. Schmitt and ligands **L1-L3** were prepared as outlined in chapter 6.

## **Chapter Five: Results and Discussion**

Having a library of organic ligand synthons at hand the final steps in producing coordination compounds designed to explore supramolecular chemical effects are to combine these ligands with transition metal salts using various solvents and different bases, all three of which are capable of influencing the crystal architecture of the resulting compound.

Several factors affect the overall structure of the complexes resulting from the reaction between a coordinating species and a transition metal ion upon their mixing under ambient conditions at various pH values. Primarily, the ligand exerts the controlling effect by virtue of its substituents and degree of deprotonation in the presence of a particular base. However, this can be complicated by the possibility of the existence of oligonuclear transition metal species under basic conditions and especially in protic solvents. It is possible by careful selection of conditions to trap these oligonuclear and often metastable species if they are present in solution in reasonable yield. In this chapter the coordination complexes of various ligands are presented. Although, in this case, no more than dinuclear species were obtained it was shown that various type of ligands can form stable complexes with transition metal ions and that the substitution pattern of the ligand has a varying effect on the structure of the resulting coordination complex. In the extreme, the variation of the substitution pattern resulted not in a large oligonuclear species but in an extended network.

These principles are discussed in the following pages with reference to the crystal structures of the coordination compounds obtained with the thirteen ligands described in the previous chapter.

### 5.1 Structure of $[\text{CuBr}_2(\text{C}_{14}\text{H}_{16}\text{N}_4)]$ , **1**.

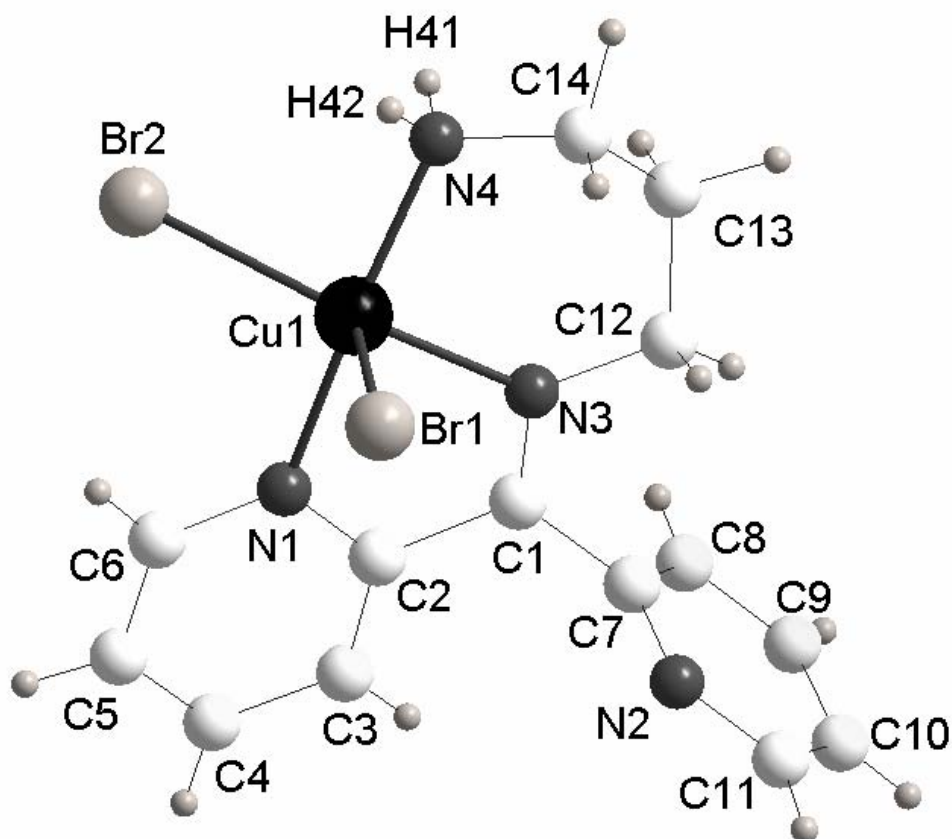


Fig. 10 Structure of the mononuclear complex  $[\text{CuBr}_2(\text{C}_{14}\text{H}_{16}\text{N}_4)]$ , **1**.

The Cu(II)-atom is coordinated in a square-based pyramidal geometry by 5 atoms, 3 nitrogen's and two Br atoms. The ligand forms a ring with the nitrogen atoms of the aliphatic arm and only the N from one of the pyridyl groups is coordinated to the metal.

The free nitrogen atom, N2, of the pyridyl group could actually coordinate to another metal-atom, but this is not the case. The protons of the N4 interact with a Br atom and a N2' atom. Although different metal-ligand-ratios (1:1 to 6:1) were tried out in order to form other compounds, it was not possible to add base, because the ligand would be destroyed by hydrolysis.

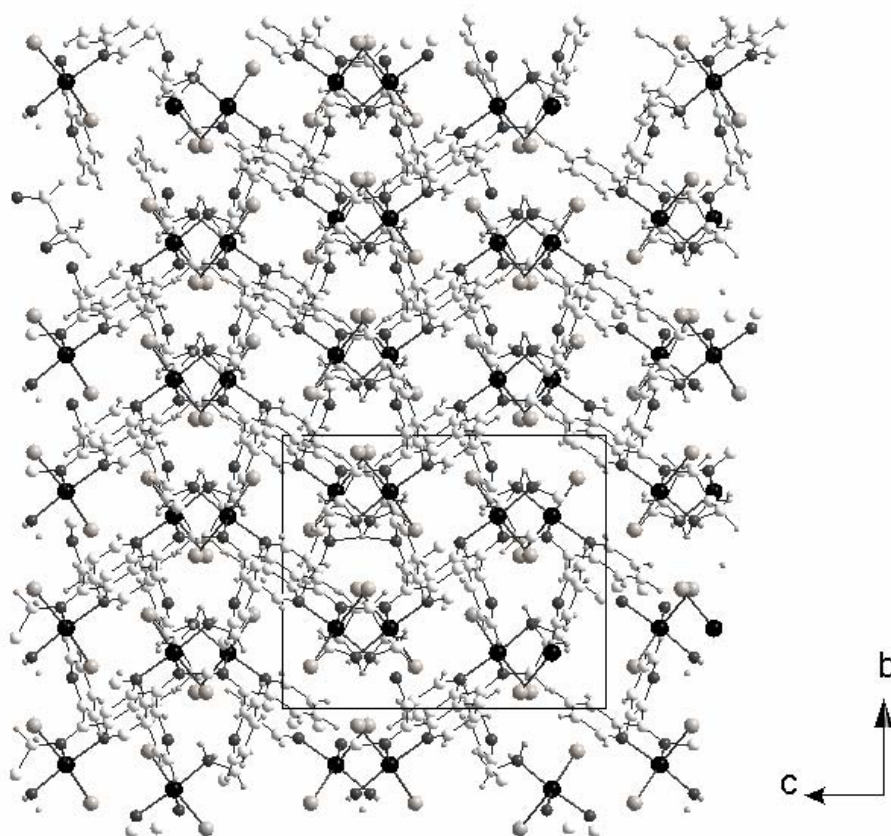
**Packing structure of  $[\text{CuBr}_2(\text{C}_{14}\text{H}_{16}\text{N}_4)]$ , 1.**

Fig. 11 View of the molecular packing  $[\text{CuBr}_2(\text{C}_{14}\text{H}_{16}\text{N}_4)]$  down the **a**-axis.

Figure 11 shows the view down the **a**-axis with isolated monomers, in which the copper atoms are ordered in pairs. In this view the pyridyl-groups appear to be a  $\pi$ - $\pi$ -stacked. It can be seen from figure 12 that the monomers from layers within the crystal structure.

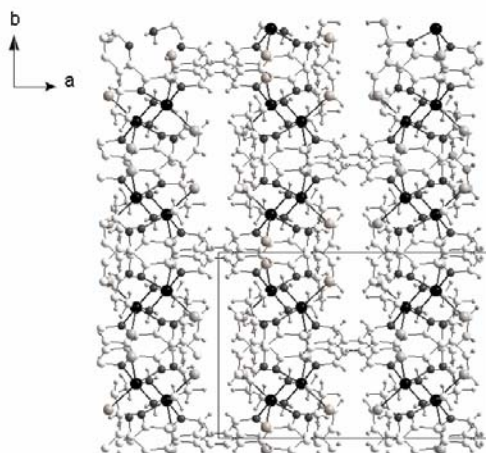


Fig. 12 View of the molecular packing  $[\text{CuBr}_2(\text{C}_{14}\text{H}_{16}\text{N}_4)]$  down the **c**-axis.

The shortest Cu...Cu displacement amounts to 7.477 Å. The view down the **c**-axis shows isolated monomers, which form a rectangular small cavity, ordered in sheets parallel in the **ab**-plane. The shortest Cu...Cu displacement amounts to 6.421 Å. The cavity has the horizontal distances of 5.638 Å and 11.609 Å and the vertical distance amounts to 12.303 Å. There is considerable current interest in the covalent and noncovalent syntheses of molecular cavities. Fujita and coworkers have synthesized three types of coordination polymers, which are formed together in one crystal, when a bifunctional ligand like 4,4' bipyridine is reacted with Cd(NO<sub>3</sub>)<sub>2</sub> in the presence of mesitylene or m-xylene or o-xylene. These molecules are also included in the crystal as guests. One type of polymer exists in a 2D-layer containing grids of 20×20 Å. The Cd atom has distorted octahedral geometry and exhibited no symmetry in coordination. The grid layers pack on each other such that there exist channels of dimensions ca. 10×20 Å with large interlayer separation of 10.9 Å [82].

## 5.2 Structure of [CuCl<sub>2</sub>(C<sub>14</sub>H<sub>16</sub>N<sub>4</sub>)]·H<sub>2</sub>O, **2**.

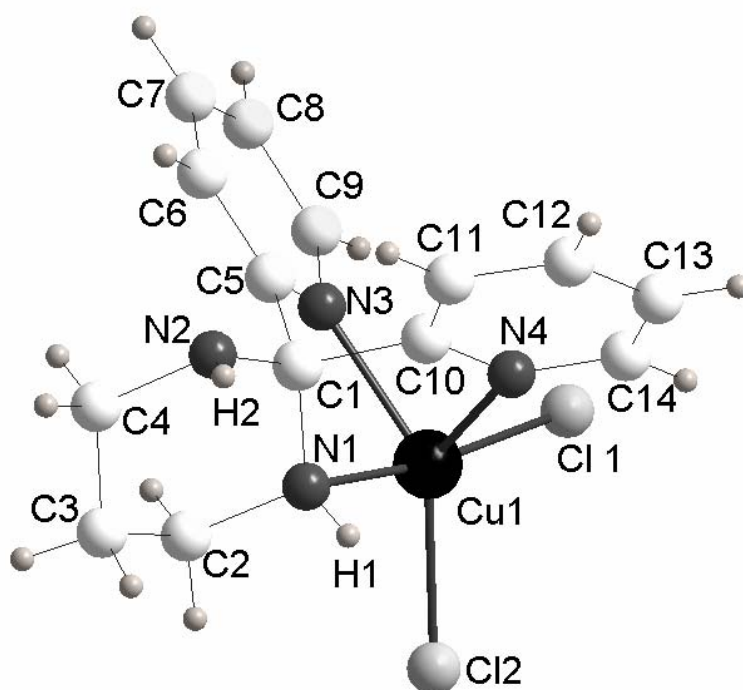
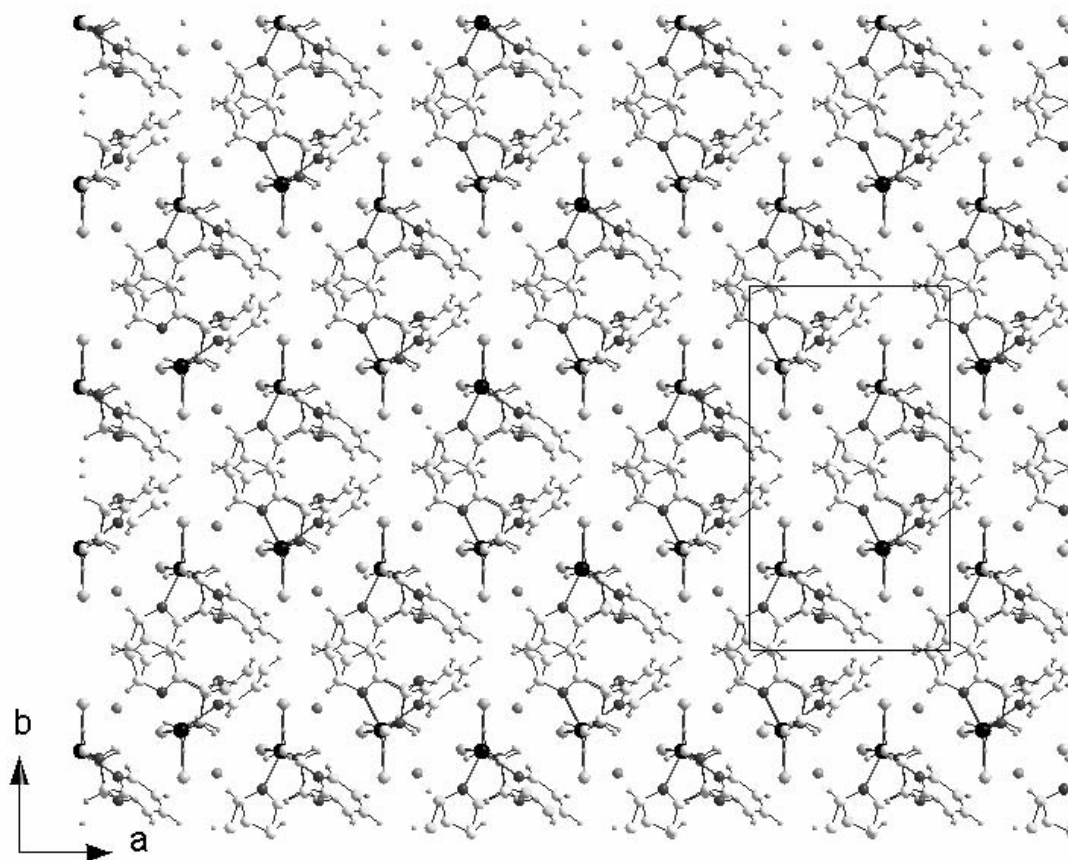


Fig. 13 Structure of the mononuclear complex [CuCl<sub>2</sub>(C<sub>14</sub>H<sub>16</sub>N<sub>4</sub>)]·H<sub>2</sub>O, **2**.

The asymmetric unit contains one mononuclear complex. The copper atom has a coordination of 5 atoms in a square bipyramid with  $\tau = 0.356$  and is coordinated with two chlorines and three nitrogen atoms. A method of assigning the geometrical nomenclature to distorted pentacoordinate complexes has been suggested and has been adopted in this work [83]. This formalism assigns a  $\tau$  value to the coordination geometry around the metal based upon the relationship:  $\tau = (\theta_1 - \theta_2)/60$ , where  $\theta_1$  the largest angle at the metal and  $\theta_2$  the second largest angle. In the case of an ideal square-based pyramidal system these would both be  $180^\circ$ , so  $\tau$  would be zero. For a perfect trigonal bipyramid base system  $\theta_1$  and  $\theta_2$  would be  $180^\circ$  and  $120^\circ$ , so  $\tau$  would be 1. Intermediate cases, as are always seen in reality, can therefore be assigned to one of the two systems by calculating  $\tau$  and seeing idealized situation it tends towards. Two nitrogen atoms of the coordination sphere of the metal come from the pyridyl-rings; a nitrogen atom N1 is still protonated and closes the ring. N2 is sterically inhibited from coordinating to a further metal center. If N1 could be deprotonated then perhaps it could bridge to a second Cu(II) ion. If these N-atoms could be deprotonated a higher coordination could be achieved. The perpendicular position of the pyridyl-rings is not favorable for  $\pi$ - $\pi$  stacking. The NH-group can make a H-bond with the chlorine building a weak dimer-unit with adjacent complexes, forming chains parallel to the a-axis. Although no base was used in the reaction, to inhibit solvolysis at the ligand, nevertheless the ligand itself has undergone intramolecular cyclization, with the terminal amino group attacking the Schiff base nucleophilically to give a six-membered ring. Different ligand-metal-ratios (1:1 to 1:6) were tried out.

A similar type of ligand cyclization can be possible with a vanadium complex of a Schiff-base. This reaction is a catalytic oxidation of the ligand by oxygen of the air [84].



Structure packing of  $[\text{CuCl}_2(\text{C}_{14}\text{H}_{16}\text{N}_4)] \cdot \text{H}_2\text{O}$ , 2.Fig. 14 View of the molecular packing  $[\text{CuCl}_2(\text{C}_{14}\text{H}_{16}\text{N}_4)] \cdot \text{H}_2\text{O}$  down the **c**-axis.

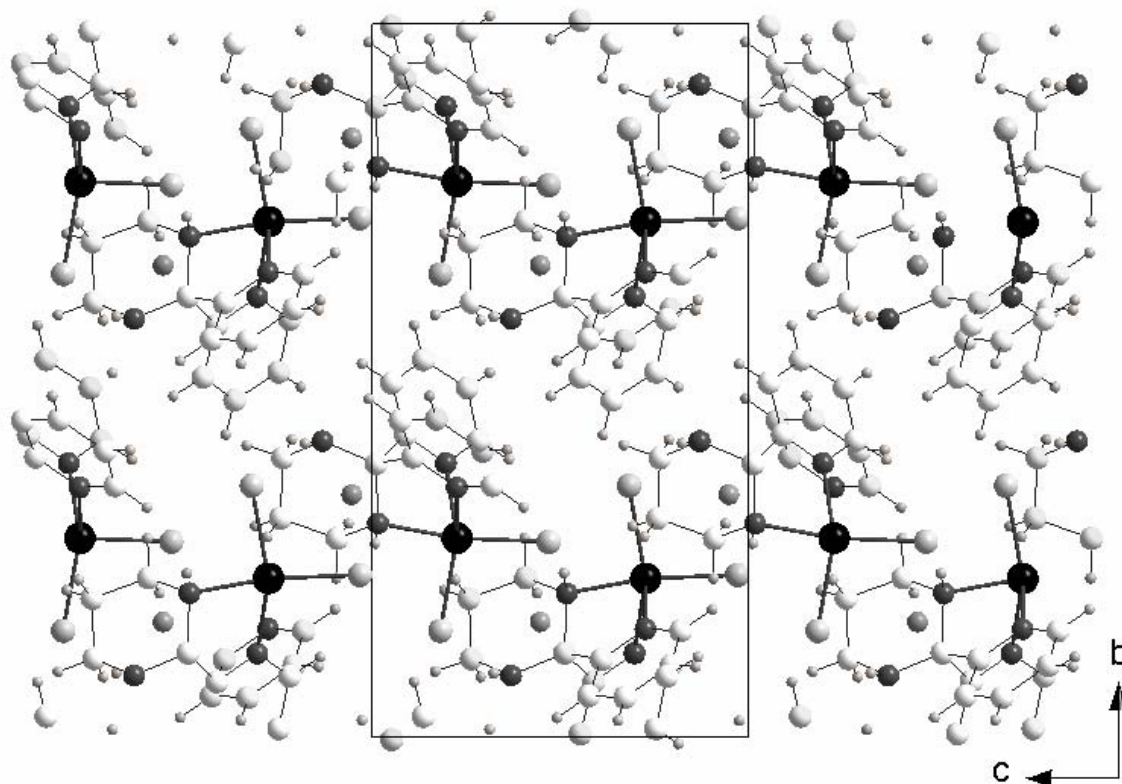


Fig. 15 View of the molecular packing  $[\text{CuCl}_2(\text{C}_{14}\text{H}_{16}\text{N}_4)] \cdot \text{H}_2\text{O}$  viewed down the **a**-axis.

The packing down the **a**-axis shows isolated monomers, in which the Cu atoms are ordered in zigzag strings. The shortest Cu...Cu displacement amounts to 5.893 Å. The copper atoms are in a zigzag-row, but they are not linked through covalent chemical bonds, and also not linked by H-bonding, because the Cl...HN distance amounts to 7.733 Å. The figure down of the **b**-axis looks like a helix going to the left, nevertheless it shows isolated monomers, which are ordered in a row. The Cu...Cu displacement within the row amount to 10.009 Å and the next Cu-atom lies diagonally across at a distance of 5.893 Å. The view along the **c**-axis shows copper atoms, which are ordered in pairs. The copper atoms are at the corners of a cavity and have a Cu...Cu distance of 9.065 Å and from a cavity diagonally to the next cavity of 5.893 Å. These cavities are 9.065Å high and 8.831Å wide.

There is considerable current interest in the covalent and noncovalent syntheses of molecular cages and capsules [85]. An intriguing feature of such hollow molecules is that they can regulate the reactivity and stability of molecules, which are accommodated in their cavities [86]. Hence if the size and shape of the cavity are rationally and precisely designed, chemical

transformations can be suitably controlled by the cavity. Large hollow molecules have been efficiently prepared by transition metal-mediated self-assembly. For example with Pd(II) and Pt(II) with pyridine and or pyrimidine based bridging ligands leads to the quantitative self-assembly of nanometer-sized hollow structures such as these cages. Fujita and coworkers have found that coordination cages can promote polycondensation of trialkoxysilanes within its cavity giving all *cis*-isomers of cyclic trimers in a “ship in a bottle fashion” [87]. Another example of nanocages is the self-assembled cage with Pd(II) and pyridyl derivatives, which promote the aerobic, aqueous oxidation of styrene and its derivatives in a Wacker oxidation.[88].

### 5.3 Structure of $[\text{Cu}(\text{C}_{14}\text{H}_{16}\text{N}_4)_2]\text{Br}_2 \cdot 2\text{MeOH}$ , **3**.

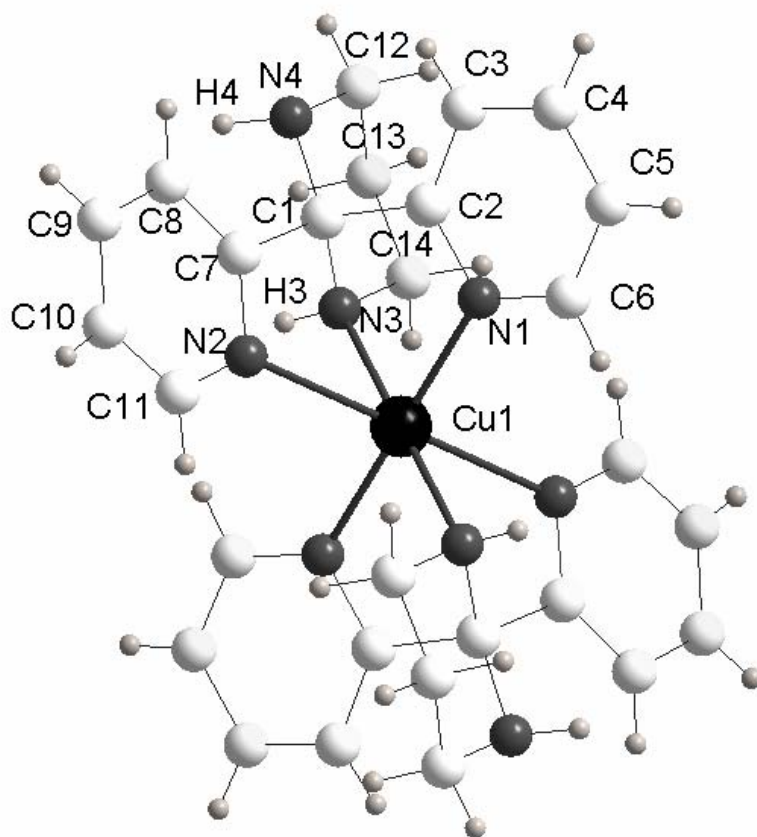


Fig. 16 Structure of the mononuclear complex  $[\text{Cu}(\text{C}_{14}\text{H}_{16}\text{N}_4)_2]\text{Br}_2 \cdot 2\text{MeOH}$ , **3**.

The asymmetric unit contains half of a monomeric complex. The Cu-atom is coordinated with 6 nitrogens with a Jahn-Teller-elongation across N2-Cu-N2'. Again no base was added,

because the ligand would be destroyed by hydrolysis. In this complex the same cyclized ligand as in **2** has been formed. In **3**, however, two such ligands coordinate to the Cu(II) ion, which lies on an inversion center in the crystal lattice. Different ligand-metal-ratios (1:1 to 1:6) were tried out. With  $[\text{CuCl}_2(\text{C}_{14}\text{H}_{16}\text{N}_4)]\cdot\text{H}_2\text{O}$  **2** a mole ratio metal:ligand (1:1) was used as in  $[\text{CuBr}_2(\text{C}_{14}\text{H}_{16}\text{N}_4)]$  **1**, and other metal salts and solvents were tried out. It is interesting then to compare  $[\text{CuCl}_2(\text{C}_{14}\text{H}_{16}\text{N}_4)]\cdot\text{H}_2\text{O}$  **2** and  $[\text{CuBr}_2(\text{C}_{14}\text{H}_{16}\text{N}_4)]$  **1** and find that in this case the solvent and mole ratio has no big influence on the formation of different compounds.

In the  $[\text{Cu}(\text{C}_{14}\text{H}_{16}\text{N}_4)_2]\text{Br}_2\cdot 2\text{H}_2\text{O}\cdot 2\text{MeOH}$  **3** a 10:1 ligand:metal ratio was used, compared to a 1:1 for  $[\text{CuCl}_2(\text{C}_{14}\text{H}_{16}\text{N}_4)]\cdot\text{H}_2\text{O}$  **2**. This shows, that the excess at ligand is insignificant in this synthesis, because similar monomers were obtained in both cases.

#### Structure packing of $[\text{Cu}(\text{C}_{14}\text{H}_{16}\text{N}_4)_2]\text{Br}_2\cdot 2\text{MeOH}$ , **3**.

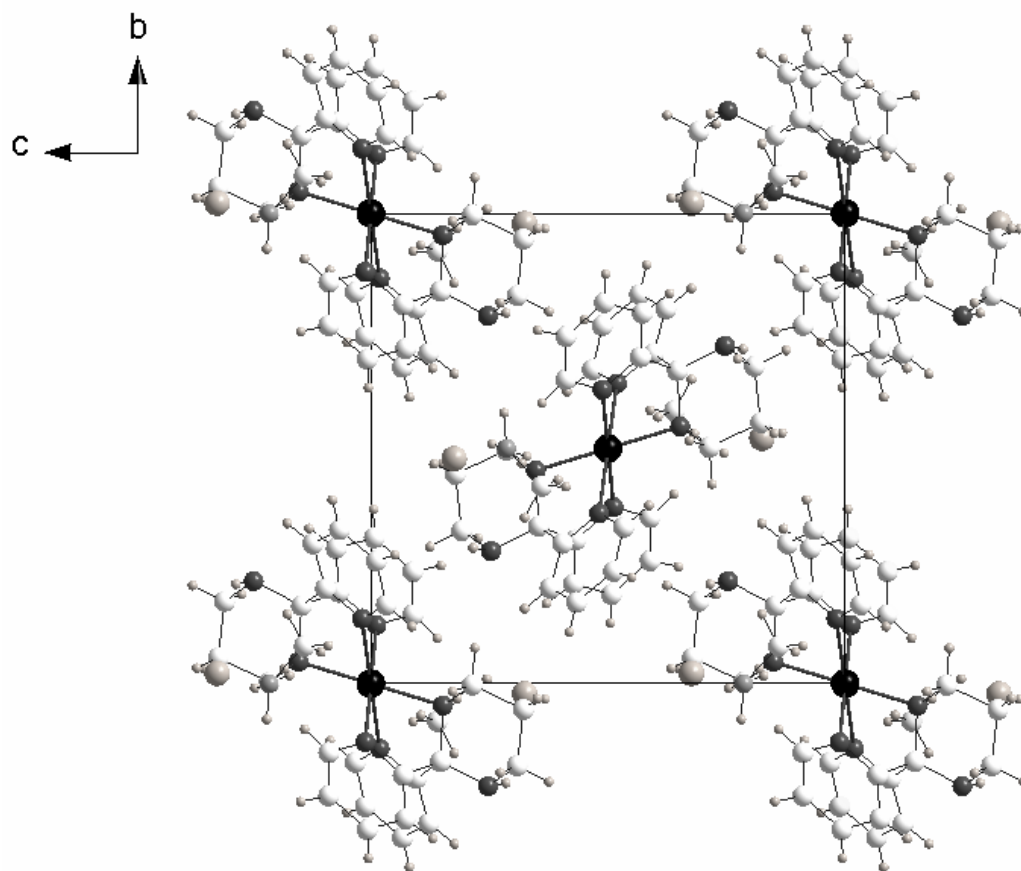


Fig. 17 View of the molecular packing  $[\text{Cu}(\text{C}_{14}\text{H}_{16}\text{N}_4)_2]\text{Br}_2\cdot 2\text{MeOH}$  down the **a**-axis.

The view along the **a**-axis shows isolated monomers. The two ligands form an organic “shell” around the Cu (II) centers, isolating them. The ligand is like a “daisy” surrounding the metal. The view down the **b**-axis also shows these isolated monomers. The shortest Cu-Cu-displacement amounts to 9.122Å. The Cu atoms are ordered vertically in rows. Between the rows are the Bromide counterions and methanol molecules. The view down the **c**-axis again shows isolated monomers. The copper atoms are coordinated in an octahedral arrangement of nitrogen atoms.

#### 5.4 Structure of $[\text{CuCl}_2(\text{C}_{12}\text{H}_{12}\text{N}_2\text{O}_2)]$ , **4**

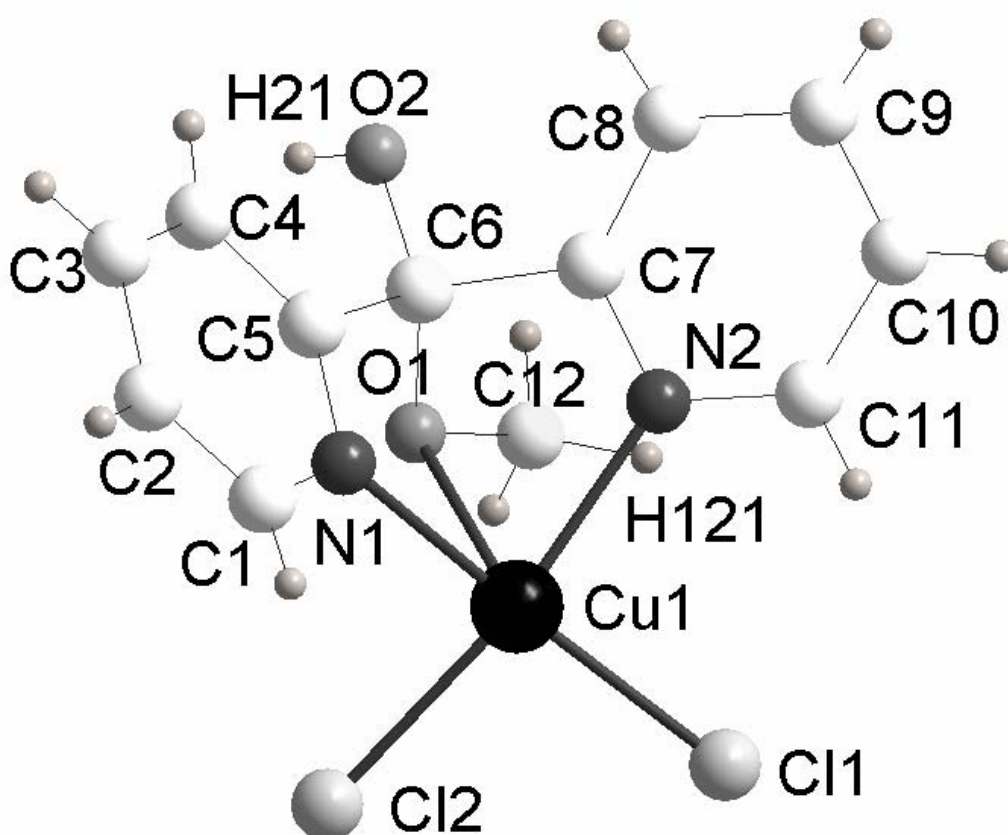


Fig. 18 Structure of the mononuclear complex  $[\text{CuCl}_2(\text{C}_{12}\text{H}_{12}\text{N}_2\text{O}_2)]$ , **4**.

The formation of **4** shows the high sensitivity of the ligand to solvolysis. This complex was previously synthesised and structurally characterised with the reaction of  $\text{CuCl}_2$  and dipyridylketone (dpk) in methanol, but in this case the compound crystallises with a different cell [89].

Another dpk compound was isolated, which was previously reported [90]. The ligand **L1** has hydrolyzed forming a copper-dimer with dipyridylketone. The water molecules present in the metal salts were responsible for this hydrolysis.

The ring-formation in the cases of **1**, **2**, **3** and **4** depends on the coordination mode and on which N-nucleophile of the ligand coordinates first to the Cu(II). There are two routes to coordination, (I) and (II) given in figure 19. If the NH<sub>2</sub> coordinates first, it is no longer a nucleophile, and the Schiff base can coordinate, forming the chelated structure in **1** with a 6-membered ring. If the Schiff-base N coordinates first, the C=N double bond will then be even more activated towards nucleophilic attack, and the free-NH<sub>2</sub> can attack intramolecularly, giving a favorable 5-membered ring as in **2** and **3**. If the nucleophile is methanol then **4** forms.

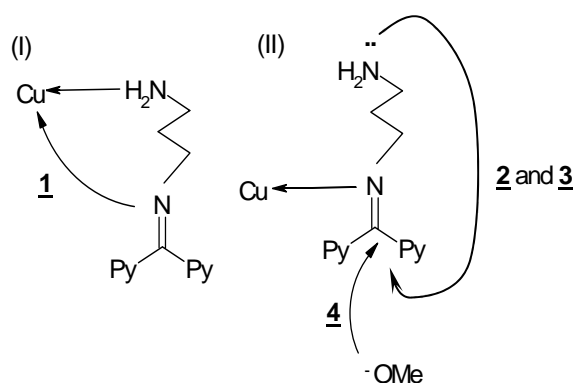


Fig. 19 Proposed reaction mechanisms in the formation of complexes **1** to **4**.

### 5.5 Structure of $[\text{Cu}_2\text{Cl}_4(1,3\text{-dipyridylpropane})_2]\cdot\text{H}_2\text{O}$ , **5**.

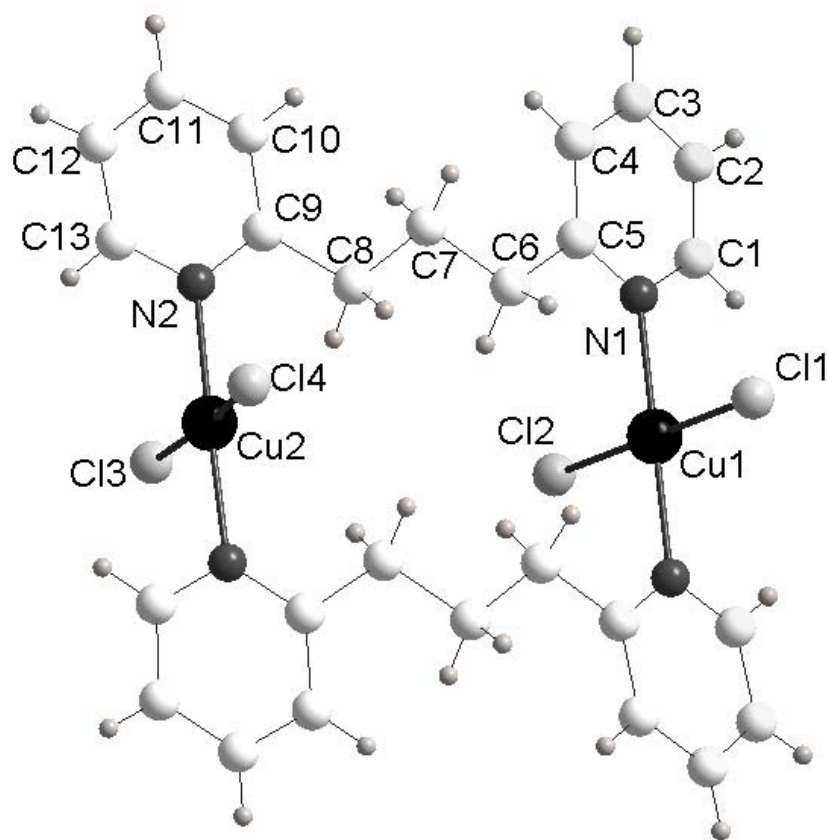


Fig. 20 Structure of the dinuclear complex  $[\text{Cu}_2\text{Cl}_4(1,3\text{-dipyridylpropane})_2]\cdot\text{H}_2\text{O}$ , **5**.

Cu1 and Cu2 are both four coordinate, with *trans* square planar geometries. Two pyridine nitrogens from different ligands and two chloride ions make up the coordination sphere. Although **5** is structurally a dimer, there is no magnetic pathway between the Cu(II) centers and the Cu...Cu separation is 7.299 Å, so magnetically we have isolated Cu(II) centers. This complex has been previously reported by Spodine et al, but as the anhydrous form with a different crystal structure [91].

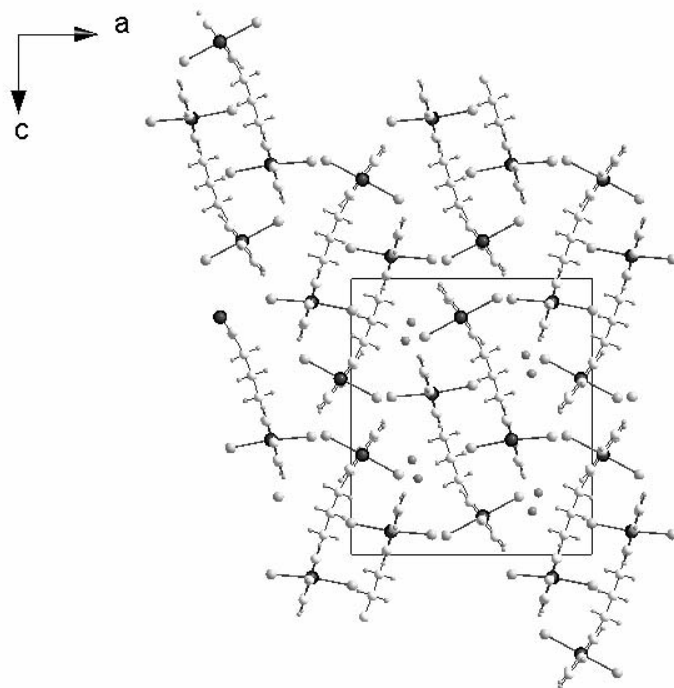
**Structure packing of  $[\text{Cu}_2\text{Cl}_4(1,3\text{-dipyridylpropane})_2]\cdot\text{H}_2\text{O}$ , 5.**

Fig. 21 View of the packing  $[\text{Cu}_2\text{Cl}_4(1,3\text{-dipyridylpropane})_2]\cdot\text{H}_2\text{O}$  viewed the **b**-axis.

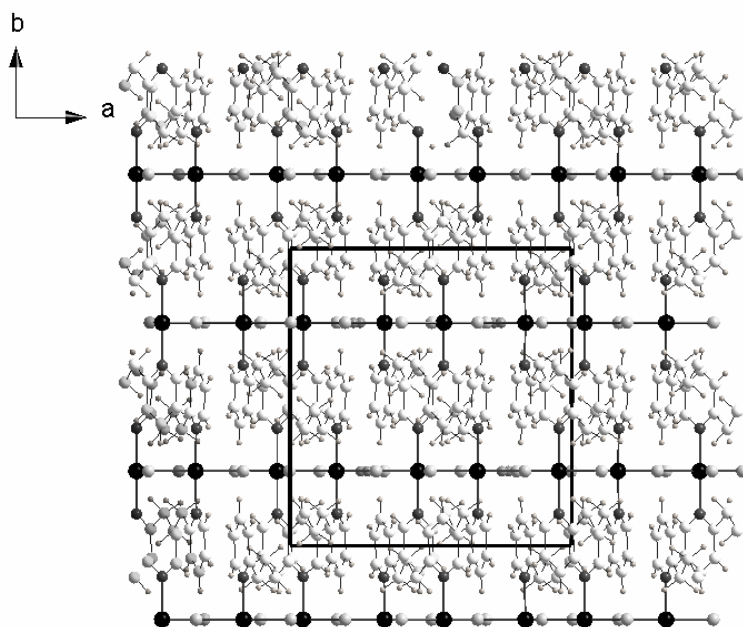


Fig. 22 View of the molecular packing  $[\text{Cu}_2\text{Cl}_4(1,3\text{-dipyridylpropane})_2]\cdot\text{H}_2\text{O}$  down the **c**-axis.



The Cu and Cl atoms lie on the crystal mirror plane perpendicular to the **b**-axis (see figure 12), which relates the two ligands in the complex. This can be seen clearly, when the packing is viewed along the **c**-axis, with alternating layers of inorganic Cu and Cl atoms and of organic ligand. Viewed down the **b**-axis, the packing within the layers seems rather irregular. Although there is an intermolecular Cu...Cu distance of 5.098 Å between the dimers in the same layer. This distance is still at the limit of magnetic interactions.

The figure from the view of the **b**-axis shows isolated monomers. The figure consists of disorganized dimers, in which the ligand is stretched out like a “worm”.

### 5.6 Structure of $[\text{Cu}_2(\text{OAc})_4(\text{C}_4\text{H}_4\text{N}_3\text{Br})]_\infty$ , 6.

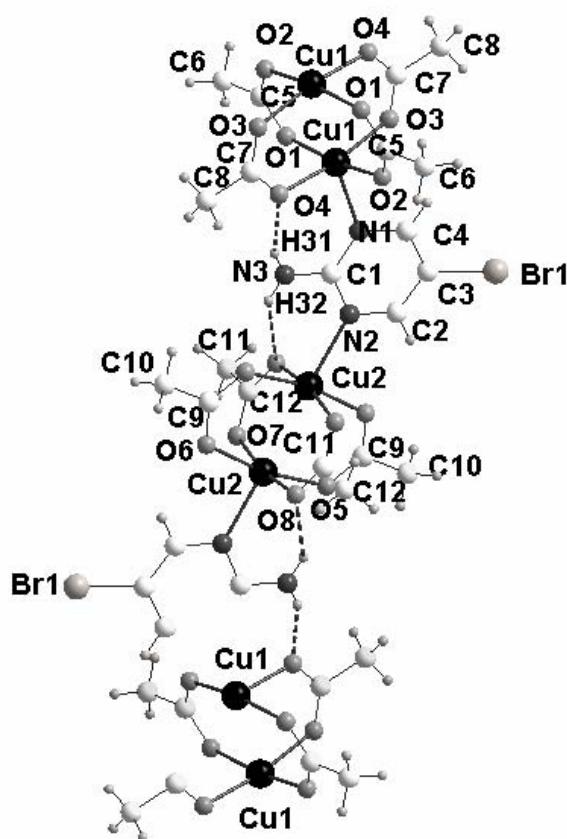


Fig. 23 Structure of the infinite complex  $[\text{Cu}_2(\text{OAc})_4(\text{C}_4\text{H}_4\text{N}_3\text{Br})]_\infty$ , 6.

This compound is a coordination polymer. The ligand **L4** was used as a building block in the structure, although working in acidic medium. The chromium was not included in the structure although Cr(III) and Cu(II) were present in the reaction solution in a ratio 4.15 :1.

The Cu has a coordination sphere of 5 atoms and the resulting polymer, which consists of Cu-acetate-dimers, which are alternate with the ligand **L4**. Smith and Graham [92] have synthesized the same polymer, but without bromine in the ligand molecule.

**Structure packing of  $[\text{Cu}_2(\text{OAc})_4(\text{C}_4\text{H}_4\text{N}_3\text{Br})]_\infty$ , **6**.**

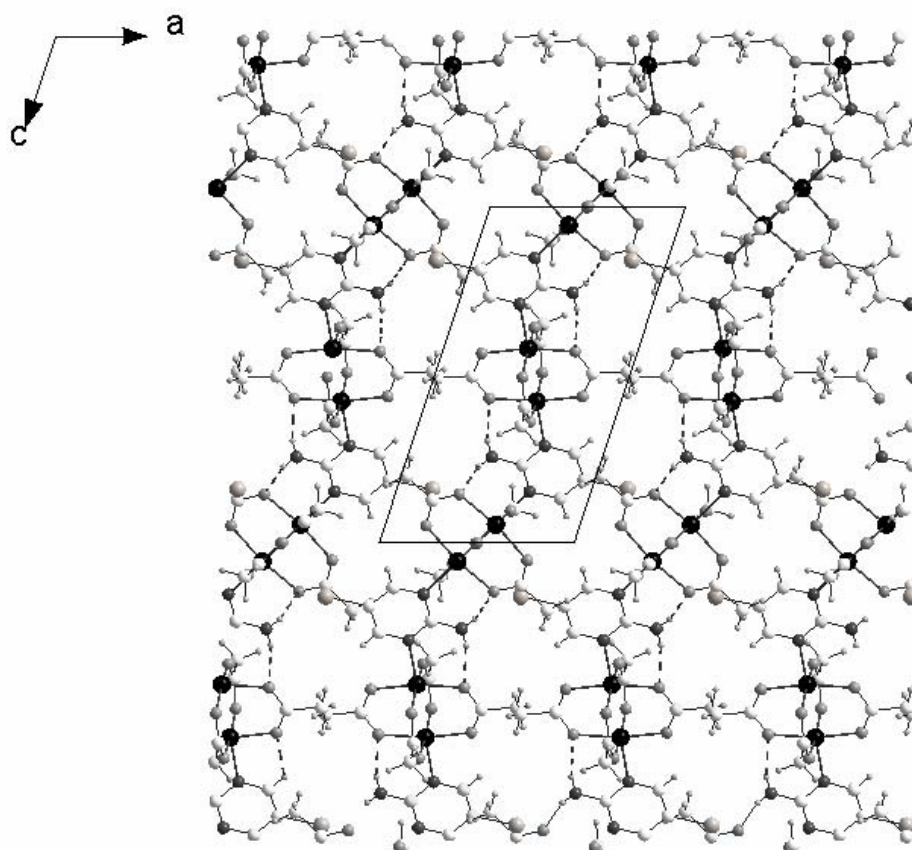


Fig. 24 View of the molecular packing in  $[\text{Cu}_2(\text{OAc})_4(\text{C}_4\text{H}_4\text{N}_3\text{Br})]_\infty$  down the **b**-axis.

The view down the **b**-axis shows the polymer chains side by side, propagating along the **c**-axis. The polymer chains are isolated and curve through the structure. The nitrogens of the ligand provide the terminal ligation for the Cu(II) centers in the classic copper(II) acetate structure. The 1,3-geometry of the nitrogens in the aromatic ring leads to the zigzag curve in the chain. The amine group is not coordinated, but forms hydrogen bonds to acetate oxygens. Alternate Cu-acetate dimers in the chain are crystallographically distinct, but similar structurally, and Cu1...Cu1 amounts to 2.601 Å and Cu2 to Cu2 amounts to 2.619 Å. The separation between Cu1 and Cu2 linked through the organic ligand is 6.453 Å. In Smith's polymer the Cu...Cu separation in the dimers is always the same and it amounts to 2.633 Å.

There is no significant inter-chain hydrogen bonding interactions, although intra-chain associations between the amine nitrogen of the 2-aminopyrimidine and the carboxyl oxygens of the dimer give rigidity to the polymer. In the case of **6** these H-bonds amount to 2.0 and 2.1 Å. In all three directions, polymer chains were observed. In the compound **6**, a polymer, and in the compound **9** a mixed-metal-chain could be obtained, the asymmetric unit is essentially the same and the structure packing consists of parallel zigzag polymer chains, in both cases the chloride of **9** is replaced by the ligand in **6** and the Mn-water-unit in **9** is replaced by a Cu-acetate-unit in **6**.

### 5.6.1 Magnetic properties of **6**

The common way to judge the qualitative magnetic interaction of a compound is to plot  $\chi^*T$  versus  $T$ . For  $J = 0$ ,  $\chi^*T$  is constant and equal to  $Ng^2\beta^2/2k$ , following the spin-only-formula [44]. For  $J > 0$ ,  $\chi^*T$  decreases with higher Temperature and is close to  $Ng^2\beta^2/2k$  at room temperature. For  $J < 0$ ,  $\chi^*T$  increases continuously with higher Temperature and decreases upon cooling; also is close to  $Ng^2\beta^2/2k$  near room temperature like it is shown in the figure 25.

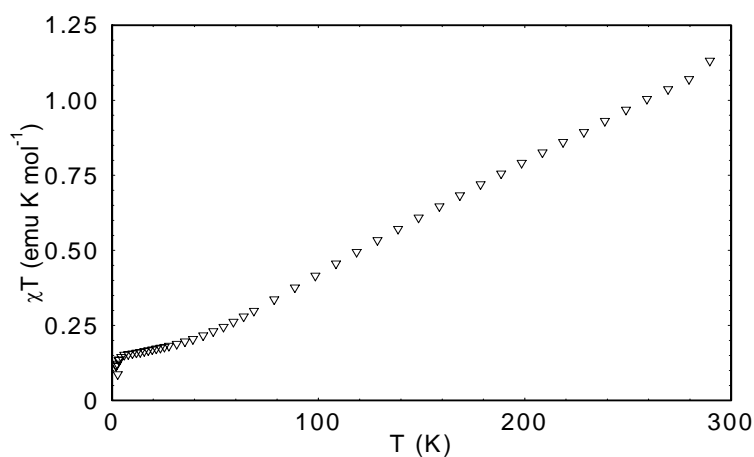


Fig. 25 The  $\chi T$  versus  $T$  plot for  $[\text{Cu}_2(\text{OAc})_4(\text{C}_4\text{H}_4\text{N}_3\text{Br})]_\infty$ , **6**.

The curve shown in figure 25 has a strong antiferromagnetic coupling of the Cu centers leading to a diamagnetic ground state, and was measured at the University of Florence. This behavior is well documented for  $[\text{Cu}_2(\text{OAc})_4\text{L}_2]$  systems in the book of Olivier Kahn [44], where values of  $J = -100 \text{ cm}^{-1}$  are expected. The curve has an intensive decrease between 0 K and 10 K, which indicates another antiferromagnetic coupling between others Cu-center units.

For this curve between 10 K and 300 K a value of 1.5 K\* $\mu_B$ /mol/emu is expected from the spin-only formula using a 4 Cu(II) centered unit. The sample was measured at 10000 Oe.

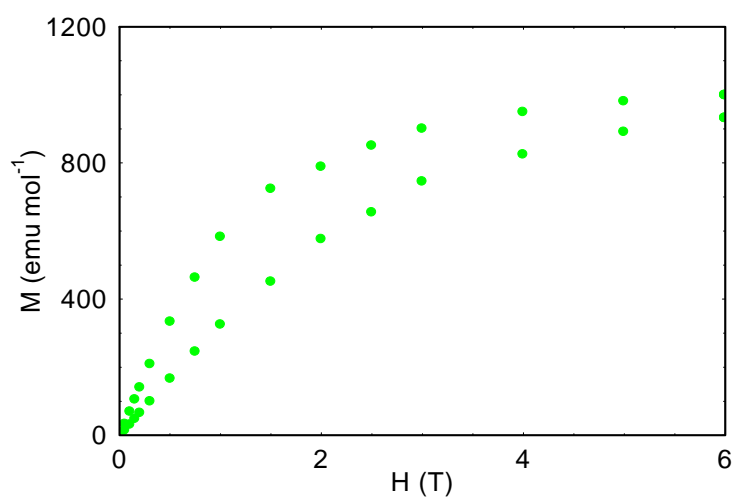
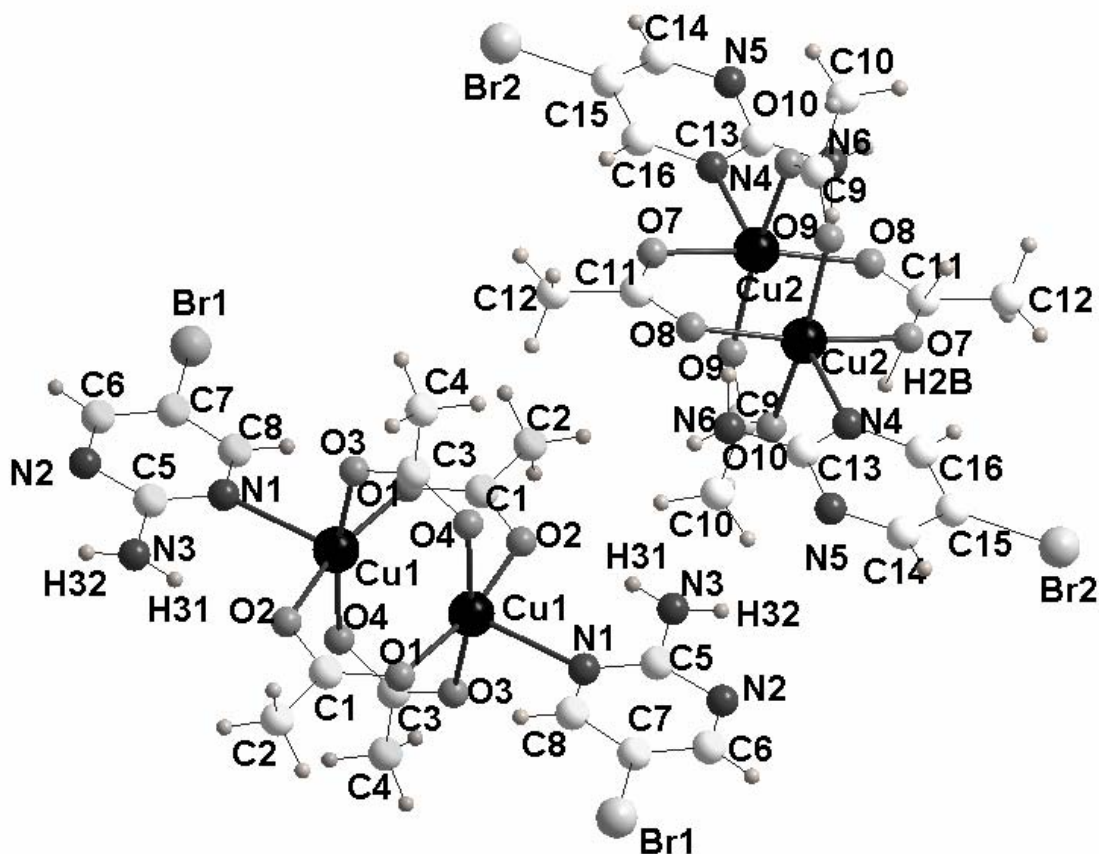
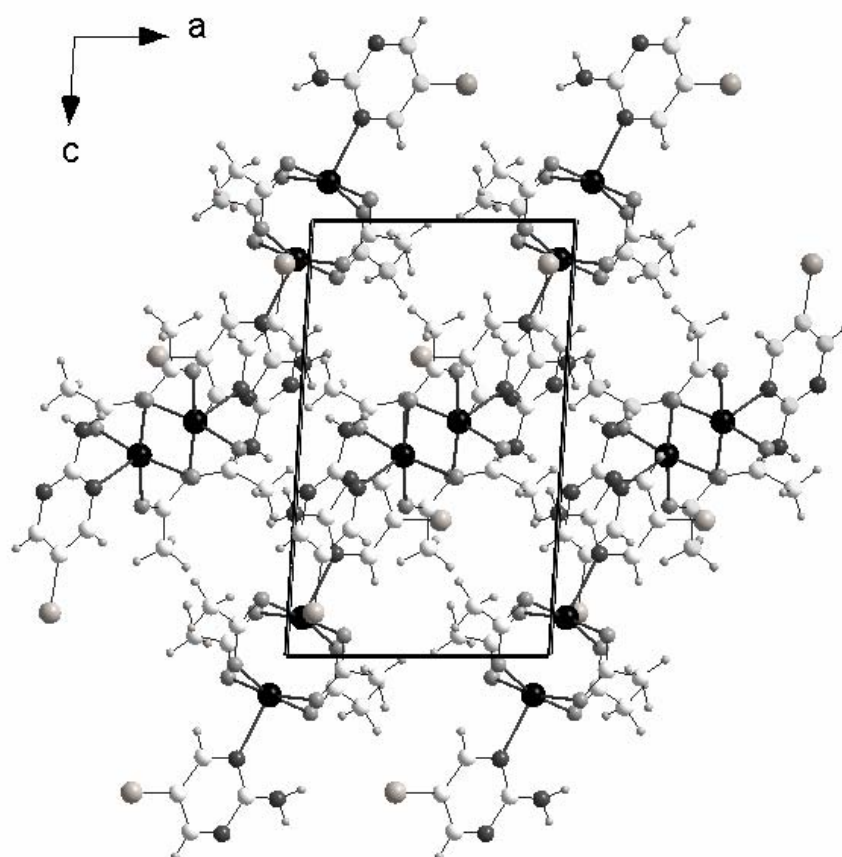
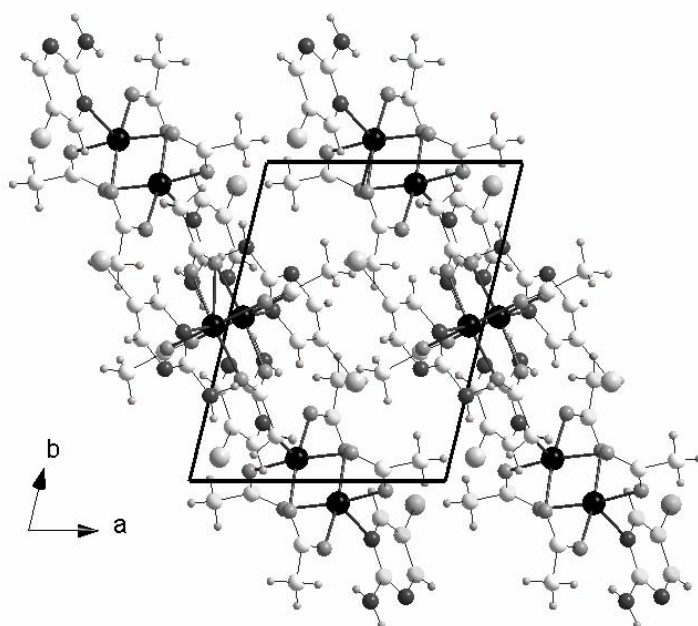


Fig. 26 The magnetization versus magnetic field H for  $[\text{Cu}_2(\text{OAc})_4(\text{C}_4\text{H}_4\text{N}_3\text{Br})]_\infty$ , **6**.

The magnetization of **6** versus H, as shown in figure 26, has saturation for 2K and 4K respectively for each curve between 900 and 1000  $\text{emu}\cdot\text{mol}^{-1}$ . This is a typical magnetization value for antiferromagnetic compounds.

5.7 Structure of  $[\text{Cu}_2(\text{OAc})_4(\text{C}_4\text{H}_4\text{N}_3\text{Br})_2]$ , **7**.Fig. 27 Structure of the dinuclear complex  $[\text{Cu}_2(\text{OAc})_4(\text{C}_4\text{H}_4\text{N}_3\text{Br})_2]$ , **7**.

Compound **7** is an example of the well studied dinuclear Cu-acetate complexes. This resulted from attempts to include  $\text{Ni}^{2+}$  in a mixed metal structure and as in **6** the ligand **L4** is incorporated as the terminal ligand in the copper(II) acetate structure without  $\text{Ni}^{2+}$  being included. Acetates enter a bond only with copper and chromium [93]. There are 4 Cu-atoms in the asymmetric unit of compound **6** and **7**. The Cu1-Cu1-distance in the asymmetric unit of **7** amounts to 2.625 Å and the Cu2-Cu2-displacement in the asymmetric unit of **7** amounts to 2.640 Å. This compound should have similar magnetic properties to other well-known Cu-acetate structures.

Structure packing of  $[\text{Cu}_2(\text{OAc})_4(\text{C}_4\text{H}_4\text{N}_3\text{Br})_2]$ , **7**.Fig. 28 View of the molecular packing in  $[\text{Cu}_2(\text{OAc})_4(\text{C}_4\text{H}_4\text{N}_3\text{Br})_2]$  down the **b**-axis.Fig. 29 View of the molecular packing in  $[\text{Cu}_2(\text{OAc})_4(\text{C}_4\text{H}_4\text{N}_3\text{Br})_2]$  down the view **c**-axis.

The views down the **a**, **b**, and **c**-axes show the isolated monomers, which are ordered in rows. Compound **6** and **7** result from attempts to create mixed metal species and it is interesting to note that with Cr(III) present a polymeric structure results whereas with Ni(II) isolated dimers are produced.

Morosin and Hughes have investigated the crystal structure of pyrazine copper acetate. It is a binuclear copper acetate system in which the Cu-Cu-separation in the triplet state has been estimated to be 0.12 Å longer than that in the singlet state. The Cu...Cu separation amounts to 2.583 Å and is significantly shorter than those found in similar dimer compounds. This structure is a linear chain. An EPR study has been carried out with this structure [95].

Evans et al reported a Cu-acetate-pyridine complex, which surprisingly doesn't build Cu-acetate dimers. The Cu(II) has a typical square-pyramidal sphere with two O-atoms of the acetate in *trans* position and 3 nitrogen atoms of three pyridine molecules [94]. Cu-acetate-complexes have important uses such as the regioselective o-hydroxylation of L-tyrosine to L-dopa on encapsulation in molecular sieves Y, MCM-22, and VPI-5 using atmospheric oxygen as oxidant [96]. Over the past 25 years extensive work on dimeric copper(II) carboxylates employing spectroscopic, magnetic and X-ray crystallographic techniques has been reported [97].  $\text{Cu}_2(\text{OCOCH}_3)_4 \cdot 2\text{H}_2\text{O}$  is the typical dimer unit which typically produces a chain-like structure [98].

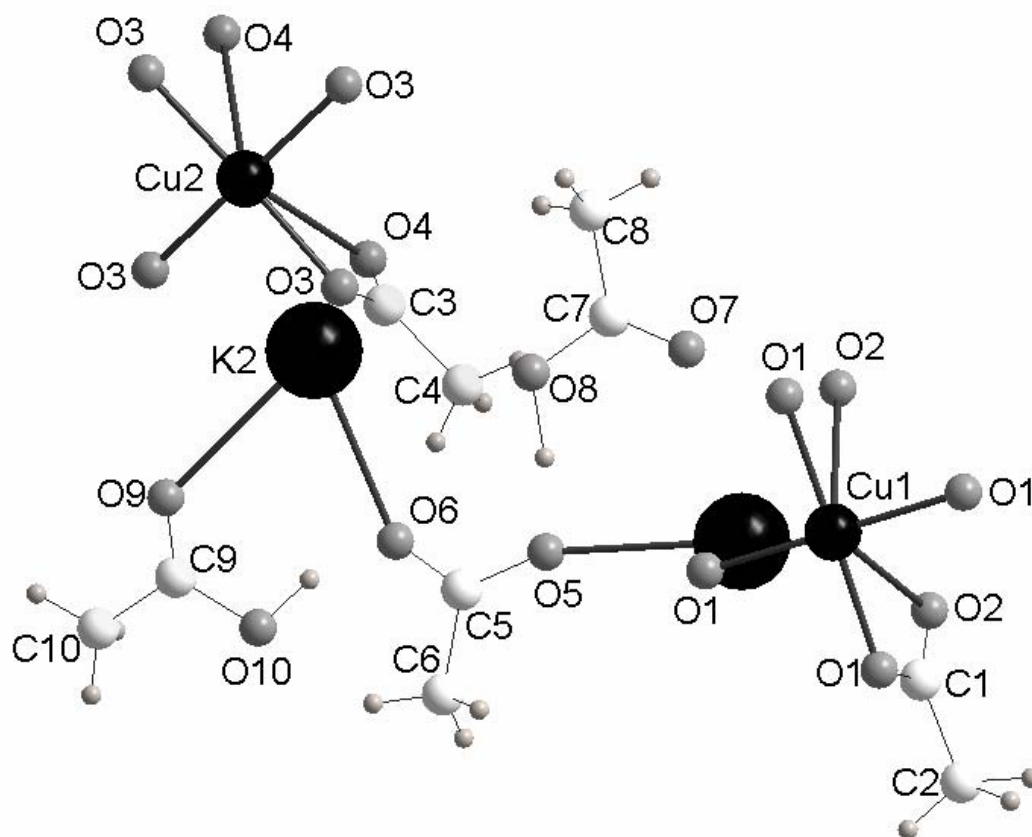
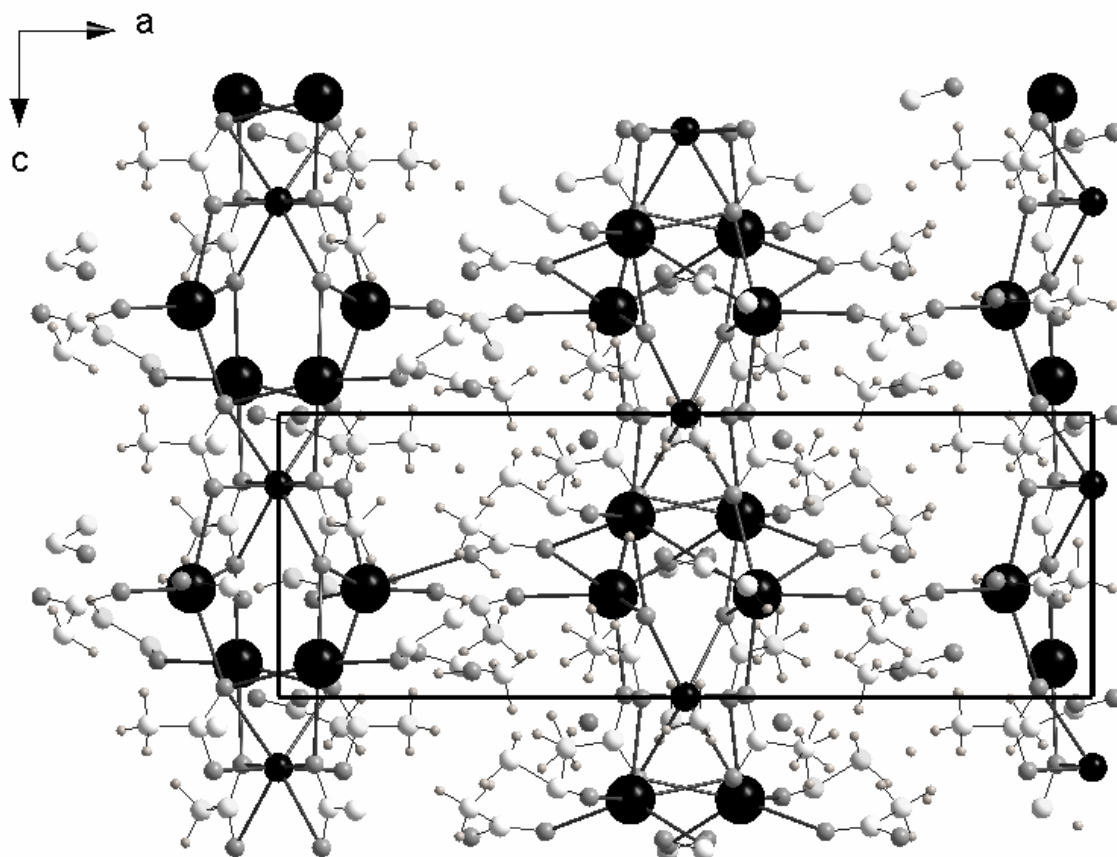
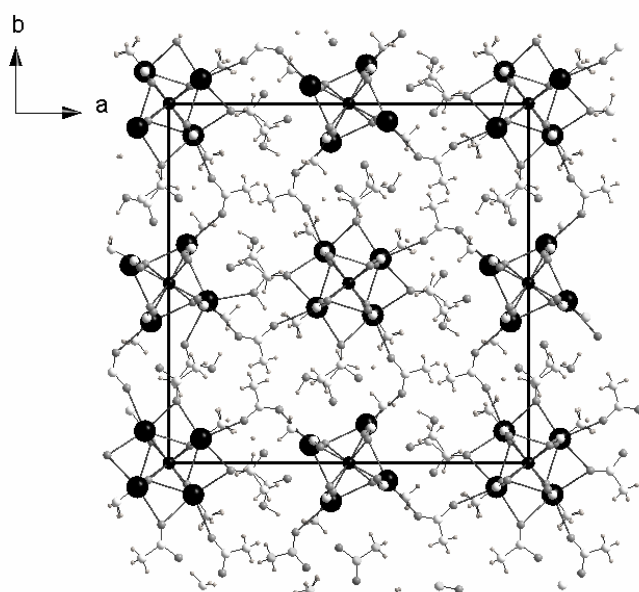
**5.8 Structure of  $K_4[Cu(OAc)_6(HOAc)_4]$ , **8**.**

Fig. 30 Structure of the infinite complex  $K_4[Cu(OAc)_6(HOAc)_4]_{\infty}$ , **8**.

This compound resulted from attempts to isolate a mixed  $Cu^{2+}/Ni^{2+}$  compound in the presence of **L10**. The protonated ligand is also present. The asymmetric unit contains two Cu-atoms, which are connected with acetate ligands to potassium ions.



Structure packing of  $K_4[Cu(OAc)_6(HOAc)_4]_{\infty}$ , **8**.Fig. 30 View of the molecular packing in  $K_4[Cu(OAc)_6(HOAc)_4]_{\infty}$  down the **b**-axis.Fig. 31 View of the molecular packing in  $K_4[Cu(OAc)_6(HOAc)_4]_{\infty}$  along the **c**-axis.

The view down the **a**- and **b**-axes are similar with chains in two directions. For the **b**-axis there is only one Cu-center between the potassium atoms instead of the two in the view down of the **a**-axis. The Cu-atoms are joined vertically through linking potassium atoms and horizontally the acetate groups connect the Cu-chains. The shortest Cu...Cu displacement amounts to 10.830 Å. The view down of the **c**-axis shows a network structure. Here we see how 4 K<sup>+</sup> atoms, which are connected through acetate in two directions, surround the Cu-monomers.

Another interesting feature of this compound is that the acetate coordinates to both Cu(1) and Cu(2) in a bidentate chelating mode (Figure 18) as well as serving to link copper centers to potassium counterions in a *syn,syn* fashion. The protonated ligand is also important in linking the metal ions together (figures 30 and 31).

A Cu<sub>6</sub>-acetate cluster could be synthesized mixing Bi(OCMe<sub>3</sub>)<sub>3</sub> with [Cu(O<sub>2</sub>CMe)<sub>2</sub>]<sub>2</sub> in THF [94]. The bismuth was not incorporated into the structure Cu<sub>6</sub>(μ-O<sub>2</sub>CCH<sub>3</sub>)<sub>4</sub>(μ<sub>4</sub>-O<sub>2</sub>CCH<sub>3</sub>)<sub>2</sub>(μ-OCMe<sub>3</sub>)<sub>6</sub>. The six copper atoms are planar in a hexagon with Cu...Cu distances of 2.989, 3.027, and 3.073 Å.

Also crystal structures of isomorphous prototypic oxo-centered trinuclear complexes [Cr<sub>3</sub>O(OOCCH<sub>3</sub>)<sub>6</sub>(H<sub>2</sub>O)<sub>3</sub>]Cl·6H<sub>2</sub>O and [Fe<sub>3</sub>O(OOCCH<sub>3</sub>)<sub>6</sub>(H<sub>2</sub>O)<sub>3</sub>]Cl·6H<sub>2</sub>O were reported by Powell *et al.* [99]. It is firmly established that the metal ions in the oxo-centered units are antiferromagnetically coupled, but all recent measurements indicate that the three magnetic coupling constants are not equal.

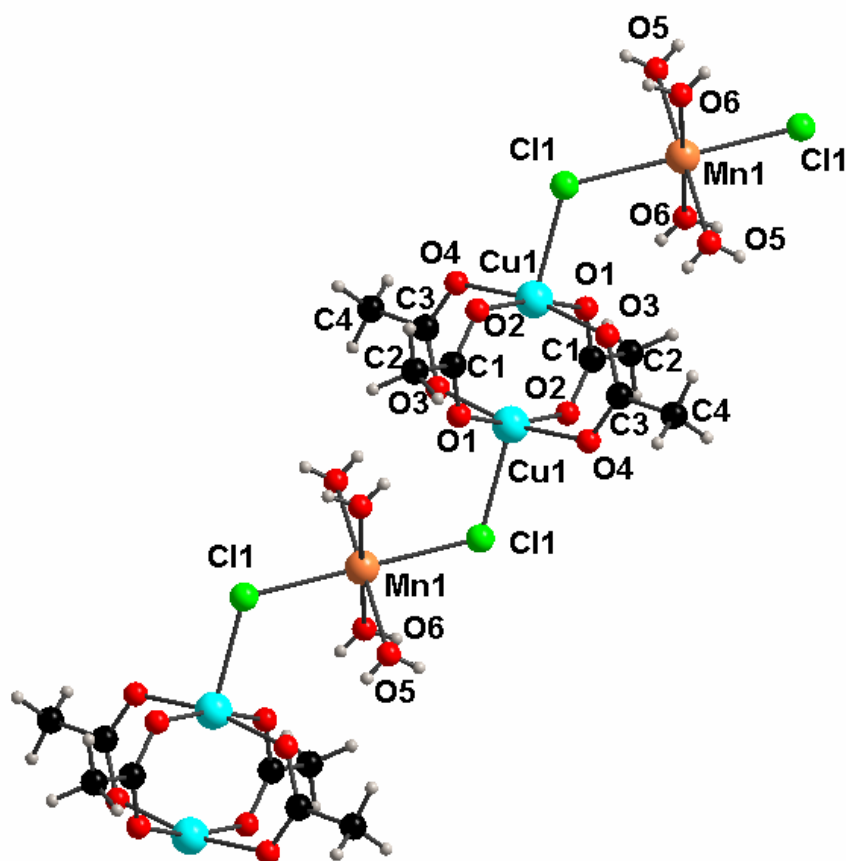
5.9 Structure of  $[\text{Cu}_2(\text{OAc})_4\text{MnCl}_2(\text{H}_2\text{O})_4]_\infty$ , **2**.

Fig. 32 Structure of the infinite complex  $[\text{Cu}_2(\text{OAc})_4\text{MnCl}_2(\text{H}_2\text{O})_4]_\infty$ , **2**.

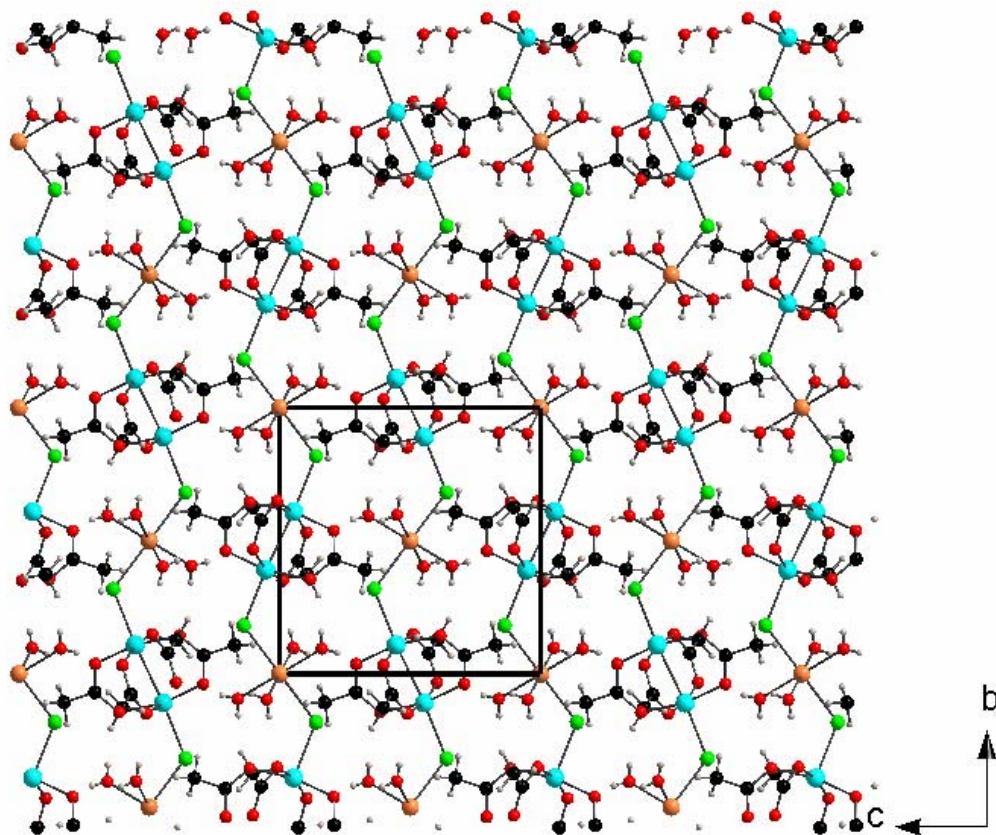
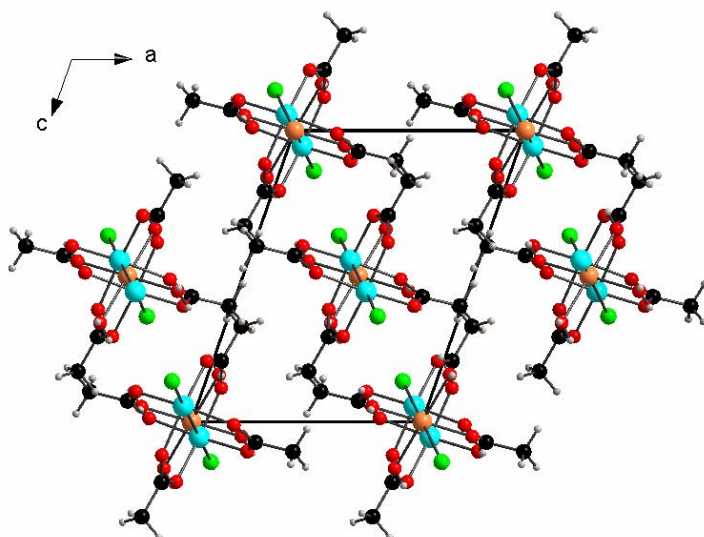
In this case the reaction of copper acetate with ligand **L10** and  $\text{Mn}^{2+}$  resulted in the incorporation of  $\text{Mn}^{2+}$  into the structure but not the ligand. Compound **2** is a polymeric mixed-metal complex. A chlorine atom links the Cu- and Mn-atoms and consequently this compound is magnetically coupled. The Mn is coordinated with 6 atoms and Cu with [4+1] coordination. Cu(II) is coordinated as a square based pyramid and Mn(II) an octahedron.

The dimeric  $[\text{Cu}_2(\text{OAc})_4]$ -units are linked through chloride ions into one-dimensional chains. The chlorides take the terminal positions in the classic copper (II) acetate structure and also form *trans* ligands for the Mn(II) which has a further four water ligands in the equatorial plane. The chloride bridges are non-linear, the Cu1..Cl1 distance amounts to 2.444 Å, the Mn1..Cl1 amounts to 2.528 Å and the Cu-Mn distance over the chloride amounts to 4.233 Å, with a Mn-Cl-Cu angle of 116.71°. Both Cu-acetate dimers and the Mn(II) units lie on

crystallographic inversion centers. Blake *et al* synthesized tri-nuclear-acetates with Cr(III), Fe(III) and Ni(II) [101, 100].

A heteropentanuclear  $[\text{Cu(II)}_2\text{Co(II)Co(III)}_2(\text{OAc})_4(\text{H}_2\text{tea})(\text{tea})_2].2(\text{OAc})$  with (tea= triethanolamine) has been reported [102]. In the centrosymmetric unit of this complex five metal ions are linked together by eight oxygen atoms of the four triethanolamine ligands and by two acetate anions, with the metal-metal separations being 2.823 and 2.964 Å for Cu(II)...Co(III) and Co(III)...Co(II), respectively. Magnetic measurements for this complex showed a marked decrease of the  $\chi^*T$  value at low temperature, indicative of antiferromagnetic interactions between the magnetic centers. A fit was attempted assuming an effective  $S = \frac{1}{2}$  ground state for Co(II) and an Ising-type anisotropy, considering only intramolecular interactions. The value obtained for  $J$  of  $36 \text{ cm}^{-1}$  must originate from the efficient role of the diamagnetic Co(III) in transmitting the interaction between Co(II) and Cu(II) below 40 K.

In addition reactions can be carried out with mixed-metal complexes like the catalytic oxidation of styrene and cumene in the absence of solvent [103]. The products of this catalysis are styrene oxide and benzaldehyde. Among the  $\mu$ -oxo mixed metal acetate complexes  $\text{Fe(III)}_2\text{Zn(II)}$ ,  $\text{Co(III)}_2\text{Co(II)}$  and  $\text{Cr(III)}_2\text{Fe(II)}$  are superior for both reactivity and epoxide selectivity to monomeric or trimeric complexes. Moderately high temperatures and decreased  $\text{O}_2$  pressure result in increased epoxide selectivity. All the complexes tested oxidized cumene, but the  $\text{Fe}_2(\text{III})\text{Mn(II)}$  complex had no activity for the oxidation of styrene. Electron transfer between metals via  $\mu$ -oxo atom is considered to be responsible for the effective catalytic feature.

Structure packing of  $[\text{Cu}_2(\text{OAc})_4\text{MnCl}_2(\text{H}_2\text{O})_4]_\infty$ , **2**.Fig. 33 View of the molecular packing in  $[\text{Cu}_2(\text{OAc})_4\text{MnCl}_2(\text{H}_2\text{O})_4]_\infty$  down the **a**-axis.Fig. 34 View of the molecular packing in  $[\text{Cu}_2(\text{OAc})_4\text{MnCl}_2(\text{H}_2\text{O})_4]_\infty$  down the **b**-axis.

The view down the **a**-axis shows polymer chains in a zigzag ordering. Here, water-molecules are between the polymer chains. The view down the **b**-axis shows the polymer chains end on. Here, we can clearly recognize that the chains are not interconnected. The magnetic interaction is only along the chain, in one dimension, along the **b**-axis.

### 5.9.1 Magnetic properties of the compound **9**.

In spite of much patience in attempting to isolate a pure sample of crystals of this compound under the microscope, it proved impossible to exclude copper(II) acetate from this sample.

The compound  $[\text{Cu}_2(\text{OAc})_4\text{MnCl}_2(\text{H}_2\text{O})_4]_\infty$  was also measured on the SQUID at the University of Florence (figure 35). The  $\chi T$  versus  $T$  shows a maximum value of 0.7 K\*mol/emu, which approximates to the interaction of two ions with spin  $S = 1/2$ . Cu (II) with  $d^9 S = 1/2$  and Mn(II) with  $d^5 S = 5/2$  have a total-spin of 3 for ferromagnetic coupling and  $S = 2$  for antiferromagnetic.

Following the formula of Curie for spin only for  $\chi^*T$  the curve should saturate at 4.75 K\*mol/emu. For  $g = 2$ ,  $\chi^*T$  is 0.375 K\*mol/emu for  $S = 1/2$  and 4.375 K\*mol/emu for  $S = 5/2$ . The addition of these values gives 4.75 K\*mol/emu. But this calculation is valid only for the isolated spins. The saturation value of the curve is lower than 4.75 K\*mol/emu and it is too high, because the curve starts at 0.7 K\*mol/emu. For antiferromagnetic interaction the formula to use is the formula of Curie-Weiss and the value of  $\theta$  should be calculated with the plot of  $1/\chi$  vs.  $T$ . But the values of this curve do not correspond to a value for spin only or for an interaction. We infer from this that the measured sample contains a high proportion of Cu-acetate. The impurities have much stronger interactions than the Cu-Mn-coupling. The sample was measured at 10000 Oe.

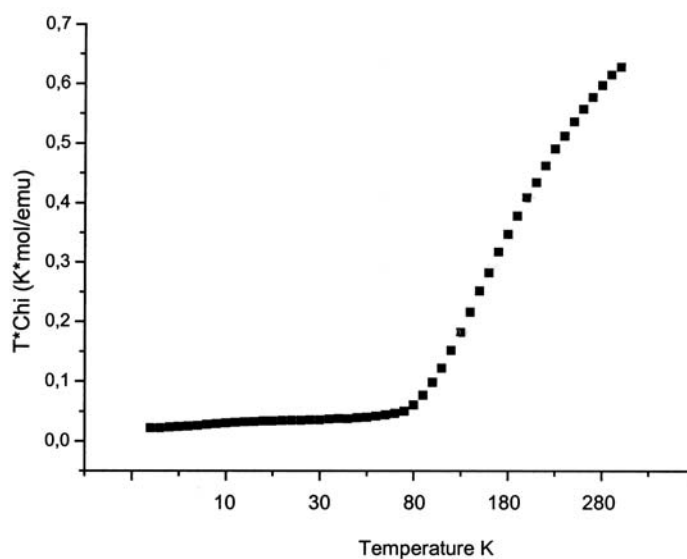


Fig. 35: The  $\chi T$  versus  $T$  plot for compound **9**.

Kahn and coworkers synthesized chains such as  $\text{MnCu}(\text{opba})(\text{H}_2\text{O})_2 \cdot \text{H}_2\text{O}$  and  $\text{MnCu}(\text{opba})(\text{DMSO})_3$  (opba=o-phenylenebisoxamate), that also adopt a zigzag shape and have Cu and Mn as paramagnetic ions. These two chain compounds have much the same physical properties. They are one-dimensional ferrimagnets. Owing to the antiferromagnetic interaction between adjacent  $\text{Mn}^{2+}$  and  $\text{Cu}^{2+}$  ions, the  $S_{\text{Mn}} = 5/2$  and  $S_{\text{Cu}} = 1/2$  local spins tend to align along opposite directions, and the ground-state spin is  $S_g = N(S_{\text{Mn}} - S_{\text{Cu}})$ , where  $N$  is the number of MnCu repeat units along the chain.

The temperature dependence of  $\chi^*T$  for such a ferromagnetic system is quite characteristic,  $\chi$  being the molar magnetic susceptibility and  $T$  the temperature. As  $T$  is lowered,  $\chi^*T$  first decreases, passes through a minimum, and then increases very rapidly. This behavior may be understood as follows: At high temperature,  $\chi^*T$  tends to the paramagnetic limit. The minimum of  $\chi^*T$  corresponds to a short-range order where the spins of adjacent centers are antiparallel, but without correlation between neighboring MnCu units. The increases of  $\chi^*T$  as  $T$  tends absolute zero is due to the increase of correlation between length along which the  $S_{\text{Mn}}$  spins are aligned along a direction and the  $S_{\text{Cu}}$  spins along the opposite direction. If the chain is infinite, long range magnetic ordering is expected at 0K. Indeed, there is no long range magnetic ordering at finite temperature for one-dimensional compounds. In  $\text{MnCu}(\text{opba})(\text{H}_2\text{O})_2 \cdot \text{H}_2\text{O}$ , the ferromagnetic chains are not perfectly isolated within the crystal lattice; they interact very weakly in an up-down fashion, and the compound shows long range antiferromagnetic ordering of the ferromagnetic chains at  $T_N = 5$  K. An external magnetic

field of 5 kOe is sufficient to overcome the interchain antiferromagnetic interactions, and to induce a transition to a ferromagnetic-like state in which the chain spins are aligned along the field direction [1].

### 5.10 Structure of $\text{K}[\text{Cu}(\text{ida})\text{Cl}(\text{H}_2\text{O})_2]$ , **10**.

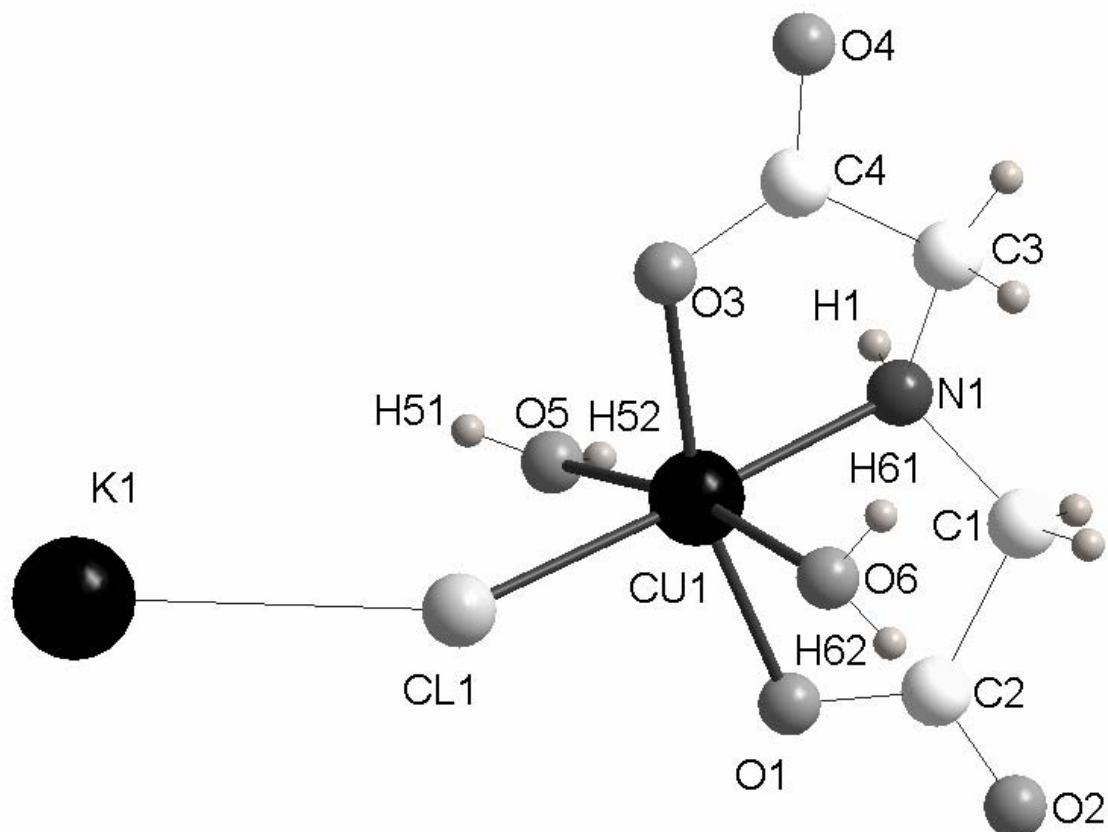


Fig. 36 Structure of the mononuclear complex  $\text{K}[\text{Cu}(\text{ida})\text{Cl}(\text{H}_2\text{O})_2]$ , **10**.

The compound is a monomer with the ligand iminodiacetic acid. There is a Jahn-Teller-Effect along the Cu-H<sub>2</sub>O axis. The Cu is coordinated by a Cl-atom, 2 molecules of water and the O-atoms and N-atom of the ligand coordinate meridional in the octahedron. The reaction was carried out at pH of 7 and Ni<sup>2+</sup> was also added, but it was not incorporated into the structure. It is remarkable at pH 3 up to pH 7 only a monomer could be obtained. In the case of Fe (III) with a pH of 7 Henderson could synthesize a Fe-hexamer with **L5** in his PhD work 1993.



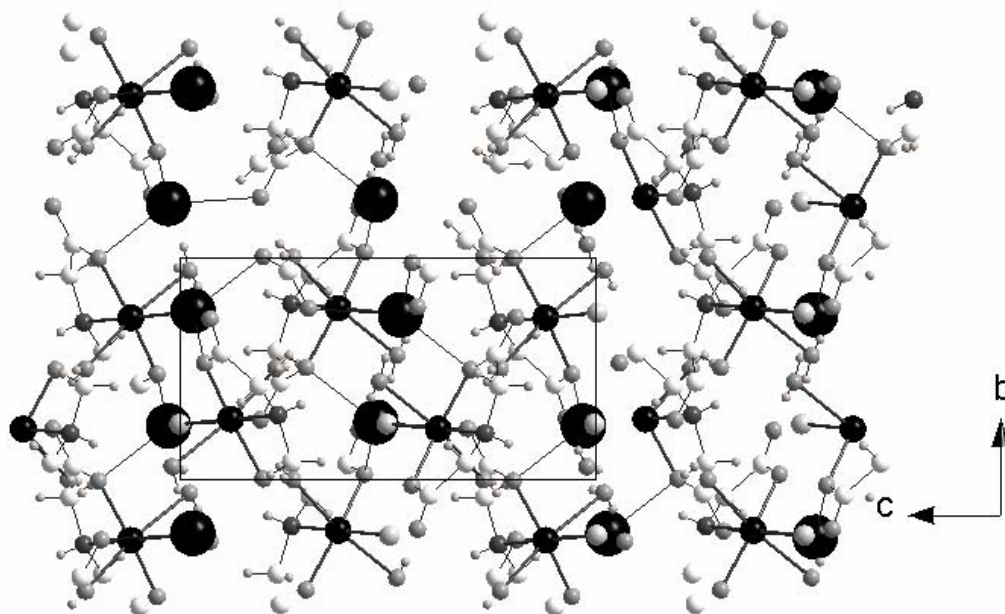
**Structure packing of  $\text{K}[\text{Cu}(\text{ida})\text{Cl}(\text{H}_2\text{O})_2]$ , 10.**

Fig. 37 View of the molecular packing in  $\text{K}[\text{Cu}(\text{ida})\text{Cl}(\text{H}_2\text{O})_2]$  down the **a**-axis.

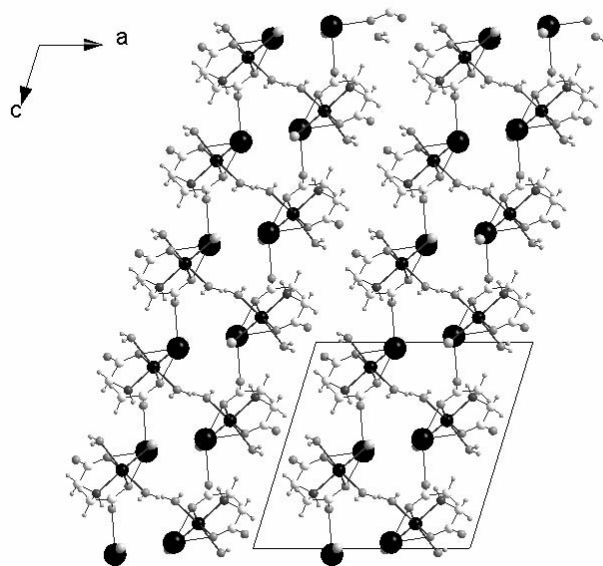


Fig. 38 View of the molecular packing in  $\text{K}[\text{Cu}(\text{ida})\text{Cl}(\text{H}_2\text{O})_2]$  down the **b**-axis.

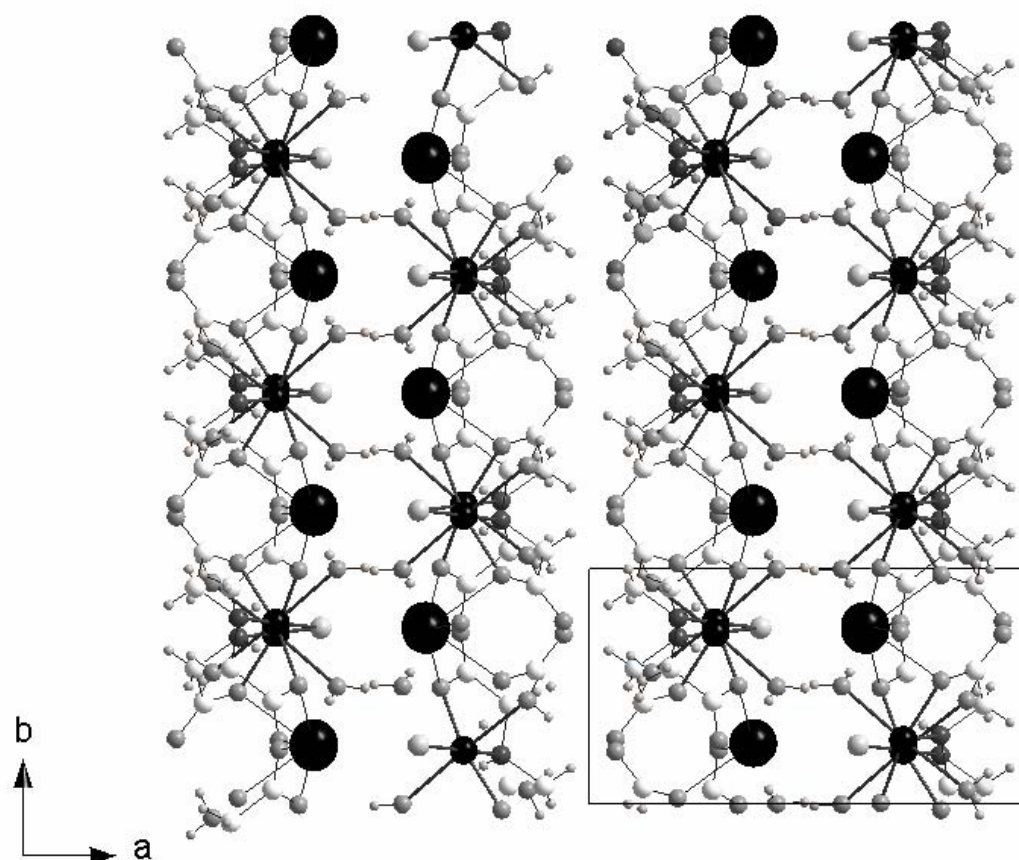


Fig. 39 View of the molecular packing in  $\text{K}[\text{Cu}(\text{ida})\text{Cl}(\text{H}_2\text{O})_2]$  down the **c**-axis.

The view down the **b**-axis shows Cu-monomer-chains, the shortest Cu-Cu-displacement amounts to  $6.26\text{\AA}$  and furthermore potassium atoms lie between the Cu-monomers. The potassium-atoms are ordered in a stair like fashion row in the same row as the Cu-atoms. Through the potassium atoms a chain results in direction along the **c**-axis. The view down the **a**-axis shows that the potassium-atoms form the monomers into a network structure, and the Cu-atoms are organised linearly. The ligand is ordered also linearly. We can speak here of a layer, because horizontally as well as vertically the structure is joined in fact together over potassium-oxygen-bridges in direction of the **c**- and **b**-axes. The view down the **c**-axis shows the potassium atoms in the same chain as the Cu-atoms. The Cu-atoms are joined through a potassium oxygen bridge. We think of this in terms of a sheet structure only along the **a**-axis and of chains along the **c**- and **b**-axes.

### 5.11 Structure of $\text{K}[\text{Cr}(\text{Hedta})\text{Cl}]\cdot\text{H}_2\text{O}$ , **11**.

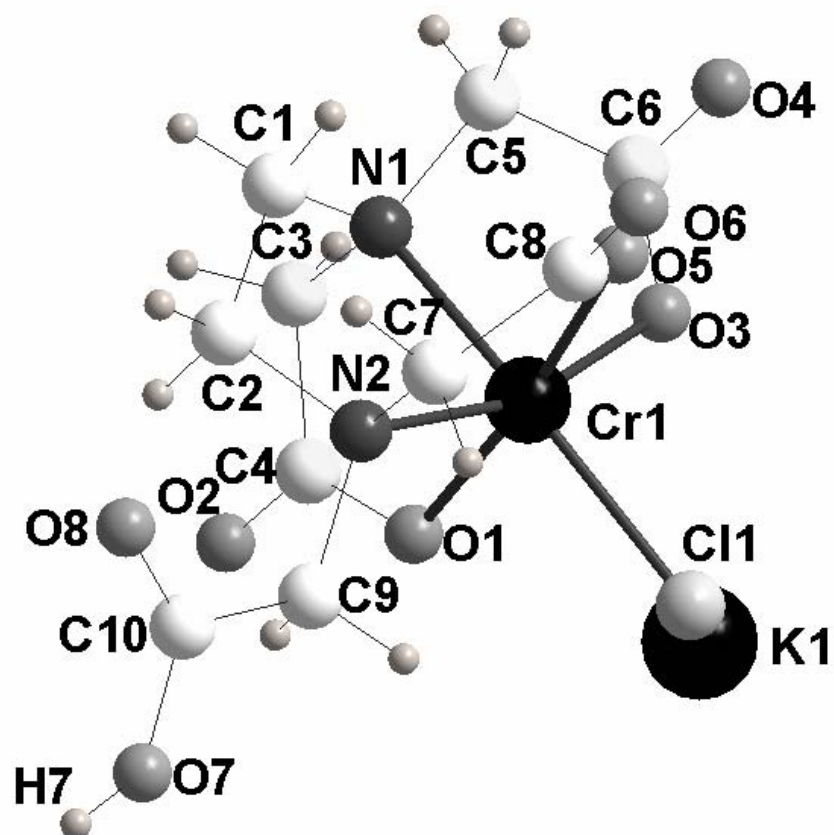
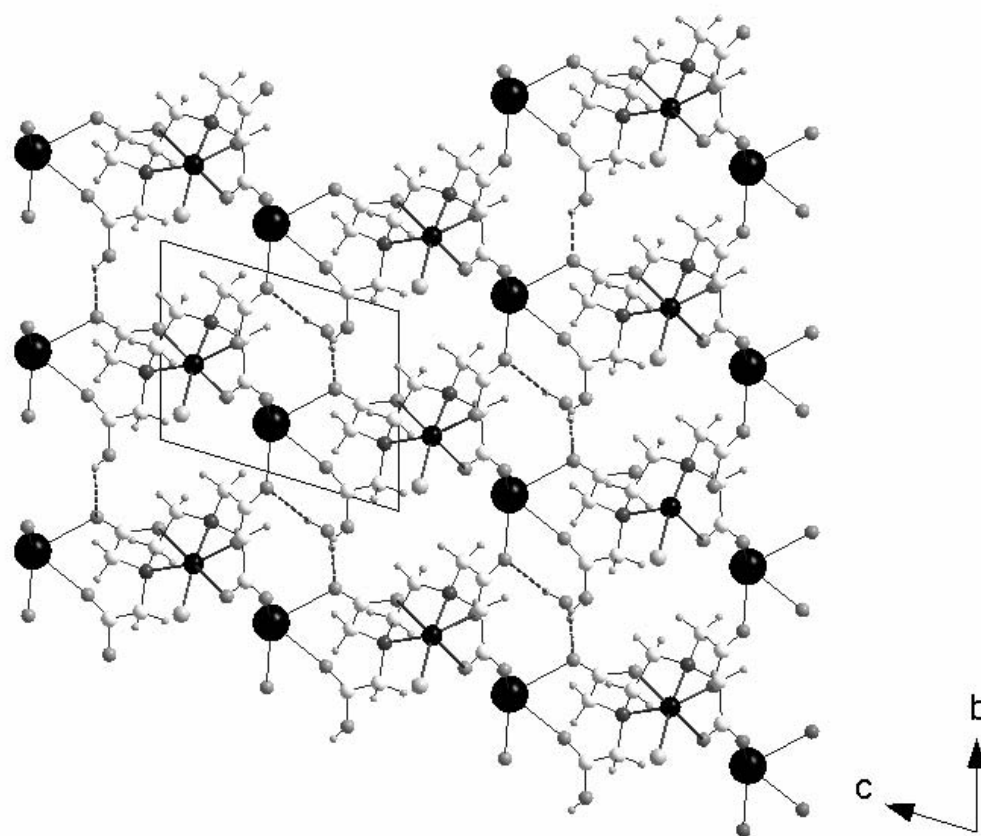
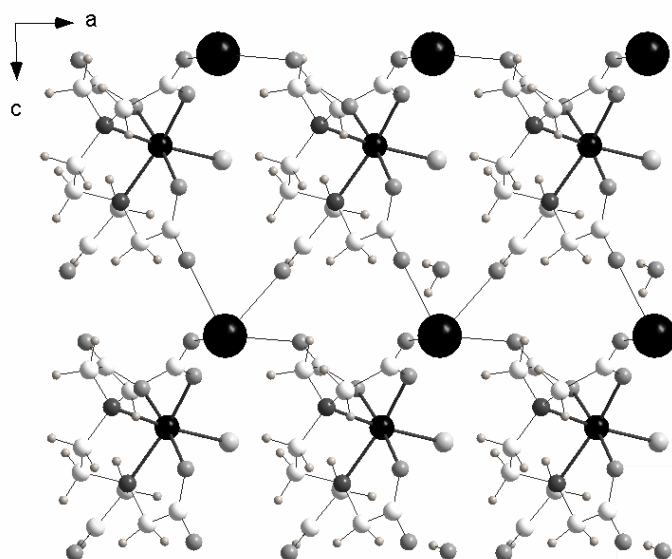


Fig. 40 Structure of the mononuclear complex  $\text{K}[\text{Cr}(\text{Hedta})\text{Cl}]\cdot\text{H}_2\text{O}$ , **11**.

The asymmetric unit contains a monomer formed with edta at pH=4 and with the octahedrally chromium, coordinated by two nitrogen atoms and three oxygen atoms from the ligand and chlorine. The protonated  $\text{CO}_2\text{H}$  group is not coordinated, but forms a hydrogen bond. The structure of **11** crystallizes in an uncommon space group, P1. That has only been detected in proteins and a few organic structures. The crystal structure is enantiomerically pure, but the crystals form a racemate of 50:50 with crystals of the mirror image of **11** also present in the product. It is necessary to have a chiral ligand to build an enantiomerically pure substance to obtain crystals of one chirality.

Structure packing of  $\text{K}[\text{Cr}(\text{Hedta})\text{Cl}]\cdot\text{H}_2\text{O}$ , 11.Fig. 41 View of the molecular packing in  $\text{K}[\text{Cr}(\text{Hedta})\text{Cl}]\cdot\text{H}_2\text{O}$  down the **a**-axis.Fig. 42 View of the molecular packing in  $\text{K}[\text{Cr}(\text{Hedta})\text{Cl}]\cdot\text{H}_2\text{O}$  down the **b**-axis.

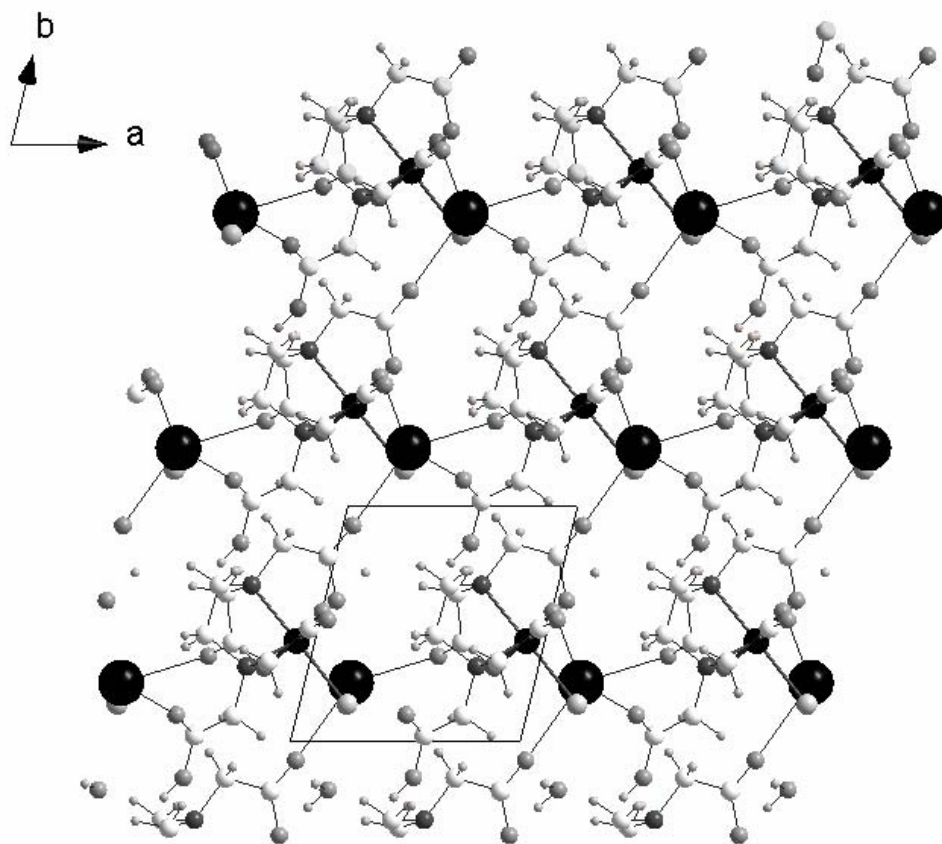


Fig. 43 View of the molecular packing in  $\text{K}[\text{Cr}(\text{Hedta})\text{Cl}]\cdot\text{H}_2\text{O}$  down the **c**-axis.

Coordination of carboxylate oxygens and chloride ligands to the  $\text{K}^+$  cations results in sheets of complexes in the *bc*-plane. Further coordination to  $\text{K}^+$ , and hydrogen-bonding from the  $\text{CO}_2\text{H}$  group and the water of crystallization link the sheets into a 3-dimensional structure. The overall coordination spheres of the  $\text{K}^+$  cation are 4 oxygens of the ligand and the chlorine. The packing viewed down the **a**-axis shows ordered layers. There are H-bonds between the protonated carboxylate group of the ligand and the oxygen on the potassium-atoms. There are also H-bonds between the water molecule and the K-O-bridge. The Cr-Cr-displacement is 8.436 Å within the chain and from a chain diagonally to the next chain 11.005 Å. The ligand is between the Cr- and K-chains. In the view down the **b**-axis shows layer-order again. The Cr-Cr-displacements amounts to 6.582 Å in direction of the **a**-axis and 9.515 Å in direction of the **c**-axis. Between the K-atoms are oxygens, and between the Cr-atoms chlorine atoms are available, sandwiched between the K and Cr-atoms are ligand molecules. The view down the **c**-axis also shows a layer. The Cr-Cr-displacements amount to 6.582 Å in direction of the **a**-axis and 9.515 Å in direction of the **b**-axis. This structure is an enantiomeric pure three



dimensional layer structure, in which the K and Cr-atoms alternate in chains. The ligand is achiral, so the overall sample is racemic.

### 5.12 Structure of $[\text{CuCl}(\text{H}_3\text{edta})]\cdot 2\text{H}_2\text{O}$ , **12**.

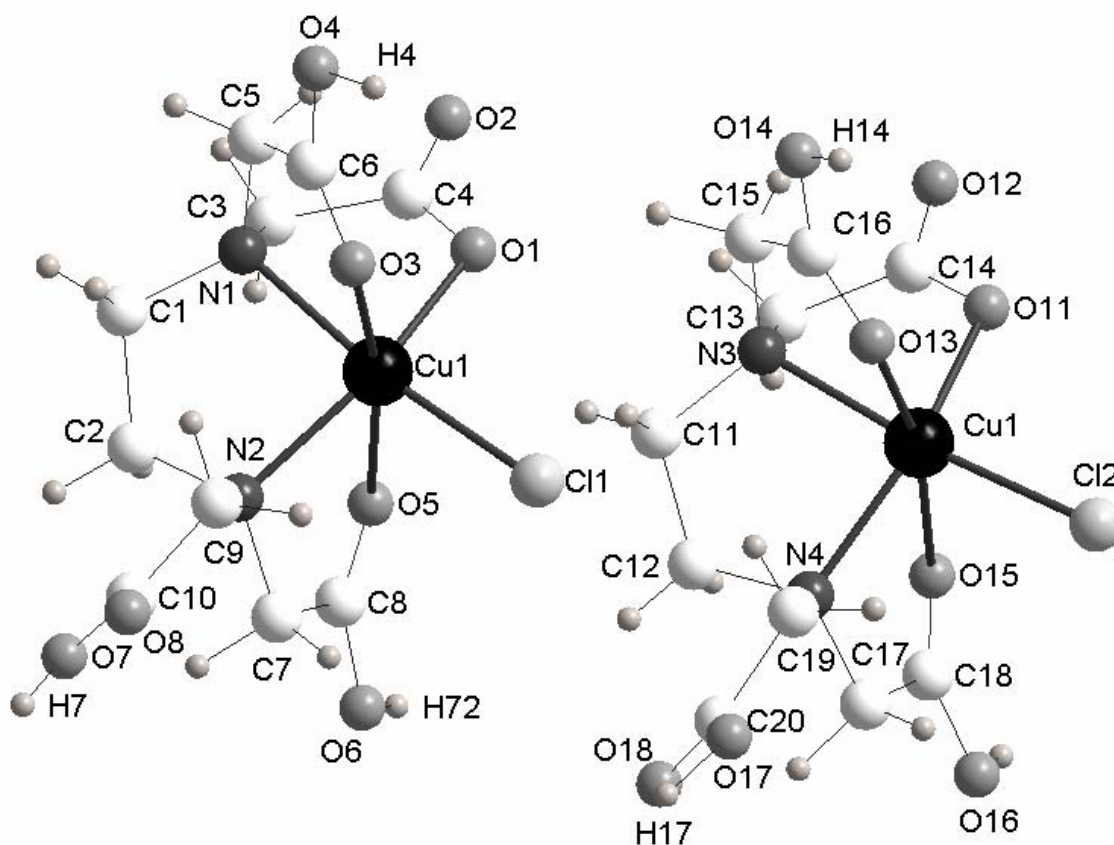


Fig. 44 Structure of the mononuclear complex  $[\text{CuCl}(\text{H}_3\text{edta})]\cdot 2\text{H}_2\text{O}$ , **12**.

Compound **12** has 2 mononuclear Cu complexes in the asymmetric unit. 5 of the 6 coordination atoms of the ligand are attached to the metal ion. Three carboxylate oxygen atoms are protonated and one of these groups does not coordinate to the metal. The six-coordinated Cu(II) centers both show the expected Jahn-Teller distortion to a tetragonally elongated  $[4+2]$  octahedron. The equatorial plane is defined by the two ligand nitrogens, the deprotonated carboxylate and the chloride. Two  $\text{CO}_2\text{H}$  groups provide the axial coordination; the third is uncoordinated. The complex has nearly a *pseudo-trans* symmetry.

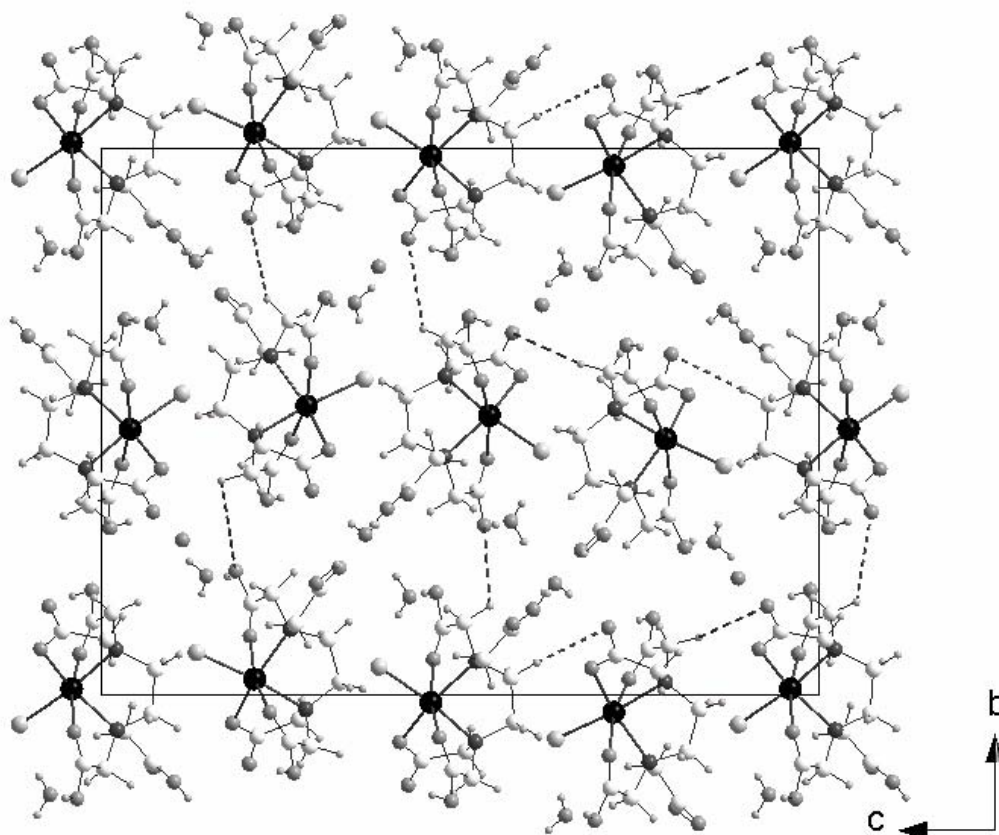
**Packing structure of  $[\text{CuCl}(\text{H}_3\text{edta})]\cdot 2\text{H}_2\text{O}$ , 12.**

Fig. 45 View of the molecular packing in  $[\text{CuCl}(\text{H}_3\text{edta})]\cdot 2\text{H}_2\text{O}$  along the *a*-axis.

The view down the *a*-axis shows the isolated Cu-monomers, where the Cu...Cu displacements from monomer to monomer are between 10.4 and 9.6 Å vertically and vary between 6.6Å and 6.9Å horizontally. Hydrogen bonds are present in the horizontal and vertical directions of the figure, giving an extensive hydrogen bonding network.

The structure of the Cr-edta monomer 11 has a sheet structure while the Cu-edta monomer 12 has a structure of isolated monomers, which are connected to each other via hydrogen bonding.

### 5.13 Structure of $[\text{Cu}(\text{Hada})_2]$ , **13**.

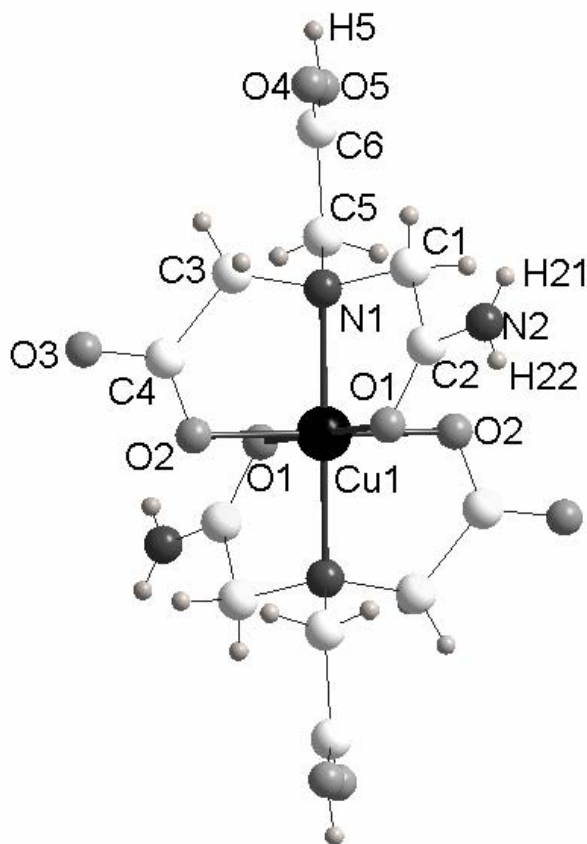


Fig. 46 Structure of the mononuclear complex  $[\text{Cu}(\text{Hada})_2]$ , **13**.

The asymmetric unit contains half a monomer with the Cu(II) center on a crystallographic inversion center, which relates the two Hada ligands. Although four equivalents of KOH were used in the reaction, one carboxylate group of each ligand is still protonated. Therefore, in the following reactions the base was increased to 8 equivalents of KOH, but without resulting in single crystal formation. Each ligand coordinates to Cu(II) via the nitrogen, an oxygen of the deprotonated carboxylate group, and the amido oxygens. These three atoms are coordinated facially. Thus, 4 oxygen- and 2 nitrogen atoms coordinate the copper in an octahedron.

There is a protonated carboxylate, which is not coordinated, showing that Cu(II) has a higher affinity for amide oxygen groups than carboxylic acids as ligand. The amide ligand is still a rather weak ligand, and forms the elongated axis of the Jahn-Teller distorted octahedral coordination.



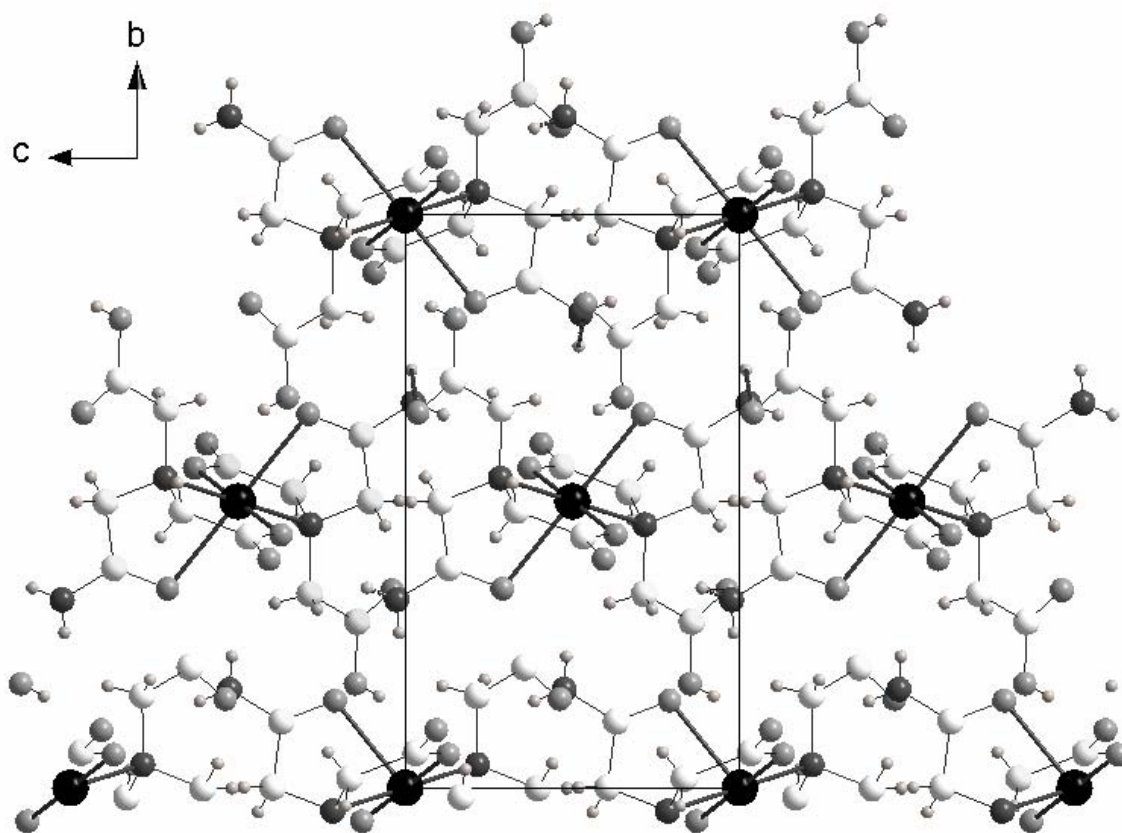
**Structure packing of [Cu(Hada)<sub>2</sub>], 13.**

Fig. 47 View of the molecular packing in [Cu(Hada)<sub>2</sub>] down the **a**-axis.

The view down the **a**-axis shows isolated monomers linked by H-bonds between the NH<sub>2</sub> and the oxygen of the ligand. The shortest Cu-Cu-displacement amounts to 7.162Å.

The monomers are isolated, but the ordering of the copper atoms in this packing is a chain, along all three axes. A [(Cu(ada)(ImH)] compound has been reported by Bugella-Altamirano et al [104] It also consists of a monomer with a pyramidal coordination sphere and a crystal packing of isolated monomers linked to other three adjacent ones by six hydrogen bonds into a zigzag chain.

### 5.14 Structure of (pyrH).[Cr(ada)<sub>2</sub>].3H<sub>2</sub>O **14**

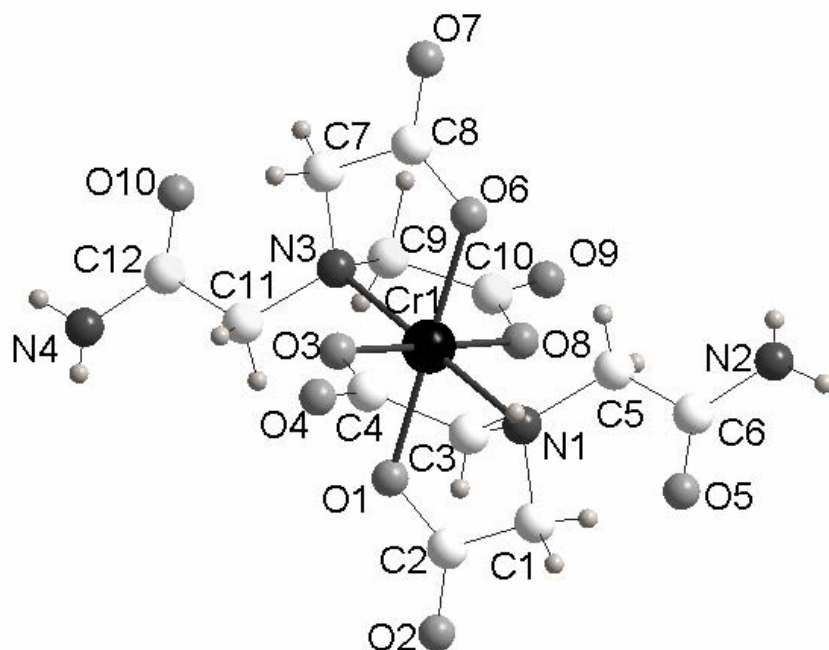


Fig. 48 Structure of the mononuclear complex [Cr(ada)<sub>2</sub>](pyrH).3H<sub>2</sub>O, **13**.

This structure has a monomer in the asymmetric unit, with a Cr(III) octahedron coordinated by 2 nitrogens and 4 oxygens. The nitrogen atoms are in equatorial *trans* positions. The octahedron is nearly perfect; the axes are approximately at 180°. In the equatorial level one plane there are angles of 95° and 84°. As in the case of **13**, two ligands coordinate to the metal to give octahedral coordination. However, in this case both carboxylate groups are deprotonated, and coordinate to Cr1 together with the amino nitrogen in a facial geometry. The complex has pseudo-inversion symmetry. Although an excess of pyridine was used as base, pyridine ligands are not found in the structure. But rather protonated pyridine acts as counteractions to the [Cr(ada)<sub>2</sub>]<sup>-</sup> anions. Richard K. Henderson has synthesized the Fe- and Cr-ada-monomers K[Fe(ada)<sub>2</sub>].3H<sub>2</sub>O and K[Cr(ada)<sub>2</sub>].2H<sub>2</sub>O. In this case using a different base results similar in a compound, but crystallizing in a different space group. In fact, the formal replacement of K<sup>+</sup> by [pyrH]<sup>+</sup> leads to a different packing arrangement in the crystal structure for whilst K<sup>+</sup> interacts with exogenous oxygen groups on the ligand shell of the complex, [pyrH]<sup>+</sup> acts more like a spacer in the structure of **14**.

Structure packing of  $[\text{Cr}(\text{ada})_2](\text{pyrH})\cdot 3\text{H}_2\text{O}$

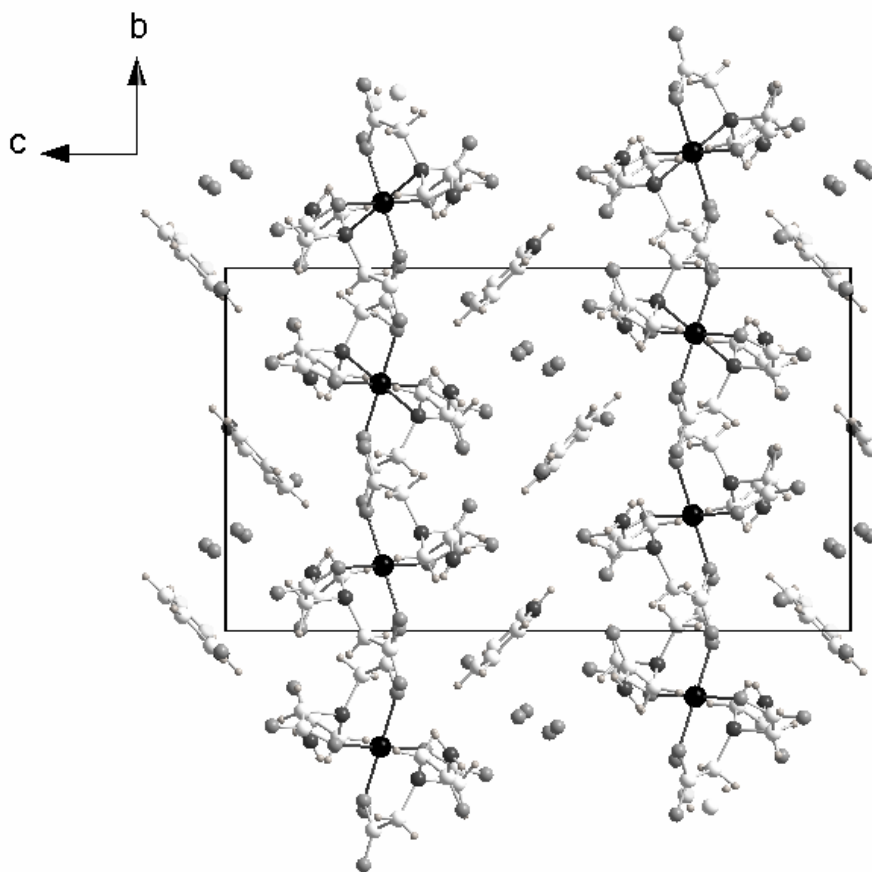


Fig. 49 View of the molecular packing in  $[\text{Cr}(\text{ada})_2](\text{pyrH})\cdot 3\text{H}_2\text{O}$  down the **a**-axis

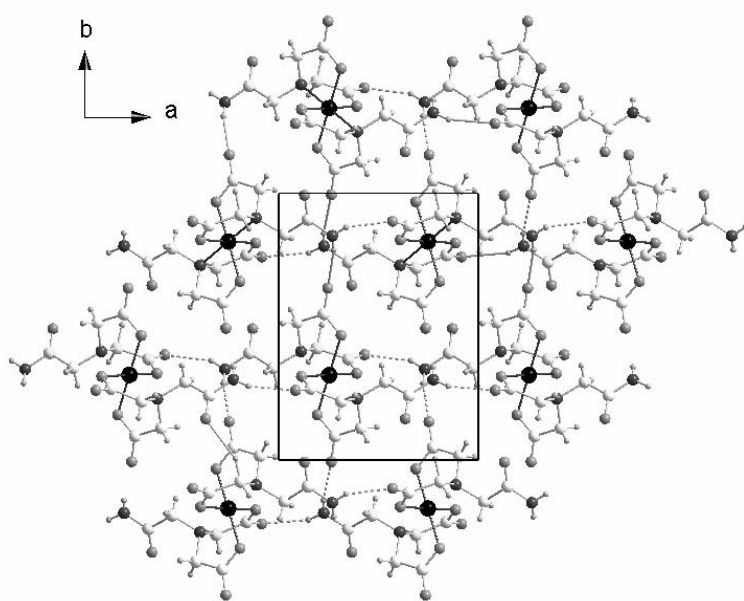


Fig. 50 View of the molecular packing in  $[\text{Cr}(\text{ada})_2](\text{pyrH})\cdot 3\text{H}_2\text{O}$  down the **c**-axis

The structure packing down the **a**-axis shows a row of the Cr monomers in vertical direction. These rows lie vertical alternate with pyridinium molecules. The Cr...Cr displacement amounts to 7.5 Å within the row and 11.3 Å from one row to the next. The pyridinium molecules are ordered diagonally to the Cr-row, so the  $\pi$ -orbitals of the pyridine ring lie perpendicular to the chromium monomers.

The view down the **b**-axis shows a string ordering of the Cr ions. All pyridinium molecules lie in a plane. The Cr-Cr-displacements remain at 7.5 Å. The ligand of a monomer lies over the ligand of the next monomer. The monomers are arranged in a row. The view down the **c**-axis shows isolated monomers in a layer-structure held together by hydrogen bonding present in the direction of the **a**- and **b**-axes of this figure.

#### 5.15 Structure of $\{(\text{pyrH})[\text{Cu}(\text{heidi})(\text{pyr})]\text{Cl}\cdot 2\text{H}_2\text{O}\}_\infty$ , 15.

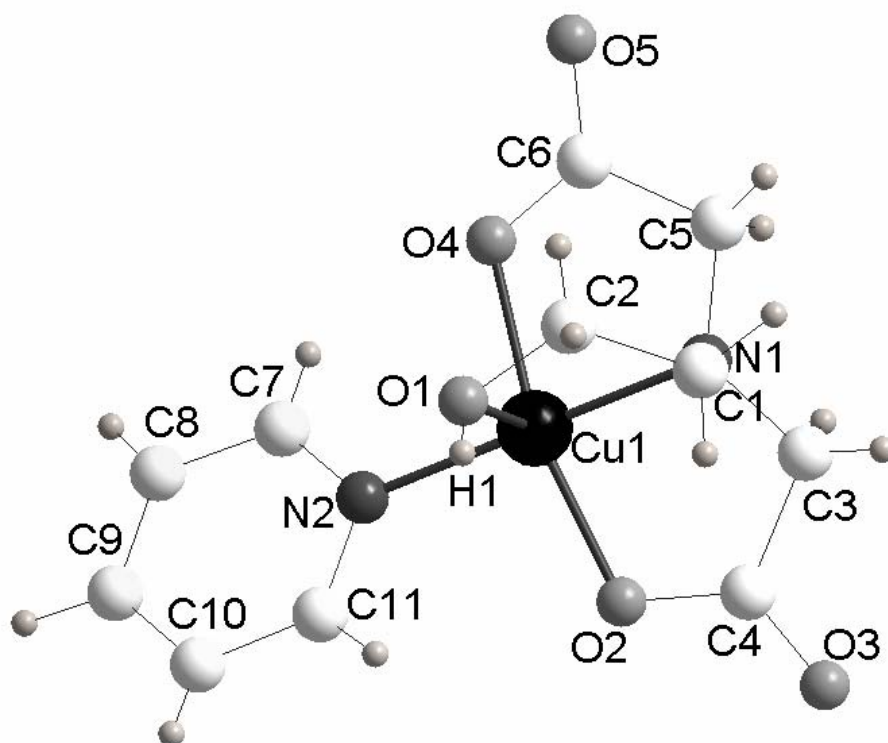


Fig. 51 Structure of the infinite complex  $\{(\text{pyrH})[\text{Cu}(\text{heidi})(\text{pyr})]\text{Cl}\cdot 2\text{H}_2\text{O}\}_\infty$

The asymmetric unit contains a monomer, which has been obtained at pH 5.96 with N-(2-hydroxyethyl) iminodiacetic acid (H<sub>3</sub>heidi, **L8**) as ligand. The copper atom is coordinated with three oxygen atoms and two nitrogen atoms. The OH-group lies axial and the other four coordination atoms two nitrogens and two oxygens, equatorial. The nitrogen atoms are in *trans* position. The square-based pyramid has equatorial angles of 95° for N-Cu-O, 84° for O-Cu-N, 84° for N-Cu-O, and 95° for O-Cu-N. In the Fe- and Cr-monomers of **L8** the O2 and O4 are *cis* to each other giving facial coordination, while with Cu these oxygen's are *trans* resulting merodinal coordination. Two oxygens are from each of the deprotonated carboxylate groups, the imino nitrogen and a pyridine nitrogen form a square-planar coordination around the Cu(II). The neutral OH group from the heidi and O from the next complex can be regarded as completing a distorted octahedral environment around the Cu(II).

**Structure packing of  $\{(\text{pyrH})[\text{Cu}(\text{heidi})(\text{pyr})]\text{Cl}\cdot 2\text{H}_2\text{O}\}_\infty$ , **15**.**

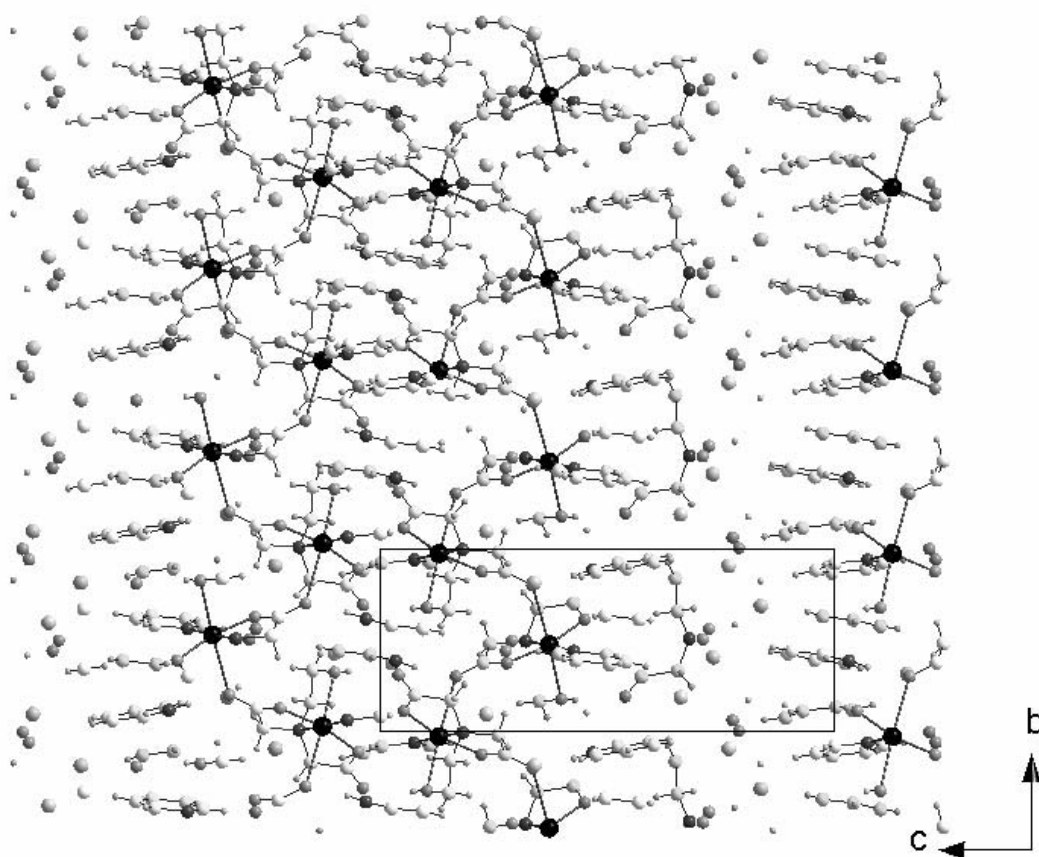


Fig. 52 View of the packing in  $\{(\text{pyrH})[\text{Cu}(\text{heidi})(\text{pyr})]\text{Cl}\cdot 2\text{H}_2\text{O}\}_\infty$  down the **a**-axis.

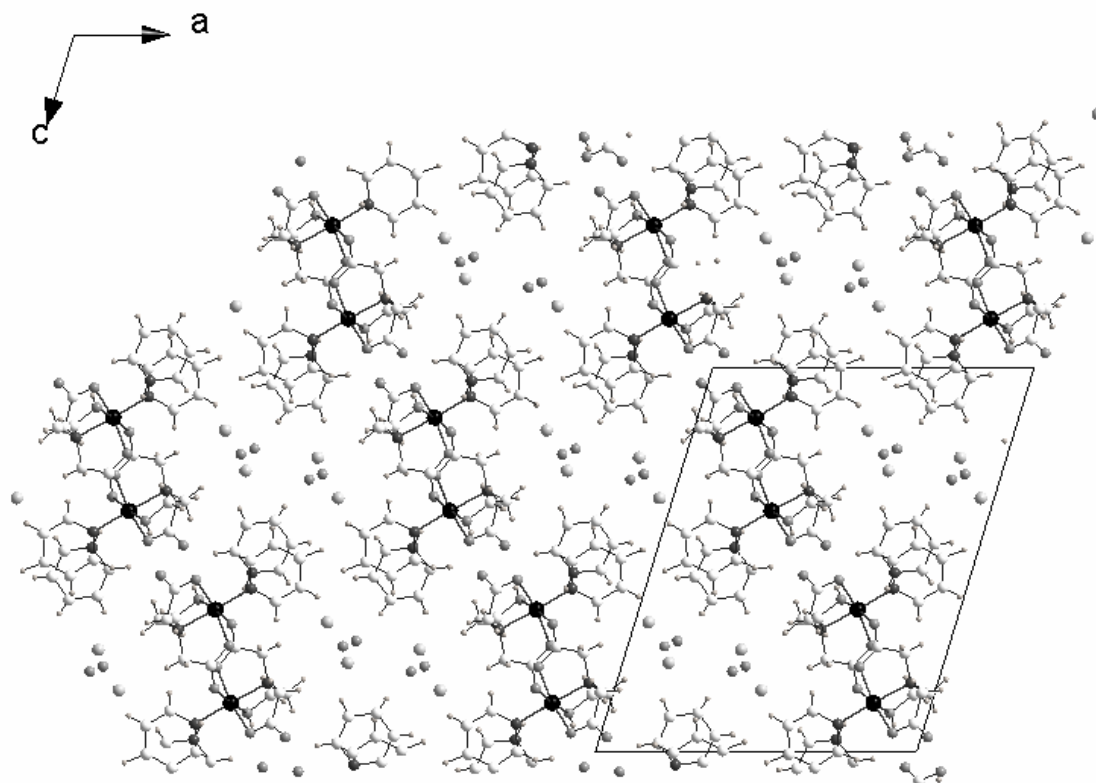


Fig. 52 View of the packing in  $\{(\text{pyrH})[\text{Cu}(\text{heidi})(\text{pyr})]\text{Cl}\cdot 2\text{H}_2\text{O}\}_\infty$  down the **b**-axis.

The coordination of Cu1 by an outer carboxylate oxygen from the complex results in infinite zigzag chains of the complex units parallel to the **b**-axis, linked by syn(ax)-anti(eq) carboxylate bridges. However, such bridges have been shown to result in very weak magnetic interactions [39], and in this case the Cu-O(ax) bond length amounts to 1.964 Å and the Cu...Cu separation amounts to 5.789 Å.

The view of the **a**-axis shows Cu zigzag chains coordinated through the ligand. Pyridinium and pyridine molecules lie perpendicular to the Cu-chain, giving  $\pi$ -stacking of 3.6 Å. In some bithiazol oligomers the  $\pi$ -stacking amounts to 3.45 Å. The molecules in this structure give a  $\pi$ -stacking tilted ca. 43°, with respect to the stacking axis, causing the molecules to assume a “staircase” structure when viewed at right angles to the molecular plane. The interstack interactions bind the  $\pi$ -stack into a 2D-sheet. Spectroscopic experiments on these bithiazol oligomers have a significantly higher emission in the UV-VIS-spectroscopy than the theoretically predicted [105].

The view by the **b**-axis shows the Cu-atoms connected over the ligand in pairs. These pairs are isolated and are surrounded by chlorine and oxygen atoms. Pyridine is also coordinated at the Cu-atom. The Cu-Cu-displacements amount to 5.78 Å in the Cu-pairs and 9.30 Å from one pair to the next pair. The view of this packing shows the overlap of the pyr.(pyrH)<sup>+</sup> rings very clearly.

### 5.16 Structure of [Cu(naphtyl-OH-ida).(H<sub>2</sub>O)], **16**.

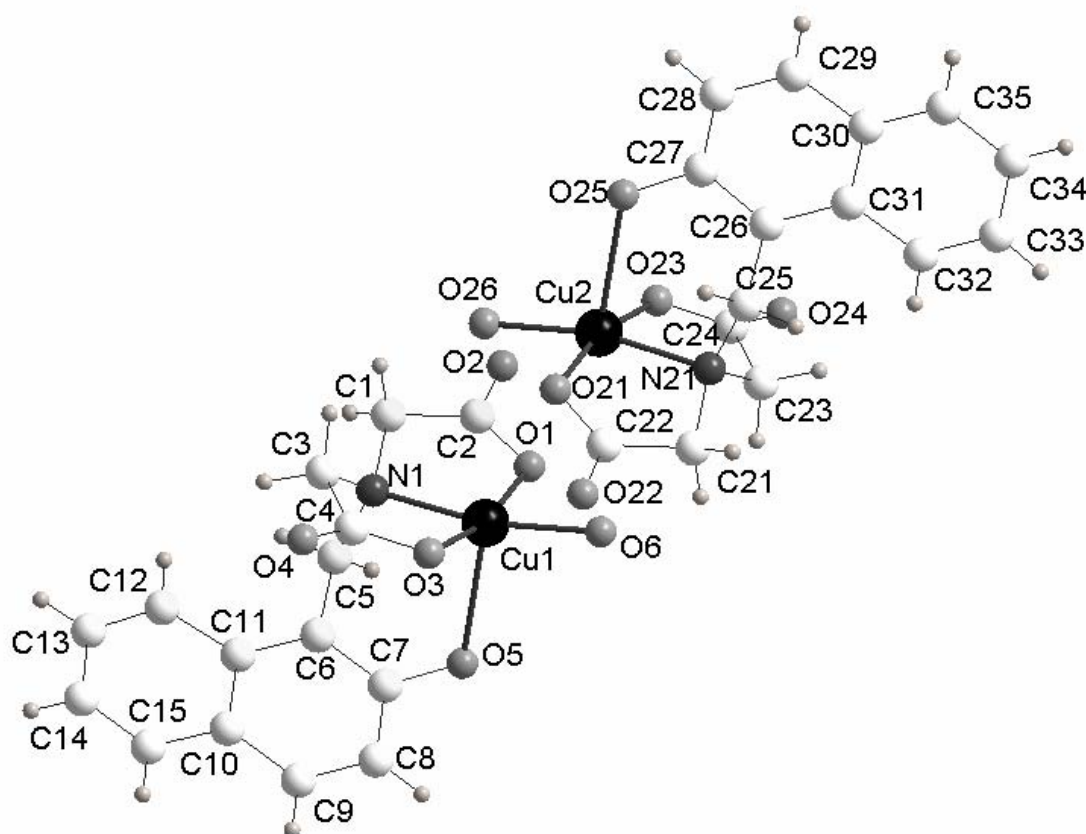


Fig. 53 Structure of the mononuclear complex [Cu(naphtyl-OH-ida).(H<sub>2</sub>O)], **16**.

Here we have monomers with two copper atoms in the asymmetrical unit and the ligand is a naphtyl derivative ligand **L11**. In the synthesis, the Mn(II) monomeric complex of this ligand was used in a reaction with Cu(II), which resulted in the substitution of the Mn(II) by Cu(II) as is obvious from the colour of the complex and the x-ray structural analysis. The Cu...Cu displacement amounts to 4.034 Å and is too long for any magnetic interactions. Reactions were carried out under mild solvothermal conditions.

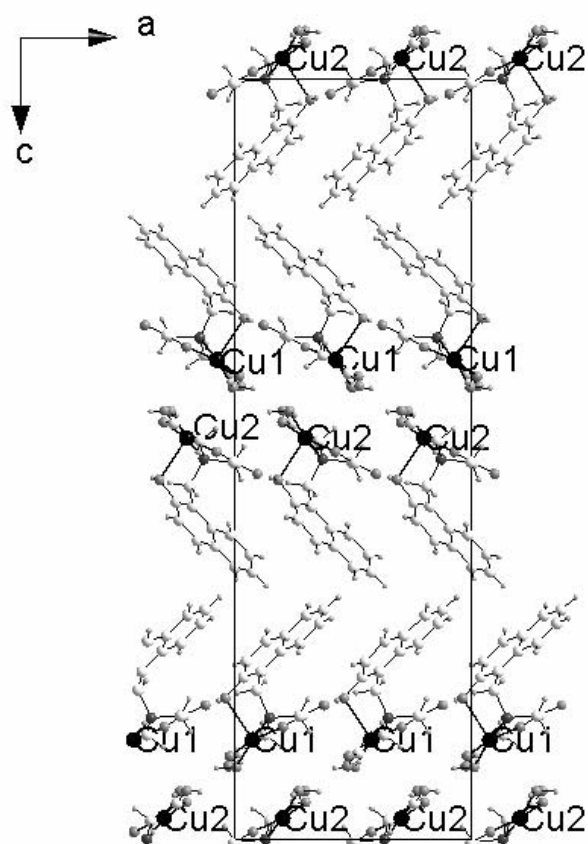
Structure packing of  $[\text{Cu}(\text{naphthyl-OH-ida})\cdot(\text{H}_2\text{O})]$ , **16**.

Fig. 54 View of the molecular packing in  $[\text{Cu}(\text{naphthyl-OH-ida})\cdot(\text{H}_2\text{O})]$  down the **b**-axis.

The view down the **b**-axis shows the isolated monomers. The Cu...Cu displacement of the Cu(1)-Atom to the opposite Cu(1)-atom in horizontal direction amounts to 6.641 Å, from the Cu(2)-Atom to the opposite Cu(1)-atom in vertical direction 4.03 Å and from the Cu(1)-atom to the opposite Cu(2)-atom, that is separated by the ligand, 15.058 Å. The view down **a**- and **b**-axes show a hydrophilic area between the Cu-atoms and a hydrophobic area between the naphthyl ligands **L11**. There is no  $\pi$ - $\pi$  stacking between the ligands, moreover the ligands are perpendicular to each other, so that the  $\pi$ -orbitals are orthogonal to each other and this is a good condition for ferromagnetic coupling. The naphthyl ligands lie orthogonal to the Cu-center in an angle of 71.42° to each other. The view down the **a**-axis also shows isolated monomers. The Cu-Cu-displacement of the Cu(2)-atom to the Cu(1)-atom opposite in horizontal direction amounts to 8.845 Å, from the Cu(1)-atom to the Cu(1)-atom opposite in vertical direction 6.641 Å and from the Cu(1)-atom to the opposite Cu(2)-atom, that is separated by the ligand, 14.786 Å. This is also seen looking down the **c**-axis.



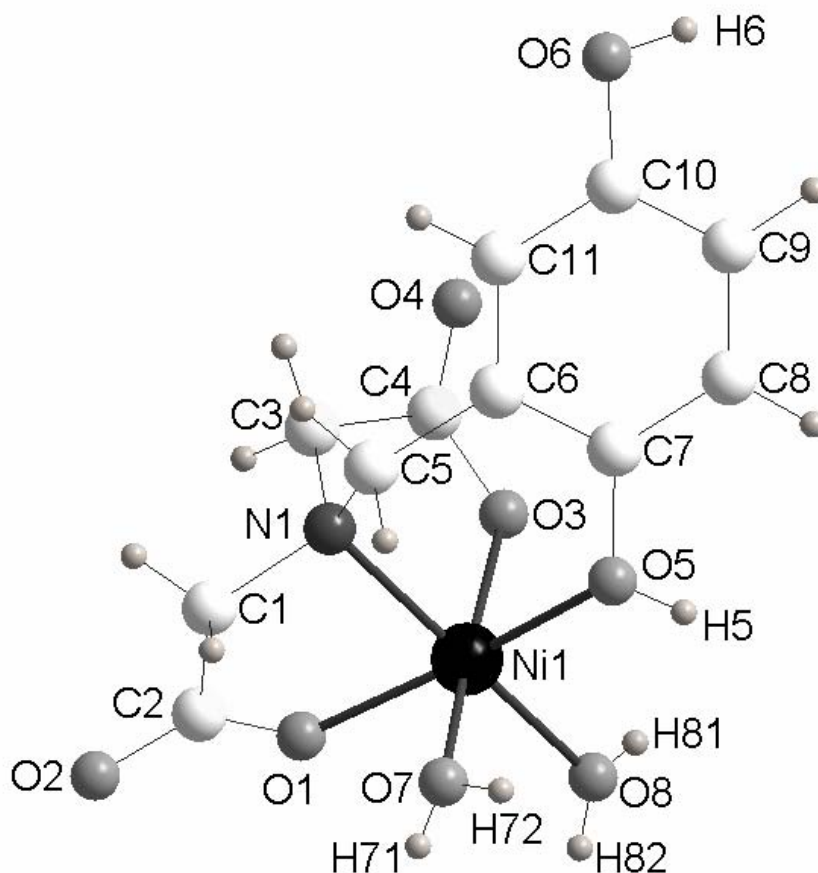
**5.17 Structure of  $[\text{Ni}(\text{Hhda-OH})(\text{H}_2\text{O})_2]\cdot\text{H}_2\text{O}$ , 17.**

Fig. 55 Structure of the mononuclear complex  $[\text{Ni}(\text{Hhda-OH})(\text{H}_2\text{O})_2]\cdot\text{H}_2\text{O}$ , 17.

This monomer was also obtained at  $\text{pH} = 4$ . The Ni atom is coordinated with an octahedron of 5 oxygen atoms and one nitrogen. The phenol groups are not deprotonated and only one carboxylic acid group loses a proton. More base could lead to oligomeric structures, but only powders and black and red solutions were obtained.

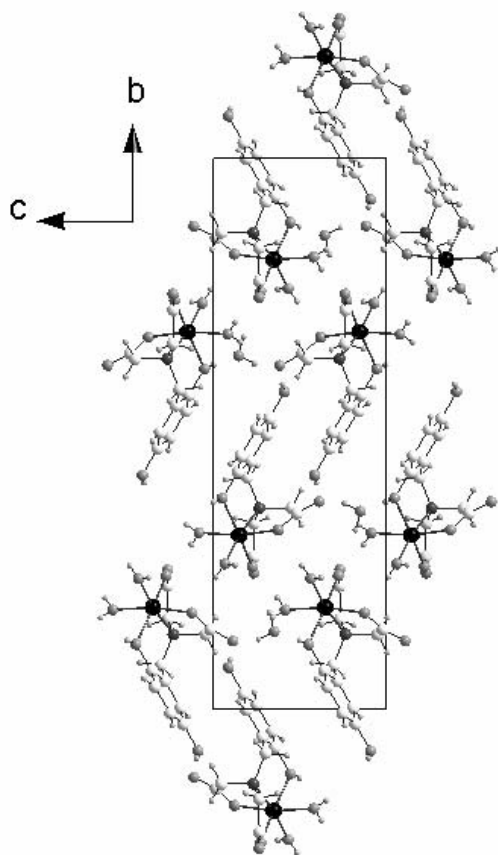
**Structure packing of  $[\text{Ni}(\text{Hhda-OH})(\text{H}_2\text{O})_2]\cdot\text{H}_2\text{O}$ , 18.**

Fig. 56 View of the molecular packing in  $[\text{Ni}(\text{hda-OH})(\text{H}_2\text{O})_2]\cdot\text{H}_2\text{O}$  down the **a**-axis.

The view down the **c**-axis shows isolated monomers that are ordered in rows. The shortest Ni-Ni-displacement amounts to 5.08 Å. The view down the **a**-axis shows isolated pairs of monomers that enclose a cavity. The Ni-Ni-displacement in the cavity amounts to 10.998 Å. The shortest Ni-Ni-displacement amounts to 5.082 Å. There is a  $\pi$ - $\pi$  stacking with a distance from C10 to C10 of 3.669 Å. The cavity encloses a hydrophobic area and from pair to pair between the Ni-centers there is a hydrophilic area.

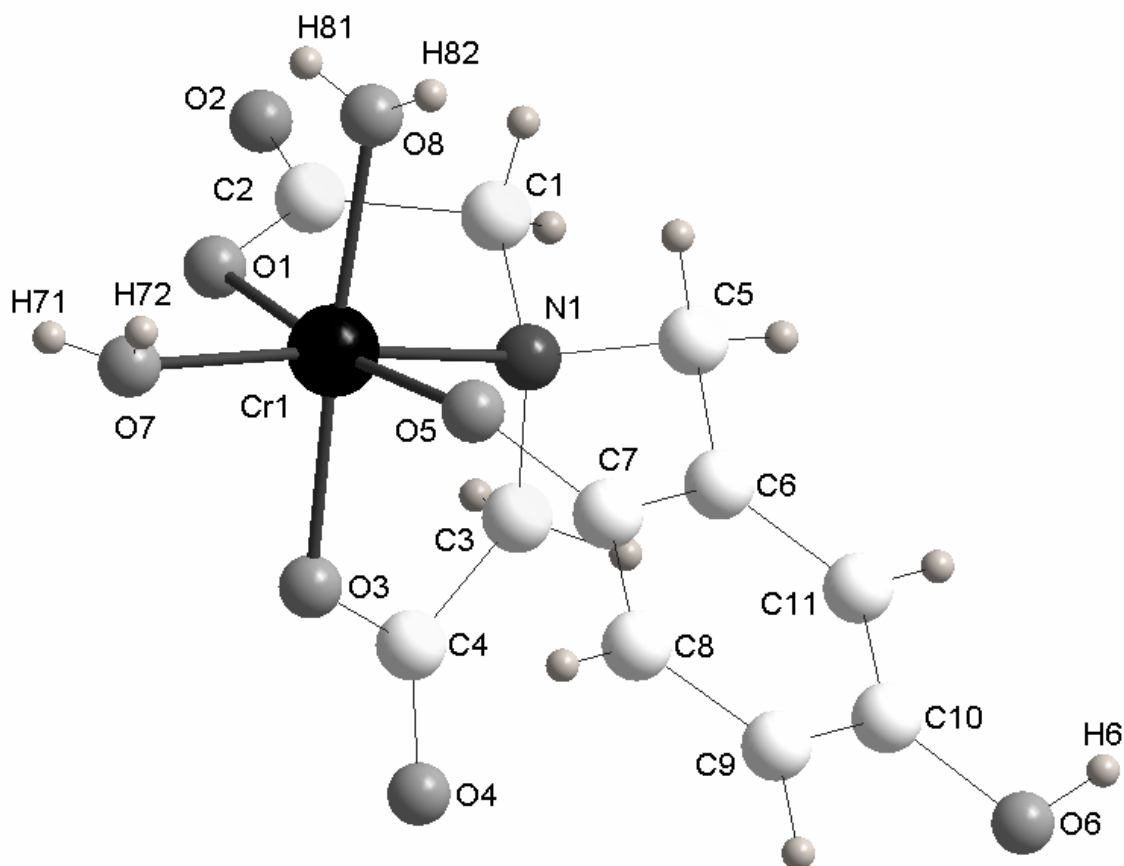
**5.18 Structure of [Cr(hda-OH)(H<sub>2</sub>O)].2H<sub>2</sub>O, 18.**

Fig. 57 View of the molecular packing in [Cr(hda-OH)(H<sub>2</sub>O)].2H<sub>2</sub>O, 18.

Again there is a monomer in the asymmetric unit, which is coordinated as an octahedron with 5 oxygen atoms and one nitrogen atom. This monomer was also obtained at pH = 4. In contrast to 17 the M(III) ion is a strong enough Lewis acid to deprotonate both carboxylic acid groups and the coordinated phenol OH. The ligand is OH. The ligand is tetradentate with 2 water ligands *cis* to each other completing the coordination sphere. This coordination mode is well suited to the stabilization of a quinone type radical and some evidence was seen for this in a reaction using argon as an inert gas resulting in a colourless solution and instable red crystals forming. With addition of ethylene diamine instead of KOH the OH-group is protonated and doesn't coordinate with the metal, while in 17 the protonated OH-group coordinates the Ni-center. Only one single crystal was obtained with this type of ligand to date [2]. Chinese scientists claim, this type of ligand could be used in the leukemia therapy [78].

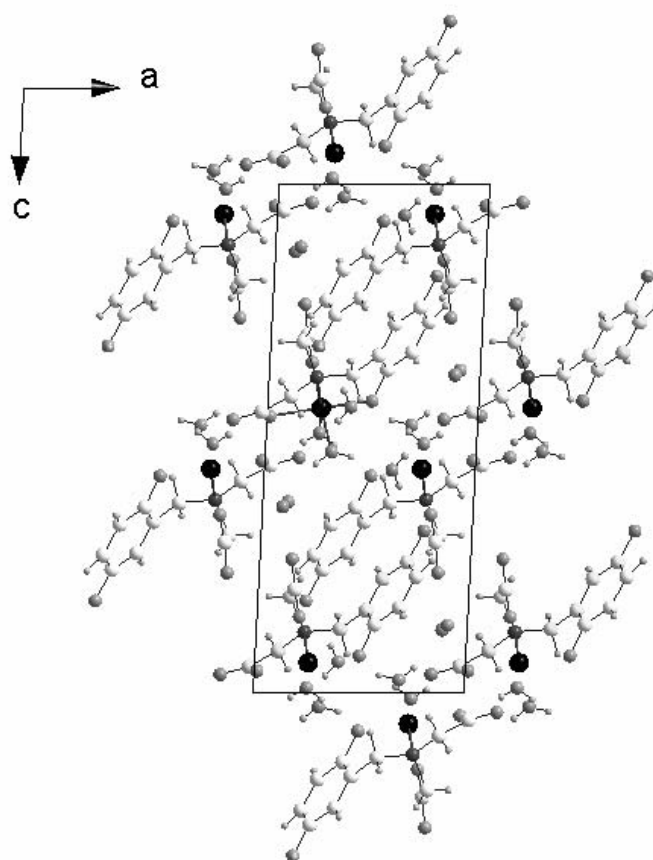
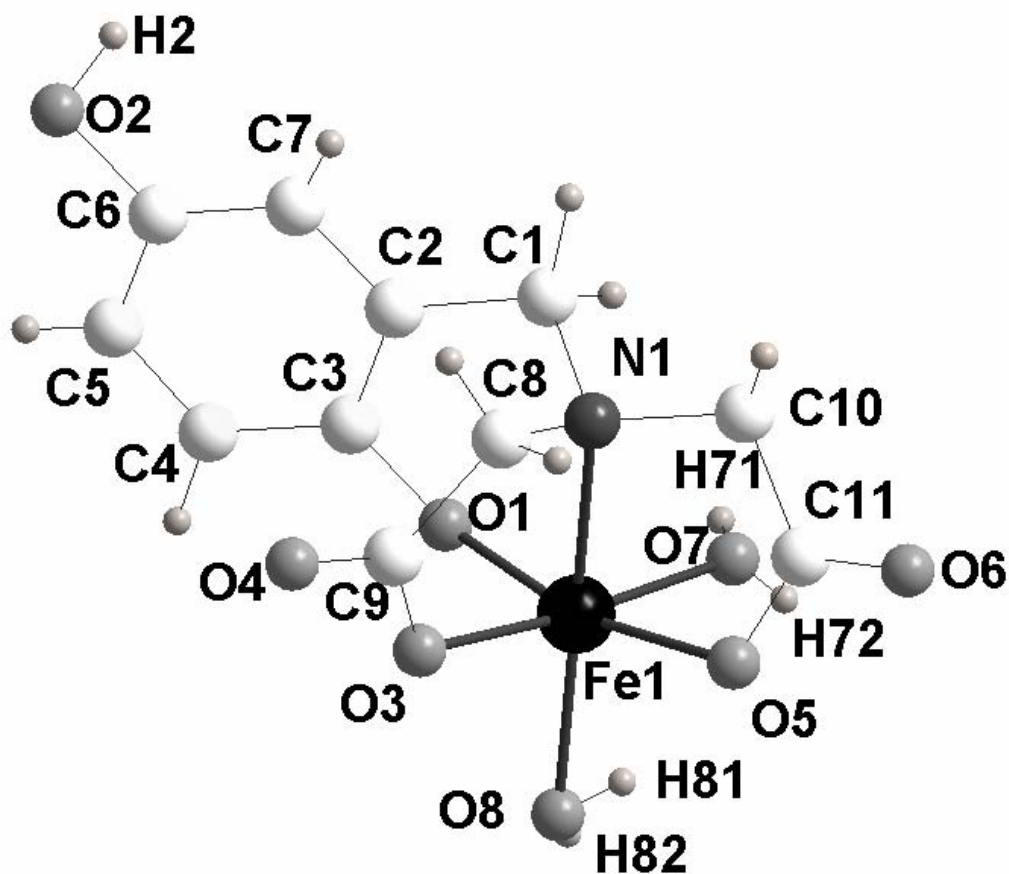
**Structure packing of [Cr(hda-OH)(H<sub>2</sub>O)].2H<sub>2</sub>O, 18.**

Fig. 58 View of the molecular packing in [Cr(hda-OH)(H<sub>2</sub>O)].2H<sub>2</sub>O down the **b**-axis.

The view down the **b**-axis shows isolated monomers, which are in a chair conformation. The shortest Cr...Cr displacement amounts to 5.12 Å. There are no chains and no  $\pi$ - $\pi$  stacking. The view down the **a**-axis also shows the isolated monomers, that the surrounded by water-molecules. The shortest Cr...Cr displacement amounts to 5.124Å.

The view down the **c**-axis shows isolated monomers. The Cr-atoms are ordered in unconnected pairs in a row, in which the Cr...Cr displacement of the pair corresponds to 9.864Å, and the Cr...Cr displacement to the next row diagonally corresponds to 5.124Å and the Cr...Cr displacement within the row corresponds to 20.333Å.

5.19 Structure of  $[\text{Fe}(\text{hda-OH})(\text{H}_2\text{O})_2]\cdot 2\text{H}_2\text{O}$ , 19.Fig. 59 Structure of the mononuclear complex  $[\text{Fe}(\text{hda-OH})(\text{H}_2\text{O})_2]\cdot 2\text{H}_2\text{O}$ , 19.

Again we see a monomer with the octahedron completed by 2 water-molecules coordinated at the Fe-atom. Thus the Fe(III) is coordinated as an octahedron of 5 oxygens and a nitrogen-atom. In spite of the addition of 4 equivalents of base, the ligand is not completely deprotonated. The structure packing is isomorphic with 18.

With this ligand, further attempts were tried with 8 and 16 equivalents KOH and different ligand: metal mol ratios, but until now only powders and colorless crystals were obtained.

### 5.20 Structure of $K_5[Fe_2(\mu-O)(\mu-NO_3)(SO_3\text{-hda-OH})_2] \cdot 15H_2O$ , 20.

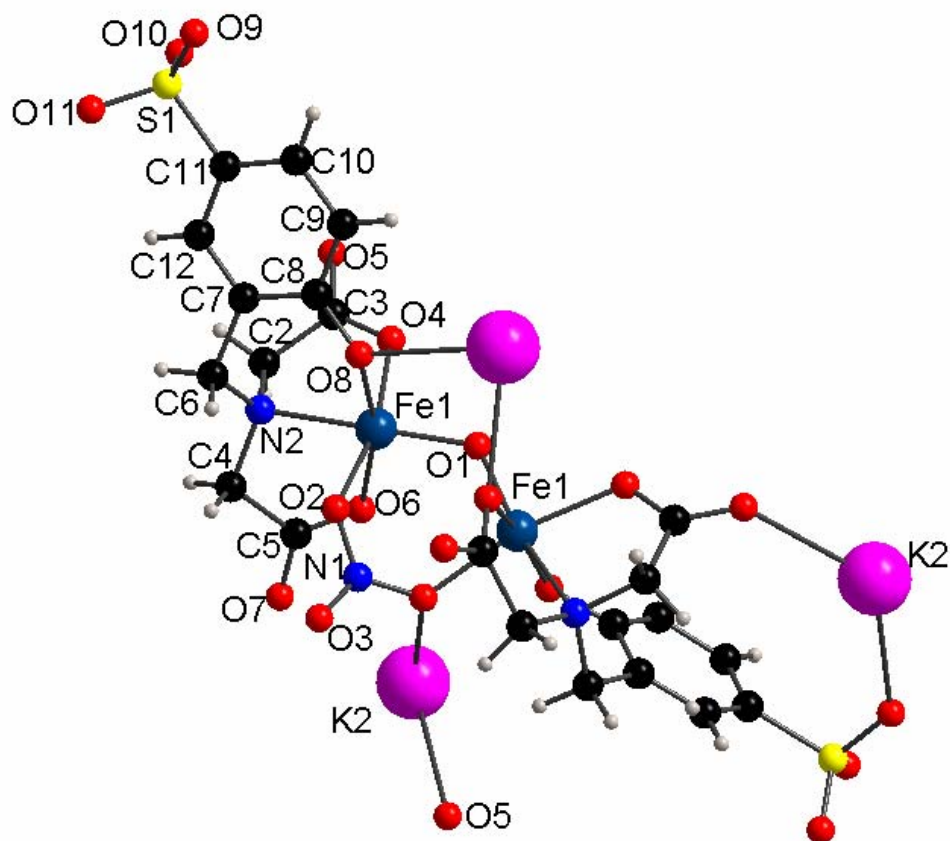


Fig. 60 Structure of the dinuclear complex  $K_5[Fe_2(\mu-O)(\mu-NO_3)(SO_3\text{-hda-OH})_2] \cdot 15H_2O$ , 20.

The asymmetric unit contains a dimeric  $[Fe(III)]_2O$  unit, where each Fe(III) has an octahedron of 5 oxygens and one nitrogen. This compound crystallises in trigonal symmetry with the space group  $P3221$ . The iron atoms are bound by one bridging-nitrate in a 1.3 mode and by one  $\mu$ -oxo-ligand. The Fe atoms are coordinated by one of the two oxygens of the terminal-COOH and by the nitrogen of the carboxymethyl-amino group.

The Fe-O distances are in the order of 1.97-2.03 Å, while the distance Fe-O(19) is only 1.826, shorter than a normal hydroxide bond and typical for an Fe-O-Fe bridge. This compound was produced with 8 equivalents of base. The same product was obtained also with 10 equivalents of KOH. The ligand-metal ratio was varied between 1:1 and 1:4 and every time the same product was isolated. Also, different metal-salt-solutions were added, to try to synthesize a mixed metal-cluster, but no other metal was successfully incorporated into the structure.

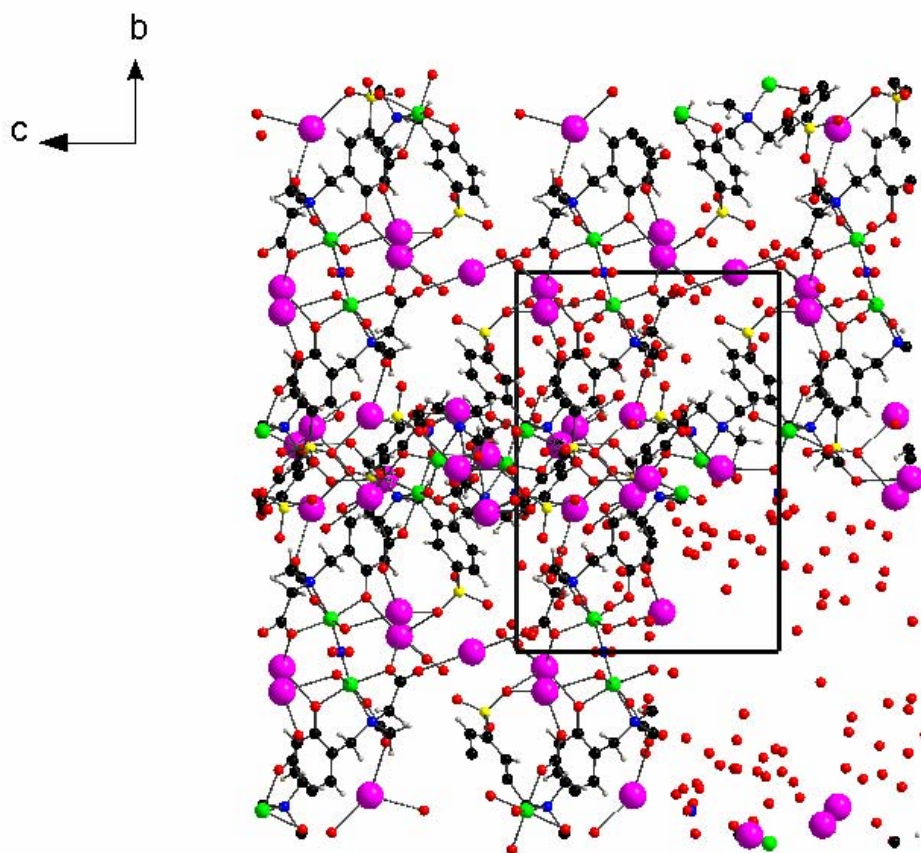
**Structure packing of  $K_5[Fe_2(\mu-O)(\mu-NO_3)(SO_3-hda-OH)_2] \cdot 15H_2O$ , 20.**

Fig. 61 View of the packing in  $K_5[Fe_2(\mu-O)(\mu-NO_3)(SO_3-hda-OH)_2] \cdot 15H_2O$  down the **a**-axis.

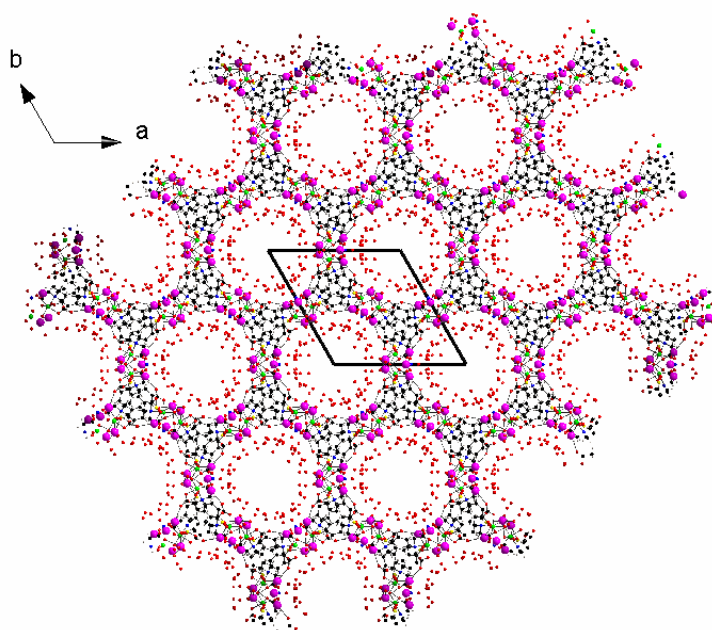


Fig. 62 View of the packing in  $K_5[Fe_2(\mu-O)(\mu-NO_3)(SO_3-hda-OH)_2] \cdot 15H_2O$  down the **c**-axis.

The view down the **a**-axis shows a network structure. The Fe<sup>3+</sup> are shown as bright green so that the Fe-dimers can be seen more clearly. The shortest Fe-Fe-displacement amounts to 3.23 Å, and is consequently sufficiently short in order to evoke magnetic interactions. The Fe-dimers are in the middle of the packing of the **a**-axis. From one dimer to the next dimer of the dimer row in the middle of the packing the Fe-Fe-displacement amounts to 8.873 Å and the Fe-Fe-displacement of the dimer to the next dimer outside of this row in the middle of the packing amounts to 24.246 Å.

The view down the **b**-axis also shows a network structure. The Fe-dimers are ordered in row. The Fe-dimers are arranged in the middle row and from one dimer to the next dimer in the middle row the Fe-Fe-displacement is 11.427 Å and the Fe-Fe-displacement of the dimer to the next dimer outside of this middle amounts to 23.985 Å. So the distances between dimers are different in the packing from the view of the **b**-axis from in the packing from the view of the **a**-axis. The Sulfonate groups hold together the potassium atoms and in this way are the foundation for the formation of the narrower middle dimer row. The Sulfonate groups of the dimer row with larger Fe-Fe-displacements on both sides of the middle dimer row are not coordinated with potassium atoms, so the dimers are further away in this case. The same thing happens with the packing along the **a**-axis. Therefore the sulfonate group “is playing an important role” in the packing to bring the dimers closer to each other. The view down the **c**-axis shows also a network structure. The packing is built of rings connected to each other through the Fe-dimers.

Six Fe-dimers produce the building blocks of each ring and every Fe-dimer lies between 2 rings. The charge balance shows, that the sulphonate and the carboxylate groups are deprotonated and the charges are saturated by K<sup>+</sup> ions, the Fe<sup>3+</sup> are saturated by nitrate and oxo-ligands and by O10 from p-hydroxybenzene-sulphonate group. O12, O8, N11 complete the coordination sphere of Fe<sup>3+</sup>.

The intermolecular connectivity is very interesting because of the presence of 5 potassium ions per molecule of compound, that are partially solvated by crystallisation waters, creating a spectacular packing of the molecules inside the unit cell, with dodecanuclear channels growing around the 3-fold axis, as shown in figure 62. The diameter of channels is about 12 Å.



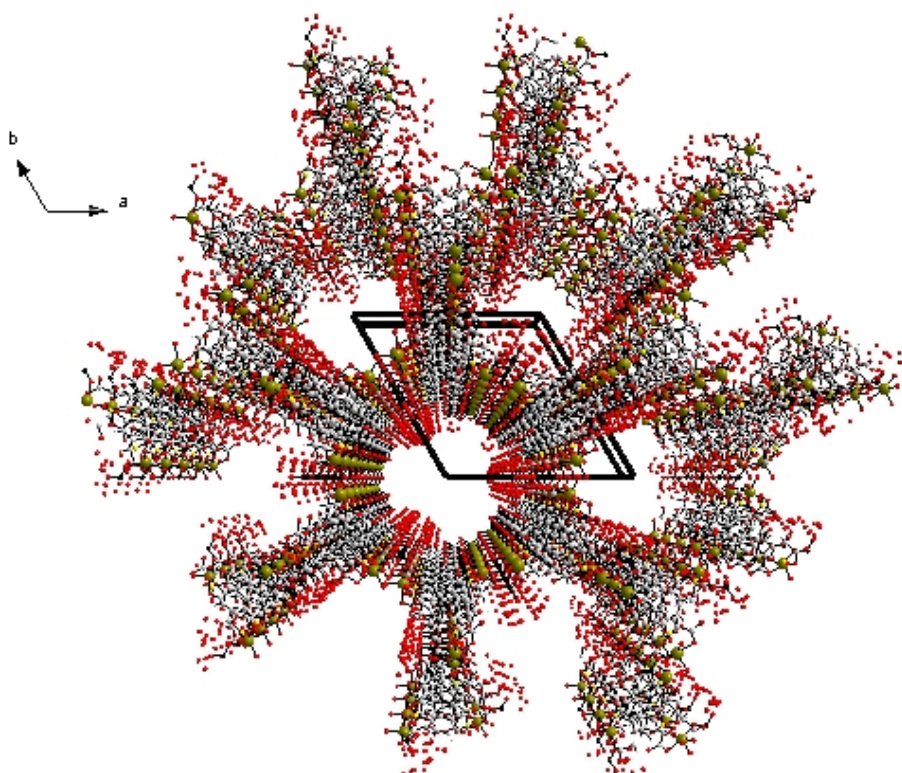


Fig. 63 The packing of the structure for **20** down the *c*-axis 001.

The  $K^+$  ions are coordinated by 8 to 6 oxygens, linked by coordination bonds to sulfonate and carboxylate groups; water molecules complete the coordination sphere in a distorted polyhedron, with distances of the order of 2.76-2.78 Å. K3 is on special position along the  $3_2$  symmetry operator, as shown in figure 63 and links four-half molecules of the compound, allowing the fragment to grow in a “helicoid mode” along the *c*-axis.

K3 is connected to O7 and O13 from two sulphonate groups and to O9 from two carboxylate groups, Ow3 from crystal water complete the coordination sphere (see figure 60).

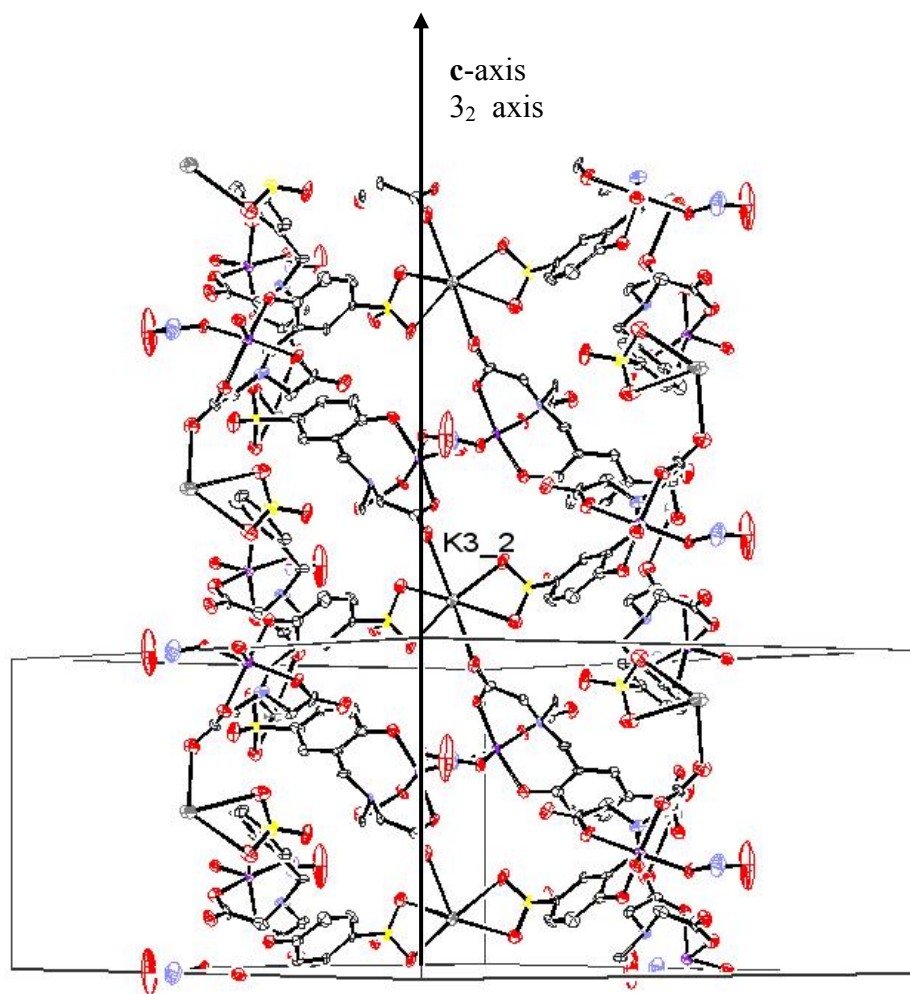


Fig. 63 View of the molecular packing in **20** down the **c**-axis; K3 is on a special position along the  $3_2$  symmetry operator. Waters, K4 and K5 are omitted for clarity.

K4 and K5 are connected by a bridging carboxylate. The distances between the water molecules are about 2.8, 2.9 Å, not allowing strong H-bonds. Because of thermal vibration and disorder the ellipsoids for Ow2, Ow4, Ow6, Ow7 were split into two positions with an half occupancy. The occupancy factor for atom Ow1 and Ow11 was reduced to 0.3333 to model the solvent disorder better; atom Ow11 is inside the channel at distances of 3.1-3.2 Å from other solvent molecules.

### 5.20.1 Magnetic properties of the compound **20**.

A magnetic measurement of the compound  $K_5[Fe_2(\mu-O)(\mu-NO_3)(SO_3-hda-OH)_2] \cdot 15H_2O$  **20** over the temperature range 6-300K was carried out. The curve  $\chi^*T$  versus T in figure 64 decreases from 300K to 50 K linearly and reaches a plateau from 50K to 2K and finally the

curve tends to zero. The decrease of the curve at very low temperature is probably a result of zero field splitting and saturation effects of the impurity.

Dr. Andrea Caneschi (University in Florence) calculated the fit of this measurement on the basis of Van Vleck formula in K, for a spin of  $S=5/2$  for Fe (III) with a paramagnetic impurity. He calculated a value of  $J = -248.7$  K corresponding to  $-173$   $\text{cm}^{-1}$  for  $-2J$ . The value of  $\rho$  the paramagnetic impurity is 0.028. The curve was confirmed by a magnetization experiment which shows that the antiferromagnetic interaction is saturated at  $1600$   $\text{emu}\cdot\text{mol}^{-1}$ .  $\chi^2$  then takes a value of 0.00055 and  $R^2$  is 0.9951. The sample was measured at 10000 Oe. The molar magnetic susceptibility was calculated using the following equation [44].

$$\chi = (\text{Ng}^2\beta^2/\text{kT}) * (\text{e}^x + 5\text{e}^{3x} + 14\text{e}^{6x} + 30\text{e}^{10x} + 55\text{e}^{15x} / 1 + 3\text{e}^x + 5\text{e}^{3x} + 7\text{e}^{6x} + 9\text{e}^{10x} + 11\text{e}^{15x})$$

With  $x = J/\text{kT}$ .

This is valid for a Hamiltonian describing the isotropic interaction for any pair of interacting magnetic centers with local spins  $S_a$  and  $S_b$ , provided that the local states have no first-order angular momentum.

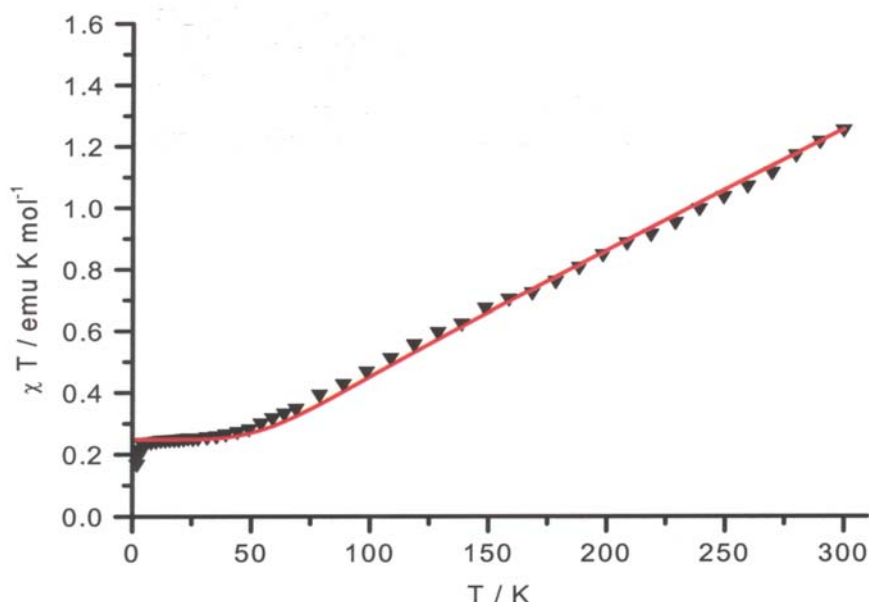


Fig. 64 The  $\chi^*T$  versus T plot for compound 20.

From the data on 36 Fe(III) dimers of the type of  $\{\text{Fe}_2\text{O}(\text{OOCR})_2(\text{Ligand})_2\}$  it has been shown that Fe-O-Fe angles between  $101$ - $105^\circ$  give J values of  $15$ - $20$   $\text{cm}^{-1}$  [106]. While with

other complexes of the type  $[\text{Fe}_2\text{O}(\text{Ligand})_2]$  [107] the Fe-O-Fe angles lie between  $129\text{-}123^\circ$  and the J - values lie between  $124$  and  $132\text{ cm}^{-1}$ , there is no correlation between J and the angle. Instead if the J-value increases, the P-value (shortest Fe-O-distance) decreases. The parameter P represents the average of the shortest distance between the metals and the bridging atoms which are part of the superexchange pathway between the two metals. A relationship exists between P and J, namely  $J = A\exp(BP)$  with  $A = 8.763 \times 10^{11}$  and  $B = -12.633$ , but this is only valid for carboxylate bridged systems [107].

In compound **20** the angle Fe-O-Fe has  $123.3^\circ$ , the Fe...Fe distance is  $3.23\text{ \AA}$ , the P-value  $1.835\text{ \AA}$  and the J value correspond to  $-86.5\text{ cm}^{-1}$ . This J-value is similar to that of  $J = -87.0\text{ cm}^{-1}$  for  $\{\text{Fe}_2\text{O}[\text{O}_2\text{PO}(\text{OPh})]_2(\text{Me}_3\text{TACN})_2\}^{2+}$  ( $\text{Me}_3\text{TACN} = 1,4,7\text{-trimethyl-}1,4,7\text{-triazacyclononane}$ ), where the Fe...Fe distance  $3.198\text{ \AA}$ , the P-value  $1.817\text{ \AA}$  and the Fe-O-Fe angle is  $123.2^\circ$  [107].

## Chapter Six: Synthetic Methods.

### 6.1 Organic synthesis.

#### 6.1.1 Synthesis of the ligand L1.

**L1** was synthesized according to a reported method [48]. A solution containing di-2-pyridylketone (1.055 g, 5.72 mmol) and 1,3-diaminopropane (0.424 g, 5.72 mmol) was heated in 100 ml acetonitrile under reflux for 18 h. The solvent was removed by rotary evaporation. The product was recrystallized from acetonitrile and dried under vacuum. 0.48 g/ 35 % of a white microcrystalline solid was obtained.

#### 6.1.2 Synthesis of the ligand L2.

A solution containing **L1** (1.989 g, 8.27 mmol) and  $\text{ClCH}_2\text{CO}_2\text{H}$  (1.564 g, 16.55 mmol) in methanol (250 ml) was refluxed for 12 h. The solvent was removed by rotary evaporation and the product was purified by column-chromatography on silica gel using methanol:hexane (1:1). The product was obtained from the first phase. Yield: 1.06 g/ 36 %.  $^1\text{H}$  NMR in ppm ( $\text{CDCl}_3$ ): 8.7 (2H, d,  $\text{C}_6\text{H}_4$ ), 8.1 (2H, d,  $\text{C}_6\text{H}_4$ ), 7.85 (2H, m,  $\text{C}_6\text{H}_4$ ), 7.45 (2H, m,  $\text{C}_6\text{H}_4$ ), 3.9 (4H, s,  $\text{CH}_2\text{COOH}$ ), 3.3 (6H, m,  $\text{NCH}_2\text{CH}_2$ ).  $^{13}\text{C}$  NMR in ppm ( $\text{CDCl}_3$ ): 193, 155, 150, 137, 126, 125, 50, 45, 37, 25. IR KBr disc ( $\text{cm}^{-1}$ ): 3230 (br), 1586 (br), 1430 (br), 1202 (sp), 1114 (sp), 991 (sp), 938 (sp), 710 (br).

#### 6.1.3 Synthesis of the ligand L3.

This was synthesized according to a reported method [108]. 2-vinylpyridine (21 g, 21.5 ml, 0.2 mol), 2-picoline (56.64 g, 60 ml, 0.6 mol), hydroquinone (5 mg, 0.045 mmol) and potassium (0.25 g/ 6.4 mmol) were mixed in toluene (20 ml) under an  $\text{N}_2$ -atmosphere and refluxed for 2 h. Isopropanol was added to remove the excess potassium. The oily orange product was washed with water and an aqueous  $\text{Na}_2\text{S}_2\text{O}_5$  solution. Excess solvent was removed by rotary evaporation. The product was triturated with acetone and isolated as a oil. Yield: 0.83 g/ 2.1 %.  $^1\text{H}$  NMR in ppm ( $\text{DMSO}-d_6$ ): 8.4 (2H, d,  $\text{C}_6\text{H}_4$ ), 7.6 (2H, d,  $\text{C}_6\text{H}_4$ ), 7.2 (4H, m,  $\text{C}_6\text{H}_4$ ), 2.7 (4H, t,  $\text{ArCH}_2$ ), 2.1 (2H, m,  $\text{ArCH}_2\text{CH}_2$ ).  $^{13}\text{C}$  NMR in ppm ( $\text{DMSO}-d_6$ ): 161.5, 149, 136, 123, 121.

#### 6.1.4 Synthesis of the ligand L13. [109]

A solution containing iminodiacetic acid (11.71 g, 0.09 mol) in water (30-40 ml) was neutralized to pH 7-8 using 40% NaOH. This was then added dropwise to 65% 4-hydroxybenzenesulfonic acid (21.43 g, 0.08 mol) in acetic acid (150 ml). To the resulting suspension one equivalent of 37% formaldehyde (6.5 g, 0.08 mol) was added drop wise. The mixture was heated for 3 h at 70°C before cooling to room temperature. Ethanol (1.2 l) was added to the yellow solution causing a white product to precipitate. The filtered product was washed with ethanol and dried at the air, because it was very sticky. Yield: 20.30 g/ 62 %. <sup>1</sup>H NMR in ppm (D<sub>2</sub>O): 7.9 (1H, (s), C<sub>6</sub>H<sub>3</sub>), 7.7 (1H, d, C<sub>6</sub>H<sub>3</sub>), 7.1 (1H, d, C<sub>6</sub>H<sub>3</sub>), 3.9 (4H, (s), NCH<sub>2</sub>COOH), 3.8 (2H, (s), ArCH<sub>2</sub>). <sup>13</sup>C-NMR in ppm (D<sub>2</sub>O): 170, 135, 130-115, 159, 56, 47.

### 6.2 Inorganic synthesis.

#### 6.2.1 [CuBr<sub>2</sub>(C<sub>14</sub>H<sub>16</sub>N<sub>4</sub>)] 1

A solution containing L1 (0.069 g, 0.287 mmol) and CuBr<sub>2</sub> (0.064 g, 0.287 mmol) in acetonitrile (40 ml) was heated with stirring. Slow evaporation of the resulting solution produced green crystals after a week. Yield: 0.0066 g/ 5 %. (based on the ligand) The infrared was not measured, because there was insufficient amount of product.

#### 6.2.2 [CuCl<sub>2</sub>(C<sub>14</sub>H<sub>16</sub>N<sub>4</sub>)]·H<sub>2</sub>O 2

A solution containing L1 (0.130 g, 0.54 mmol) and CuCl<sub>2</sub>·2H<sub>2</sub>O (0.092 g, 0.54 mmol) in methanol (20 ml) was heated with stirring. Slow evaporation of the resulting solution produced green crystals after a week (0.0046 g/ 5 %). (Yield based on the ligand) The infrared was not measured, because there was insufficient amount of product.

#### 6.2.3 [Cu(C<sub>14</sub>H<sub>16</sub>N<sub>4</sub>)<sub>2</sub>]Br<sub>2</sub>·2MeOH 3

A solution containing L1 (0.032 g, 0.133 mmol) and CuBr<sub>2</sub> (0.021 g, 0.094 mmol) in acetonitrile (40 ml) was heated with stirring. Slow evaporation of the resulting solution produced green crystals after a week. Yield (based on the ligand): 0.0102 g/ 5 %. The infrared was not measured, because there was insufficient amount of product.

**6.2.4**  $[\text{CuCl}_2(\text{C}_{12}\text{H}_{12}\text{N}_2\text{O}_2)]$  4

A solution containing **L1** (2.65 g, 9.53 mmol) and  $\text{CuCl}_2 \cdot 2\text{H}_2\text{O}$  (0.276 g, 1.61 mmol) in methanol (20 ml) was heated with stirring. Slow evaporation of the resulting solution produced green crystals after a week. Yield (based on the ligand): 0.083 g/ 2.5 %. The infrared was not measured, because there was insufficient amount of product.

**6.2.5**  $[\text{Cu}_2\text{Cl}_4(1,3\text{-dpp})_2] \cdot \text{H}_2\text{O}$  5

A solution containing **L3** (0.124 g, 0.626 mmol) and  $\text{CuCl}_2 \cdot 2\text{H}_2\text{O}$  (0.214 g, 1.25 mmol) in methanol (20 ml) was heated with stirring. The product was filtered off and dissolved in distilled water. Slow evaporation of the resulting solution produced black crystals after 4 weeks. Yield (based on the ligand): 0.064 g/ 15 %. IR KBr disc ( $\text{cm}^{-1}$ ): 3443 (br), 1607 (s), 1571 (s), 1491 (s), 1428 (s), 1384 (w), 1160 (m), 1110 (w), 1065 (w), 1028 (m), 775 (s), 653 (w), 440 (m).

**6.2.6**  $[\text{Cu}_2(\text{OAc})_4(\text{C}_4\text{H}_4\text{N}_3\text{Br})]_{\infty}$  6

To a solution containing **L9** (0.128 g, 0.735 mmol),  $\text{Cu}(\text{NO}_3)_2 \cdot 3\text{H}_2\text{O}$  (0.177 g, 0.180 mmol) and  $\text{Cr}(\text{NO}_3)_3 \cdot 9\text{H}_2\text{O}$  (0.299 g, 0.747 mmol) in methanol (40 ml) was added KOH (2.5 ml, 1M) and glacial acetic acid (2.5 ml). Slow evaporation of the resulting solution produced blue crystals after a week. Yield (based on the ligand): 0.216 g/ 55%. IR KBr disc ( $\text{cm}^{-1}$ ): 3369 (br), 3221 (m), 1615 (s), 1564 (m), 1436 (s), 1384 (w), 1326 (w), 1223 (m), 825 (w), 792 (w), 687 (w), 671 (w), 627 (w).

**6.2.7**  $[\text{Cu}_2(\text{OAc})_4(\text{C}_4\text{H}_4\text{N}_3\text{Br})_2]$  7

To a solution containing **L9** (0.079 g, 0.453 mmol),  $\text{Cu}(\text{NO}_3)_2 \cdot 3\text{H}_2\text{O}$  (0.110 g, 0.453 mmol) and  $\text{Ni}(\text{NO}_3)_2 \cdot 6\text{H}_2\text{O}$  (0.139 g, 0.477 mmol) in methanol (40 ml) was added KOH (2.5 ml, 1M) and glacial acetic acid (2.5 ml). Slow evaporation of the resulting solution produced blue crystals after a week. Yield (based on the ligand): 0.288 g/ 45%. IR KBr disc ( $\text{cm}^{-1}$ ): 3366 (m), 3220 (m), 1614 (s), 1436 (s), 1223 (w), 1139 (w), 825 (w), 792 (w), 682 (w), 623 (w), 498 (w).

**6.2.8  $\text{K}_4[\text{Cu}(\text{OAc})_6(\text{HOAc})_4]$  8**

To a solution containing **L10** (0.070 g, 0.233 mmol),  $\text{Cu}(\text{NO}_3)_2 \cdot 3\text{H}_2\text{O}$  (0.057 g, 0.235 mmol) and  $\text{Ni}(\text{NO}_3)_2 \cdot 6\text{H}_2\text{O}$  (0.063 g, 0.216 mmol) in methanol (40 ml) was added KOH (2.5 ml, 1M) and glacial acetic acid (2.5 ml). Slow evaporation of the resulting solution produced blue crystals after a week. Yield (based on Cu): 0.032 g/ 57% IR KBr disc ( $\text{cm}^{-1}$ ): 3441 (br), 1566 (s), 1417 (s), 1280 (w), 1020 (w), 929 (w), 666 m.

**6.2.9  $[\text{Cu}_2(\text{OAc})_4\text{MnCl}_2(\text{H}_2\text{O})_4]_\infty$  9**

To a solution containing  $\text{Cu}(\text{NO}_3)_2 \cdot 3\text{H}_2\text{O}$  (0.261 g, 1.08 mmol) and  $\text{MnCl}_2 \cdot 2\text{H}_2\text{O}$  (0.183 g, 1.13 mmol) in methanol (40 ml) was added KOH (2.5 ml, 1M) and glacial acetic acid (2.5 ml). Slow evaporation of the resulting solution produced green-blue crystals after a week. Yield (based on the Cu): 0.169 g/ 65%. IR KBr disc ( $\text{cm}^{-1}$ ): 3417 (s), 1613 (s), 1384 (s), 1114 (w), 1047 (w), 689 (w), 625 (w).

**6.2.10  $\text{K}[\text{Cu}(\text{ida})\text{Cl}(\text{H}_2\text{O})_2]$  10**

To a solution containing **L5** (0.278 g, 2.08 mmol),  $\text{NiSO}_4 \cdot 6\text{H}_2\text{O}$  (0.182 g, 0.69 mmol) and  $\text{CuCl}_2 \cdot 2\text{H}_2\text{O}$  (0.118 g, 0.69 mmol) in distilled water (20 ml) was added KOH until pH 7. Slow evaporation of the resulting solution produced blue crystals after 4 weeks. Yield (based on the ligand): 0.066 g/ 10.5 %. The infrared was not measured, because there was insufficient amount of product.

**6.2.11  $\text{K}[\text{Cr}(\text{Hedta})\text{Cl}] \cdot \text{H}_2\text{O}$  11**

To a solution containing **L5** (0.542 g, 1.85 mmol),  $\text{NiSO}_4 \cdot 6\text{H}_2\text{O}$  (0.247 g, 0.927 mmol) and  $\text{CrCl}_3 \cdot 6\text{H}_2\text{O}$  (0.247 g, 0.927 mmol) in distilled water (20 ml) was added KOH until pH 4. Slow evaporation of the resulting solution produced blue crystals after 4 weeks. Yield (based on the ligand): 0.053 g/ 6.6 %. The infrared was not measured, because there was insufficient amount of product.



**6.2.12 [CuCl(H<sub>3</sub>edta)].2H<sub>2</sub>O 12**

A solution containing **L6** (0.523 g, 1.78 mmol) and CuCl<sub>2</sub>·2H<sub>2</sub>O (0.917 g, 5.36 mmol) in distilled water (20 ml) was refluxed for 30 min. Slow evaporation of the resulting solution produced blue crystals after 4 weeks. Yield (based on the ligand): 0.273 g/ 36 %. IR KBr disc (cm<sup>-1</sup>): 3444 (br), 2769 (s), 2624 (s), 2568 (s), 1968 (s), 1723 (s), 1566 (s), 1459 (s), 1417 (s), 1368 (m), 1323 (m), 1299 (s), 1256 (s), 1231 (s), 1110 (w), 1028 (w), 1008 (w), 985 (w), 960 (w), 911 (w), 856 (w), 820 (w), 784 (w), 744 (w), 729 (w), 695 (w), 660 (w), 620 (w), 552 (w), 522 (w), 475 (w).

**6.2.13 [Cu(Hada)<sub>2</sub>] 13**

To a solution containing **L7** (0.1 g, 0.525 mmol), Cu(NO<sub>3</sub>)<sub>2</sub>·3H<sub>2</sub>O (0.042 g, 0.175 mmol), and CrCl<sub>3</sub>·6H<sub>2</sub>O (0.028 g, 0.175 mmol) in distilled water (20 ml) was added KOH until pH 3. Slow evaporation of the resulting solution produced blue crystals after 4 weeks. Yield (based on the ligand): 2.086 g/ 45 %. IR KBr disc (cm<sup>-1</sup>): 3433 (s), 1729 (s), 1650 (s), 1586 (s), 1403 (s), 1215 (s), 1109 (m), 977 (m), 717 (w), 646 (w).

**6.2.14 [Cr(ada)<sub>2</sub>](pyrH).3H<sub>2</sub>O 14**

A solution containing **L7** (0.423 g, 2.22 mmol) and CrCl<sub>3</sub>·6H<sub>2</sub>O (0.149 g, 0.559 mmol) and pyridine (2 ml) in distilled water (20 ml) was refluxed for 30 min. Slow evaporation of the resulting solution produced blue crystals after 4 weeks. Yield (based on the ligand): 0.698 g/ 28 %. IR KBr disc (cm<sup>-1</sup>): 3427 (br), 2034 (w), 1638 (s), 1618 (s), 1489 (w), 1445 (w), 1384 (w), 1220 (w), 1113 (w), 988 (w), 617 (w).

**6.2.15 {(pyrH)[Cu(heidi)(pyr)]Cl.2H<sub>2</sub>O}<sub>∞</sub> 15**

A solution containing **L8** (0.162 g, 0.914 mmol), CuCl<sub>2</sub>·2H<sub>2</sub>O (0.155 g, 0.914 mmol) and pyridine (1 ml) in distilled water (7 ml) was prepared with pH 6. Slow evaporation of the resulting solution produced blue crystals after 3 weeks. Yield (based on the ligand): 1.501 g/ 35 %. IR KBr disc (cm<sup>-1</sup>): 3555 (br), 1650 (s), 1524 (m), 1478 (m), 1388 (m), 1050 (w), 745 (w), 674 (w).

**6.2.16 [Cu(naphthyl-OH-ida)(H<sub>2</sub>O)] 16**

A solution containing 0.162g of a mononuclear Mn-L11 complex (synthesized by Dr. J. Hill) and CuCl<sub>2</sub>·2H<sub>2</sub>O (0.305 g, 1.78 mmol) in 7.5 ml methanol was placed in a 10 ml autoclave. This was heated at 40°C for 4 h. Slow evaporation of the resulting solution gave light-blue crystals after 4 weeks. Yield (based on the Cu): 0.075 g/ 25%. IR KBr disc (cm<sup>-1</sup>): 3343 (br), 3220 (m), 2930 (m), 1600 (s), 1578 (s), 1517 (m), 1444 (m), 1396 (m), 1360 (m), 1310 (m), 1275 (m), 1241 (w), 1177 (w), 1147 (w), 1125 (w), 1072 (w), 1044 (w), 1081 (w), 985 (w), 944 (w), 921 (w), 898 (w), 856 (w), 813 (w), 784 (w), 742 (w), 717 (w), 641 (w), 596 (w), 535 (w), 495, 463 (w), 412 (w).

**6.2.17 [Ni(hda-OH)(H<sub>2</sub>O)<sub>2</sub>].H<sub>2</sub>O 17**

To a solution containing L12 (0.117 g, 0.46 mmol) and NiSO<sub>4</sub>·6H<sub>2</sub>O (0.079 g, 0.3 mmol) in distilled water (40 ml) was added KOH until pH 4. Slow evaporation of the resulting solution produced green crystals after 4 weeks. Yield (based on the ligand): 0.075 g/ 45 %. IR KBr disc (cm<sup>-1</sup>): 3550 (s), 3416 (s), 3235 (s), 1637 (s), 1617 (s), 1586 (s), 1514 (m), 1408 (m), 1227 (w), 1121 (w), 978 (w), 910 (w), 814 (w), 622 (w).

**6.2.18 [Cr(hda-OH)(H<sub>2</sub>O)].2H<sub>2</sub>O 18**

To a solution containing L12 (0.107 g, 0.42 mmol) and CrCl<sub>3</sub>·6H<sub>2</sub>O (0.073 g, 0.274 mmol) in distilled water (40 ml) was added KOH until pH 4. Slow evaporation of the resulting solution gave red crystals after 4 weeks. Yield (based on the ligand): 0.063 g/ 40 %. IR KBr disc (cm<sup>-1</sup>): 3103 (s), 1660 (s), 1491 (s), 1449 (s), 1364 (s), 1293 (s), 1260 (s), 1217 (s), 1157 (s), 1098 (m), 1076 (m), 1015 (s), 965 (s), 870 (s), 845 (s), 669 (s), 600 (s), 526 (s), 489 s.

**6.2.19 [Fe(hda-OH)(H<sub>2</sub>O)<sub>2</sub>].2H<sub>2</sub>O 19**

To a solution containing L12 (0.128 g, 0.5 mmol), Cu(NO<sub>3</sub>)<sub>2</sub>·3H<sub>2</sub>O (0.258 g, 0.638 mmol) and NiSO<sub>4</sub>·6H<sub>2</sub>O (0.161 g, 0.612 mmol) in methanol (40 ml) was added KOH (2ml, 1M) to give pH 4. The solution was gently heated for 20 min. Slow evaporation gave brown crystals after a week. Yield (based on the ligand): 0.066 g/ 35 %. IR KBr disc (cm<sup>-1</sup>): 3415 (br), 1638 (s), 1491 (m), 1451 (m), 1384 (s), 1363 (s), 1258 (m), 1220 (m), 1203 (m), 1158 (w), 1114 (w), 1013 (w), 967 (w), 925 (w), 869 (w), 805 (w), 669 (w), 481 (w).

**6.2.20  $\text{K}_5[\text{Fe}_2(\mu\text{-O})(\mu\text{-NO}_3)(\text{SO}_3\text{-hda-OH})_2] \cdot 15\text{H}_2\text{O}$  20**

A solution containing **L13** (0.464 g, 1.13 mmol) and KOH (4 ml, 2M) in methanol (10 ml) was added dropwise to  $\text{Fe}(\text{NO}_3)_3 \cdot 9\text{H}_2\text{O}$  (0.206 g, 0.5 mmol) and  $\text{MnCl}_2 \cdot 2\text{H}_2\text{O}$  (0.325 g, 2.0 mmol) in methanol (10 ml). The filtered solution was slowly evaporated giiving brown crystals after 3 weeks. Yield (based on the ligand): 1.306 g/ 45 %. IR KBr disc ( $\text{cm}^{-1}$ ): 3475 (br), 2576 (m), 1610 (s), 1480 (s), 1385 (s), 1295 (s), 1213 (s), 1183 (s), 1132 (s), 1104 (s), 1034 (s), 977 (w), 934 (w), 916 (w), 861 (w), 833 (w), 794 (w), 746 (w), 724 (w), 665 (w), 610 (s), 549 (w), 517 (w), 414 (w).

## Chapter Seven: Experimental methods

### 7.1 X-ray-diffraction on single crystals.

The structural characterization of the compounds in this work was carried out on a Stoe IPDS or a Bruker SMART Apex area-detector diffractometer using graphite-monochromated Mo- $K_{\alpha}$  radiation ( $\lambda = 0.71069 \text{ \AA}$ ). Structures were solved by direct methods and refined using the full-matrix least-squares package. The function minimized was:

$$wR2 = (\{\sum[\omega(F_0^2 - F_c^2)]\} / \sum |F_0^2|)^{1/2} \quad (15)$$

with

$$1/w = \sigma^2(F_0^2) + (aP)^2 + bP \quad (16)$$

where

$$P = [\text{Max}(F_0^2, 0) + 2F_c^2] / 3 \quad (17)$$

and

$$R_1 = [\sum |F_0^2 - F_c^2| / \sum |F_0^2|] \quad (18)$$

The goodness of the fit  $S$  is defined as:

$$S = [\sum w(F_0^2 - F_c^2)^2 / (n-p)]^{1/2} \quad (19)$$

where  $n$  is the number of reflections and  $p$  is the total number of parameters refined. On completion of the refinement, a conventional  $R$  was calculated for reflections with  $I \geq 2\sigma(z)$ .

### 7.2 FT-IR Spectroscopy

KBr was mixed with the sample in a ratio of approximately 100:1 and ground together and pressed under a pressure of approximately 7 tonnes to transparent pellets. The spectra were measured on a Perkin Elmer Spectra one in transmissions over the range of  $400 \text{ cm}^{-1}$  to  $4000 \text{ cm}^{-1}$ . The resolution of the spectra was  $4 \text{ cm}^{-1}$ .

### 7.3 FT-NMR spectroscopy

The  $^1\text{H}$ -NMR spectra were measured on a *Bruker* AC 250 at 250.133 MHz (NMR) and the  $^{13}\text{C}$ -NMR spectra on a *Bruker* AMX 300 at 62.896 MHz. 5 mm NMR tubes were filled with

---

saturated solutions in deuterated solvents to depth of 6 cm. Measurements were recorded at room temperature. The chemical shifts given according to the  $\delta$ -scale in ppm.

#### **7.4 Elemental Analysis**

The C, H and N elemental analysis was performed using an *Elementar Vario EL* analyzer at the University of Karlsruhe (TH).

#### **7.5 Magnetic Measurements**

The measurement of the magnetic properties of the compounds took place with a *Cryonic S600 SQUID-Magnetometer* at 6.5 T at the University in Florence. The measurements were performed on pure crystalline samples. The magnetic data were corrected for the sample holder and the magnetic contribution calculated from Pascal's constants.

## Chapter Eight: Crystallographic data

Table 1: Crystallographic Data

Compound	<b>1</b>	<b>2</b>	<b>3</b>
Formula	C <sub>14</sub> H <sub>16</sub> Br <sub>2</sub> CuN <sub>4</sub>	C <sub>14</sub> H <sub>18</sub> Cl <sub>2</sub> CuN <sub>4</sub> O	C <sub>30</sub> H <sub>40</sub> Br <sub>2</sub> CuN <sub>8</sub> O <sub>2</sub>
Formula weight	463.67	350.68	768.06
Crystal System	Monoclinic	Monoclinic	Monoclinic
Space Group	C2/c	I2/a	P2 <sub>1</sub> /c
<i>a</i> / Å	21.111(3)	13.9715(8)	10.0434(18)
<i>b</i> / Å	11.8661(13)	9.0809(3)	12.576(2)
<i>c</i> / Å	17.2669(19)	20.6710(11)	13.218(2)
$\alpha$ / °	90	90	90
$\beta$ / °	125.451(2)	90.330(7)	106.225(3)
$\gamma$ / °	90	90	90
<i>U</i> / Å <sup>3</sup>	3523.6(7)	2622.6(2)	1603.0(5)
<i>Z</i>	8	4	2
T / K	200	200	200
<i>F</i> (000)	1816	1416	782
<i>D</i> <sub>c</sub> / Mg m <sup>-3</sup>	1.748	1.776	1.591
$\mu$ (Mo-K $\alpha$ ) / mm <sup>-1</sup>	5.774	2.070	3.215
Diffractometer	Bruker Smart Apex	Stoe IPDS	Bruker Smart Apex
Data Measured	8806	7124	7827
Unique Data	3962	2565	3567
<i>R</i> <sub>int</sub>	0.0332	0.0463	0.0256
Observed Data	2.09 to 27.93°	2.68 to 25.97°	2.11 to 27.96°
Parameters/Restraints	254/ 0	220/0	266/ 0
Completeness to 2 $\theta$ = 50°	100.0 %	99.8%	99.8 %
<i>wR</i> <sub>2</sub> , <i>R</i> <sub>1</sub> (all data)	<i>R</i> <sub>1</sub> = 0.0379, <i>wR</i> <sub>2</sub> = 0.0627	<i>R</i> <sub>1</sub> = 0.0440, <i>wR</i> <sub>2</sub> = 0.0809	<i>R</i> <sub>1</sub> = 0.0326, <i>wR</i> <sub>2</sub> = 0.0725
<i>wR</i> <sub>2</sub> , <i>R</i> <sub>1</sub> [ <i>I</i> ≥ 2 $\sigma$ ( <i>I</i> )]	<i>R</i> <sub>1</sub> = 0.0281, <i>wR</i> <sub>2</sub> = 0.0608	<i>R</i> <sub>1</sub> = 0.0330, <i>wR</i> <sub>2</sub> = 0.0784	<i>R</i> <sub>1</sub> = 0.0281, <i>wR</i> <sub>2</sub> = 0.0709
<i>S</i> (all data)	0.928	0.951	1.030
Biggest diff. peak/hole	0.703 and -0.494 e.Å <sup>3</sup>	0.560 and -0.269 e.Å <sup>3</sup>	0.510 and -0.609 e.Å <sup>3</sup>

Table 2: Crystallographic Data

Compound	<b>5</b>	<b>6</b>	<b>7</b>	<b>8</b>
Formula	C <sub>13</sub> H <sub>15</sub> C <sub>12</sub> CuN <sub>2</sub> O <sub>0.50</sub>	C <sub>12</sub> H <sub>14</sub> BrCu <sub>2</sub> N <sub>3</sub> O <sub>8</sub>	C <sub>16</sub> H <sub>20</sub> Br <sub>2</sub> Cu <sub>2</sub> N <sub>6</sub> O <sub>8</sub>	C <sub>20</sub> H <sub>34</sub> CuK <sub>4</sub> O <sub>20</sub>
Formula weight	341.71	535.25	711.28	814.41
Crystal System	orthorhombic	triclinic	triclinic	tetragonal
Space Group	Pnma	P-1	P-1	I-4
<i>a</i> / Å	13.227(3)	8.5614(13)	8.3573(17)	21.3410(18)
<i>b</i> / Å	13.944(3)	8.7329(12)	11.651(2)	21.3410(18)
<i>c</i> / Å	15.136(3)	14.819(2)	14.645(3)	7.4108(6)
$\alpha$ / °	90	93.822(17)	66.72(3)	90
$\beta$ / °	90	106.143(17)	87.82(3)	90
$\gamma$ / °	90	107.812(17)	76.60(3)	90
<i>U</i> / Å <sup>3</sup>	2791.7(10)	999.2(3)	1271.9(4)	3375.2(5)
<i>Z</i>	8	2	2	4
T / K	200	200	200	200
<i>F</i> (000)	1392	528	700	1676
<i>D<sub>c</sub></i> / Mg m <sup>-3</sup>	1.626	1.779	1.857	1.603
$\mu$ (Mo-K $\alpha$ ) / mm <sup>-1</sup>	1.934	4.169	4.864	1.218
Diffractometer	Bruker Smart Apex	Stoe IPDS	Stoe IPDS	Stoe IPDS
Data Measured	12211	6445	8433	6597
Unique Data	2847	3603	4705	3234
<i>R<sub>int</sub></i>	0.1244	0.0542	0.1376	0.0816
Observed Data	1.99 to 26.03°	2.48 to 25.99°	1.94 to 26.18°	2.70 to 26.00°
Parameters/Restraints	184/ 6	244/ 0	323/ 4	213/ 1
Completeness to 2 $\theta$ = 50°	99.1 %	93.7 %	94.3 %	99.8 %
<i>wR<sub>2</sub></i> , <i>R<sub>I</sub></i> (all data)	<i>R</i> <sub>1</sub> = 0.1224, <i>wR</i> <sub>2</sub> = 0.0912	<i>R</i> <sub>1</sub> = 0.0706, <i>wR</i> <sub>2</sub> = 0.1125	<i>R</i> <sub>1</sub> = 0.1651, <i>wR</i> <sub>2</sub> = 0.2349	<i>R</i> <sub>1</sub> = 0.0757, <i>wR</i> <sub>2</sub> = 0.1070
<i>wR<sub>2</sub></i> , <i>R<sub>I</sub></i> [ <i>I</i> ≥ 2 $\sigma$ ( <i>I</i> )]	<i>R</i> <sub>1</sub> = 0.0412, <i>wR</i> <sub>2</sub> = 0.0795	<i>R</i> <sub>1</sub> = 0.0460, <i>wR</i> <sub>2</sub> = 0.1052	<i>R</i> <sub>1</sub> = 0.0889, <i>wR</i> <sub>2</sub> = 0.2047	<i>R</i> <sub>1</sub> = 0.0446, <i>wR</i> <sub>2</sub> = 0.0933
<i>S</i> (all data)	0.673	0.873	0.795	0.852
Biggest diff. peak/hole	0.674 and -0.351 e.Å <sup>3</sup>	1.047 and -0.649 e.Å <sup>3</sup>	1.402 and -0.775 e.Å <sup>3</sup>	0.525 and -0.667 e.Å <sup>3</sup>

Table 3: Crystallographic Data

Compound	<b>9</b>	<b>10</b>	<b>11</b>	<b>12</b>
Formula	C <sub>8</sub> H <sub>20</sub> Cl <sub>2</sub> Cu <sub>2</sub> MnO <sub>12</sub>	C <sub>4</sub> H <sub>9</sub> ClCuKNO <sub>6</sub>	C <sub>10</sub> H <sub>15</sub> ClCrKN <sub>2</sub> O <sub>9</sub>	C <sub>10</sub> H <sub>19</sub> ClCuN <sub>2</sub> O <sub>10</sub>
Formula weight	561.16	305.21	433.79	426.26
Crystal System	Monoclinic	Monoclinic	Triclinic	Orthorhombic
Space Group	P2 <sub>1</sub> /n	P2 <sub>1</sub> /c	P1	P2 <sub>1</sub> 2 <sub>1</sub> 2 <sub>1</sub>
<i>a</i> / Å	8.3226(15)	12.5088(14)	6.5816(14)	7.2107(4)
<i>b</i> / Å	10.7109(14)	6.3889(5)	7.2180(16)	18.3410(13)
<i>c</i> / Å	11.137(2)	12.4659(14)	8.753(2)	24.1302(12)
$\alpha$ / °	90	90	72.41(3)	90
$\beta$ / °	109.48(2)	106.939(13)	84.26(3)	90
$\gamma$ / °	90	90	75.21(3)	90
<i>U</i> / Å <sup>3</sup>	935.9(3)	953.02(17)	383.14(15)	3191.3(3)
<i>Z</i>	2	4	1	8
T / K	293	200	200	200
<i>F</i> (000)	562	612	221	1752
<i>D<sub>c</sub></i> / Mg m <sup>-3</sup>	1.991	2.127	1.880	1.774
$\mu$ (Mo-K $\alpha$ ) / mm <sup>-1</sup>	3.255	3.011	1.243	1.592
Diffractometer	Stoe IPDS	Stoe IPDS	Stoe IPDS	Stoe IPDS
Data Measured	4033	4489	2517	25138
Unique Data	1808	1822	2517	6070
<i>R<sub>int</sub></i>	0.0385	0.0383	0.0000	0.0378
Observed Data	3.22 to 26.11°	3.41 to 26.03°	2.44 to 26.12°	2.02 to 26.02°
Parameters/Restraints	129/ 0	163/ 0	226/ 6	577/ 3
Completeness to 2 $\theta$ = 50°	98.9 %	98.0 %	94.7 %	97.2 %
<i>wR<sub>2</sub></i> , <i>R<sub>I</sub></i> (all data)	<i>R<sub>1</sub></i> = 0.0528, <i>wR<sub>2</sub></i> = 0.0762	<i>R<sub>1</sub></i> = 0.0542, <i>wR<sub>2</sub></i> = 0.0913	<i>R<sub>1</sub></i> = 0.0581, <i>wR<sub>2</sub></i> = 0.1201	<i>R<sub>1</sub></i> = 0.0355, <i>wR<sub>2</sub></i> = 0.0899
<i>wR<sub>2</sub></i> , <i>R<sub>I</sub></i> [ <i>I</i> ≥ 2 $\sigma$ ( <i>I</i> )]	<i>R<sub>1</sub></i> = 0.0328, <i>wR<sub>2</sub></i> = 0.0713	<i>R<sub>1</sub></i> = 0.0400, <i>wR<sub>2</sub></i> = 0.0879	<i>R<sub>1</sub></i> = 0.0442, <i>wR<sub>2</sub></i> = 0.1083	<i>R<sub>1</sub></i> = 0.0337, <i>wR<sub>2</sub></i> = 0.0888
<i>S</i> (all data)	0.862	0.962	1.091	1.092
Biggest diff. peak/hole	0.585 and -0.423 e.Å <sup>3</sup>	0.659 and -0.376 e.Å <sup>3</sup>	0.513 and -0.341 e.Å <sup>3</sup>	0.603 and -0.529 e.Å <sup>3</sup>



Table 4: Crystallographic Data

Compound	<b>13</b>	<b>14</b>	<b>15</b>	<b>16</b>
Formula	C <sub>12</sub> H <sub>18</sub> CuN <sub>4</sub> O <sub>10</sub>	C <sub>17</sub> H <sub>28</sub> CrN <sub>5</sub> O <sub>13</sub>	C <sub>16</sub> H <sub>24</sub> ClCuN <sub>3</sub> O <sub>7</sub>	C <sub>15</sub> H <sub>15</sub> CuNO <sub>6</sub>
Formula weight	441.84	562.44	469.37	368.82
Crystal System	Monoclinic	Orthorhombic	Monoclinic	Orthorhombic
Space Group	P2 <sub>1</sub> /c	P2 <sub>1</sub> 2 <sub>1</sub> 2 <sub>1</sub>	P2 <sub>1</sub> /n	Pna2 <sub>1</sub>
<i>a</i> / Å	9.3094(13)	9.0428(7)	15.1944(9)	11.378(2)
<i>b</i> / Å	12.0957(18)	12.0476(7)	7.3376(6)	7.2488(14)
<i>c</i> / Å	7.6714(11)	20.7393(14)	18.9990(11)	36.410(7)
$\alpha$ / °	90	90	90	90
$\beta$ / °	112.850(15)	90	106.997(7)	90
$\gamma$ / °	90	90	90	90
<i>U</i> / Å <sup>3</sup>	796.0(2)	2259.4(3)	2025.7(2)	3002.9(10)
<i>Z</i>	2	4	4	8
T / K	200	200	200	200
<i>F</i> (000)	454	1172	972	1512
<i>D<sub>c</sub></i> / Mg m <sup>-3</sup>	1.843	1.653	1.539	1.632
$\mu$ (Mo-K $\alpha$ ) / mm <sup>-1</sup>	1.440	0.587	1.253	1.486
Diffractometer	Stoe IPDS	Stoe IPDS	Stoe IPDS	Stoe IPDS
Data Measured	3786	11147	11061	10478
Unique Data	1537	4369	3867	5254
<i>R<sub>int</sub></i>	0.0333	0.0351	0.0746	0.0971
Observed Data	2.37 to 26.13°	1.95 to 26.00°	2.03 to 25.97°	2.24 to 25.99°
Parameters/Restraints	160/ 3	394/ 0	312/ 0	415/ 1
Completeness to 2 $\theta$ = 50°	98.2 %	99.2 %	98.8 %	99.4 %
<i>wR<sub>2</sub></i> , <i>R<sub>1</sub></i> (all data)	<i>R<sub>1</sub></i> = 0.0478, <i>wR<sub>2</sub></i> = 0.1208	<i>R<sub>1</sub></i> = 0.0519, <i>wR<sub>2</sub></i> = 0.0893	<i>R<sub>1</sub></i> = 0.0803, <i>wR<sub>2</sub></i> = 0.1766	<i>R<sub>1</sub></i> = 0.1071, <i>wR<sub>2</sub></i> = 0.1350
<i>wR<sub>2</sub></i> , <i>R<sub>1</sub></i> [ <i>I</i> ≥ 2 $\sigma$ ( <i>I</i> )]	<i>R<sub>1</sub></i> = 0.0414, <i>wR<sub>2</sub></i> = 0.1156	<i>R<sub>1</sub></i> = 0.0379, <i>wR<sub>2</sub></i> = 0.0859	<i>R<sub>1</sub></i> = 0.0636, <i>wR<sub>2</sub></i> = 0.1675	<i>R<sub>1</sub></i> = 0.0587, <i>wR<sub>2</sub></i> = 0.1235
<i>S</i> (all data)	1.025	0.900	0.979	0.775
Biggest diff. peak/hole	0.448 and -0.677 e.Å <sup>3</sup>	0.402 and -0.389 e.Å <sup>3</sup>	2.345 and -0.700 e.Å <sup>3</sup>	1.593 and -0.443 e.Å <sup>-3</sup>

Table 5: Crystallographic Data

Compound	<b>17</b>	<b>18</b>	<b>19</b>	<b>20</b>
Formula	C <sub>11</sub> H <sub>17</sub> NNiO <sub>9</sub>	C <sub>11</sub> H <sub>18</sub> CrNO <sub>10</sub>	C <sub>11</sub> H <sub>18</sub> FeNO <sub>10</sub>	C <sub>22</sub> H <sub>48</sub> Fe <sub>2</sub> K <sub>5</sub> N <sub>3</sub> O <sub>35</sub> S <sub>2</sub>
Formula weight	365.97	376.26	380.11	1285.95
Crystal System	Monoclinic	Monoclinic	Monoclinic	Trigonal
Space Group	P2 <sub>1</sub> /c	P2 <sub>1</sub> /c	P2 <sub>1</sub> /c	P3 <sub>2</sub> 2 <sub>1</sub>
<i>a</i> / Å	7.3360(4)	7.9048(8)	7.9420(9)	20.7925(13)
<i>b</i> / Å	24.6917(17)	10.0075(8)	10.0644(10)	20.7925(13)
<i>c</i> / Å	7.8386(4)	19.142(2)	19.2511(20)	12.4716(6)
$\alpha$ / °	90	90	90	90
$\beta$ / °	99.999(6)	92.929(12)	92.513(13)	90
$\gamma$ / °	90	90	90	120
<i>U</i> / Å <sup>3</sup>	1398.30(14)	1512.3(3)	1537.3(3)	4669.5(5)
<i>Z</i>	4	4	4	3
T / K	200	200	200	200
<i>F</i> (000)	760	780	788	1980
<i>D<sub>c</sub></i> / Mg m <sup>-3</sup>	1.738	1.653	1.642	1.372
$\mu$ (Mo-K $\alpha$ ) / mm <sup>-1</sup>	1.436	0.810	1.034	0.949
Diffractometer	Stoe IPDS	Stoe IPDS	Stoe IPDS	Stoe IPDS
Data Measured	6560	6435	5266	30650
Unique Data	2634	2688	264	6072
<i>R<sub>int</sub></i>	0.0378	0.0633	0.0769	0.1382
Observed Data	2.76 to 26.06°	2.58 to 25.97°	2.28 to 25.98°	1.96 to 26.01°
Parameters/Restraints	267/ 2	265/ 4	260/ 8	344/ 0
Completeness to 2 $\theta$ = 50°	96.3 %	91.1 %	88.4 %	99.7 %
<i>wR<sub>2</sub></i> , <i>R<sub>1</sub></i> (all data)	<i>R</i> <sub>1</sub> = 0.0455, <i>wR</i> <sub>2</sub> = 0.1241	<i>R</i> <sub>1</sub> = 0.0896, <i>wR</i> <sub>2</sub> = 0.0977	<i>R</i> <sub>1</sub> = 0.1287, <i>wR</i> <sub>2</sub> = 0.0978	<i>R</i> <sub>1</sub> = 0.1074, <i>wR</i> <sub>2</sub> = 0.1839
<i>wR<sub>2</sub></i> , <i>R<sub>1</sub></i> [ <i>I</i> ≥ 2 $\sigma$ ( <i>I</i> )]	<i>R</i> <sub>1</sub> = 0.0424, <i>wR</i> <sub>2</sub> = 0.1219	<i>R</i> <sub>1</sub> = 0.0457, <i>wR</i> <sub>2</sub> = 0.0898	<i>R</i> <sub>1</sub> = 0.0485, <i>wR</i> <sub>2</sub> = 0.0843	<i>R</i> <sub>1</sub> = 0.0838, <i>wR</i> <sub>2</sub> = 0.1735
<i>S</i> (all data)	1.122	0.784	0.684	0.948
Biggest diff.peak/hole	0.439 and -0.603e.Å <sup>3</sup>	0.589 and -0.306e.Å <sup>3</sup>	0.851 and -0.310e.Å <sup>3</sup>	0.788 and -0.592e.Å <sup>3</sup>

**8.1 [CuCl<sub>2</sub>(C<sub>14</sub>H<sub>16</sub>N<sub>4</sub>)]·H<sub>2</sub>O 2 : Bond lengths [Å] and angles [°].**

Cu(1)-N(1)	1.978(10)	Cl(1)-Cu(1)-Cl(2)	97.89(11)	N(3)-C(5)-C(6)	122.7(8)
Cu(1)-N(3)	2.116(7)	N(1)-C(2)-H(2A)	109.1	N(3)-C(5)-C(1)	113.3(7)
Cu(1)-N(4)	2.220(7)	C(3)-C(2)-H(2A)	109.1	N(3)-C(9)-C(8)	121.5(10)
Cu(1)-Cl(1)	2.243(3)	N(1)-C(2)-H(2B)	109.1	N(3)-C(9)-H(9)	119.2
Cu(1)-Cl(2)	2.293(2)	C(3)-C(2)-H(2B)	109.1	C(5)-N(3)-C(9)	119.3(8)
		H(2A)-C(2)-H(2B)	107.9	C(5)-N(3)-Cu(1)	111.6(6)
N(1)-Cu(1)-N(3)	78.0(3)	C(4)-C(3)-C(2)	108.9(9)	C(9)-N(3)-Cu(1)	128.4(7)
N(1)-Cu(1)-N(4)	76.9(3)	C(4)-C(3)-H(3A)	109.9	N(4)-C(10)-C(11)	122.9(8)
N(3)-Cu(1)-N(4)	86.2(3)	C(2)-C(3)-H(3A)	109.9	N(4)-C(10)-C(1)	114.4(8)
N(1)-Cu(1)-Cl(1)	171.6(3)	N(2)-C(4)-C(3)	114.2(9)	N(4)-C(14)-C(13)	120.2(9)
N(3)-Cu(1)-Cl(1)	95.8(2)	N(2)-C(4)-H(4A)	108.7	N(4)-C(14)-H(14)	119.9
N(4)-Cu(1)-Cl(1)	97.3(2)	C(3)-C(4)-H(4A)	108.7	C(10)-N(4)-C(14)	120.9(8)
N(1)-Cu(1)-Cl(2)	90.3(2)	N(2)-C(4)-H(4B)	108.7	C(10)-N(4)-Cu(1)	108.8(5)
N(3)-Cu(1)-Cl(2)	144.9(2)	C(3)-C(4)-H(4B)	108.7	C(14)-N(4)-Cu(1)	130.4(6)
N(4)-Cu(1)-Cl(2)	123.6(2)	H(4A)-C(4)-H(4B)	107.6		

**8.2 [Cu(C<sub>14</sub>H<sub>16</sub>N<sub>4</sub>)<sub>2</sub>]Br<sub>2</sub>·2MeOH 3 : Bond lengths [Å] and angles [°].**

Cu(1)-N(3)	2.0167(15)	N(3)-Cu(1)-N(1)#1	99.42(6)	N(3)-C(1)-C(2)	106.65(13)
Cu(1)-N(3)#1	2.0167(15)	N(3)#1-Cu(1)-N(1)#1	80.58(6)	N(4)-C(1)-C(7)	110.23(14)
Cu(1)-N(1)#1	2.0464(15)	N(3)-Cu(1)-N(1)	80.58(6)	N(3)-C(1)-C(7)	107.21(14)
Cu(1)-N(1)	2.0464(15)	N(3)#1-Cu(1)-N(1)	99.42(6)	C(2)-C(1)-C(7)	105.91(14)
Cu(1)-N(2)	2.4312(15)	N(1)#1-Cu(1)-N(1)	180.0	N(1)-C(2)-C(3)	122.06(16)
Cu(1)-N(2)#1	2.4312(15)	N(3)-Cu(1)-N(2)	73.21(6)	N(1)-C(2)-C(1)	113.81(14)
C(1)-N(4)	1.448(2)	N(3)#1-Cu(1)-N(2)	106.79(6)	N(1)-C(6)-C(5)	122.17(17)
C(1)-N(3)	1.500(2)	N(1)#1-Cu(1)-N(2)	95.69(6)	N(1)-C(6)-H(6)	114.8(14)
C(2)-N(1)	1.349(2)	N(1)-Cu(1)-N(2)	84.31(6)	C(6)-N(1)-C(2)	118.48(16)
N(3)-C(14)	1.488(2)	N(3)-Cu(1)-N(2)#1	106.79(6)	C(6)-N(1)-Cu(1)	128.96(12)
N(3)-H(3)	0.77(2)	N(3)#1-Cu(1)-N(2)#1	73.21(6)	C(2)-N(1)-Cu(1)	112.48(11)
C(12)-N(4)	1.472(2)	N(1)#1-Cu(1)-N(2)#1	84.31(6)	N(2)-C(7)-C(8)	123.15(17)
N(4)-H(4)	0.90(2)	N(1)-Cu(1)-N(2)#1	95.69(6)	N(2)-C(7)-C(1)	114.36(15)
C(21)-O(21)	1.396(3)	N(2)-Cu(1)-N(2)#1	180.0	N(2)-C(11)-C(10)	122.63(19)
O(21)-H(21)	0.71(4)	N(4)-C(1)-N(3)	114.51(14)	N(2)-C(11)-H(11)	115.3(13)
N(3)-Cu(1)-N(3)#1	180.0	N(4)-C(1)-C(2)	111.85(14)	C(7)-N(2)-C(11)	117.64(16)

C(7)-N(2)-Cu(1)	105.70(11)	N(4)-C(12)-H(12A)	107.3(13)	C(12)-N(4)-H(4)	109.1(13)
C(11)-N(2)-Cu(1)	136.36(13)	C(13)-C(12)-H(12A)	110.3(13)	O(21)-C(21)-H(21A)	109.5
C(14)-N(3)-C(1)	111.96(14)	N(4)-C(12)-H(12B)	109.2(12)	O(21)-C(21)-H(21B)	109.5
C(14)-N(3)-Cu(1)	114.26(12)	C(13)-C(12)-H(12B)	107.1(12)	H(21A)-C(21)-H(21B)	109.5
C(1)-N(3)-Cu(1)	104.18(10)	N(3)-C(14)-C(13)	112.27(16)	O(21)-C(21)-H(21C)	109.5
C(14)-N(3)-H(3)	106.7(14)	N(3)-C(14)-H(14A)	106.7(12)	C(21)-O(21)-H(21)	111(3)
C(1)-N(3)-H(3)	106.8(15)	N(3)-C(14)-H(14B)	107.9(11)		
Cu(1)-N(3)-H(3)	112.8(14)	C(1)-N(4)-C(12)	113.46(15)		
N(4)-C(12)-C(13)	112.56(16)	C(1)-N(4)-H(4)	108.6(14)		

Symmetry transformations used to generate equivalent atoms:

#1 -x+1,-y+1,-z+1

### 8.3 [CuBr<sub>2</sub>(C<sub>14</sub>H<sub>16</sub>N<sub>4</sub>)] **1** : Bond lengths [Å] and angles [°].

Cu(1)-N(4)	1.968(2)	N(4)-Cu(1)-N(3)	93.69(10)	C(6)-N(1)-Cu(1)	126.80(19)
Cu(1)-N(1)	2.007(2)	N(1)-Cu(1)-N(3)	79.59(8)	C(2)-N(1)-Cu(1)	114.64(17)
Cu(1)-N(3)	2.055(2)	N(4)-Cu(1)-Br(2)	89.63(7)	N(2)-C(7)-C(8)	123.3(3)
Cu(1)-Br(2)	2.4329(4)	N(1)-Cu(1)-Br(2)	92.08(6)	N(2)-C(7)-C(1)	113.8(2)
Cu(1)-Br(1)	2.5973(5)	N(3)-Cu(1)-Br(2)	149.75(7)	N(4)-C(14)-C(13)	110.9(3)
C(1)-N(3)	1.272(3)	N(4)-Cu(1)-Br(1)	95.34(8)	N(4)-C(14)-H(14A)	109.2(18)
C(2)-N(1)	1.343(3)	N(1)-Cu(1)-Br(1)	93.75(7)	C(13)-C(14)-H(14A)	108.8(19)
C(6)-N(1)	1.338(3)	N(3)-Cu(1)-Br(1)	97.06(6)	N(4)-C(14)-H(14B)	109(2)
C(6)-H(6)	0.91(3)	Br(2)-Cu(1)-Br(1)	112.575(17)	C(13)-C(14)-H(14B)	109(2)
C(7)-N(2)	1.328(3)	N(3)-C(1)-C(2)	116.4(2)	H(14A)-C(14)-H(14B)	110(3)
C(11)-N(2)	1.338(4)	N(3)-C(1)-C(7)	125.3(2)	C(14)-N(4)-Cu(1)	118.95(19)
N(3)-C(12)	1.470(3)	N(1)-C(2)-C(3)	122.2(2)	C(14)-N(4)-H(41)	106.0(19)
C(14)-N(4)	1.481(4)	N(1)-C(2)-C(1)	114.2(2)	Cu(1)-N(4)-H(41)	109.4(19)
N(4)-H(41)	0.86(3)	N(1)-C(6)-C(5)	122.0(3)	C(14)-N(4)-H(42)	108(2)
N(4)-H(42)	0.85(3)	N(1)-C(6)-H(6)	115.8(18)	Cu(1)-N(4)-H(42)	105(2)
N(4)-Cu(1)-N(1)	169.30(11)	C(6)-N(1)-C(2)	118.6(2)	H(41)-N(4)-H(42)	109(3)

### 8.4 [Cu<sub>2</sub>Cl<sub>4</sub>(1,3-dpp)<sub>2</sub>].H<sub>2</sub>O **5** : Bond lengths [Å] and angles [°].

Cu(1)-N(1)	2.012(4)	Cu(2)-N(2)#1	1.995(4)	N(1)-C(1)	1.324(8)
Cu(1)-N(1)#1	2.012(4)	Cu(2)-N(2)	1.995(4)	N(1)-C(5)	1.333(7)
Cu(1)-Cl(1)	2.255(2)	Cu(2)-Cl(4)	2.243(2)	N(2)-C(13)	1.323(7)
Cu(1)-Cl(2)	2.259(2)	Cu(2)-Cl(3)	2.260(3)	N(2)-C(9)	1.327(7)

O(1A)-O(1B)	1.06(4)	N(2)-Cu(2)-Cl(4)	89.06(14)	C(9)-N(2)-Cu(2)	123.5(4)
N(1)-Cu(1)-N(1)#1	180.0(4)	N(2)#1-Cu(2)-Cl(3)	91.00(14)	N(1)-C(1)-C(2)	122.7(6)
N(1)-Cu(1)-Cl(1)	90.01(14)	N(2)-Cu(2)-Cl(3)	91.00(14)	N(1)-C(5)-C(4)	119.0(6)
N(1)#1-Cu(1)-Cl(1)	90.01(14)	Cl(4)-Cu(2)-Cl(3)	173.21(13)	N(1)-C(5)-C(6)	117.6(5)
N(1)-Cu(1)-Cl(2)	89.99(14)	C(1)-N(1)-C(5)	120.3(5)	C(4)-C(5)-C(6)	123.4(6)
N(1)#1-Cu(1)-Cl(2)	89.99(14)	C(1)-N(1)-Cu(1)	117.6(4)	N(2)-C(9)-C(10)	119.9(6)
Cl(1)-Cu(1)-Cl(2)	179.07(11)	C(5)-N(1)-Cu(1)	122.1(4)	N(2)-C(9)-C(8)	117.0(5)
N(2)#1-Cu(2)-N(2)	177.8(3)	C(13)-N(2)-C(9)	120.0(5)	N(2)-C(13)-C(12)	122.4(6)
N(2)#1-Cu(2)-Cl(4)	89.06(14)	C(13)-N(2)-Cu(2)	116.4(4)		

Symmetry transformations used to generate equivalent atoms:

#1 x, -y+1/2, z

### 8.5 [Cu<sub>2</sub>(OAc)<sub>4</sub>(C<sub>4</sub>H<sub>4</sub>N<sub>3</sub>Br)]<sub>∞</sub> **6** : Bond lengths [Å] and angles [°].

Cu(1)-O(1)	1.947(4)	O(1)-C(5)	1.278(6)	O(2)#1-Cu(1)-O(3)#1	87.85(19)
Cu(1)-O(2)#1	1.955(4)	C(5)-O(2)	1.261(7)	O(1)-Cu(1)-O(4)	88.12(18)
Cu(1)-O(3)#1	1.984(4)	C(5)-C(6)	1.475(9)	O(2)#1-Cu(1)-O(4)	90.8(2)
Cu(1)-O(4)	1.985(4)	C(6)-H(6A)	0.9600	O(3)#1-Cu(1)-O(4)	169.26(14)
Cu(1)-N(1)	2.223(4)	C(6)-H(6B)	0.9600	O(1)-Cu(1)-N(1)	98.60(16)
Cu(1)-Cu(1)#1	2.6007(12)	C(6)-H(6C)	0.9600	O(2)#1-Cu(1)-N(1)	92.23(16)
Cu(2)-O(8)#2	1.944(4)	O(2)-Cu(1)#1	1.955(4)	O(3)#1-Cu(1)-N(1)	93.99(15)
Cu(2)-O(7)	1.946(4)	O(3)-C(7)	1.257(6)	O(4)-Cu(1)-N(1)	96.71(14)
Cu(2)-O(5)	1.991(4)	O(3)-Cu(1)#1	1.984(4)	O(1)-Cu(1)-Cu(1)#1	85.18(11)
Cu(2)-O(6)#2	1.994(4)	C(7)-O(4)	1.269(7)	O(2)#1-Cu(1)-Cu(1)#1	84.00(11)
Cu(2)-N(2)	2.228(4)	C(7)-C(8)	1.502(8)	O(3)#1-Cu(1)-Cu(1)#1	86.43(10)
Cu(2)-Cu(2)#2	2.6181(12)	C(8)-H(8A)	0.9600	O(4)-Cu(1)-Cu(1)#1	82.83(10)
N(1)-C(4)	1.326(7)	C(8)-H(8B)	0.9600	N(1)-Cu(1)-Cu(1)#1	176.18(13)
N(1)-C(1)	1.357(6)	C(8)-H(8C)	0.9600	O(8)#2-Cu(2)-O(7)	168.29(15)
C(1)-N(3)	1.317(7)	O(5)-C(9)	1.249(6)	O(8)#2-Cu(2)-O(5)	89.7(2)
C(1)-N(2)	1.368(6)	C(9)-O(6)	1.253(6)	O(7)-Cu(2)-O(5)	89.4(2)
N(3)-H(31)	0.78(7)	C(9)-C(10)	1.500(8)	O(8)#2-Cu(2)-O(6)#2	88.9(2)
N(3)-H(32)	0.81(6)	O(6)-Cu(2)#2	1.994(4)	O(7)-Cu(2)-O(6)#2	89.6(2)
N(2)-C(2)	1.315(7)	O(7)-C(11)	1.257(6)	O(5)-Cu(2)-O(6)#2	168.46(14)
C(2)-C(3)	1.377(7)	C(11)-O(8)	1.250(7)	O(8)#2-Cu(2)-N(2)	97.08(16)
C(2)-H(2)	0.9300	C(11)-C(12)	1.481(10)	O(7)-Cu(2)-N(2)	94.60(16)
C(3)-C(4)	1.373(7)	O(8)-Cu(2)#2	1.944(4)	O(5)-Cu(2)-N(2)	98.40(15)
C(3)-Br(1)	1.886(5)	O(1)-Cu(1)-O(2)#1	169.18(14)	O(6)#2-Cu(2)-N(2)	93.13(14)
C(4)-H(4)	0.9300	O(1)-Cu(1)-O(3)#1	91.26(17)	O(8)#2-Cu(2)-Cu(2)#2	84.20(11)

O(7)-Cu(2)-Cu(2)#2	84.10(11)	C(2)-N(2)-Cu(2)	115.6(3)	O(3)-C(7)-O(4)	123.9(5)
O(5)-Cu(2)-Cu(2)#2	82.71(10)	C(1)-N(2)-Cu(2)	127.4(3)	O(3)-C(7)-C(8)	118.2(5)
O(6)#2-Cu(2)-Cu(2)#2	85.76(10)	N(2)-C(2)-C(3)	122.9(5)	O(4)-C(7)-C(8)	117.9(4)
N(2)-Cu(2)-Cu(2)#2	178.30(12)	N(2)-C(2)-H(2)	118.6	C(7)-O(4)-Cu(1)	125.3(3)
C(4)-N(1)-C(1)	118.0(4)	C(4)-C(3)-Br(1)	121.3(4)	C(9)-O(5)-Cu(2)	125.3(3)
C(4)-N(1)-Cu(1)	114.8(3)	C(2)-C(3)-Br(1)	121.3(4)	O(5)-C(9)-O(6)	124.9(5)
C(1)-N(1)-Cu(1)	127.1(3)	N(1)-C(4)-C(3)	121.7(4)	O(5)-C(9)-C(10)	117.3(5)
N(3)-C(1)-N(1)	118.7(4)	N(1)-C(4)-H(4)	119.1	O(6)-C(9)-C(10)	117.9(5)
N(3)-C(1)-N(2)	118.3(4)	C(5)-O(1)-Cu(1)	123.1(4)	C(9)-O(6)-Cu(2)#2	121.4(4)
N(1)-C(1)-N(2)	123.0(4)	O(2)-C(5)-O(1)	123.1(6)	C(11)-O(7)-Cu(2)	123.4(4)
C(1)-N(3)-H(31)	120(5)	O(2)-C(5)-C(6)	118.2(5)	O(8)-C(11)-O(7)	124.8(6)
C(1)-N(3)-H(32)	118(4)	O(1)-C(5)-C(6)	118.7(5)	O(8)-C(11)-C(12)	117.8(5)
H(31)-N(3)-H(32)	121(6)	C(5)-O(2)-Cu(1)#1	124.5(4)	O(7)-C(11)-C(12)	117.4(6)
C(2)-N(2)-C(1)	117.0(4)	C(7)-O(3)-Cu(1)#1	121.4(4)	C(11)-O(8)-Cu(2)#2	123.5(4)

Symmetry transformations used to generate equivalent atoms:

#1 -x+1,-y+1,-z #2 -x+1,-y,-z+1

## 8.6 [Cu<sub>2</sub>(OAc)<sub>4</sub>(C<sub>4</sub>H<sub>4</sub>N<sub>3</sub>Br)<sub>2</sub>] $\bar{2}$ : Bond lengths [Å] and angles [°].

Cu(1)-O(2)#1	1.956(10)	Cu(2)-O(7)	1.943(10)	C(15)-Br(2)	1.885(12)
Cu(1)-O(1)	1.967(9)	Cu(2)-O(10)#2	1.945(10)	O(2)#1-Cu(1)-O(1)	167.9(3)
Cu(1)-O(3)	1.972(9)	Cu(2)-O(9)	1.949(10)	O(2)#1-Cu(1)-O(3)	88.7(4)
Cu(1)-O(4)#1	1.979(9)	Cu(2)-O(8)#2	1.974(10)	O(1)-Cu(1)-O(3)	90.0(4)
Cu(1)-N(1)	2.237(8)	Cu(2)-N(4)	2.251(9)	O(2)#1-Cu(1)-O(4)#1	89.7(4)
Cu(1)-Cu(1)#1	2.625(3)	Cu(2)-Cu(2)#2	2.640(3)	O(1)-Cu(1)-O(4)#1	89.0(4)
O(1)-C(1)	1.229(15)	O(7)-C(11)	1.253(15)	O(3)-Cu(1)-O(4)#1	167.8(3)
C(1)-O(2)	1.301(14)	C(9)-O(10)	1.219(15)	O(2)#1-Cu(1)-N(1)	98.4(4)
O(2)-Cu(1)#1	1.956(10)	C(9)-O(9)	1.266(16)	O(1)-Cu(1)-N(1)	93.6(3)
O(3)-C(3)	1.247(14)	C(9)-C(10)	1.51(2)	O(3)-Cu(1)-N(1)	97.4(3)
C(3)-O(4)	1.247(13)	O(8)-C(11)	1.263(14)	O(4)#1-Cu(1)-N(1)	94.8(4)
C(3)-C(4)	1.478(19)	O(8)-Cu(2)#2	1.974(10)	O(2)#1-Cu(1)-Cu(1)#1	83.9(2)
O(4)-Cu(1)#1	1.979(9)	O(10)-Cu(2)#2	1.945(10)	O(1)-Cu(1)-Cu(1)#1	84.0(2)
N(1)-C(5)	1.299(15)	N(4)-C(16)	1.319(15)	O(3)-Cu(1)-Cu(1)#1	84.2(2)
N(1)-C(8)	1.313(16)	N(4)-C(13)	1.327(16)	O(4)#1-Cu(1)-Cu(1)#1	83.6(2)
C(5)-N(2)	1.353(14)	C(13)-N(6)	1.299(18)	N(1)-Cu(1)-Cu(1)#1	177.2(3)
C(5)-N(3)	1.367(18)	C(13)-N(5)	1.392(15)	C(1)-O(1)-Cu(1)	125.6(7)
N(3)-H(31)	0.85(4)	N(6)-H(61)	0.87(4)	O(1)-C(1)-O(2)	122.0(12)
N(3)-H(32)	0.87(4)	N(6)-H(62)	0.88(4)	O(1)-C(1)-C(2)	121.9(11)
N(2)-C(6)	1.325(18)	N(5)-C(14)	1.28(2)	O(2)-C(1)-C(2)	116.0(12)

C(1)-C(2)-H(2A)	109.5	N(1)-C(8)-C(7)	122.3(13)	C(9)-O(9)-Cu(2)	121.4(9)
C(1)-C(2)-H(2B)	109.5	N(1)-C(8)-H(8)	118.8	O(7)-C(11)-O(8)	122.4(13)
H(2A)-C(2)-H(2B)	109.5	C(7)-C(8)-H(8)	118.8	O(7)-C(11)-C(12)	119.5(11)
C(1)-O(2)-Cu(1)#1	124.5(8)	O(7)-Cu(2)-O(10)#2	89.2(5)	O(8)-C(11)-C(12)	118.1(12)
C(3)-O(3)-Cu(1)	123.8(8)	O(7)-Cu(2)-O(9)	89.7(5)	C(9)-O(10)-Cu(2)#2	125.9(10)
O(4)-C(3)-O(3)	124.3(12)	O(10)#2-Cu(2)-O(9)	167.2(4)	C(16)-N(4)-C(13)	120.1(10)
O(4)-C(3)-C(4)	116.1(11)	O(7)-Cu(2)-O(8)#2	167.3(4)	C(16)-N(4)-Cu(2)	115.1(8)
O(3)-C(3)-C(4)	119.6(11)	O(10)#2-Cu(2)-O(8)#2	89.6(4)	C(13)-N(4)-Cu(2)	124.6(7)
C(3)-O(4)-Cu(1)#1	124.1(9)	O(9)-Cu(2)-O(8)#2	88.7(4)	N(6)-C(13)-N(4)	122.3(11)
C(5)-N(1)-C(8)	117.1(10)	O(7)-Cu(2)-N(4)	92.9(4)	N(6)-C(13)-N(5)	115.0(13)
C(5)-N(1)-Cu(1)	128.6(8)	O(10)#2-Cu(2)-N(4)	94.6(4)	N(4)-C(13)-N(5)	122.6(12)
C(8)-N(1)-Cu(1)	114.3(8)	O(9)-Cu(2)-N(4)	98.2(4)	C(13)-N(6)-H(61)	108(10)
N(1)-C(5)-N(2)	125.9(12)	O(8)#2-Cu(2)-N(4)	99.9(3)	C(13)-N(6)-H(62)	129(10)
N(1)-C(5)-N(3)	118.6(11)	O(7)-Cu(2)-Cu(2)#2	84.5(3)	H(61)-N(6)-H(62)	105(10)
N(2)-C(5)-N(3)	115.2(11)	O(10)#2-Cu(2)-Cu(2)#2	82.3(3)	C(14)-N(5)-C(13)	116.0(13)
C(5)-N(3)-H(31)	117(10)	O(9)-Cu(2)-Cu(2)#2	84.9(3)	N(5)-C(14)-C(15)	124.6(13)
C(5)-N(3)-H(32)	116(10)	O(8)#2-Cu(2)-Cu(2)#2	82.8(2)	N(5)-C(14)-H(14)	117.7
H(31)-N(3)-H(32)	126(10)	N(4)-Cu(2)-Cu(2)#2	175.9(3)	C(15)-C(14)-H(14)	117.7
C(6)-N(2)-C(5)	115.9(11)	C(11)-O(7)-Cu(2)	124.9(8)	C(14)-C(15)-C(16)	116.5(12)
N(2)-C(6)-C(7)	121.8(12)	O(10)-C(9)-O(9)	125.4(14)	C(14)-C(15)-Br(2)	121.9(10)
N(2)-C(6)-H(6)	119.1	O(10)-C(9)-C(10)	118.8(13)	C(16)-C(15)-Br(2)	121.3(11)
C(6)-C(7)-Br(1)	121.3(10)	O(9)-C(9)-C(10)	115.8(12)	N(4)-C(16)-C(15)	120.2(12)
C(8)-C(7)-Br(1)	121.9(11)	C(11)-O(8)-Cu(2)#2	125.2(9)	N(4)-C(16)-H(16)	119.9

Symmetry transformations used to generate equivalent atoms:

#1 -x+1,-y+2,-z+1 #2 -x,-y+1,-z #3 -x,-y+3,-z+1

#4 x,y-1,z

### 8.7 $\text{K}_4[\text{Cu}(\text{OAc})_6(\text{HOAc})_4]$ **8** : Bond lengths [ $\text{\AA}$ ] and angles [ $^\circ$ ].

Cu(1)-O(1)#1	1.960(4)	K(1)-O(2)#7	2.706(4)	K(2)-O(6)	2.793(4)
Cu(1)-O(1)#2	1.960(4)	K(1)-O(7)#8	2.782(5)	K(2)-O(9)	2.934(5)
Cu(1)-O(1)	1.960(4)	K(1)-O(5)	2.785(4)	K(2)-O(8)	2.941(5)
Cu(1)-O(1)#3	1.960(4)	K(1)-O(7)	2.859(5)	K(2)-O(9)#10	2.942(5)
Cu(2)-O(3)#4	1.949(4)	K(1)-O(2)#3	2.876(4)	O(1)-C(1)	1.262(7)
Cu(2)-O(3)#5	1.949(4)	K(1)-O(2)	2.985(5)	O(1)-K(1)#2	2.672(4)
Cu(2)-O(3)	1.949(4)	K(2)-O(3)	2.701(4)	C(1)-O(2)	1.241(7)
Cu(2)-O(3)#6	1.949(4)	K(2)-O(4)#9	2.740(5)	O(2)-K(1)#8	2.706(4)
K(1)-O(1)#1	2.672(4)	K(2)-O(4)#4	2.791(5)	O(2)-K(1)#3	2.876(4)

O(3)-C(3)	1.261(7)	O(2)#7-K(1)-O(7)#8	72.96(15)	O(3)-K(2)-O(9)#10	129.11(15)
O(4)-K(2)#11	2.740(5)	O(1)#1-K(1)-O(5)	97.11(14)	O(4)#9-K(2)-O(9)#10	67.93(15)
O(4)-K(2)#5	2.791(5)	O(2)#7-K(1)-O(5)	107.23(14)	O(4)#4-K(2)-O(9)#10	73.83(14)
O(5)-C(5)	1.267(7)	O(7)#8-K(1)-O(5)	99.79(13)	O(6)-K(2)-O(9)#10	100.76(14)
O(5)-H(8)	1.32(9)	O(1)#1-K(1)-O(7)	114.41(14)	O(9)-K(2)-O(9)#10	138.97(7)
C(5)-O(6)	1.237(7)	O(2)#7-K(1)-O(7)	69.38(14)	O(8)-K(2)-O(9)#10	68.32(14)
C(5)-C(6)	1.492(9)	O(7)#8-K(1)-O(7)	136.51(5)	C(1)-O(1)-Cu(1)	108.0(4)
O(7)-C(7)	1.202(8)	O(5)-K(1)-O(7)	72.12(13)	C(1)-O(1)-K(1)#2	151.6(4)
O(7)-K(1)#7	2.782(5)	O(1)#1-K(1)-O(2)#3	70.94(12)	Cu(1)-O(1)-K(1)#2	100.30(16)
C(7)-O(8)	1.324(8)	O(2)#7-K(1)-O(2)#3	88.88(14)	O(2)-C(1)-O(1)	123.0(5)
C(7)-C(8)	1.476(10)	O(7)#8-K(1)-O(2)#3	131.04(13)	O(2)-C(1)-C(2)	119.8(5)
C(8)-H(8A)	0.9600	O(5)-K(1)-O(2)#3	129.14(13)	O(1)-C(1)-C(2)	117.1(5)
C(8)-H(8B)	0.9600	O(7)-K(1)-O(2)#3	69.36(12)	C(1)-O(2)-K(1)#8	126.1(4)
C(8)-H(8C)	0.9600	O(1)#1-K(1)-O(2)	72.21(11)	C(1)-O(2)-K(1)#3	123.0(4)
O(8)-H(8)	1.22(9)	O(2)#7-K(1)-O(2)	86.67(14)	K(1)#8-O(2)-K(1)#3	89.28(12)
O(9)-C(9)	1.213(7)	O(7)#8-K(1)-O(2)	66.58(12)	C(1)-O(2)-K(1)	115.8(3)
O(9)-K(2)#12	2.942(5)	O(5)-K(1)-O(2)	157.32(13)	K(1)#8-O(2)-K(1)	87.06(12)
C(9)-O(10)	1.303(7)	O(7)-K(1)-O(2)	130.37(12)	K(1)#3-O(2)-K(1)	108.14(13)
C(9)-C(10)	1.466(9)	O(2)#3-K(1)-O(2)	67.32(13)	C(3)-O(3)-Cu(2)	111.4(4)
O(10)-H(10)	1.01(4)	O(3)-K(2)-O(4)#9	148.83(13)	C(3)-O(3)-K(2)	143.8(4)
O(1)#1-Cu(1)-O(1)#2	177.2(2)	O(3)-K(2)-O(4)#4	69.88(14)	Cu(2)-O(3)-K(2)	104.56(17)
O(1)#1-Cu(1)-O(1)	90.035(7)	O(4)#9-K(2)-O(4)#4	95.97(18)	O(4)-C(3)-O(3)	123.2(6)
O(1)#2-Cu(1)-O(1)	90.035(8)	O(3)-K(2)-O(6)	101.76(16)	O(4)-C(3)-C(4)	121.1(6)
O(1)#1-Cu(1)-O(1)#3	90.035(8)	O(4)#9-K(2)-O(6)	99.24(16)	O(3)-C(3)-C(4)	115.6(6)
O(1)#2-Cu(1)-O(1)#3	90.035(7)	O(4)#4-K(2)-O(6)	160.51(15)	C(3)-O(4)-K(2)#11	128.3(4)
O(1)-Cu(1)-O(1)#3	177.2(2)	O(3)-K(2)-O(9)	91.82(15)	C(3)-O(4)-K(2)#5	126.4(4)
O(3)#4-Cu(2)-O(3)#5	175.0(2)	O(4)#9-K(2)-O(9)	74.69(16)	K(2)#11-O(4)-K(2)#5	94.75(15)
O(3)#4-Cu(2)-O(3)	90.109(12)	O(4)#4-K(2)-O(9)	127.62(15)	C(5)-O(5)-K(1)	158.8(4)
O(3)#5-Cu(2)-O(3)	90.110(11)	O(6)-K(2)-O(9)	68.72(12)	C(5)-O(5)-H(8)	108(3)
O(3)#4-Cu(2)-O(3)#6	90.109(11)	O(3)-K(2)-O(8)	84.07(14)	K(1)-O(5)-H(8)	93(3)
O(3)#5-Cu(2)-O(3)#6	90.109(12)	O(4)#9-K(2)-O(8)	126.52(15)	O(6)-C(5)-O(5)	122.1(6)
O(3)-Cu(2)-O(3)#6	175.0(2)	O(4)#4-K(2)-O(8)	99.94(14)	O(6)-C(5)-C(6)	119.4(6)
O(1)#1-K(1)-O(2)#7	155.00(12)	O(6)-K(2)-O(8)	61.08(13)		
O(1)#1-K(1)-O(7)#8	108.95(15)	O(9)-K(2)-O(8)	127.41(14)		

Symmetry transformations used to generate equivalent atoms:

#1  $y, -x+1, -z+2$  #2  $-y+1, x, -z+2$  #3  $-x+1, -y+1, z$  #4  $-y+1/2, x+1/2, -z+1/2$  #5  $y-1/2, -x+1/2, -z+1/2$   
 #6  $-x, -y+1, z$  #7  $y, -x+1, -z+1$  #8  $-y+1, x, -z+1$  #9  $x, y, z+1$  #10  $-y+1/2, x+1/2, -z+3/2$  #11  $x, y, z-1$   
 #12  $y-1/2, -x+1/2, -z+3/2$



**8.8** [Cu<sub>2</sub>(OAc)<sub>4</sub>MnCl<sub>2</sub>(H<sub>2</sub>O)<sub>4</sub>]<sub>∞</sub> **9** : Bond lengths [Å] and angles [°].

Cu(1)-O(4)#1	1.972(3)	O(4)#1-Cu(1)-O(3)	167.63(12)	C(3)-O(4)-Cu(1)#1	122.6(3)
Cu(1)-O(3)	1.979(3)	O(4)#1-Cu(1)-O(2)#1	89.62(12)	Cu(1)-Cl(1)-Mn(1)	116.71(4)
Cu(1)-O(2)#1	1.981(3)	O(3)-Cu(1)-O(2)#1	88.35(12)	O(6)-Mn(1)-O(6)#2	180.00(18)
Cu(1)-O(1)	1.986(3)	O(4)#1-Cu(1)-O(1)	88.70(12)	O(6)-Mn(1)-O(5)	87.91(13)
Cu(1)-Cl(1)	2.4436(11)	O(3)-Cu(1)-O(1)	90.59(12)	O(6)#2-Mn(1)-O(5)	92.09(13)
Cu(1)-Cu(1)#1	2.6600(10)	O(2)#1-Cu(1)-O(1)	167.27(11)	O(6)-Mn(1)-O(5)#2	92.09(13)
O(1)-C(1)	1.260(5)	O(4)#1-Cu(1)-Cl(1)	97.42(9)	O(6)#2-Mn(1)-O(5)#2	87.91(13)
C(1)-O(2)	1.257(5)	O(3)-Cu(1)-Cl(1)	94.95(9)	O(5)-Mn(1)-O(5)#2	180.00(15)
C(1)-C(2)	1.492(5)	O(2)#1-Cu(1)-Cl(1)	98.06(9)	O(6)-Mn(1)-Cl(1)#2	89.84(9)
O(2)-Cu(1)#1	1.981(3)	O(1)-Cu(1)-Cl(1)	94.67(9)	O(6)#2-Mn(1)-Cl(1)#2	90.16(9)
O(3)-C(3)	1.266(5)	O(4)#1-Cu(1)-Cu(1)#1	85.00(9)	O(5)-Mn(1)-Cl(1)#2	92.03(9)
C(3)-O(4)	1.260(5)	O(3)-Cu(1)-Cu(1)#1	82.69(8)	O(5)#2-Mn(1)-Cl(1)#2	87.97(9)
C(3)-C(4)	1.495(6)	O(2)#1-Cu(1)-Cu(1)#1	86.07(8)	O(6)-Mn(1)-Cl(1)	90.16(9)
O(4)-Cu(1)#1	1.972(3)	O(1)-Cu(1)-Cu(1)#1	81.21(8)	O(6)#2-Mn(1)-Cl(1)	89.84(9)
Cl(1)-Mn(1)	2.5280(10)	Cl(1)-Cu(1)-Cu(1)#1	175.20(4)	O(5)-Mn(1)-Cl(1)	87.97(9)
Mn(1)-O(6)	2.152(3)	C(1)-O(1)-Cu(1)	127.1(3)	O(5)#2-Mn(1)-Cl(1)	92.03(9)
Mn(1)-O(6)#2	2.152(3)	O(2)-C(1)-O(1)	123.9(3)	Cl(1)#2-Mn(1)-Cl(1)	180.00(5)
Mn(1)-O(5)	2.205(4)	O(2)-C(1)-C(2)	118.8(3)	Mn(1)-O(5)-H(51)	112(5)
Mn(1)-O(5)#2	2.205(4)	O(1)-C(1)-C(2)	117.4(4)	Mn(1)-O(5)-H(52)	118(6)
Mn(1)-Cl(1)#2	2.5280(10)	C(1)-O(2)-Cu(1)#1	121.6(2)	H(51)-O(5)-H(52)	108(7)
O(5)-H(51)	0.72(6)	C(3)-O(3)-Cu(1)	124.9(3)	Mn(1)-O(6)-H(61)	119(5)
O(5)-H(52)	0.67(7)	O(4)-C(3)-O(3)	124.6(4)	Mn(1)-O(6)-H(62)	119(5)
O(6)-H(61)	0.74(6)	O(4)-C(3)-C(4)	117.5(4)	H(61)-O(6)-H(62)	114(7)
O(6)-H(62)	0.67(7)	O(3)-C(3)-C(4)	117.8(4)		

Symmetry transformations used to generate equivalent atoms:

#1 -x,-y+1,-z #2 -x,-y,-z #3 -x-1/2,y-1/2,-z-1/2

**8.9** K[Cu(ida)Cl(H<sub>2</sub>O)<sub>2</sub>] **10** : Bond lengths [Å] and angles [°].

Cu(1)-O(1)	1.973(3)	N(1)-C(1)	1.465(5)	O(3)-K(1)#3	2.758(3)
Cu(1)-O(3)	1.979(3)	N(1)-H(1)	0.78(5)	O(4)-K(1)#2	2.654(3)
Cu(1)-N(1)	1.999(3)	C(2)-O(2)	1.237(4)	O(5)-K(1)#1	2.898(4)
Cu(1)-Cl(1)	2.2800(10)	C(2)-O(1)	1.260(5)	O(5)-H(51)	0.76(7)
Cu(1)-O(5)	2.377(3)	O(1)-K(1)#1	2.726(3)	O(5)-H(52)	0.63(8)
Cu(1)-O(6)	2.519(4)	C(4)-O(4)	1.227(5)	O(6)-K(1)#3	3.370(4)
N(1)-C(3)	1.463(5)	C(4)-O(3)	1.276(5)	O(6)-H(61)	0.81(6)

O(6)-H(62)	0.74(5)	N(1)-C(1)-H(12)	114(4)	Cu(1)-Cl(1)-K(1)#3	84.57(3)
Cl(1)-K(1)	3.0986(12)	O(2)-C(2)-O(1)	124.4(4)	K(1)-Cl(1)-K(1)#3	95.58(3)
Cl(1)-K(1)#3	3.1768(12)	O(2)-C(2)-C(1)	118.0(4)	Cu(1)-Cl(1)-K(1)#1	77.66(3)
Cl(1)-K(1)#1	3.2923(12)	O(1)-C(2)-C(1)	117.6(3)	K(1)-Cl(1)-K(1)#1	97.19(3)
K(1)-O(4)#4	2.654(3)	C(2)-O(1)-Cu(1)	114.8(2)	K(1)#3-Cl(1)-K(1)#1	161.94(4)
K(1)-O(1)#1	2.726(3)	C(2)-O(1)-K(1)#1	131.5(2)	O(4)#4-K(1)-O(1)#1	91.50(9)
K(1)-O(3)#3	2.758(3)	Cu(1)-O(1)-K(1)#1	98.04(10)	O(4)#4-K(1)-O(3)#3	137.70(8)
K(1)-O(5)#1	2.898(4)	N(1)-C(3)-C(4)	109.8(3)	O(1)#1-K(1)-O(3)#3	84.91(8)
K(1)-Cl(1)#3	3.1768(12)	N(1)-C(3)-H(31)	109(3)	O(4)#4-K(1)-O(5)#1	141.06(9)
K(1)-Cl(1)#1	3.2923(12)	C(4)-C(3)-H(31)	112(3)	O(1)#1-K(1)-O(5)#1	64.61(9)
K(1)-O(6)#3	3.370(4)	N(1)-C(3)-H(32)	109(3)	O(3)#3-K(1)-O(5)#1	73.51(10)
O(1)-Cu(1)-O(3)	164.98(11)			O(4)#4-K(1)-Cl(1)	88.06(7)
O(1)-Cu(1)-N(1)	83.75(12)	O(4)-C(4)-O(3)	123.8(3)	O(1)#1-K(1)-Cl(1)	145.79(6)
O(3)-Cu(1)-N(1)	82.74(12)	O(4)-C(4)-C(3)	119.3(4)	O(3)#3-K(1)-Cl(1)	117.30(6)
O(1)-Cu(1)-Cl(1)	97.52(9)	O(3)-C(4)-C(3)	116.9(3)	O(5)#1-K(1)-Cl(1)	95.48(9)
O(3)-Cu(1)-Cl(1)	96.19(8)	O(4)-C(4)-K(1)#2	40.41(18)	O(4)#4-K(1)-Cl(1)#3	87.24(6)
N(1)-Cu(1)-Cl(1)	177.83(10)	O(3)-C(4)-K(1)#2	127.5(2)	O(1)#1-K(1)-Cl(1)#3	129.74(6)
O(1)-Cu(1)-O(5)	87.02(12)	C(3)-C(4)-K(1)#2	101.6(2)	O(3)#3-K(1)-Cl(1)#3	64.25(6)
O(3)-Cu(1)-O(5)	99.63(12)	C(4)-O(3)-Cu(1)	114.2(2)	O(5)#1-K(1)-Cl(1)#3	131.69(8)
N(1)-Cu(1)-O(5)	90.52(15)	C(4)-O(3)-K(1)#3	120.9(2)	Cl(1)-K(1)-Cl(1)#3	84.42(3)
Cl(1)-Cu(1)-O(5)	87.79(11)	Cu(1)-O(3)-K(1)#3	102.67(11)	O(4)#4-K(1)-Cl(1)#1	79.62(6)
O(1)-Cu(1)-O(6)	88.12(12)	C(4)-O(4)-K(1)#2	122.2(2)	O(1)#1-K(1)-Cl(1)#1	63.53(6)
O(3)-Cu(1)-O(6)	86.84(12)	Cu(1)-O(5)-K(1)#1	84.94(11)	O(3)#3-K(1)-Cl(1)#1	133.42(6)
N(1)-Cu(1)-O(6)	96.21(13)	Cu(1)-O(5)-H(51)	139(4)	O(5)#1-K(1)-Cl(1)#1	62.52(8)
Cl(1)-Cu(1)-O(6)	85.60(9)	K(1)#1-O(5)-H(51)	103(5)	Cl(1)-K(1)-Cl(1)#1	82.81(3)
O(5)-Cu(1)-O(6)	171.23(13)	Cu(1)-O(5)-H(52)	114(7)	Cl(1)#3-K(1)-Cl(1)#1	161.94(4)
C(3)-N(1)-C(1)	117.8(3)	K(1)#1-O(5)-H(52)	99(7)	O(4)#4-K(1)-O(6)#3	78.87(9)
C(3)-N(1)-Cu(1)	107.4(2)	H(51)-O(5)-H(52)	105(7)	O(1)#1-K(1)-O(6)#3	70.73(9)
C(1)-N(1)-Cu(1)	108.5(3)	Cu(1)-O(6)-K(1)#3	77.12(9)	O(3)#3-K(1)-O(6)#3	60.14(9)
C(3)-N(1)-H(1)	102(3)	Cu(1)-O(6)-H(61)	125(4)	O(5)#1-K(1)-O(6)#3	116.98(11)
C(1)-N(1)-H(1)	112(3)	K(1)#3-O(6)-H(61)	84(4)	Cl(1)-K(1)-O(6)#3	142.07(8)
Cu(1)-N(1)-H(1)	109(3)	Cu(1)-O(6)-H(62)	105(3)	Cl(1)#3-K(1)-O(6)#3	59.75(7)
N(1)-C(1)-C(2)	110.2(3)	K(1)#3-O(6)-H(62)	170(4)	Cl(1)#1-K(1)-O(6)#3	128.35(7)
N(1)-C(1)-H(11)	112(3)	H(61)-O(6)-H(62)	102(5)		
C(2)-C(1)-H(11)	100(3)	Cu(1)-Cl(1)-K(1)	145.34(4)		

Symmetry transformations used to generate equivalent atoms:

#1 -x+1,-y,-z+1 #2 -x+1,y+1/2,-z+1/2 #3 -x+1,-y+1,-z+1 #4 -x+1,y-1/2,-z+1/2 #5 x,-y+1/2,z-1/2  
 #6 x,y-1,z #7 x,y+1,z #8 -x+2,-y,-z+1

**8.10 K[Cr(Hedta)Cl].H<sub>2</sub>O 11 : Bond lengths [Å] and angles [°].**

Cr(1)-O(1)	1.948(5)	O(1)-Cr(1)-N(1)	84.1(2)	O(1)-C(4)-C(3)	116.1(6)
Cr(1)-O(5)	1.962(5)	O(5)-Cr(1)-N(1)	91.0(2)	C(4)-O(1)-Cr(1)	117.9(4)
Cr(1)-O(3)	1.972(5)	O(3)-Cr(1)-N(1)	80.3(2)	C(4)-O(1)-K(1)	116.8(4)
Cr(1)-N(1)	2.062(6)	O(1)-Cr(1)-N(2)	93.2(2)	Cr(1)-O(1)-K(1)	93.50(19)
Cr(1)-N(2)	2.117(5)	O(5)-Cr(1)-N(2)	82.2(2)	C(4)-O(2)-K(1)#1	142.9(4)
Cr(1)-Cl(1)	2.306(2)	O(3)-Cr(1)-N(2)	164.49(18)	N(1)-C(5)-C(6)	109.1(6)
Cl(1)-K(1)	3.171(2)	N(1)-Cr(1)-N(2)	86.2(2)	N(1)-C(5)-H(5A)	109.9
N(1)-C(5)	1.483(9)	O(1)-Cr(1)-Cl(1)	90.57(15)	N(1)-C(5)-H(5B)	109.9
N(1)-C(1)	1.484(8)	O(5)-Cr(1)-Cl(1)	94.54(15)	O(4)-C(6)-O(3)	125.1(6)
N(1)-C(3)	1.499(9)	O(3)-Cr(1)-Cl(1)	96.54(15)	O(4)-C(6)-C(5)	120.2(6)
C(2)-N(2)	1.506(9)	N(1)-Cr(1)-Cl(1)	173.66(16)	O(3)-C(6)-C(5)	114.7(6)
N(2)-C(9)	1.481(8)	N(2)-Cr(1)-Cl(1)	97.63(16)	C(6)-O(3)-Cr(1)	115.9(4)
N(2)-C(7)	1.484(10)	Cr(1)-Cl(1)-K(1)	81.14(7)	C(6)-O(3)-K(1)	143.6(4)
C(4)-O(2)	1.219(8)	C(5)-N(1)-C(1)	113.7(5)	Cr(1)-O(3)-K(1)	89.52(17)
C(4)-O(1)	1.283(8)	C(5)-N(1)-C(3)	111.5(5)	C(6)-O(4)-K(1)#2	144.6(5)
O(1)-K(1)	2.938(5)	C(1)-N(1)-C(3)	112.3(5)	N(2)-C(7)-C(8)	112.9(6)
O(2)-K(1)#1	2.682(6)	C(5)-N(1)-Cr(1)	104.9(4)	N(2)-C(7)-H(7A)	109.0
C(6)-O(4)	1.212(9)	C(1)-N(1)-Cr(1)	106.4(4)	N(2)-C(7)-H(7B)	109.0
C(6)-O(3)	1.290(8)	C(3)-N(1)-Cr(1)	107.3(4)	H(7A)-C(7)-H(7B)	107.8
O(3)-K(1)	3.055(5)	N(1)-C(1)-C(2)	108.8(5)	O(6)-C(8)-O(5)	125.1(6)
O(4)-K(1)#2	2.792(5)	N(1)-C(1)-H(1A)	109.9	O(6)-C(8)-C(7)	117.8(6)
C(8)-O(6)	1.224(8)	N(1)-C(1)-H(1B)	109.9	O(5)-C(8)-C(7)	117.0(6)
C(8)-O(5)	1.287(8)	C(1)-C(2)-N(2)	112.2(5)	C(8)-O(5)-Cr(1)	116.9(4)
O(6)-K(1)#3	2.678(6)	N(2)-C(2)-H(2A)	109.2	C(8)-O(6)-K(1)#3	126.3(4)
C(10)-O(8)	1.212(8)	N(2)-C(2)-H(2B)	109.2	N(2)-C(9)-C(10)	116.3(5)
C(10)-O(7)	1.294(9)	C(9)-N(2)-C(7)	110.9(5)	N(2)-C(9)-H(9A)	108.2
O(7)-H(7)	0.85(4)	C(9)-N(2)-C(2)	109.8(5)	N(2)-C(9)-H(9B)	108.2
O(8)-K(1)#4	2.797(5)	C(7)-N(2)-C(2)	112.9(5)	O(8)-C(10)-O(7)	125.2(7)
K(1)-O(6)#5	2.678(6)	C(9)-N(2)-Cr(1)	112.9(4)	O(8)-C(10)-C(9)	124.6(6)
K(1)-O(2)#6	2.682(6)	C(7)-N(2)-Cr(1)	106.5(4)	O(7)-C(10)-C(9)	110.2(6)
K(1)-O(4)#7	2.792(5)	C(2)-N(2)-Cr(1)	103.7(4)	C(10)-O(7)-H(7)	132(6)
K(1)-O(8)#8	2.797(5)	N(1)-C(3)-C(4)	112.8(6)	C(10)-O(8)-K(1)#4	167.9(5)
O(11)-H(111)	0.84(4)	N(1)-C(3)-H(3A)	109.0	O(6)#5-K(1)-O(2)#6	102.61(16)
O(11)-H(112)	0.86(4)	N(1)-C(3)-H(3B)	109.0	O(6)#5-K(1)-O(4)#7	102.89(17)
O(1)-Cr(1)-O(5)	173.5(2)	H(3A)-C(3)-H(3B)	107.8	O(2)#6-K(1)-O(4)#7	143.74(17)
O(1)-Cr(1)-O(3)	92.9(2)	O(2)-C(4)-O(1)	124.3(6)	O(6)#5-K(1)-O(8)#8	80.04(16)
O(5)-Cr(1)-O(3)	90.47(19)	O(2)-C(4)-C(3)	119.6(6)	O(2)#6-K(1)-O(8)#8	76.38(16)

O(4)#7-K(1)-O(8)#8	83.14(15)	O(2)#6-K(1)-O(3)	75.52(15)	O(4)#7-K(1)-Cl(1)	93.19(12)
O(6)#5-K(1)-O(1)	93.01(15)	O(4)#7-K(1)-O(3)	132.58(14)	O(8)#8-K(1)-Cl(1)	134.62(14)
O(2)#6-K(1)-O(1)	127.53(15)	O(8)#8-K(1)-O(3)	143.53(15)	O(1)-K(1)-Cl(1)	59.40(11)
O(4)#7-K(1)-O(1)	76.11(15)	O(1)-K(1)-O(3)	56.57(13)	O(3)-K(1)-Cl(1)	61.82(10)
O(8)#8-K(1)-O(1)	156.09(16)	O(6)#5-K(1)-Cl(1)	143.79(12)	H(111)-O(11)-H(112)	103(10)
O(6)#5-K(1)-O(3)	83.89(14)	O(2)#6-K(1)-Cl(1)	80.93(12)		

Symmetry transformations used to generate equivalent atoms:

#1 x-1,y,z #2 x,y+1,z #3 x,y,z+1 #4 x-1,y,z+1 #5 x,y,z-1 #6 x+1,y,z #7 x,y-1,z #8 x+1,y,z-1  
#9 x,y-1,z+1 #10 x-1,y,z-1

### 8.11 [CuCl(H<sub>3</sub>edta)] .2H<sub>2</sub>O 12 : Bond lengths [Å] and angles [°].

Cu(1)-O(1)	1.993(2)	Cu(2)-N(4)	2.072(3)	C(18)-O(16)	1.323(5)
Cu(1)-N(1)	2.039(3)	Cu(2)-Cl(2)	2.2484(9)	O(16)-H(16)	0.89(7)
Cu(1)-N(2)	2.078(3)	Cu(2)-O(13)	2.342(3)	C(19)-C(20)	1.510(5)
Cu(1)-Cl(1)	2.2446(9)	Cu(2)-O(15)	2.585(3)	C(19)-H(191)	0.91(4)
Cu(1)-O(3)	2.349(3)	N(3)-C(13)	1.468(5)	C(19)-H(192)	0.93(4)
Cu(1)-O(5)	2.491(3)	N(3)-C(15)	1.481(4)	C(20)-O(18)	1.216(5)
N(1)-C(3)	1.465(5)	N(3)-C(11)	1.490(4)	C(20)-O(17)	1.303(5)
N(1)-C(5)	1.478(4)	C(12)-N(4)	1.499(4)	O(17)-H(17)	1.03(5)
N(1)-C(1)	1.489(4)	N(4)-C(19)	1.467(5)	O(21)-H(211)	0.85(5)
C(2)-N(2)	1.491(4)	N(4)-C(17)	1.472(4)	O(21)-H(212)	0.77(4)
N(2)-C(7)	1.481(4)	C(13)-C(14)	1.520(4)	O(22)-H(221)	0.72(5)
N(2)-C(9)	1.485(5)	C(13)-H(131)	0.83(4)	O(22)-H(222)	0.69(8)
C(4)-O(2)	1.248(4)	C(13)-H(132)	0.97(5)	O(23)-H(231)	0.84(3)
C(4)-O(1)	1.257(5)	C(14)-O(11)	1.248(5)	O(23)-H(232)	0.78(3)
C(6)-O(3)	1.212(4)	C(14)-O(12)	1.262(5)		
C(6)-O(4)	1.303(4)	C(15)-C(16)	1.505(5)	O(1)-Cu(1)-N(1)	80.38(11)
O(4)-H(4)	1.09(7)	C(15)-H(151)	0.88(4)	O(1)-Cu(1)-N(2)	155.32(12)
C(8)-O(5)	1.217(4)	C(15)-H(152)	1.05(4)	N(1)-Cu(1)-N(2)	86.24(11)
C(8)-O(6)	1.308(4)	C(16)-O(13)	1.217(5)	O(1)-Cu(1)-Cl(1)	97.10(7)
O(6)-H(6)	0.83(6)	C(16)-O(14)	1.299(5)	N(1)-Cu(1)-Cl(1)	170.22(9)
C(10)-O(8)	1.203(5)	O(14)-H(14)	0.79(7)	N(2)-Cu(1)-Cl(1)	99.32(8)
C(10)-O(7)	1.307(5)	C(17)-C(18)	1.514(5)	O(1)-Cu(1)-O(3)	100.47(10)
O(7)-H(7)	0.91(6)	C(17)-H(171)	0.89(4)	N(1)-Cu(1)-O(3)	77.10(11)
Cu(2)-O(11)	1.983(2)	C(17)-H(172)	1.03(4)	N(2)-Cu(1)-O(3)	96.59(11)
Cu(2)-N(3)	2.044(3)	C(18)-O(15)	1.195(5)	Cl(1)-Cu(1)-O(3)	94.18(7)

---

O(1)-Cu(1)-O(5)	88.51(10)	H(51)-C(5)-H(52)	115(4)	O(13)-Cu(2)-O(15)	169.32(9)
N(1)-Cu(1)-O(5)	100.16(11)	O(3)-C(6)-O(4)	124.6(4)	C(13)-N(3)-C(15)	109.7(3)
N(2)-Cu(1)-O(5)	73.47(10)	O(3)-C(6)-C(5)	122.5(3)	C(13)-N(3)-C(11)	115.6(3)
Cl(1)-Cu(1)-O(5)	89.18(7)	O(4)-C(6)-C(5)	112.8(3)	C(15)-N(3)-C(11)	109.9(3)
O(3)-Cu(1)-O(5)	169.92(9)	C(6)-O(3)-Cu(1)	106.5(2)	C(13)-N(3)-Cu(2)	101.5(2)
C(3)-N(1)-C(5)	109.4(3)	C(6)-O(4)-H(4)	109(3)	C(15)-N(3)-Cu(2)	111.6(2)
C(3)-N(1)-C(1)	115.1(3)	N(2)-C(7)-C(8)	111.1(3)	C(11)-N(3)-Cu(2)	108.2(2)
C(5)-N(1)-C(1)	111.1(3)	N(2)-C(7)-H(71)	108(2)	N(3)-C(11)-C(12)	109.6(3)
C(3)-N(1)-Cu(1)	101.3(2)	N(2)-C(7)-H(72)	108(2)	N(3)-C(11)-H(111)	107(2)
C(5)-N(1)-Cu(1)	110.7(2)	H(71)-C(7)-H(72)	114(3)	C(12)-C(11)-H(111)	115(2)
C(1)-N(1)-Cu(1)	108.9(2)	O(5)-C(8)-O(6)	125.0(4)	N(3)-C(11)-H(112)	112(2)
N(1)-C(1)-C(2)	110.5(3)	O(5)-C(8)-C(7)	124.1(3)	C(12)-C(11)-H(112)	109(2)
N(1)-C(1)-H(11)	107(2)	O(6)-C(8)-C(7)	110.9(3)	H(111)-C(11)-H(112)	104(3)
C(2)-C(1)-H(11)	113(2)	C(8)-O(5)-Cu(1)	102.2(2)	N(4)-C(12)-C(11)	110.9(3)
N(1)-C(1)-H(12)	113(2)	C(8)-O(6)-H(6)	116(4)	N(4)-C(12)-H(121)	104(2)
C(2)-C(1)-H(12)	115(2)	N(2)-C(9)-C(10)	119.7(3)	C(11)-C(12)-H(121)	114(2)
H(11)-C(1)-H(12)	98(3)	N(2)-C(9)-H(91)	109(2)	N(4)-C(12)-H(122)	110(2)
N(2)-C(2)-C(1)	110.9(3)	C(10)-C(9)-H(91)	109(2)	C(11)-C(12)-H(122)	110(2)
N(2)-C(2)-H(21)	109(3)	N(2)-C(9)-H(92)	106(3)	H(121)-C(12)-H(122)	107(3)
C(1)-C(2)-H(21)	112(3)	C(10)-C(9)-H(92)	108(3)	C(19)-N(4)-C(17)	111.0(3)
N(2)-C(2)-H(22)	109(2)	H(91)-C(9)-H(92)	104(4)	C(19)-N(4)-C(12)	113.3(3)
C(1)-C(2)-H(22)	111(2)	O(8)-C(10)-O(7)	124.6(3)	C(17)-N(4)-C(12)	109.9(3)
H(21)-C(2)-H(22)	105(4)	O(8)-C(10)-C(9)	119.0(3)	C(19)-N(4)-Cu(2)	107.5(2)
C(7)-N(2)-C(9)	112.5(3)	O(7)-C(10)-C(9)	116.3(3)	C(17)-N(4)-Cu(2)	110.9(2)
C(7)-N(2)-C(2)	110.5(3)	C(10)-O(7)-H(7)	99(4)	C(12)-N(4)-Cu(2)	104.10(19)
C(9)-N(2)-C(2)	112.6(3)	O(11)-Cu(2)-N(3)	79.99(10)	N(3)-C(13)-C(14)	105.3(3)
C(7)-N(2)-Cu(1)	109.1(2)	O(11)-Cu(2)-N(4)	153.03(12)	N(3)-C(13)-H(131)	113(3)
C(9)-N(2)-Cu(1)	107.3(2)	N(3)-Cu(2)-N(4)	86.62(10)	N(3)-C(13)-H(132)	110(3)
C(2)-N(2)-Cu(1)	104.34(19)	O(11)-Cu(2)-Cl(2)	98.17(8)	H(131)-C(13)-H(132)	104(4)
N(1)-C(3)-C(4)	106.4(3)	N(3)-Cu(2)-Cl(2)	172.22(9)	O(11)-C(14)-O(12)	122.9(3)
N(1)-C(3)-H(31)	110(2)	N(4)-Cu(2)-Cl(2)	97.98(8)	O(11)-C(14)-C(13)	117.5(3)
N(1)-C(3)-H(32)	114(2)	O(11)-Cu(2)-O(13)	101.14(10)	O(12)-C(14)-C(13)	119.6(3)
O(2)-C(4)-O(1)	123.8(3)	N(3)-Cu(2)-O(13)	76.25(11)	C(14)-O(11)-Cu(2)	112.1(2)
O(2)-C(4)-C(3)	119.7(3)	N(4)-Cu(2)-O(13)	98.22(11)	N(3)-C(15)-C(16)	111.3(3)
O(1)-C(4)-C(3)	116.5(3)	Cl(2)-Cu(2)-O(13)	96.81(7)	N(3)-C(15)-H(151)	103(3)
C(4)-O(1)-Cu(1)	112.0(2)	O(11)-Cu(2)-O(15)	86.90(10)	N(3)-C(15)-H(152)	109(2)
N(1)-C(5)-C(6)	112.2(3)	N(3)-Cu(2)-O(15)	98.52(10)	C(16)-C(15)-H(152)	113(3)
N(1)-C(5)-H(51)	107(3)	N(4)-Cu(2)-O(15)	71.96(10)	O(13)-C(16)-O(14)	125.5(4)
N(1)-C(5)-H(52)	100(3)	Cl(2)-Cu(2)-O(15)	88.90(7)	O(13)-C(16)-C(15)	122.3(3)

O(14)-C(16)-C(15)	112.2(3)	O(15)-C(18)-C(17)	124.4(3)	O(18)-C(20)-O(17)	125.0(3)
C(16)-O(13)-Cu(2)	107.4(2)	O(16)-C(18)-C(17)	110.6(3)	O(18)-C(20)-C(19)	123.8(4)
C(16)-O(14)-H(14)	110(4)	C(18)-O(15)-Cu(2)	99.8(2)	O(17)-C(20)-C(19)	111.2(3)
N(4)-C(17)-C(18)	112.0(3)	C(18)-O(16)-H(16)	108(3)	C(20)-O(17)-H(17)	116(3)
N(4)-C(17)-H(171)	106(2)	N(4)-C(19)-C(20)	117.4(3)	H(211)-O(21)-H(212)	106(4)
C(18)-C(17)-H(171)	107(2)	N(4)-C(19)-H(191)	111(3)	H(221)-O(22)-H(222)	122(7)
N(4)-C(17)-H(172)	108(2)	N(4)-C(19)-H(192)	101(3)	H(231)-O(23)-H(232)	99(4)
O(15)-C(18)-O(16)	125.0(4)				

Symmetry transformations used to generate equivalent atoms:

#1  $x+1,y,z$  #2  $x-1,y,z$  #3  $x+1/2,-y+1/2,-z+1$  #4  $x-1/2,-y+1/2,-z+1$  #5  $-x+1,y-1/2,-z+1/2$

#6  $-x,y-1/2,-z+1/2$

### 8.12 [Cu(Hada)<sub>2</sub>] **13** : Bond lengths [Å] and angles [°].

Ni(1)-O(8)	2.008(2)	C(6)-C(11)	1.398(4)	O(3)-Ni(1)-O(1)	99.68(8)
Ni(1)-O(3)	2.035(2)	C(7)-C(8)	1.379(4)	O(7)-Ni(1)-O(1)	88.61(10)
Ni(1)-O(7)	2.039(2)	C(7)-O(5)	1.380(3)	O(8)-Ni(1)-N(1)	172.47(9)
Ni(1)-O(1)	2.0398(19)	O(5)-H(5)	0.81(4)	O(3)-Ni(1)-N(1)	84.01(8)
Ni(1)-N(1)	2.072(2)	C(8)-C(9)	1.387(4)	O(7)-Ni(1)-N(1)	91.94(9)
Ni(1)-O(5)	2.0816(19)	C(8)-H(8)	1.01(3)	O(1)-Ni(1)-N(1)	80.17(8)
N(1)-C(3)	1.481(4)	C(9)-C(10)	1.381(4)	O(8)-Ni(1)-O(5)	93.07(9)
N(1)-C(1)	1.484(3)	C(9)-H(9)	1.03(4)	O(3)-Ni(1)-O(5)	88.72(8)
N(1)-C(5)	1.486(3)	C(10)-O(6)	1.379(3)	O(7)-Ni(1)-O(5)	82.21(9)
C(1)-C(2)	1.517(4)	C(10)-C(11)	1.386(4)	O(1)-Ni(1)-O(5)	167.41(8)
C(1)-H(11)	0.92(3)	O(6)-H(6)	0.85(5)	N(1)-Ni(1)-O(5)	91.50(8)
C(1)-H(12)	0.94(3)	C(11)-H(11A)	0.98(4)	C(3)-N(1)-C(1)	111.5(2)
C(2)-O(2)	1.242(3)	O(7)-H(71)	0.70(5)	C(3)-N(1)-C(5)	111.0(2)
C(2)-O(1)	1.277(3)	O(7)-H(72)	0.75(5)	C(1)-N(1)-C(5)	110.7(2)
C(3)-C(4)	1.523(4)	O(8)-H(81)	0.79(4)	C(3)-N(1)-Ni(1)	105.55(16)
C(3)-H(31)	0.98(4)	O(8)-H(82)	0.74(5)	C(1)-N(1)-Ni(1)	105.02(16)
C(3)-H(32)	0.96(4)	O(9)-H(91)	0.79(4)	C(5)-N(1)-Ni(1)	112.75(17)
C(4)-O(4)	1.247(3)	O(9)-H(92)	0.88(5)	N(1)-C(1)-C(2)	110.8(2)
C(4)-O(3)	1.267(3)			N(1)-C(1)-H(11)	110.4(19)
C(5)-C(6)	1.508(4)	O(8)-Ni(1)-O(3)	90.12(9)	C(2)-C(1)-H(11)	106.2(19)
C(5)-H(51)	0.97(3)	O(8)-Ni(1)-O(7)	94.60(10)	N(1)-C(1)-H(12)	112(2)
C(5)-H(52)	0.97(4)	O(3)-Ni(1)-O(7)	169.98(10)	C(2)-C(1)-H(12)	112(2)
C(6)-C(7)	1.394(4)	O(8)-Ni(1)-O(1)	96.24(9)	H(11)-C(1)-H(12)	105(3)

O(2)-C(2)-O(1)	124.2(3)	N(1)-C(5)-H(52)	105(2)	C(8)-C(9)-H(9)	122(2)
O(2)-C(2)-C(1)	118.9(2)	C(6)-C(5)-H(52)	109(2)	O(6)-C(10)-C(9)	122.9(3)
O(1)-C(2)-C(1)	116.9(2)	H(51)-C(5)-H(52)	113(3)	O(6)-C(10)-C(11)	117.1(3)
C(2)-O(1)-Ni(1)	112.88(17)	C(7)-C(6)-C(11)	117.9(2)	C(9)-C(10)-C(11)	120.0(3)
N(1)-C(3)-C(4)	111.9(2)	C(7)-C(6)-C(5)	122.4(2)	C(10)-O(6)-H(6)	105(3)
N(1)-C(3)-H(31)	109(2)	C(11)-C(6)-C(5)	119.6(2)	C(10)-C(11)-C(6)	121.1(3)
C(4)-C(3)-H(31)	106(2)	C(8)-C(7)-O(5)	121.6(2)	C(10)-C(11)-H(11A)	120(2)
N(1)-C(3)-H(32)	111(2)	C(8)-C(7)-C(6)	121.0(2)	C(6)-C(11)-H(11A)	119(2)
C(4)-C(3)-H(32)	112(2)	O(5)-C(7)-C(6)	117.4(2)	Ni(1)-O(7)-H(71)	127(4)
H(31)-C(3)-H(32)	107(3)	C(7)-O(5)-Ni(1)	120.99(16)	Ni(1)-O(7)-H(72)	117(3)
O(4)-C(4)-O(3)	125.0(3)	C(7)-O(5)-H(5)	114(3)	H(71)-O(7)-H(72)	101(5)
O(4)-C(4)-C(3)	118.2(2)	Ni(1)-O(5)-H(5)	114(3)	Ni(1)-O(8)-H(81)	115(4)
O(3)-C(4)-C(3)	116.8(2)	C(7)-C(8)-C(9)	120.4(3)	Ni(1)-O(8)-H(82)	121(4)
C(4)-O(3)-Ni(1)	113.40(17)	C(7)-C(8)-H(8)	118(2)	H(81)-O(8)-H(82)	118(5)
N(1)-C(5)-C(6)	113.0(2)	C(9)-C(8)-H(8)	121(2)	H(91)-O(9)-H(92)	102(4)
N(1)-C(5)-H(51)	109(2)	C(10)-C(9)-C(8)	119.6(3)		
C(6)-C(5)-H(51)	109(2)	C(10)-C(9)-H(9)	118(2)		

Symmetry transformations used to generate equivalent atoms:

#1 -x+1,-y+1,-z+1 #2 x,y,z-1 #3 x,-y+3/2,z-1/2  
 #4 -x,y-1/2,-z+1/2

### 8.13 [Cr(ada)<sub>2</sub>](pyrH).3H<sub>2</sub>O **14** : Bond lengths [Å] and angles [°].

Cr(1)-O(8)	1.945(2)	C(4)-O(4)	1.243(4)	C(12)-N(4)	1.324(5)
Cr(1)-O(6)	1.951(2)	C(4)-O(3)	1.263(4)	N(4)-N(41)	0.81(4)
Cr(1)-O(1)	1.953(2)	C(6)-O(5)	1.225(4)	N(4)-N(42)	0.81(4)
Cr(1)-O(3)	1.955(2)	C(6)-N(2)	1.317(5)	N(21)-C(22)	1.340(7)
Cr(1)-N(3)	2.082(3)	N(2)-H(21)	0.89(4)	N(21)-C(26)	1.358(8)
Cr(1)-N(1)	2.096(3)	N(2)-H(22)	0.65(4)	N(21)-H(21A)	0.8600
C(1)-C(2)	1.506(4)	N(3)-C(11)	1.482(5)	O(23A)-O(23B)	1.620(18)
C(1)-H(11)	0.84(3)	N(3)-C(7)	1.489(5)	O(8)-Cr(1)-O(6)	89.91(11)
C(1)-H(12)	0.96(5)	N(3)-C(9)	1.495(5)	O(8)-Cr(1)-O(1)	89.65(11)
C(2)-O(2)	1.228(4)	C(8)-O(7)	1.225(4)	O(6)-Cr(1)-O(1)	179.44(12)
C(2)-O(1)	1.278(4)	C(8)-O(6)	1.283(4)	O(8)-Cr(1)-O(3)	179.31(13)
C(3)-C(4)	1.498(5)	C(10)-O(9)	1.230(4)	O(6)-Cr(1)-O(3)	89.44(11)
C(3)-H(31)	0.98(3)	C(10)-O(8)	1.286(4)	O(1)-Cr(1)-O(3)	91.00(11)
C(3)-H(32)	0.78(5)	C(12)-O(10)	1.225(4)	O(8)-Cr(1)-N(3)	84.69(10)

O(6)-Cr(1)-N(3)	82.69(10)	O(4)-C(4)-C(3)	118.2(3)	C(8)-O(6)-Cr(1)	116.5(2)
O(1)-Cr(1)-N(3)	97.62(10)	O(3)-C(4)-C(3)	118.7(3)	N(3)-C(9)-C(10)	113.6(3)
O(3)-Cr(1)-N(3)	95.45(11)	C(4)-O(3)-Cr(1)	116.8(2)	N(3)-C(9)-H(91)	111.5(19)
O(8)-Cr(1)-N(1)	95.44(10)	N(1)-C(5)-C(6)	116.5(3)	N(3)-C(9)-H(92)	106(2)
O(6)-Cr(1)-N(1)	97.25(11)	N(1)-C(5)-H(51)	104(2)	O(9)-C(10)-O(8)	122.8(3)
O(1)-Cr(1)-N(1)	82.45(10)	N(1)-C(5)-H(52)	109(2)	O(9)-C(10)-C(9)	119.8(3)
O(3)-Cr(1)-N(1)	84.41(10)	O(5)-C(6)-N(2)	123.9(3)	O(8)-C(10)-C(9)	117.4(3)
N(3)-Cr(1)-N(1)	179.85(13)	O(5)-C(6)-C(5)	122.3(3)	C(10)-O(8)-Cr(1)	116.9(2)
C(5)-N(1)-C(1)	112.8(3)	N(2)-C(6)-C(5)	113.8(3)	N(3)-C(11)-C(12)	115.6(3)
C(5)-N(1)-C(3)	113.0(3)	C(6)-N(2)-H(21)	118(2)	N(3)-C(11)-H(111)	107(2)
C(1)-N(1)-C(3)	112.2(3)	C(6)-N(2)-H(22)	118(4)	N(3)-C(11)-H(112)	108(3)
C(5)-N(1)-Cr(1)	107.5(2)	H(21)-N(2)-H(22)	124(4)	O(10)-C(12)-N(4)	124.2(3)
C(1)-N(1)-Cr(1)	104.56(19)	C(11)-N(3)-C(7)	112.5(3)	O(10)-C(12)-C(11)	122.9(3)
C(3)-N(1)-Cr(1)	106.1(2)	C(11)-N(3)-C(9)	112.6(3)	N(4)-C(12)-C(11)	113.0(3)
N(1)-C(1)-C(2)	111.6(3)	C(7)-N(3)-C(9)	111.5(3)	C(12)-N(4)-N(41)	114(3)
N(1)-C(1)-H(11)	106(2)	C(11)-N(3)-Cr(1)	108.6(2)	C(12)-N(4)-N(42)	117(3)
N(1)-C(1)-H(12)	103(3)	C(7)-N(3)-Cr(1)	104.4(2)	N(41)-N(4)-N(42)	124(4)
O(2)-C(2)-O(1)	123.6(3)	C(9)-N(3)-Cr(1)	106.8(2)	C(22)-N(21)-C(26)	122.2(5)
O(2)-C(2)-C(1)	119.7(3)	N(3)-C(7)-C(8)	111.8(3)	C(22)-N(21)-H(21A)	118.9
O(1)-C(2)-C(1)	116.6(3)	N(3)-C(7)-H(71)	111(2)	C(26)-N(21)-H(21A)	118.9
C(2)-O(1)-Cr(1)	116.9(2)	N(3)-C(7)-H(72)	111(2)	C(23)-C(22)-N(21)	119.1(5)
C(4)-C(3)-N(1)	113.9(3)	H(71)-C(7)-H(72)	103(3)	N(21)-C(22)-H(22A)	120.4
N(1)-C(3)-H(31)	106.6(19)	O(7)-C(8)-O(6)	123.7(3)	N(21)-C(26)-C(25)	115.9(6)
N(1)-C(3)-H(32)	110(3)	O(7)-C(8)-C(7)	120.2(3)	N(21)-C(26)-H(26)	122.0
O(4)-C(4)-O(3)	123.1(3)	O(6)-C(8)-C(7)	116.1(3)		

Symmetry transformations used to generate equivalent atoms:

#1  $x+1, y, z$  #2  $-x+1, y+1/2, -z+1/2$  #3  $x-1, y, z$

#4  $-x, y-1/2, -z+1/2$

#### 8.14 $\{(\text{pyrH})\cdot[\text{Cu}(\text{heidi})(\text{pyr})]\text{Cl}\cdot 2\text{H}_2\text{O}\}_\infty$ **15**: Bond lengths [Å] and angles [°].

Cu(1)-O(2)	1.962(3)	N(1)-C(5)	1.459(6)	C(4)-O(2)	1.282(5)
Cu(1)-O(4)	1.963(3)	N(1)-C(3)	1.477(5)	C(6)-O(5)	1.240(5)
Cu(1)-N(2)	1.971(4)	N(1)-C(1)	1.492(5)	C(6)-O(4)	1.272(5)
Cu(1)-N(1)	2.000(3)	C(2)-O(1)	1.411(6)	O(5)-Cu(1)#2	2.618(3)
Cu(1)-O(1)	2.363(3)	O(1)-H(1)	0.65(6)	N(2)-C(11)	1.329(6)
Cu(1)-O(5)#1	2.618(3)	C(4)-O(3)	1.222(5)	N(2)-C(7)	1.330(6)



N(21)-C(25)	1.326(8)	C(3)-N(1)-Cu(1)	103.8(3)	C(6)-O(5)-Cu(1)#2	132.6(3)
N(21)-C(21)	1.333(7)	C(1)-N(1)-Cu(1)	108.1(3)	C(11)-N(2)-C(7)	117.5(4)
N(21)-H(21)	0.89(6)	N(1)-C(1)-C(2)	111.7(4)	C(11)-N(2)-Cu(1)	119.7(3)
C(21)-C(22)	1.373(8)	N(1)-C(1)-H(1A)	110(3)	C(7)-N(2)-Cu(1)	122.7(3)
C(21)-H(21A)	0.92(6)	N(1)-C(1)-H(1B)	110(3)	N(2)-C(7)-C(8)	122.5(5)
C(22)-C(23)	1.372(9)	O(1)-C(2)-C(1)	111.7(4)	N(2)-C(7)-H(7)	119(4)
C(22)-H(22)	0.97(7)	O(1)-C(2)-H(2A)	103(4)	C(8)-C(7)-H(7)	118(4)
O(2)-Cu(1)-O(4)	165.94(12)	C(1)-C(2)-H(2A)	106(3)	C(9)-C(8)-C(7)	119.4(6)
O(2)-Cu(1)-N(2)	95.64(14)	O(1)-C(2)-H(2B)	107(3)	C(9)-C(8)-H(8)	123(4)
O(4)-Cu(1)-N(2)	95.87(14)	C(2)-O(1)-Cu(1)	101.0(2)	C(7)-C(8)-H(8)	117(4)
O(2)-Cu(1)-N(1)	84.14(13)	C(2)-O(1)-H(1)	106(6)	C(8)-C(9)-C(10)	118.5(5)
O(4)-Cu(1)-N(1)	84.89(13)	Cu(1)-O(1)-H(1)	107(6)	C(8)-C(9)-H(9)	118(4)
N(2)-Cu(1)-N(1)	176.29(14)	N(1)-C(3)-C(4)	109.7(3)	C(10)-C(9)-H(9)	123(4)
O(2)-Cu(1)-O(1)	100.48(12)	N(1)-C(3)-H(3A)	110(3)	C(11)-C(10)-C(9)	119.2(5)
O(4)-Cu(1)-O(1)	86.83(12)	N(1)-C(3)-H(3B)	107(3)	C(11)-C(10)-H(10)	118(5)
N(2)-Cu(1)-O(1)	93.64(13)	O(3)-C(4)-O(2)	125.1(4)	C(9)-C(10)-H(10)	122(5)
N(1)-Cu(1)-O(1)	82.77(12)	O(3)-C(4)-C(3)	118.0(4)	N(2)-C(11)-C(10)	123.0(5)
O(2)-Cu(1)-O(5)#1	81.04(11)	O(2)-C(4)-C(3)	116.9(4)	N(2)-C(11)-H(11)	116(3)
O(4)-Cu(1)-O(5)#1	90.95(11)	C(4)-O(2)-Cu(1)	112.3(3)	C(25)-N(21)-C(21)	122.3(5)
N(2)-Cu(1)-O(5)#1	89.77(12)	N(1)-C(5)-C(6)	111.0(3)	C(25)-N(21)-H(21)	120(4)
N(1)-Cu(1)-O(5)#1	93.85(11)	N(1)-C(5)-H(5A)	106(3)	C(21)-N(21)-H(21)	117(4)
O(1)-Cu(1)-O(5)#1	176.10(11)	N(1)-C(5)-H(5B)	104(4)	N(21)-C(21)-C(22)	119.7(5)
C(5)-N(1)-C(3)	115.8(3)	O(5)-C(6)-O(4)	123.7(4)	N(21)-C(21)-H(21A)	119(4)
C(5)-N(1)-C(1)	111.6(3)	O(5)-C(6)-C(5)	119.5(4)	N(21)-C(25)-C(24)	119.5(6)
C(3)-N(1)-C(1)	109.6(3)	O(4)-C(6)-C(5)	116.7(4)	N(21)-C(25)-H(25)	120(5)
C(5)-N(1)-Cu(1)	107.3(3)	C(6)-O(4)-Cu(1)	114.2(3)		

Symmetry transformations used to generate equivalent atoms:

#1 -x+1/2,y-1/2,-z+1/2 #2 -x+1/2,y+1/2,-z+1/2

### 8.15 [Cu(naphtyl-OH-ida)(H<sub>2</sub>O)] **16**: Bond lengths [Å] and angles [°].

Cu(1)-O(3)	1.911(7)	N(1)-C(3)	1.487(12)	C(5)-C(6)	1.502(16)
Cu(1)-O(1)	1.913(8)	C(1)-C(2)	1.516(15)	C(6)-C(7)	1.368(15)
Cu(1)-O(6)	1.939(7)	C(2)-O(1)	1.268(12)	C(6)-C(11)	1.404(18)
Cu(1)-N(1)	2.014(8)	C(2)-O(2)	1.278(12)	C(7)-O(5)	1.351(13)
Cu(1)-O(5)	2.448(8)	C(3)-C(4)	1.558(14)		
N(1)-C(5)	1.463(16)	C(4)-O(4)	1.224(13)	Cu(2)-O(21)	1.910(7)
N(1)-C(1)	1.468(13)	C(4)-O(3)	1.299(12)	Cu(2)-O(23)	1.917(7)

Cu(2)-O(26)	1.936(7)	C(3)-N(1)-Cu(1)	103.2(6)	O(23)-Cu(2)-O(25)	90.1(3)
Cu(2)-N(21)	1.993(9)	N(1)-C(1)-C(2)	109.8(8)	O(26)-Cu(2)-O(25)	101.6(3)
Cu(2)-O(25)	2.432(9)	O(1)-C(2)-O(2)	119.4(10)	N(21)-Cu(2)-O(25)	88.7(3)
N(21)-C(25)	1.484(17)	O(1)-C(2)-C(1)	118.7(9)	C(25)-N(21)-C(23)	113.2(9)
N(21)-C(23)	1.494(12)	O(2)-C(2)-C(1)	121.9(8)	C(25)-N(21)-C(21)	108.9(8)
N(21)-C(21)	1.522(14)	C(2)-O(1)-Cu(1)	112.9(7)	C(23)-N(21)-C(21)	113.5(8)
O(3)-Cu(1)-O(1)	165.7(3)	N(1)-C(3)-C(4)	111.0(8)	C(25)-N(21)-Cu(2)	111.5(6)
O(3)-Cu(1)-O(6)	100.3(3)	O(4)-C(4)-O(3)	127.0(9)	C(23)-N(21)-Cu(2)	103.5(6)
O(1)-Cu(1)-O(6)	85.6(3)	O(4)-C(4)-C(3)	118.2(9)	C(21)-N(21)-Cu(2)	106.0(7)
O(3)-Cu(1)-N(1)	87.1(3)	O(3)-C(4)-C(3)	114.7(9)	C(22)-C(21)-N(21)	108.5(8)
O(1)-Cu(1)-N(1)	85.1(3)	C(4)-O(3)-Cu(1)	114.5(6)	O(22)-C(22)-O(21)	123.9(10)
O(6)-Cu(1)-N(1)	168.1(4)	N(1)-C(5)-C(6)	113.0(9)	O(22)-C(22)-C(21)	119.3(9)
O(3)-Cu(1)-O(5)	91.0(3)	O(5)-C(7)-C(6)	120.5(10)	O(21)-C(22)-C(21)	116.8(9)
O(1)-Cu(1)-O(5)	100.8(3)	O(5)-C(7)-C(8)	118.9(10)	C(22)-O(21)-Cu(2)	115.2(7)
O(6)-Cu(1)-O(5)	101.0(3)	O(21)-Cu(2)-O(23)	166.3(3)	N(21)-C(23)-C(24)	110.5(8)
N(1)-Cu(1)-O(5)	88.0(3)	O(21)-Cu(2)-O(26)	86.9(3)	O(24)-C(24)-O(23)	126.4(9)
C(5)-N(1)-C(1)	111.6(8)	O(23)-Cu(2)-O(26)	100.2(3)	O(24)-C(24)-C(23)	116.3(9)
C(5)-N(1)-C(3)	111.9(8)	O(21)-Cu(2)-N(21)	84.0(3)	O(23)-C(24)-C(23)	117.2(9)
C(1)-N(1)-C(3)	112.1(8)	O(23)-Cu(2)-N(21)	87.0(4)	C(24)-O(23)-Cu(2)	113.9(7)
C(5)-N(1)-Cu(1)	112.6(6)	O(26)-Cu(2)-N(21)	167.3(4)	N(21)-C(25)-C(26)	113.6(8)
C(1)-N(1)-Cu(1)	104.9(7)	O(21)-Cu(2)-O(25)	100.0(3)		

### 8.16 [Ni(hda-OH)(H<sub>2</sub>O)<sub>2</sub>].H<sub>2</sub>O 17: Bond lengths [Å] and angles [°].

Ni(1)-O(8)	2.008(2)	O(6)-H(6)	0.85(5)	O(7)-Ni(1)-N(1)	91.94(9)
Ni(1)-O(3)	2.035(2)	O(7)-H(71)	0.70(5)	O(1)-Ni(1)-N(1)	80.17(8)
Ni(1)-O(7)	2.039(2)	O(7)-H(72)	0.75(5)	O(8)-Ni(1)-O(5)	93.07(9)
Ni(1)-O(1)	2.0398(19)	O(8)-H(81)	0.79(4)	O(3)-Ni(1)-O(5)	88.72(8)
Ni(1)-N(1)	2.072(2)	O(8)-H(82)	0.74(5)	O(7)-Ni(1)-O(5)	82.21(9)
Ni(1)-O(5)	2.0816(19)	O(9)-H(91)	0.79(4)	O(1)-Ni(1)-O(5)	167.41(8)
N(1)-C(3)	1.481(4)	O(9)-H(92)	0.88(5)	N(1)-Ni(1)-O(5)	91.50(8)
N(1)-C(1)	1.484(3)	O(8)-Ni(1)-O(3)	90.12(9)	C(3)-N(1)-C(1)	111.5(2)
N(1)-C(5)	1.486(3)	O(8)-Ni(1)-O(7)	94.60(10)	C(3)-N(1)-C(5)	111.0(2)
C(2)-O(2)	1.242(3)	O(3)-Ni(1)-O(7)	169.98(10)	C(1)-N(1)-C(5)	110.7(2)
C(2)-O(1)	1.277(3)	O(8)-Ni(1)-O(1)	96.24(9)	C(3)-N(1)-Ni(1)	105.55(16)
C(4)-O(4)	1.247(3)	O(3)-Ni(1)-O(1)	99.68(8)	C(1)-N(1)-Ni(1)	105.02(16)
C(4)-O(3)	1.267(3)	O(7)-Ni(1)-O(1)	88.61(10)	C(5)-N(1)-Ni(1)	112.75(17)
C(7)-O(5)	1.380(3)	O(8)-Ni(1)-N(1)	172.47(9)	N(1)-C(1)-C(2)	110.8(2)
C(10)-O(6)	1.379(3)	O(3)-Ni(1)-N(1)	84.01(8)	N(1)-C(1)-H(11)	110.4(19)

C(2)-C(1)-H(11)	106.2(19)	O(4)-C(4)-C(3)	118.2(2)	C(7)-O(5)-H(5)	114(3)
N(1)-C(1)-H(12)	112(2)	O(3)-C(4)-C(3)	116.8(2)	Ni(1)-O(5)-H(5)	114(3)
C(2)-C(1)-H(12)	112(2)	C(4)-O(3)-Ni(1)	113.40(17)	C(7)-C(8)-C(9)	120.4(3)
H(11)-C(1)-H(12)	105(3)	N(1)-C(5)-C(6)	113.0(2)	C(10)-O(6)-H(6)	105(3)
O(2)-C(2)-O(1)	124.2(3)	N(1)-C(5)-H(51)	109(2)	Ni(1)-O(7)-H(71)	127(4)
O(2)-C(2)-C(1)	118.9(2)	N(1)-C(5)-H(52)	105(2)	Ni(1)-O(7)-H(72)	117(3)
O(1)-C(2)-C(1)	116.9(2)	C(6)-C(5)-H(52)	109(2)	H(71)-O(7)-H(72)	101(5)
C(2)-O(1)-Ni(1)	112.88(17)	H(51)-C(5)-H(52)	113(3)	Ni(1)-O(8)-H(81)	115(4)
N(1)-C(3)-C(4)	111.9(2)	C(8)-C(7)-O(5)	121.6(2)	Ni(1)-O(8)-H(82)	121(4)
N(1)-C(3)-H(31)	109(2)	C(8)-C(7)-C(6)	121.0(2)	H(81)-O(8)-H(82)	118(5)
N(1)-C(3)-H(32)	111(2)	O(5)-C(7)-C(6)	117.4(2)	H(91)-O(9)-H(92)	102(4)
O(4)-C(4)-O(3)	125.0(3)	C(7)-O(5)-Ni(1)	120.99(16)		

Symmetry transformations used to generate equivalent atoms:

#1 -x+1,-y+1,-z+1 #2 x,-y+1/2,z+1/2 #3 x,y,z+1 #4 x+1,y,z #5 -x+1,-y+1,-z+2 #6 x+1,-y+1/2,z+1/2

### 8.17 [Cr(hda-OH)(H<sub>2</sub>O)].2H<sub>2</sub>O **18**: Bond lengths [Å] and angles [°].

Cr(1)-O(5)	1.929(2)	O(11)-H(111)	0.72(6)	C(1)-N(1)-Cr(1)	104.9(3)
Cr(1)-O(3)	1.964(3)	O(11)-H(112)	0.83(6)	C(3)-N(1)-Cr(1)	107.7(3)
Cr(1)-O(8)	1.964(3)	O(12A)-O(12B)	0.576(10)	C(5)-N(1)-Cr(1)	110.5(3)
Cr(1)-O(7)	1.978(4)	O(5)-Cr(1)-O(3)	90.71(11)	N(1)-C(1)-C(2)	109.8(4)
Cr(1)-O(1)	1.996(2)	O(5)-Cr(1)-O(8)	88.15(12)	N(1)-C(1)-H(1A)	110(3)
Cr(1)-N(1)	2.068(4)	O(3)-Cr(1)-O(8)	176.09(15)	N(1)-C(1)-H(1B)	112(3)
N(1)-C(1)	1.477(5)	O(5)-Cr(1)-O(7)	91.70(12)	O(2)-C(2)-O(1)	125.0(4)
N(1)-C(3)	1.482(6)	O(3)-Cr(1)-O(7)	90.57(14)	O(2)-C(2)-C(1)	119.4(4)
N(1)-C(5)	1.512(5)	O(8)-Cr(1)-O(7)	93.20(16)	O(1)-C(2)-C(1)	115.6(3)
C(2)-O(2)	1.224(4)	O(5)-Cr(1)-O(1)	171.90(14)	C(2)-O(1)-Cr(1)	114.9(2)
C(2)-O(1)	1.293(5)	O(3)-Cr(1)-O(1)	93.93(12)	N(1)-C(3)-C(4)	112.6(4)
C(3)-C(4)	1.507(7)	O(8)-Cr(1)-O(1)	86.78(12)	N(1)-C(3)-H(3A)	109(3)
C(4)-O(4)	1.232(5)	O(7)-Cr(1)-O(1)	94.89(12)	N(1)-C(3)-H(3B)	106(3)
C(4)-O(3)	1.277(5)	O(5)-Cr(1)-N(1)	93.71(12)	O(4)-C(4)-O(3)	123.8(5)
C(7)-O(5)	1.370(5)	O(3)-Cr(1)-N(1)	82.87(15)	O(4)-C(4)-C(3)	120.6(4)
C(10)-O(6)	1.380(5)	O(8)-Cr(1)-N(1)	93.46(16)	O(3)-C(4)-C(3)	115.6(4)
O(6)-H(6)	0.91(5)	O(7)-Cr(1)-N(1)	171.55(14)	C(4)-O(3)-Cr(1)	118.1(3)
O(7)-H(71)	0.73(4)	O(1)-Cr(1)-N(1)	80.30(11)	C(6)-C(5)-N(1)	110.0(4)
O(7)-H(72)	0.73(4)	C(1)-N(1)-C(3)	110.4(3)	N(1)-C(5)-H(5A)	110.2(19)
O(8)-H(81)	0.73(4)	C(1)-N(1)-C(5)	111.8(4)	N(1)-C(5)-H(5B)	102(2)
O(8)-H(82)	0.77(4)	C(3)-N(1)-C(5)	111.3(3)	O(5)-C(7)-C(6)	120.5(4)

O(5)-C(7)-C(8)	119.9(4)	C(10)-C(11)-C(6)	120.4(4)	Cr(1)-O(8)-H(81)	110(5)
C(7)-O(5)-Cr(1)	120.3(2)	C(10)-C(11)-H(11)	118(2)	Cr(1)-O(8)-H(82)	119(5)
O(6)-C(10)-C(9)	118.3(4)	C(6)-C(11)-H(11)	121(2)	H(81)-O(8)-H(82)	127(7)
O(6)-C(10)-C(11)	122.2(4)	Cr(1)-O(7)-H(71)	121(5)	H(111)-O(11)-H(112)	107(6)
C(9)-C(10)-C(11)	119.5(4)	Cr(1)-O(7)-H(72)	114(5)		
C(10)-O(6)-H(6)	109(3)	H(71)-O(7)-H(72)	109(7)		

Symmetry transformations used to generate equivalent atoms:

#1 -x+1,y+1/2,-z+1/2 #2 -x,-y,-z+1 #3 -x+1,-y,-z+1 #4 x+1,y,z #5 x,-y+1/2,z+1/2

### 8.18 [Fe(hda-OH)(H<sub>2</sub>O)<sub>2</sub>].2H<sub>2</sub>O **19**: Bond lengths [Å] and angles [°].

Fe(1)-O(1)	1.923(5)	O(8)-Fe(1)-O(7)	94.9(2)	C(5)-C(6)-O(2)	118.2(6)
Fe(1)-O(8)	1.988(4)	O(1)-Fe(1)-O(3)	90.86(18)	C(6)-O(2)-H(2)	93(5)
Fe(1)-O(7)	2.003(4)	O(8)-Fe(1)-O(3)	90.34(16)	N(1)-C(8)-C(9)	113.3(5)
Fe(1)-O(3)	2.007(3)	O(7)-Fe(1)-O(3)	174.8(2)	N(1)-C(8)-H(8A)	112(4)
Fe(1)-O(5)	2.040(5)	O(1)-Fe(1)-O(5)	166.8(2)	N(1)-C(8)-H(8B)	113(3)
Fe(1)-N(1)	2.173(5)	O(8)-Fe(1)-O(5)	94.01(19)	O(4)-C(9)-O(3)	123.2(6)
N(1)-C(10)	1.479(9)	O(7)-Fe(1)-O(5)	85.9(2)	O(4)-C(9)-C(8)	120.7(5)
N(1)-C(8)	1.481(7)	O(3)-Fe(1)-O(5)	94.06(17)	O(3)-C(9)-C(8)	116.0(5)
N(1)-C(1)	1.491(9)	O(1)-Fe(1)-N(1)	91.2(2)	C(9)-O(3)-Fe(1)	119.2(4)
C(6)-O(2)	1.403(8)	O(8)-Fe(1)-N(1)	167.05(19)	N(1)-C(10)-C(11)	110.9(6)
O(2)-H(2)	0.90(8)	O(7)-Fe(1)-N(1)	94.4(2)	N(1)-C(10)-H(10A)	107(5)
C(9)-O(4)	1.220(6)	O(3)-Fe(1)-N(1)	80.54(16)	O(6)-C(11)-O(5)	123.4(7)
C(9)-O(3)	1.301(6)	O(5)-Fe(1)-N(1)	77.6(2)	O(6)-C(11)-C(10)	120.8(6)
C(11)-O(6)	1.226(8)	C(10)-N(1)-C(8)	111.5(5)	O(5)-C(11)-C(10)	115.9(7)
C(11)-O(5)	1.296(7)	C(10)-N(1)-C(1)	111.8(5)	C(11)-O(5)-Fe(1)	116.7(5)
O(7)-H(71)	0.85(4)	C(8)-N(1)-C(1)	111.6(5)	Fe(1)-O(7)-H(71)	127(5)
O(7)-H(72)	0.85(4)	C(10)-N(1)-Fe(1)	103.9(4)	Fe(1)-O(7)-H(72)	116(4)
O(8)-H(81)	0.81(3)	C(8)-N(1)-Fe(1)	107.8(4)	H(71)-O(7)-H(72)	116(6)
O(8)-H(82)	0.90(4)	C(1)-N(1)-Fe(1)	109.9(4)	Fe(1)-O(8)-H(81)	126(5)
O(9)-H(91)	0.89(4)	C(2)-C(1)-N(1)	110.9(6)	Fe(1)-O(8)-H(82)	121(5)
O(9)-H(92)	0.89(4)	N(1)-C(1)-H(1A)	114(4)	H(81)-O(8)-H(82)	94(7)
O(10A)-O(10B)	0.715(15)	N(1)-C(1)-H(1B)	97(4)	H(91)-O(9)-H(92)	101(7)
O(1)-Fe(1)-O(8)	98.2(2)	C(3)-O(1)-Fe(1)	123.2(4)		
O(1)-Fe(1)-O(7)	88.1(2)	C(7)-C(6)-O(2)	122.4(6)		

Symmetry transformations used to generate equivalent atoms:

#1 -x+1,y+1/2,-z+1/2 #2 -x+1,-y,-z+1 #3 -x,-y,-z+1 #4 x,-y+1/2,z+1/2 #5 x+1,y,z

**8.19  $K_5[Fe_2(\mu-O)(\mu-NO_3)(SO_3-hda-OH)_2] \cdot 15H_2O$  20 : Bond lengths [Å] and angles [°].**

Fe(1)-O(1)	1.835(4)	S(1)-O(11)	1.433(6)	O(25A)-K(2)#2	3.26(5)
Fe(1)-O(8)	1.977(4)	S(1)-O(10)	1.452(5)	O(25B)-K(2)#2	3.09(3)
Fe(1)-O(2)	2.038(5)	S(1)-O(9)	1.462(5)	O(25C)-O(27A)	1.59(8)
Fe(1)-O(4)	2.080(5)	S(1)-K(3)#3	3.422(2)	O(26A)-O(26B)	1.12(4)
Fe(1)-O(6)	2.098(4)	S(1)-K(2)#2	3.790(2)	O(26B)-O(26C)	1.70(8)
Fe(1)-N(2)	2.198(5)	O(9)-K(3)#3	2.903(6)	O(27A)-O(27B)	1.45(7)
Fe(1)-K(1)#1	3.614(3)	O(10)-K(2)#2	2.718(6)		
Fe(1)-K(1)	3.683(2)	O(10)-K(1)#4	2.748(6)	O(1)-Fe(1)-O(8)	100.54(15)
Fe(1)-K(2)#1	3.947(2)	O(10)-K(3)#3	2.919(6)	O(1)-Fe(1)-O(2)	99.9(2)
O(1)-Fe(1)#1	1.835(4)	K(1)-O(22B)	1.704(18)	O(8)-Fe(1)-O(2)	87.0(2)
O(1)-K(1)#1	2.965(3)	K(1)-O(6)#1	2.717(6)	O(1)-Fe(1)-O(4)	93.4(3)
O(1)-K(1)	2.965(3)	K(1)-O(22A)	2.748(13)	O(8)-Fe(1)-O(4)	89.5(2)
O(2)-N(1)	1.271(7)	K(1)-O(10)#5	2.748(6)	O(2)-Fe(1)-O(4)	166.7(2)
O(2)-K(2)#1	2.726(5)	K(1)-O(28)	3.40(5)	O(1)-Fe(1)-O(6)	94.77(15)
N(1)-O(3)#1	1.265(16)	K(1)-Fe(1)#1	3.614(3)	O(8)-Fe(1)-O(6)	164.2(2)
N(1)-O(3)	1.265(16)	K(1)-K(2)#1	3.937(4)	O(2)-Fe(1)-O(6)	86.6(2)
N(1)-O(2)#1	1.271(7)	K(1)-K(3)#6	4.796(3)	O(4)-Fe(1)-O(6)	93.4(2)
N(1)-K(2)	3.3648(19)	K(2)-O(10)#7	2.718(6)	O(1)-Fe(1)-N(2)	166.15(17)
N(1)-K(2)#1	3.3648(19)	K(2)-O(2)#1	2.726(5)	O(8)-Fe(1)-N(2)	90.23(19)
O(3)-O(3)#1	0.78(2)	K(2)-O(5)#7	2.812(6)	O(2)-Fe(1)-N(2)	89.3(2)
O(3)-K(2)	3.375(16)	K(2)-O(8)#1	2.995(6)	O(4)-Fe(1)-N(2)	77.9(2)
N(2)-C(2)	1.455(8)	K(2)-O(21)	3.001(13)	O(6)-Fe(1)-N(2)	75.27(18)
N(2)-C(6)	1.492(8)	K(2)-O(25B)#7	3.09(3)	O(1)-Fe(1)-K(1)#1	54.84(6)
N(2)-C(4)	1.496(9)	K(2)-O(25A)#7	3.26(5)	O(8)-Fe(1)-K(1)#1	146.38(18)
C(3)-O(5)	1.245(10)	K(3)-O(7)#8	2.786(5)	O(2)-Fe(1)-K(1)#1	117.17(15)
C(3)-O(4)	1.270(9)	K(3)-O(9)#9	2.903(7)	O(4)-Fe(1)-K(1)#1	71.68(17)
O(5)-K(2)#2	2.812(6)	K(3)-O(9)#7	2.903(6)	O(6)-Fe(1)-K(1)#1	48.33(14)
C(5)-O(6)	1.238(9)	K(3)-O(21)	2.915(15)	N(2)-Fe(1)-K(1)#1	111.69(14)
C(5)-O(7)	1.258(8)	K(3)-O(21)#8	2.915(15)	O(1)-Fe(1)-K(1)	52.97(6)
C(5)-K(2)	3.368(7)	K(3)-O(10)#9	2.919(6)	O(8)-Fe(1)-K(1)	47.62(15)
O(6)-K(1)#1	2.717(6)	K(3)-O(10)#7	2.919(6)	O(2)-Fe(1)-K(1)	93.11(15)
O(6)-K(2)	3.207(5)	K(3)-S(1)#9	3.422(2)	O(4)-Fe(1)-K(1)	94.03(16)
O(7)-K(3)	2.786(5)	K(3)-S(1)#7	3.422(2)	O(6)-Fe(1)-K(1)	147.25(14)
O(7)-K(2)	2.945(6)	K(3)-K(2)#8	3.9769(18)	N(2)-Fe(1)-K(1)	137.48(14)
C(8)-O(8)	1.310(8)	O(22A)-O(22B)	1.23(2)	K(1)#1-Fe(1)-K(1)	104.76(7)
		O(24A)-O(24B)	1.04(3)	O(1)-Fe(1)-K(2)#1	97.78(12)
O(8)-K(1)	2.767(5)	O(25A)-O(27A)	1.21(7)	O(8)-Fe(1)-K(2)#1	47.64(16)
O(8)-K(2)#1	2.995(6)	O(25A)-O(25B)	1.54(5)	O(2)-Fe(1)-K(2)#1	40.12(14)

O(4)-Fe(1)-K(2)#1	136.95(16)	O(5)-C(3)-O(4)	124.4(8)	O(11)-S(1)-K(3)#3	152.5(2)
O(6)-Fe(1)-K(2)#1	126.61(15)	O(5)-C(3)-C(2)	119.3(6)	O(10)-S(1)-K(3)#3	57.8(2)
N(2)-Fe(1)-K(2)#1	95.91(14)	O(4)-C(3)-C(2)	116.3(7)	O(9)-S(1)-K(3)#3	57.2(2)
K(1)#1-Fe(1)-K(2)#1	145.42(6)	C(3)-O(4)-Fe(1)	118.3(5)	C(11)-S(1)-K(3)#3	100.8(2)
K(1)-Fe(1)-K(2)#1	62.01(5)	C(3)-O(5)-K(2)#2	137.6(5)	O(11)-S(1)-K(2)#2	122.6(3)
Fe(1)#1-O(1)-Fe(1)	123.3(4)	N(2)-C(4)-C(5)	108.6(5)	O(10)-S(1)-K(2)#2	34.4(2)
Fe(1)#1-O(1)-K(1)#1	97.42(6)	O(6)-C(5)-O(7)	124.4(6)	O(9)-S(1)-K(2)#2	122.4(3)
Fe(1)-O(1)-K(1)#1	94.76(6)	O(6)-C(5)-C(4)	117.9(6)	C(11)-S(1)-K(2)#2	71.3(2)
Fe(1)#1-O(1)-K(1)	94.76(6)	O(7)-C(5)-C(4)	117.6(6)	K(3)#3-S(1)-K(2)#2	66.71(5)
Fe(1)-O(1)-K(1)	97.42(6)	O(6)-C(5)-K(2)	71.9(4)	S(1)-O(9)-K(3)#3	97.7(3)
K(1)#1-O(1)-K(1)	154.2(3)	O(7)-C(5)-K(2)	59.9(4)	S(1)-O(10)-K(2)#2	128.1(3)
N(1)-O(2)-Fe(1)	125.8(5)	C(4)-C(5)-K(2)	147.5(5)	S(1)-O(10)-K(1)#4	128.6(3)
N(1)-O(2)-K(2)#1	109.2(3)	C(5)-O(6)-Fe(1)	115.5(4)	K(2)#2-O(10)-K(1)#4	92.15(16)
Fe(1)-O(2)-K(2)#1	111.1(2)	C(5)-O(6)-K(1)#1	146.8(4)	S(1)-O(10)-K(3)#3	97.3(2)
O(3)#1-N(1)-O(3)	35.8(12)	Fe(1)-O(6)-K(1)#1	96.45(19)	K(2)#2-O(10)-K(3)#3	89.66(18)
O(3)#1-N(1)-O(2)	114.5(11)	C(5)-O(6)-K(2)	86.5(4)	K(1)#4-O(10)-K(3)#3	115.55(19)
O(3)-N(1)-O(2)	120.0(12)	Fe(1)-O(6)-K(2)	123.65(19)	O(22B)-K(1)-O(6)#1	74.2(6)
O(3)#1-N(1)-O(2)#1	120.0(12)	K(1)#1-O(6)-K(2)	82.85(14)	O(22B)-K(1)-O(22A)	17.5(6)
O(3)-N(1)-O(2)#1	114.5(11)	C(5)-O(7)-K(3)	128.0(5)	O(6)#1-K(1)-O(22A)	89.8(3)
O(2)-N(1)-O(2)#1	122.6(10)	C(5)-O(7)-K(2)	98.4(4)	O(22B)-K(1)-O(10)#5	76.3(5)
O(3)#1-N(1)-K(2)	108.8(8)	K(3)-O(7)-K(2)	87.83(14)	O(6)#1-K(1)-O(10)#5	81.25(17)
O(3)-N(1)-K(2)	79.7(7)	N(2)-C(6)-C(7)	111.0(5)	O(22A)-K(1)-O(10)#5	86.1(5)
O(2)-N(1)-K(2)	124.9(4)	C(12)-C(7)-C(8)	121.1(6)	O(22B)-K(1)-O(8)	149.5(6)
O(2)#1-N(1)-K(2)	49.9(2)	Fe(1)-O(8)-K(1)	100.52(19)	O(6)#1-K(1)-O(8)	85.37(16)
O(3)#1-N(1)-K(2)#1	79.7(7)	C(8)-O(8)-K(2)#1	114.5(4)	O(22A)-K(1)-O(8)	164.2(5)
O(3)-N(1)-K(2)#1	108.8(8)	Fe(1)-O(8)-K(2)#1	103.2(2)	O(10)#5-K(1)-O(8)	78.38(16)
O(2)-N(1)-K(2)#1	49.9(2)	K(1)-O(8)-K(2)#1	86.10(14)	O(22B)-K(1)-O(1)	123.0(5)
O(2)#1-N(1)-K(2)#1	124.9(4)	C(8)-C(9)-C(10)	120.6(7)	O(6)#1-K(1)-O(1)	61.19(15)
K(2)-N(1)-K(2)#1	171.4(4)	C(11)-C(10)-C(9)	119.4(6)	O(22A)-K(1)-O(1)	128.4(5)
O(3)#1-O(3)-N(1)	72.1(6)	C(10)-C(11)-C(12)	120.9(7)	O(10)#5-K(1)-O(1)	125.3(2)
O(3)#1-O(3)-K(2)	134(3)	C(10)-C(11)-S(1)	118.9(5)	O(8)-K(1)-O(1)	61.44(11)
N(1)-O(3)-K(2)	78.7(7)	C(12)-C(11)-S(1)	120.2(5)	O(22B)-K(1)-O(28)	131.5(10)
C(2)-N(2)-C(6)	112.6(5)	C(7)-C(12)-C(11)	119.9(6)	O(6)#1-K(1)-O(28)	114.9(8)
C(2)-N(2)-C(4)	110.3(5)	O(11)-S(1)-O(10)	113.2(3)	O(22A)-K(1)-O(28)	117.9(10)
C(6)-N(2)-C(4)	109.7(5)	O(11)-S(1)-O(9)	113.3(4)	O(10)#5-K(1)-O(28)	149.7(8)
C(2)-N(2)-Fe(1)	108.4(4)	O(10)-S(1)-O(9)	111.2(3)	O(8)-K(1)-O(28)	77.7(9)
C(6)-N(2)-Fe(1)	110.4(4)	O(11)-S(1)-C(11)	106.7(3)	O(1)-K(1)-O(28)	55.4(8)
C(4)-N(2)-Fe(1)	105.1(4)	O(10)-S(1)-C(11)	105.6(3)	O(22B)-K(1)-Fe(1)#1	93.8(5)
N(2)-C(2)-C(3)	112.2(5)	O(9)-S(1)-C(11)	106.1(3)	O(6)#1-K(1)-Fe(1)#1	35.22(10)

O(22A)-K(1)-Fe(1)#1	103.1(5)	O(2)#1-K(2)-O(8)#1	57.57(15)	O(2)#1-K(2)-C(5)	72.86(15)
O(10)#5-K(1)-Fe(1)#1	114.43(15)	O(5)#7-K(2)-O(8)#1	100.75(17)	O(5)#7-K(2)-C(5)	147.67(19)
O(8)-K(1)-Fe(1)#1	81.45(11)	O(7)-K(2)-O(8)#1	115.00(15)	O(7)-K(2)-C(5)	21.70(15)
O(1)-K(1)-Fe(1)#1	30.40(7)	O(10)#7-K(2)-O(21)	85.1(3)	O(8)#1-K(2)-C(5)	94.90(16)
O(28)-K(1)-Fe(1)#1	79.9(8)	O(2)#1-K(2)-O(21)	141.3(3)	O(21)-K(2)-C(5)	86.9(2)
O(22B)-K(1)-Fe(1)	143.4(6)	O(5)#7-K(2)-O(21)	88.1(3)	O(25B)#7-K(2)-C(5)	92.5(7)
O(6)#1-K(1)-Fe(1)	69.59(11)	O(7)-K(2)-O(21)	65.2(2)	O(6)-K(2)-C(5)	21.52(15)
O(22A)-K(1)-Fe(1)	155.6(5)	O(8)#1-K(2)-O(21)	159.5(3)	O(25A)#7-K(2)-C(5)	80.4(9)
O(10)#5-K(1)-Fe(1)	102.94(13)	O(10)#7-K(2)-O(25B)#7	123.2(6)	N(1)-K(2)-C(5)	58.38(12)
O(8)-K(1)-Fe(1)	31.86(9)	O(2)#1-K(2)-O(25B)#7	108.8(6)	O(10)#7-K(2)-O(3)	142.4(3)
O(1)-K(1)-Fe(1)	29.61(7)	O(5)#7-K(2)-O(25B)#7	64.9(7)	O(2)#1-K(2)-O(3)	39.1(3)
O(28)-K(1)-Fe(1)	63.4(9)	O(7)-K(2)-O(25B)#7	75.6(7)	O(5)#7-K(2)-O(3)	87.3(4)
Fe(1)#1-K(1)-Fe(1)	52.54(4)	O(8)#1-K(2)-O(25B)#7	161.2(6)	O(7)-K(2)-O(3)	70.5(4)
O(22B)-K(1)-K(2)#1	100.1(6)	O(21)-K(2)-O(25B)#7	38.1(7)	O(8)#1-K(2)-O(3)	96.6(3)
O(6)#1-K(1)-K(2)#1	53.94(12)	O(10)#7-K(2)-O(6)	73.29(14)	O(21)-K(2)-O(3)	102.3(4)
O(22A)-K(1)-K(2)#1	116.4(3)	O(2)#1-K(2)-O(6)	63.82(14)	O(25B)#7-K(2)-O(3)	71.7(7)
O(10)#5-K(1)-K(2)#1	43.62(12)	O(5)#7-K(2)-O(6)	154.60(15)	O(6)-K(2)-O(3)	69.2(3)
O(8)-K(1)-K(2)#1	49.38(12)	O(7)-K(2)-O(6)	41.79(14)	O(25A)#7-K(2)-O(3)	43.8(8)
O(1)-K(1)-K(2)#1	81.67(15)	O(8)#1-K(2)-O(6)	73.57(13)	N(1)-K(2)-O(3)	21.6(3)
O(28)-K(1)-K(2)#1	124.4(9)	O(21)-K(2)-O(6)	105.8(2)	C(5)-K(2)-O(3)	62.7(4)
Fe(1)#1-K(1)-K(2)#1	76.97(6)	O(25B)#7-K(2)-O(6)	113.7(7)	O(7)-K(3)-O(7)#8	153.0(3)
Fe(1)-K(1)-K(2)#1	62.29(5)	O(10)#7-K(2)-O(25A)#7	143.7(9)	O(7)-K(3)-O(9)#9	69.71(15)
O(22B)-K(1)-K(3)#6	48.9(5)	O(2)#1-K(2)-O(25A)#7	81.1(8)	O(7)#8-K(3)-O(9)#9	128.04(15)
O(6)#1-K(1)-K(3)#6	59.37(10)	O(5)#7-K(2)-O(25A)#7	68.9(9)	O(7)-K(3)-O(9)#7	128.04(15)
O(22A)-K(1)-K(3)#6	63.7(4)	O(7)-K(2)-O(25A)#7	71.6(9)	O(7)#8-K(3)-O(9)#7	69.71(15)
O(10)#5-K(1)-K(3)#6	33.31(12)	O(8)#1-K(2)-O(25A)#7	137.6(9)	O(9)#9-K(3)-O(9)#7	109.5(2)
O(8)-K(1)-K(3)#6	101.15(13)	O(21)-K(2)-O(25A)#7	62.9(9)	O(7)-K(3)-O(21)	68.4(3)
O(1)-K(1)-K(3)#6	119.01(15)	O(25B)#7-K(2)-O(25A)#7	28.0(10)	O(7)#8-K(3)-O(21)	90.0(3)
O(28)-K(1)-K(3)#6	174.3(8)	O(6)-K(2)-O(25A)#7	98.1(9)	O(9)#9-K(3)-O(21)	137.8(3)
Fe(1)#1-K(1)-K(3)#6	94.34(6)	O(10)#7-K(2)-N(1)	127.2(2)	O(9)#7-K(3)-O(21)	99.8(3)
Fe(1)-K(1)-K(3)#6	112.70(7)	O(2)#1-K(2)-N(1)	20.90(15)	O(7)-K(3)-O(21)#8	90.0(3)
K(2)#1-K(1)-K(3)#6	53.08(5)	O(5)#7-K(2)-N(1)	98.13(17)	O(7)#8-K(3)-O(21)#8	68.4(3)
O(10)#7-K(2)-O(2)#1	122.32(18)	O(7)-K(2)-N(1)	73.65(10)	O(9)#9-K(3)-O(21)#8	99.8(2)
O(10)#7-K(2)-O(5)#7	130.07(17)	O(8)#1-K(2)-N(1)	76.20(19)	O(9)#7-K(3)-O(21)#8	137.8(3)
O(2)#1-K(2)-O(5)#7	91.97(16)	O(21)-K(2)-N(1)	121.2(3)	O(21)-K(3)-O(21)#8	75.8(5)
O(10)#7-K(2)-O(7)	79.93(16)	O(25B)#7-K(2)-N(1)	93.3(7)	O(7)-K(3)-O(10)#9	115.26(15)
O(2)#1-K(2)-O(7)	91.37(15)	O(6)-K(2)-N(1)	56.51(15)	O(7)#8-K(3)-O(10)#9	79.28(15)
O(5)#7-K(2)-O(7)	139.3(2)	O(25A)#7-K(2)-N(1)	65.4(8)	O(9)#9-K(3)-O(10)#9	48.77(14)
O(10)#7-K(2)-O(8)#1	75.01(16)	O(10)#7-K(2)-C(5)	81.23(17)	O(9)#7-K(3)-O(10)#9	93.67(16)

O(21)-K(3)-O(10)#9	158.8(3)	O(7)-K(3)-S(1)#7	103.37(12)	S(1)#9-K(3)-K(2)	128.26(5)
O(21)#8-K(3)-O(10)#9	83.2(3)	O(7)#8-K(3)-S(1)#7	90.66(12)	S(1)#7-K(3)-K(2)	61.07(4)
O(7)-K(3)-O(10)#7	79.28(15)	O(9)#9-K(3)-S(1)#7	107.80(14)	O(7)-K(3)-K(2)#8	127.71(12)
O(7)#8-K(3)-O(10)#7	115.26(15)	O(9)#7-K(3)-S(1)#7	25.05(9)	O(7)#8-K(3)-K(2)#8	47.74(12)
O(9)#9-K(3)-O(10)#7	93.67(16)	O(21)-K(3)-S(1)#7	86.4(2)	O(9)#9-K(3)-K(2)#8	85.52(10)
O(9)#7-K(3)-O(10)#7	48.77(14)	O(21)#8-K(3)-S(1)#7	152.1(2)	O(9)#7-K(3)-K(2)#8	103.22(10)
O(21)-K(3)-O(10)#7	83.2(3)	O(10)#9-K(3)-S(1)#7	111.76(14)	O(21)-K(3)-K(2)#8	117.0(3)
O(21)#8-K(3)-O(10)#7	158.8(3)	O(10)#7-K(3)-S(1)#7	24.89(10)	O(21)#8-K(3)-K(2)#8	48.7(3)
O(10)#9-K(3)-O(10)#7	117.9(2)	S(1)#9-K(3)-S(1)#7	117.32(11)	O(10)#9-K(3)-K(2)#8	43.11(11)
O(7)-K(3)-S(1)#9	90.66(12)	O(7)-K(3)-K(2)	47.74(11)	O(10)#7-K(3)-K(2)#8	149.83(13)
O(7)#8-K(3)-S(1)#9	103.37(12)	O(7)#8-K(3)-K(2)	127.71(12)	S(1)#9-K(3)-K(2)#8	61.07(4)
O(9)#9-K(3)-S(1)#9	25.05(9)	O(9)#9-K(3)-K(2)	103.22(10)	S(1)#7-K(3)-K(2)#8	128.26(5)
O(9)#7-K(3)-S(1)#9	107.80(14)	O(9)#7-K(3)-K(2)	85.52(10)	K(2)-K(3)-K(2)#8	165.02(11)
O(21)-K(3)-S(1)#9	152.1(2)	O(21)-K(3)-K(2)	48.7(3)	K(3)-O(21)-K(2)	84.5(4)
O(21)#8-K(3)-S(1)#9	86.4(2)	O(21)#8-K(3)-K(2)	117.0(3)	O(22B)-O(22A)-K(1)	24.5(7)
O(10)#9-K(3)-S(1)#9	24.89(10)	O(10)#9-K(3)-K(2)	149.83(13)		
O(10)#7-K(3)-S(1)#9	111.76(14)	O(10)#7-K(3)-K(2)	43.11(11)		

Symmetry transformations used to generate equivalent atoms:

#1  $y, x, -z$  #2  $x-y+1, -y+1, -z+1/3$  #3  $-x+y+1, -x+1, z-2/3$  #4  $-x+y+1, -x+1, z+1/3$  #5  $-y+1, x-y, z-1/3$  #6  $x, y, z-1$   
 #7  $x-y, -y+1, -z+1/3$  #8  $y, x, -z+1$  #9  $-y+1, x-y, z+2/3$



## Chapter Nine : Conclusions

The research into supramolecular chemistry presented in this work has resulted in the synthesis and characterization of twenty coordination compounds. These can be considered to fall into three categories:

1. Compounds **1-5** all have N-containing ligands with pyridine groups and other nitrogen ligands coordinated to Cu(II) coordination sphere is evident with 4,5 and 6 coordination geometries being observed.
2. Compounds **6**, **7** and **9** all contain the classic  $\{LCu(OAc)_2\}_2$  units as a synthon. In compounds **6** and **9** these are linked into chains by a pyrimidine based ligand in **6** and a  $[Mn(H_2O)_4Cl_2]$  unit in **9**. In compound **7** the pyrimidine based ligand takes the position of the terminal ligand L in the classic structure. Compound **8** contains  $Cu^{2+}$  and  $K^+$  centres linked through a network of OAc- and HOAc ligands.
3. Compounds **10-20** all have ligands incorporating the iminodiacetate functionality. In compound **15** Cu(II) centres are linked into a chain stabilised by  $\pi$ - $\pi$ -stacking between coordinated pyridine and pyridinium counterions. In compound **20** an oxo-bridged di iron(III) complex forms a mesoporous honeycomb lattice. Magnetic measurements on compound **20** showed the predicted behaviour.

Future research should concentrate on investigating the physical properties of the compounds presented here and the development of a systematic approach aimed in tailoring supramolecular interactions.

The advantage of molecular based magnets, compared with other types of magnetic nanoparticles is that their structure is known and it is possible to measure their properties using instruments such as SQUID or X-ray-diffractometer on single crystals. I have synthesized a range of interesting compounds in my research work, from which valuable and stunning conclusions can be drawn regarding the synthetic strategies.

Solvolysis reactions were tried at 200°C, 120°C and 80°C in hydrothermal reactors at high pressure and temperature with mononuclear complexes and Fe(III)-nitrate in order to produce

assorted metal clusters but the mononuclear complex in most of the cases crystallized again and the ligand disintegrated at 200°C.

The synthesis and the structures of  $[\text{CuBr}_2(\text{C}_{14}\text{H}_{17}\text{N}_4)]$  **1** and  $[\text{Cu}(\text{C}_{14}\text{H}_{16}\text{N}_4)_2]\text{Br}_2 \cdot 2\text{MeOH}$  **3** are similar. Compound **1** was obtained with a metal-ligand ratio of 1:1, whereas compound **3** required a metal-ligand ratio of 1:10. In  $[\text{Cu}(\text{C}_{14}\text{H}_{16}\text{N}_4)_2]\text{Br}_2 \cdot 2\text{MeOH}$  **3** a ring, closing reaction was observed, which was not the case with  $[\text{CuBr}_2(\text{C}_{14}\text{H}_{17}\text{N}_4)]$  **1**. The mechanism of the ring formation was explained in chapter 5.

Using **L1**, solvents were not observed to influence the formation of clusters. This is seen in  $[\text{CuCl}_2(\text{C}_{14}\text{H}_{16}\text{N}_4)] \cdot \text{H}_2\text{O}$  **2** which was synthesized using a 1:1 metal:ligand ratio as was  $[\text{CuBr}_2(\text{C}_{14}\text{H}_{17}\text{N}_4)]$  **1**, but using different metal salts and solvents.

The ligand  $\text{H}_3\text{hda-OH}$ , **L12**, has been synthesized by Dr. Jonathan Hill. This quinoide type ligand has useful qualities in the area of the leukemia therapy and in the UV/VIS spectroscopy on the basis of its ability to form radicals. However, only one metal-compound with magnetic properties has been synthesized with this ligand until now [2]. Furthermore, reactions with increased amounts of base (8-16 equiv.) and different metal:ligand ratios have been attempted with this ligand to produce aggregates with shorter metal-metal distances. And colorless crystals were obtained. Mononuclear complexes were produced in these studies with the  $\text{H}_3\text{hda-OH}$  ligand and some red crystals were obtained in an Ar-atmosphere, however these were not single crystals.

$[\text{Cr}(\text{hda-OH})(\text{H}_2\text{O})_2] \cdot 2\text{H}_2\text{O}$  **18**,  $[\text{Fe}(\text{hda-OH})(\text{H}_2\text{O})_2] \cdot 2\text{H}_2\text{O}$  **19** and  $[\text{Ni}(\text{hda-OH})(\text{H}_2\text{O})_2] \cdot \text{H}_2\text{O}$  **17** are obtained using a similar synthesis, but different metal-metal distances and molecular packings are observed.  $[\text{Cr}(\text{hda-OH})(\text{H}_2\text{O})_2] \cdot 2\text{H}_2\text{O}$  **18** and  $[\text{Fe}(\text{hda-OH})(\text{H}_2\text{O})_2] \cdot 2\text{H}_2\text{O}$  **19** are isomorphous. However the ligand in  $[\text{Ni}(\text{hda-OH})(\text{H}_2\text{O})_2] \cdot \text{H}_2\text{O}$  arranges itself differently compared with  $[\text{Cr}(\text{hda-OH})(\text{H}_2\text{O})_2] \cdot 2\text{H}_2\text{O}$  **18**, although the composition and synthesis of these are the same.  $[\text{Ni}(\text{hda-OH})(\text{H}_2\text{O})_2] \cdot \text{H}_2\text{O}$  **17** is ordered in pairs and in rows, but the rows are not exactly like in  $[\text{Cr}(\text{hda-OH})(\text{H}_2\text{O})_2] \cdot 2\text{H}_2\text{O}$  **18** and  $[\text{Fe}(\text{hda-OH})(\text{H}_2\text{O})_2] \cdot 2\text{H}_2\text{O}$  **19**. By  $[\text{Fe}(\text{hda-OH})(\text{H}_2\text{O})_2] \cdot 2\text{H}_2\text{O}$  **19** were given 4 equivalent of base and a molar ratio of 1:1 ligand:metal, while with the Ni and Cr complexes, at a pH = 4 were worked and with a molar ratio 2:1 ligand:metal. In these named structures the shortest metal-metal distances are 4.969 Å Fe...Fe, 5.12 Å Cr...Cr and 5.08 Å Ni...Ni. From these distances, one might infer

that the more base is admitted, the shorter the metal-metal-distances become. The ligand:metal ratio determines the structure packing in the case of the copper acetate family, but not with H<sub>3</sub>hda-OH.

It was surprising that a polymer and a mononuclear complex can be isolated with similar synthetic conditions. With the polymer [Cu<sub>2</sub>(OAc)<sub>4</sub>(C<sub>4</sub>H<sub>4</sub>N<sub>3</sub>Br)]<sub>∞</sub> **6** four times more ligand than copper was used, with the ratio 4:1:4 (L4:Cu:Cr), while with the copper acetate complex [Cu<sub>2</sub>(OAc)<sub>4</sub>(C<sub>4</sub>H<sub>4</sub>N<sub>3</sub>Br)<sub>2</sub>] **7** a ratio 1:1 ligand:copper was used with the ratio 1:1:1 (L4:Cu:Ni), the other synthetic conditions (e.g. solvents, base and acidity) were the same in both cases. So the amount of ligand L4 appears to play a role in the determination of the structure packing.

With the ligand H<sub>3</sub>had-SO<sub>3</sub>H, different metal:ligand:base ratios were attempted, but all attempts led to the same structure. The binuclear Fe compound **20** proved to be extremely stable.

With the compound [CuCl<sub>2</sub>(C<sub>12</sub>H<sub>12</sub>N<sub>2</sub>O<sub>2</sub>)] **4** a short Cu...Cu-distance of 3.931 Å was observed, however no magnetic measurement of this compound was undertaken and this could be examined in the future. Also more than 2 compounds reported in this work, could be magnetically active, then by a metal-metal distance of 5.45 Å a cooperative ferromagnetic interaction was measured for a mixed-metal-cluster reported by Pilkington and Decurtins [110]. Compound **16** could exhibit interesting magnetic properties.

Some compounds could be synthesized in non-aqueous solvents so that no water accumulates at the metal and clusters could be formed, for example in the case of [Fe(hda-OH)(H<sub>2</sub>O)<sub>2</sub>].2H<sub>2</sub>O **19**. In the future, the reaction under Ar-atmosphere could be optimized with the radical ligand of the quinon-type ligand L12 in order to obtain single crystals.

## Chapter Ten: Bibliography

- [1] O. Kahn, *Accounts of Chemical Research*, **2000**, *33*, 647.
- [2] C. Drouza, V. Tolis, V. Gramlich, C. Raptopoulou, A. Terzis, M. P. Sigalas, T. A. Kabanos, A. D. Keramidas, *Chem. Comm.* **2002**, *23*, 2786.
- [3] L. S. Miller, A. J. Epstein, *MRS Bulletin*, November **2000**, 21-28.
- [4] R.-D. Schnebeck, L. Randaccio, E. Zangrando, B. Lippert, *Angew. Chem., Int. Ed.* **1998**, *37*, 119.
- [5] M. Fujita, *Chem. Comm.* **1996**, *13*, 1535.
- [6] P. J. Stang, D. H. Cao, S. Saito, A. M. Arif, *J. Am. Chem. Soc.* **1995**, *117*, 6273.
- [7] C. J. Kuehl, S. D. Huang, P. J. Stang, *J. Am. Chem. Soc.* **2001**, *123*, 9634.
- [8] S. Roche, C. Haslam, H. Adams, S. L. Heath, J. A. Thomas, *Chem. Comm.* **1998**, 1681.
- [9] M. Fujita, *Chem. Soc. Rev.* **1998**, *27*, 417.
- [10] B. J. Holliday, C. A. Mirkin, *Angew. Chem., Int. Ed.* **2001**, *40*, 2022.
- [11] N. Olenyuk, A. Fechtenkötter, P. Stang, *J. Chem. Soc., Dalton Trans.* **1998**, 1707.
- [12] F. Hasenkopf, R. Tschewitschke, *Ger. Offen.* **1996**, 6.
- [13] H., Shuichi, K. Yasuo, M. Fujita, *Chem. Comm.* **2000**, *16*, 1509.
- [14] F. Ibukuro, T. Kusukawa, M. Fujita, *J. Am. Chem. Soc.* **1998**, *120*, 8561.
- [15] B. Olenyuk, J. A. Whiteford, A. Fechtenkötter, P. J. Stang, *Nature* **1999**, *398*, 796.
- [16] M. H. Keefe, R. V. Slone, J. T. Hupp, K. F. Czaplewski, R. Q. Snurr, C. L. Stern, *Langmuir* **2000**, *16*, 3964.
- [17] C. B. Aakeröy, A. M. Beatty, *Aust. J. Chem.* **2001**, *54*, 409.
- [18] D. C. Sherrington, K. A. Taskinen, *Chem. Soc. Rev.* **2001**, *30*, 83.
- [19] P. Dapporto, P. Paoli, S. Roelens, *J. Org. Chem.* **2001**, *66*, 4930.
- [20] Y. Tokunaga, D. M. Rudkevich, J. Santamaria, G. Hilmersson, J. Rebek, *Chem. Eur. J.* **1998**, *4*, 1449.
- [21] L. R. MacGillivray, P. R. Diamente, J. L. Reid, J. A. Ripmeester, *Chem. Comm.* **2000**, 359.
- [22] K. Kobayashi, T. Shirasaka, K. Yamaguchi, S. Sakamoto, E. Horn, N. Furukawa, *Chem. Commun.* **2000**, 41.

- [23] Kobayashi, *Angew. Chem., Int. Ed.* **2000**, 39, 3110.
- [24] M. J. Hardie, M. Makha, C. L. Raston, *Chem. Comm.* **1999**, 2409.
- [25] Y. L. Cho, D. M. Rudkevich, A. Shivamjuk, K. Rissamen, J. Rebek, *Chem. Eur. J.* **2000**, 6, 3788.
- [26] Y. L. Cho, D. M. Rudkevich, J. Rebek, *J. Am. Chem. Soc.* **2000**, 122, 9868.
- [27] Castellano, *Proc. Natl. Acad. Sci. U.S.A.* **1997**, 94, 7132.
- [28] M. Pilkington; M. Gross; P. Franz.; M. Biner; S. Decurtins; H. Stoeckli-Evans; A. Neels, *Journal of Solid State Chem.* **2001**, 159, 262.
- [29] J.B Goodenough, Magnetism and the Chemical Bond, Hrsg. : F.A. Cotton : Interscience Publishers, New York, London, Sydney, **1966**.
- [30] W. Urland, *Angew. Chem. Intern. Ed.* **1981**, 20, 210.
- [31] W. Klemm, Magnetochemie, Akadem. Verlagsgesellschaft G.m.b.H., Leipzig, **1936**.
- [32] S. Boersma, *Rev. Sci. Intr.* **1949**, 20, 660.
- [33] L.S. Gouy, *C.R. Acad. Sci. Paris* **1889**, 109, 935.
- [34] G. Quincke, *Ann. Phys. (Leipzig)* **1885**, 24, 347.
- [35] G. Quincke, *Ann. Phys. (Leipzig)* **1888**, 34, 401
- [36] S. Boersma, *Rev. Sci. Intr.* **1949**, 20, 660.
- [37] R.L. Fagaly, *Sci. Pro., Oxford* **1987**, 71, 181.
- [38] J.C. Gallop, Squids, the Josephson Effects und Superconducting Electronics, Adam Hilger, Bristol, Philadelphia, New York, **1991**.
- [39] M. Murugesu, PhD Thesis **2002** Universiät Karlsruhe (TH); P. King, PhD Thesis **2003** Universiät Karlsruhe (TH).
- [40] S. Kawano, N. Fujita, K. Van Bommel, Shinkai ; *Chem. Lett.* **2003**, 32, 12.
- [41] (a) J. D. Woodward, R. Backov, K. A. Abboud, H. Ohnuki,, M. W. Meisel, D. R. Talham, *Polyhedron*, **2003**, 22, 2821; (b) H. N. Bordallo, L. Chapon, J. L. Manson, C. D. Ling, J. S. Qualls, D. Hall, D. N. Argyriou, *Polyhedron* **2003**, 22, 2045.
- [42] O. Sato; *Accounts of Chemical Research* **2003**, 36, 692.
- [43] D. Gatteschi, *Adv. Matter* **1994**, 6, 35.
- [44] O. Kahn, Molecular Magnetism; VCH: New York, **1993**.

- [45] H. Iwamura, *Pure Appl. Chem.* **1987**, *59*, 1595.
- [46] P. M. Lathi, *Magnetic properties of organic materials*; Marcel Dekker: New York, **1999**.
- [47] J.S. Miller; A. J. Epstein, *Angew. Chem., Int. Ed. Engl.* **1994**, *33*, 385.
- [48] J. Dale Ortego, *J. Chem. Eng. Data* **1986**, *31*, 365.
- [49] M. Murugesu, *J. Chem. Soc., Chem. Comm.* **2002**, 1054.
- [50] W. Schmitt, M. Murugesu, J. C. Goodwin, J. P. Hill, A. Mandel, R. Bhalla, C. E. Anson, S. L. Heath, A. K. Powell, *Polyhedron* **2001**, *20*, 1687.
- [51] J. T. Brockman, J. C. Huffman, G. Christou, *Angewandte Chemie International Edition*, **2002**, *41*, 2506.
- [52] A.K.Powell, S.L. Heath, D. Gatteschi, L.Pardi, R. Sessoli, G. Spina, F. Del Giallo, F. Pieralli, *J. Am. Chem. Soc.* **1995**, *117*, 2491.
- [53] (a) Schmitt, Henderson, Powell, Anson, Moore, Jordan, *Coord. Chem. Rev.* **2002**, *228*, 115. (b) C.J. Harding, R.K. Henderson, A. K. Powell, *Angew. Chem. Int. Ed. Engl.* **1993**, *32*, 570.
- [54] (a) W. Schmitt, C. E. Anson, R. Sessoli, M. van Veen, A. K. Powell, *J. Inorg. Biochem.* **2002**, *91*, 173. (b) W. Schmitt, C. E. Anson, B. Pilawa, A. K. Powell, *Z. Anorg. Allg. Chem.* **2002**, *628*, 2443.
- [55] F. Neese und E. I. Solomon, *Inorg. Chem.*, **1998**, *37*, 6568.
- [56] A. Saeed, *Canadian Journal of Applied Spectroscopy* **1994**, *39*, 173.
- [57] Buehler, *Chimia* **1970**, *24*, 433, G. Schwarzenbach, *Helv. Chim. Acta* **35** (1952) 2344.
- [58] P.Gütlich, A.Hauser, H.Spiering. *Angew.Chem. Int. Ed. Engl.*, **1994**, *33*, 2024.
- [59] J. A. Real, A. B. Gaspar, V. Niel, M. C. Munioz, *Coord. Chem. Rev.* **2003**, *236*, 121.
- [60] Baker, *Inorg. Chem.* **1964**, *3*, 1184.
- [61] D. M. Shin, I. S. Lee, Y.-A Lee, Y. K. Chung, *Inorg. Chem.* **2003**, *42*, 2977.
- [62] C. J. Janiak, *J. Chem. Soc., Dalton Trans.* **2000**, 3885.
- [63] R. K. Henderson, University of East Anglia, **1993**.
- [64] Podder, *Acta. Cryst. B* **1979**, *35*, 53.
- [65] N. J. Mammano, *Acta. Cryst. B* **1977**, *33*, 1251.
- [66] A. Podder, J. K. Dattagupta, N. N. Saha, *Acta. Cryst. B* **1979**, *35*, 53.
- [67] Radanović, T. Ama, D. M. Guršić, D. M. Ristanović, D. D. Radanović, H. Kawaguchi,

- Bull. Chem. Soc. Jpn.* **2000**, *73*, 2283.
- [68] K. Hoard, Smith, *Inorg. Chem.*, **1963**, *2*, 1316.
- [69] X. Solans, M. Font-Altaba, J. Oliva, J. Herrera, *Acta. Cryst. C* **1983**, *39*, 435.
- [70] K. Kanamori, A. Kyotoh, K. Fujimoto, K. Nagata, H. Suzuki, K. Okamoto, *Bull. Chem. Soc. Jpn.*, **2001**, *74*, 2113.
- [71] K. Kanamori, E. Kameda, K. Okamoto, *Bull. Chem. Soc. Jpn.*, **1996**, *69*, 2901.
- [72] (a) X. Solans, M. Font-Altaba, J. Oliva, J. Herrera, *Acta Cryst. C*, **1983**, *39*, 435; (b) M.A. Porai-Koshits, N. V. Novozhilova, T. N. Polynova, T. V. Filippova, L. I. Martynenko, *Kristallografiya*, **1973**, *17*, 89; (c) T. F. Sysoeva, V. M. Agre, V. K. Trunov, N. M. Dyatlova, N. N. Barkhanova, *Zh. Strukt. Khim.*, **1984**, *25*, 107; (d) M. V. Leont'eva, A. Ya. Fridman, N. M. Dyatlova, V. M. Agre, T.F. Sysoeva, *Zh. Neorg. Khim.*, **1987**, *32*, 2494.
- [73] Y. Kushi, K. Morimasa, H. Yoneda, "Presented at the 49<sup>th</sup> Annual Meeting of the Chemical Society of Japan", Tokyo, April **1984**, Abstr. No. 1 N31.
- [74] F. S. Stephens, *J. Chem. Soc. A*, **1969**, 1723.
- [75] R. H. Nuttall, D. M. Stalker, *Talanta*, **1977**, *24*, 355.
- [76] (a) Temkina, V. Ya et al, *Zhurnal Oshchei Khimii*, **1971**, *41*, 1334. (b) Timakova, L. M.; Zhadanov, B. V.; Yaroshenko, G. F.; Polyakova, I. A.; Temkina, V. Ya.; Lastovskii, R. P. Vses. Nauchno-Issled. Inst. Khim. Reakt. Osobo Chist. Khim. Veshchestv, Moscow, USSR. *Zhurnal Obshchei Khimii* **1978**, *48*, 1846.
- [77] Coronado, NATO ASI Series, Series E: *Applied Sciences* **1991**, *198*, 267-79.
- [78] Xu, Meizhong, Xie, Yuyuan, *Chinese Journal of Medicinal Chemistry*, **1993**, *3*, 27.
- [79] E. A. Solov'ev, G. F. Yaroshenko, M. A. Ratina, Bozhevol'nov, E. A., *Koordinatsionnaya Khimiya* **1976**, *2*, 1477.
- [80] Tsirul'nikova, N. V., Temkina, V. Ya; Dyatlova, N. M., Rusina, M. N., Zhadanov, B. V., Lastovskii, R.P., *Zhurnal Analiticheskoi Khimii* **1970**, *25*, 839.
- [81] Timakova, L. M.; Yaroshenko, G. F.; Khavchenko, N. E.; Temkina, V. Ya. Vses. Nauchno-Issled. Inst. Khim. Reakt. Osobo Chist. Khim. Veshchestv, Moscow, USSR. *Doklady Akademii Nauk SSSR* **1977**, *234*, 610.
- [82] M. Fujita; *Chem. Comm.*, **2002**, 1866.
- [83] Adisson, A; Rao, T.; Reedijk, J.; Van Rijn, J.; Vershoor, G.; *J. Chem. Soc. Dalton Trans.* **1984**, 1349.
- [84] A. G. J., Ligtenbarg, A. L. Spek, R. Hage, B. L. Feringa, *J. Chem. Soc., Dalton Trans.*, **1999**, 659.

- [85] (a) D. K. Chand, K. Biradha, M. Fujita, *Chem. Comm.*, **2001**, 1652. T. Kusakawa, M. Fujita, *J. Am. Chem. Soc.* **1999**, *121*, 1397; (b) D. K. Chaud, M. Fujita, K. Biradha, S. Sakamoto, K. Yamaguchi, *J. Chem. Soc., Dalton Trans.* **2003**, 2750; (c) F. M. Tabellion, S. Russell Seidel, A. M. Arif, P. Stang, *J. Am. Chem. Soc.* **2001**, *123*, 11982; B. Olenyuk, A. Fechtenkötter, P. J. Stang, *J. Chem. Soc., Dalton Transc.* **1998**, 1707; (d) D. H. Cao, K. Chen, J. Fan, J. Manna, B. Olenyuk, J. A. Whiteford, P. J. Stang, *Pure & Appl. Chem.* **1997**, *69*, 1979; (e) F. M. Tabellion, S. Russell Seidel, A. M. Arif, P. J. Stang, *J. Am. Chem. Soc.* **2001**, *123*, 7740; (f) K. Biradha, M. Fujita, *J. Chem. Soc., Dalton Trans.*, **2000**, 3805.
- [86] D.J.Cram; M.E. Tanner; R. Thomas, *Angew. Chem., Int. Ed. Engl.* **1991**, *30*, 1024. J.Rebek, *Chem. Eur. J.* **2000**, *6*, 187. M. Ziegler; *Angew. Chem., Int. Ed.* **2000**, *39*, 4119.
- [87] (a) M.Fujita; *J. Am. Chem. Soc.* **2000**, *122*, 6311; (b) M. Fujita; *J. Am. Chem. Soc.* **2001**, *123*, 10454.
- [88] M. Fujita; *Chem. Lett.*, **2000**, 598.
- [89] (a) C. A. Kavounis, *Polyhedron*, **1996**, *15*(3), 385-90; (b) A. C. Deveson, Ph. D. thesis, University of East Anglia, **1995**; (c) A. C. Deveson, S. L. Heath, C. J. Harding, A. K. Powell, *J. Chem. Soc. Dalton Trans.*, **1996**, 3173.
- [90] R. A. Mariezcurrena, A. W. Mombru, L. Sescun, E. Kremer, R. Gonzalez, *Acta Cryst. C* **1999**, *55*, 1989.
- [91] Spodine, Atria, Calvo, Manzur, Garland, Grandjean, Penia, *Bol. Soc. Chil. Chim.* **1991**, *36*, 209.
- [92] Smith, Graham, *Polyhedron*, **1991**, *10*, 873.
- [93] F.A.Cotton; *Inorg. Chem.* **1978**, *17*, 2004, S. F. Rice, R. B. Wilson, E. J. Solomon, *Inorg. Chem.* **1980**, *19*, 3425.
- [94] W. J.Evans; *J. Coord. Chem.*, **1999**, *47*, 199.
- [95] B.Morosin; R. C.Hughes; *Acta. Cryst. B* **1975**, *31*, 762.
- [96] (a) R.Raja, P, J. Ratnasamy, *Mol.Catal. A* **1995**, *100*, 93; (b) P. Ratnasamy, *Journal of Catalysis* **2000**, *192*, 286.
- [97] (a) J. Catterick, I. Thornton, *Adv. Inorg. Chem. Radiochem.*, **1977**, *20*, 316; (b) R. J. Doedens, *Prog. Inorg. Chem.*, **1976**, *21*, 288; (c) R. W. Jotham, *J. Chem. Soc., Dalton Trans.* **1972**, 428; (d) J.N. Van Niekerk, F.K.L. Schoening, *Acta Chrystallogr.* **1953**, *6*, 227; (e) G. M. Brown, R. Chidambaram, *Acta Chrystallogr., Sect. B*, **1973**, *29*, 2393.
- [98] J. Rao, *J. Chem. Soc., Dalton Trans.* **1983**, 2167.
- [99] A. K. Powell et al, *Inorg. Chem.* **1997**, *36*, 1265-1267.



- 
- [100] A. B. Blake, E. Sinn, A. Yavari, K. S. Murray, B. Moubarakki, *J. Chem. Soc., Dalton Trans.* **1998**, 45.
- [101] A. B. Blake, *J. Chem. Soc., Dalton Trans.* **1998**, 45.
- [102] V. G. Makkanhova, O. Yu, V. Vassilyeva, N. Kokozay, B. W. Skelton, J. Reedijk, G. A. Van Albada, L. Sorace, D. Gatteschi, *New J. Chem.*, **2001**, 25, 685.
- [103] M. Matsumoto, *Journal of Catalysis* **1992**, 138, 611.
- [104] E. Bugella-Altamarino, J. M. Gonzalez-Perez, A. G. Sicilia- Zafra, J. Niclos-Gutierrez, A. Castineiras-Campos, *Polyhedron* **1999**, 18, 3333.
- [105] M. D. Curtis, *J. Am. Chem. Soc.* **2003**, 125, 5040.
- [106] F. Le Gall, F. Fabrizi de Biani, A. Caneschi, P. Cinelli, A. Cornia, A. C. Fabretti, D. Gatteschi, *Inorg. Chim. Acta* **1997**, 262, 123-132.
- [107] S. M. Gorun, S. J. Lippard, *Inorg.Chem.* **1991**, 30, 1625.
- [108] L. M. Jampolsky, *Notes* **1952**, May 16, 74, 5222
- [109] Personal communication with Dr. J. Hill
- [110] M. Pilkington, S. Decurtins, *Chimia* **2000**, 54, 593.

**Appendix A: List of crystalline compounds.**

- 1** [CuBr<sub>2</sub>(C<sub>14</sub>H<sub>16</sub>N<sub>4</sub>)]
- 2** [CuCl<sub>2</sub>(C<sub>14</sub>H<sub>16</sub>N<sub>4</sub>).H<sub>2</sub>O]
- 3** [Cu(C<sub>14</sub>H<sub>16</sub>N<sub>4</sub>)<sub>2</sub>]Br<sub>2</sub>.2MeOH
- 4** [CuCl<sub>2</sub>(C<sub>12</sub>H<sub>12</sub>N<sub>2</sub>O<sub>2</sub>)]
- 5** [CuCl<sub>4</sub>(1,3dpp)<sub>2</sub>].H<sub>2</sub>O
- 6** [Cu<sub>2</sub>(OAc)<sub>4</sub>(C<sub>4</sub>H<sub>4</sub>N<sub>3</sub>Br)]<sub>∞</sub>
- 7** [Cu<sub>2</sub>(OAc)<sub>4</sub>(C<sub>4</sub>H<sub>4</sub>N<sub>3</sub>Br)<sub>2</sub>]
- 8** K<sub>4</sub>[Cu(OAc)<sub>6</sub>(HOAc)<sub>4</sub>]
- 9** [Cu<sub>2</sub>(OAc)<sub>4</sub>MnCl<sub>2</sub>(H<sub>2</sub>O)<sub>4</sub>]<sub>∞</sub>
- 10** K[Cu(ida)Cl(H<sub>2</sub>O)<sub>2</sub>]
- 11** K[Cr(Hedta)Cl].H<sub>2</sub>O
- 12** [CuCl(H<sub>3</sub>edta)].2H<sub>2</sub>O
- 13** [Cu(Hada)<sub>2</sub>]
- 14** [Cr(ada)<sub>2</sub>](pyrH).3H<sub>2</sub>O
- 15** {(pyrH).[Cu(heidi)(pyr)]Cl.2H<sub>2</sub>O}<sub>∞</sub>
- 16** [Cu(naphtyl-OH-ida)(H<sub>2</sub>O)]
- 17** [Ni(hda-OH)(H<sub>2</sub>O)].H<sub>2</sub>O
- 18** [Cr(hda-OH)(H<sub>2</sub>O)].2H<sub>2</sub>O
- 19** [Fe(hda-OH)(H<sub>2</sub>O)<sub>2</sub>].2H<sub>2</sub>O
- 20** K<sub>5</sub>[Fe<sub>2</sub>(μ-O)(μ-NO<sub>3</sub>)(SO<sub>3</sub>-hda)<sub>2</sub>].15H<sub>2</sub>O

**Appendix B: List of Ligands.**

- L1** N-[(1E)-Dipyridin-2-ylmethylene]propane-1,3-diamine (C<sub>14</sub>H<sub>16</sub>N<sub>3</sub>)
- L2** [(Carboxymethyl)(3-{{(1E)-dipyridin-2-ylmethylene}amino}propyl)amino]acetic acid (C<sub>18</sub>H<sub>22</sub>N<sub>4</sub>O<sub>4</sub>)
- L3** 2-(3-Pyridin-2ylpropyl)pyridine (dpp)
- L4** 5-Bromo-2-pyrimidine-amine (C<sub>4</sub>H<sub>4</sub>N<sub>3</sub>Br)
- L5** Iminodiacetic acid (H<sub>2</sub>ida)
- L6** Ethyldiamine-N,N,N,N-tetraacetic acid (H<sub>4</sub>edta)
- L7** [(Aminocarbonyl)(carboxymethyl) methylamino]acetic acid (H<sub>2</sub>ada)
- L8** N-(2-Hydroxyethyl)iminodiacetic acid (H<sub>3</sub>heidi)
- L9** 1, 3-Diimino 2 hydroxy propane N, N N', N', tetraacetic acid (H<sub>3</sub>hpta)
- L10** [(Carboxymethyl)(2,5-dihydroxy-3,4,6-trimethylphenyl)methylamino]acetic acid (Me-hda-OH)
- L11** [(Carboxymethyl)(2 hydroxy-1 naphtyl)methylamino]acetic acid (naphtyl-OH-ida)
- L12** [(Carboxymethyl)(2,5-dihydroxyphenyl)methylamino]acetic acid (hda-OH)
- L13** [(Carboxymethyl)(2-hydroxy-5-sulfophenyl)methylamino]acetic acid (SO<sub>3</sub>-had-OH)

---

**Appendix C: List of abbreviations.**

br	broad
d	Doublet
FT	Fourier-transform
IR	Infra-red
L	Ligand
MeOH	Methanol
m	Multiplet (NMR), medium (IR)
NMR	Nuclear magnetic resonance
Ph	Phenyl
s	Singlet (NMR), strong (IR)
t	Triplet
T	Temperature
T <sub>c</sub>	Critical Temperature
T <sub>N</sub>	Néel-Temperature
w	weak
χ	Molar magnetic susceptibility

# **Curriculum Vitae**

## **Personal data**

Name: Maria Paula Juanico  
Born: at the 20.11.73 in Buenos Aires (Argentina)  
Passport: Italian  
Marital status: single

## **Education and study**

1991: Bilingual Argentinean high school diploma at the Goethe-School Buenos Aires.  
1992: Technical German high school at the university in Bonn.  
1993-1995: Vordiplom in chemistry at the university in Bonn.  
1996-1999: Diploma in chemistry at the technical university Berlin.  
2000: Doctor position in the technical chemistry at the research center Karlsruhe.  
2001-2003: Doctor position in the inorganic department at the university Karlsruhe.

## **Stages at the industry**

1995: three months stage at San Roque in Montevideo, Uruguay.  
1996: 13 weeks stage at the BASF, Ludwigshafen.  
1998: 5 weeks stage at the Schering AG, Berlin.

## **Research works**

2001: Poster presentation on the international conference in Davos, Molecular Magnets.  
2002: 4 month research stay at the university in Florence, Italy.

## **Language knowledge**

Spanish: Mother language  
German: fluently spoken and written.  
English: very good spoken and written.  
Italian: good spoken and written.

## **Additional qualification:**

Classes in management of quality at the TH-Karlsruhe  
Seminar in patent law and investment.



## Acknowledgments

The present work was prepared in the time of January 2001 until October 2003 at the institute for inorganic chemistry of the technical university Karlsruhe under the management of *Prof. A. K. Powell*. Particular thanks is applied to her for the interesting topic, her personal care as well as granting of long-range freedoms to the independent scientific work, for “pulating” my English of this manuscript and the permission of a 4 month research-stay at the university in Florence, Italy.

The further I thank:

*Prof. Dante Gatteschi* and *Dr. Andrea Caneschi* for their successful cooperation in the area of the magnetism at the university in Florence.

Especially to *Dr. C. Anson* for his help and evaluation of the structure database and to *Dr. Jonathan Hill* (=big Jony-boy) for his generous help in organic synthesis, and for the wonderful friendship.

And therefore *D. Rovai*, *E. Berti*, *C. Carbonera*, *Dr. F. Constantino* and *Dr. O. Cador* for their generous help at the university of Florence and for the hospitality of all the group. I thank also grateful to the ESF (=European Science Foundation) for the financial support of my research stay in Florence.

To *Gabi Kuhne* and *Achim Balloff* for the efficient sale of chemicals. And also thank you very much to Mister Lehmann for the technical work.

A respectable Thank you also to *Gertraud Amschlinger*, our diverse secretary.

I would like to thank also *Christian Jones*, *Leonardo Ana* and *Martin Viertelhaus* for the help with computer programs. And I would like to thank *Ian Hewitt* for doing some corrections for the final version of my PhD.

I would like to thank *Dr. H. Henke* for his constructive criticism and *Dr. Wolfgang Schmitt* for his attention into my work. I would like to thank also *Dr. Muralee Murugesu* for giving me tips about synthesis.

For the financial support of my thesis I thank to the Landesgraduiertenförderung, Prof. Annie K. Powell, Prof. Dieter Fenske, Gertraud Amschlinger, Klaus Maisch and Annette Baust.

Finalmente quiero agradecer a mi *madre* y difunto *padre* por su apoyo económico y espiritual durante mis estudios, y por haberme apoyado en cada decisión que he tomado en mi vida. A mi familia en Uruguay y Argentina y a mis amigas de la infancia tanto en Uruguay como en Argentina también les agradezco de corazón todo su apoyo.